Interdisciplinary Perspectives on Infectious Diseases

Network Perspectives on Infectious Disease Dynamics

Guest Editors: Lauren Ancel Meyers, Ben Kerr, and Katia Koelle

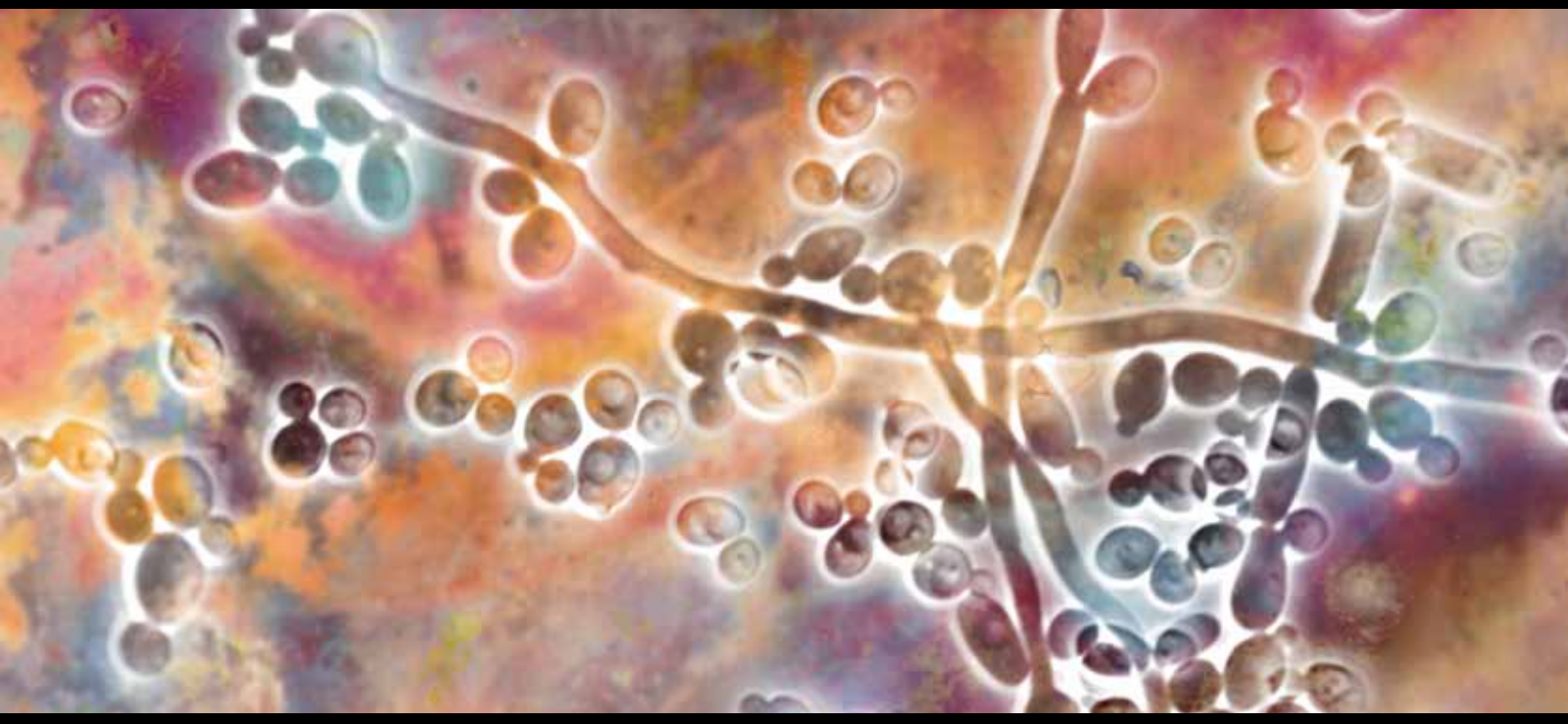

Network Perspectives on Infectious Disease Dynamics

Interdisciplinary Perspectives on Infectious Diseases

Network Perspectives on Infectious Disease Dynamics

Guest Editors: Lauren Ancel Meyers, Ben Kerr, and Katia Koelle

Editorial Board

Contents

Network Perspectives on Infectious Disease Dynamics, Lauren Ancel Meyers, Ben Kerr, and Katia Koelle
Volume 2011, Article ID 146765, 2 pages

Networks and the Epidemiology of Infectious Disease, Leon Danon, Ashley P. Ford, Thomas House, Chris P. Jewell, Matt J. Keeling, Gareth O. Roberts, Joshua V. Ross, and Matthew C. Vernon
Volume 2011, Article ID 284909, 28 pages

Epidemic Percolation Networks, Epidemic Outcomes, and Interventions, Eben Kenah and Joel C. Miller
Volume 2011, Article ID 543520, 13 pages

Contact Heterogeneity and Phylodynamics: How Contact Networks Shape Parasite Evolutionary Trees, Eamon B. O'Dea and Claus O. Wilke
Volume 2011, Article ID 238743, 9 pages

Assortativity and the Probability of Epidemic Extinction: A Case Study of Pandemic Influenza A (H1N1-2009), Hiroshi Nishiura, Alex R. Cook, and Benjamin J. Cowling
Volume 2011, Article ID 194507, 9 pages

Pathogens, Social Networks, and the Paradox of Transmission Scaling, Matthew J. Ferrari, Sarah E. Perkins, Laura W. Pomeroy, and Ottar N. Bjørnstad
Volume 2011, Article ID 267049, 10 pages

Network Models: An Underutilized Tool in Wildlife Epidemiology?, Meggan E. Craft and Damien Caillaud
Volume 2011, Article ID 676949, 12 pages

Empiricism and Theorizing in Epidemiology and Social Network Analysis, Richard Rothenberg and Elizabeth Costenbader
Volume 2011, Article ID 157194, 5 pages

Hindawi Publishing Corporation
Interdisciplinary Perspectives on Infectious Diseases
Volume 2011, Article ID 146765, 2 pages
doi:10.1155/2011/146765

Editorial

Network Perspectives on Infectious Disease Dynamics

Lauren Ancel Meyers,[1] Ben Kerr,[2] and Katia Koelle[3]

[1] *Section of Integrative Biology, The University of Texas at Austin, 1 University Station C0930, Austin, TX 78712, USA*
[2] *Department of Biology, University of Washington, P. O. Box 351800 Seattle, WA 98195, USA*
[3] *Department of Biology, Duke University, P. O. Box 90338 Durham, NC 27708, USA*

Correspondence should be addressed to Lauren Ancel Meyers, laurenmeyers@mail.utexas.edu

Received 31 December 2011; Accepted 31 December 2011

Over the last two decades, network perspectives have become ubiquitous in the life sciences, ranging from the consideration of microscopic molecular networks to macroscopic social interaction networks. These perspectives have provided new insights into the patterns and processes that we, as scientists, aim to understand. They have also encouraged the development of new mathematical and statistical approaches for rigorous examination of biological networks. This special issue focuses specifically on pioneering network perspectives in the field of infectious disease epidemiology, which have already yielded important new understanding of the dynamics of infectious disease outbreaks in humans and animals.

This special issue begins with an excellent introduction for newcomers to the field of network epidemiology by L. Danon and coauthors. This review gives an accessible overview of the types of networks relevant to the study of epidemiological interactions and methods for characterizing structural properties of networks. It also concisely summarizes new mathematical and simulation-based approaches for determining epidemiological dynamics on networks and statistical approaches for estimating epidemiological quantities for contact networks.

The special issue continues with several research articles that present new methodological developments in the field of network epidemiology. The first of these articles, by E. Kenah and J. C. Cohen, examines "epidemic percolation networks" (EPNs), a mathematical approach to modeling infectious disease transmission in networks that unifies and generalizes several existing mathematical approaches for studying infectious disease models (e.g., branching processes and network models). The article demonstrates the application of the methodology to the practical public health problem of designing effective vaccine priorities. The second article, by E. B. O'Dea and C. Wilke, also addresses the unification of existing approaches. Specifically, the authors posit that the evolutionary dynamics of viruses will be shaped by the contact patterns of the hosts they infect. They quantify the impact of host contact networks on viral gene genealogies and demonstrate the importance of explicitly considering network structure when estimating epidemiological parameters from viral sequence data.

The third research article, by H. Nishiura et al. addresses assortativity in networks, that is, the commonly observed phenomenon that nodes tend to connect to other nodes with similar properties. For example, in social networks, individuals may be most likely to associate with others in the same age group or other sociodemographic categories. The article presents quantitative approaches for analyzing the impacts of assortative mixing patterns on the probability of pandemic emergence. Based on such analyses, the article offers a plausible explanation for the early delay in geographic spread of the 2009 H1N1 influenza pandemic. This is a clear example of a network perspective on infectious disease dynamics providing a more in-depth understanding of observed epidemiological patterns. The last research article, by M. J. Ferrari and coauthors, also illustrates the scientific value of network concepts. Specifically, using a network perspective, the authors are able to reconcile conflicting patterns of density-dependent and frequency-dependent transmission dynamics. They show that, when comparing across populations, intrapopulation density-dependent transmission on networks can result in apparent frequency-dependent transmission dynamics.

The first five articles in the special issue review past work and present new results in network epidemiology. However, the field is quite young, with many exciting developments

and applications still to come. Thus, we devote the last third of this special issue to future research. The first article in this section, by M. E. Craft and D. Caillaud, argues that network perspectives have been largely limited to human applications and encourages their use in other systems, particularly wildlife populations. The article describes advances in data collection that must come first and touches on the critical need for iterative interplay between theory and data. This iterative interplay is the major focus of our special issue's last article, by R. Rothenberg and E. Costenbader, which tackles the issue of connecting theory and data to advance network epidemiology. The authors end with a directive for our theoretical colleagues to more closely "snuggle to the facts" to ensure that our modeling efforts translate into meaningful and practical insights into the spread of infectious diseases.

Taken together, we hope that these articles give you, the reader, a taste of the past, present, and future of network epidemiology. Most of all, we hope that this issue whets your appetite and stimulates further interest in developing and harnessing network perspectives on infectious disease dynamics.

Acknowledgment

We would like to thank all of the contributors to this special issue, for making it a diverse and interesting set of reviews, research articles, and commentaries. Many thanks are also due to Betsy Foxman, Editor-in-Chief, for the invitation to contribute this special issue and to the Hindawi staff for facilitating the submission, review, and publication of these exciting articles, which we have very much enjoyed reading and hope you will as well.

Lauren Ancel Meyers
Ben Kerr
Katia Koelle

Hindawi Publishing Corporation
Interdisciplinary Perspectives on Infectious Diseases
Volume 2011, Article ID 284909, 28 pages
doi:10.1155/2011/284909

Review Article

Networks and the Epidemiology of Infectious Disease

Leon Danon,[1] Ashley P. Ford,[2] Thomas House,[3] Chris P. Jewell,[2] Matt J. Keeling,[1,3] Gareth O. Roberts,[2] Joshua V. Ross,[4] and Matthew C. Vernon[1]

[1] *School of Life Sciences, University of Warwick, Coventry CV4 7AL, UK*
[2] *Department of Statistics, University of Warwick, Coventry CV4 7AL, UK*
[3] *Warwick Mathematics Institute, University of Warwick, Coventry CV4 7AL, UK*
[4] *School of Mathematical Sciences, University of Adelaide, SA 5005, Australia*

Correspondence should be addressed to Matt J. Keeling, m.j.keeling@warwick.ac.uk

Received 4 June 2010; Accepted 24 December 2010

Academic Editor: Ben Kerr

The science of networks has revolutionised research into the dynamics of interacting elements. It could be argued that epidemiology in particular has embraced the potential of network theory more than any other discipline. Here we review the growing body of research concerning the spread of infectious diseases on networks, focusing on the interplay between network theory and epidemiology. The review is split into four main sections, which examine: the types of network relevant to epidemiology; the multitude of ways these networks can be characterised; the statistical methods that can be applied to infer the epidemiological parameters on a realised network; and finally simulation and analytical methods to determine epidemic dynamics on a given network. Given the breadth of areas covered and the ever-expanding number of publications, a comprehensive review of all work is impossible. Instead, we provide a personalised overview into the areas of network epidemiology that have seen the greatest progress in recent years or have the greatest potential to provide novel insights. As such, considerable importance is placed on analytical approaches and statistical methods which are both rapidly expanding fields. Throughout this review we restrict our attention to epidemiological issues.

1. Introduction

The science of networks has revolutionised research into the dynamics of interacting elements. The associated techniques have had a huge impact in a range of fields, from computer science to neurology, from social science to statistical physics. However, it could be argued that epidemiology has embraced the potential of network theory more than any other discipline. There is an extremely close relationship between epidemiology and network theory that dates back to the mid-1980s [1, 2]. This is because the connections between individuals (or groups of individuals) that allow an infectious disease to propagate naturally define a network, while the network that is generated provides insights into the epidemiological dynamics. In particular, an understanding of the structure of the transmission network allows us to improve predictions of the likely distribution of infection and the early growth of infection (following invasion), as well as allowing the simulation of the full dynamics. However the interplay between networks and epidemiology goes further; because the network defines potential transmission routes, knowledge of its structure can be used as part of disease control. For example, contact tracing aims to identify likely transmission network connections from known infected cases and hence treat or contain their contacts thereby reducing the spread of infection. Contact tracing is a highly effective public health measure as it uses the underlying transmission dynamics to target control efforts and does not rely on a detailed understanding of the etiology of the infection. It is clear, therefore, that the study of networks and how they relate to the propagation of infectious diseases is a vital tool to understanding disease spread and, therefore, informing disease control.

Here, we review the growing body of research concerning the spread of infectious diseases on networks, focusing on the interplay between network theory and epidemiology. The paper is split into four main sections which examine the types of network relevant to epidemiology, the multitude

of ways these networks can be characterised, the statistical methods that can be applied to either infer the likely network structure or the epidemiological parameters on a realised network, and finally simulation and analytical methods to determine epidemic dynamics on a given network. Given the breadth of areas covered and the ever-expanding number of publications (over seven thousand papers have been published concerning infectious diseases and networks) a comprehensive review of all work is impossible. Instead, we provide a personalised overview into the areas of network epidemiology that have seen the greatest progress in recent years or have the greatest potential to provide novel insights. As such considerable importance is placed on analytical approaches and statistical methods which are both rapidly expanding fields. We note that a range of other network-based processes (such as the spread of ideas or panic) can be modelled in a similar manner to the spread of infection; however, in these contexts, the transmission process is far less clear; therefore, throughout this paper, we restrict our attention to epidemiological issues.

2. Networks, Data, and Simulations

There are a wide number of network structures and types that have been utilised when considering the spread of infectious diseases. Here, we consider the most common forms and explain their uses and limitations. Later, we review the implications of these structures for the spread and control of infectious diseases.

2.1. The Ideal Network. We start our examination of network forms by considering the ideal network that would allow us to completely describe the spread of any infectious pathogen. Such a network would be derived from an omniscient knowledge of individual behaviour. We define $G_{i,j}(t)$ to be a time-varying, real, and high-dimensional variable that informs about the strength of all potential transmission routes from individual i to individual j at time t. Any particular infectious disease can then be represented as a function (f_{pathogen}) translating this high-dimensional variable into an instantaneous probabilistic transmission rate (a single real variable). In this ideal, G subsumes all possible transmission networks, from sexual relations to close physical contact, face-to-face conversations, or brief encounters, and quantifies the time-varying strength of this contact. The disease function then picks out (and combines) those elements of G that are relevant for transmission of this pathogen, delivering a new (single-valued) time-varying infection-specific matrix ($T_{i,j}(t) = f_{\text{pathogen}}(G_{i,j}(t))$). This infection-specific matrix then allows us to define the stochastic dynamics of the infection process for a given pathogen. (For even greater generality, we may want to let the pathogen-specific function f also depend on the time since an individual was infected, such that time-varying infectivity or even time-varying transmission routes can be accommodated.)

Obviously, the reality of transmission networks is far from this ideal. Information on the potential transmission routes within a population tends to be limited in a number of aspects. Firstly, it is rare to have information on the entire population; most networks rely on obtaining personal information on participants, and therefore participation is often limited. Secondly, information is generally only recorded on a single transmission route (e.g., face-to-face conversation or sexual partnership) and often this is merely recorded as the presence or absence of a contact rather than attempting to quantify the strength or frequency of the interaction. Finally, data on contact networks are rarely dynamic; what is generally recorded is whether a contact was present during a particular period with little consideration given to how this pattern may change over time. In the light of these departures from the ideal, it is important to consider the specifics of different networks that have been recorded or generated and understand their structure, uses, and limitations.

2.2. Realised Encounter Networks. One of the few examples of where many of the potential transmission routes within a population have been documented comes from the spread of sexually transmitted infections (STIs). In contrast with airborne infections, STIs have very obvious transmission routes—sex acts (or sharing needles during intravenous drug use)—and as such these potential transmission routes should be easily remembered (Figure 1(a)). Generally the methodology replicates that adopted during contact tracing, getting an individual to name all their sexual partners over a given period, these partners are then traced and asked for their partners, and the process is repeated—this is known as *snowball sampling* [4] (Figure 1(b)). A related methodology is *respondent-driven sampling*, where individuals are paid both for their participation and the participation of their contacts while protecting each individual's anonymity [5]. This approach, while suitable for hidden and hard to reach populations, has a number of limitations, both practical and theoretical: recruiting people into the study, getting them to disclose such highly personal information, imperfect recall from participants, the inability to find all partners, and the clustering of contacts. In addition, there is the theoretical issue that this algorithm will only find a single connected component within the population, and it is quite likely that multiple disjoint networks exist [6].

Despite these problems, and motivated by the desire to better understand the spread of HIV and other STIs, several pioneering studies were performed. Probably the earliest is discussed by Klovdahl [1] and utilises data collected by the Center for Disease Control from 19 patients in California suffering from AIDS, leading to a network of 40 individuals. Other larger-scale studies have been performed in Winnipeg, Manitoba, Canada [7] and Colorado Springs, Colorado, USA [8]. In both of these studies, participants were tested for STIs, and the distribution of infection compared to the underlying network structure. Work done on both of these networks has generally focused on network properties and the degree to which these can explain the observed cases; no attempt was made to use these networks predictively in simulations. In addition, in the Colorado Springs study,

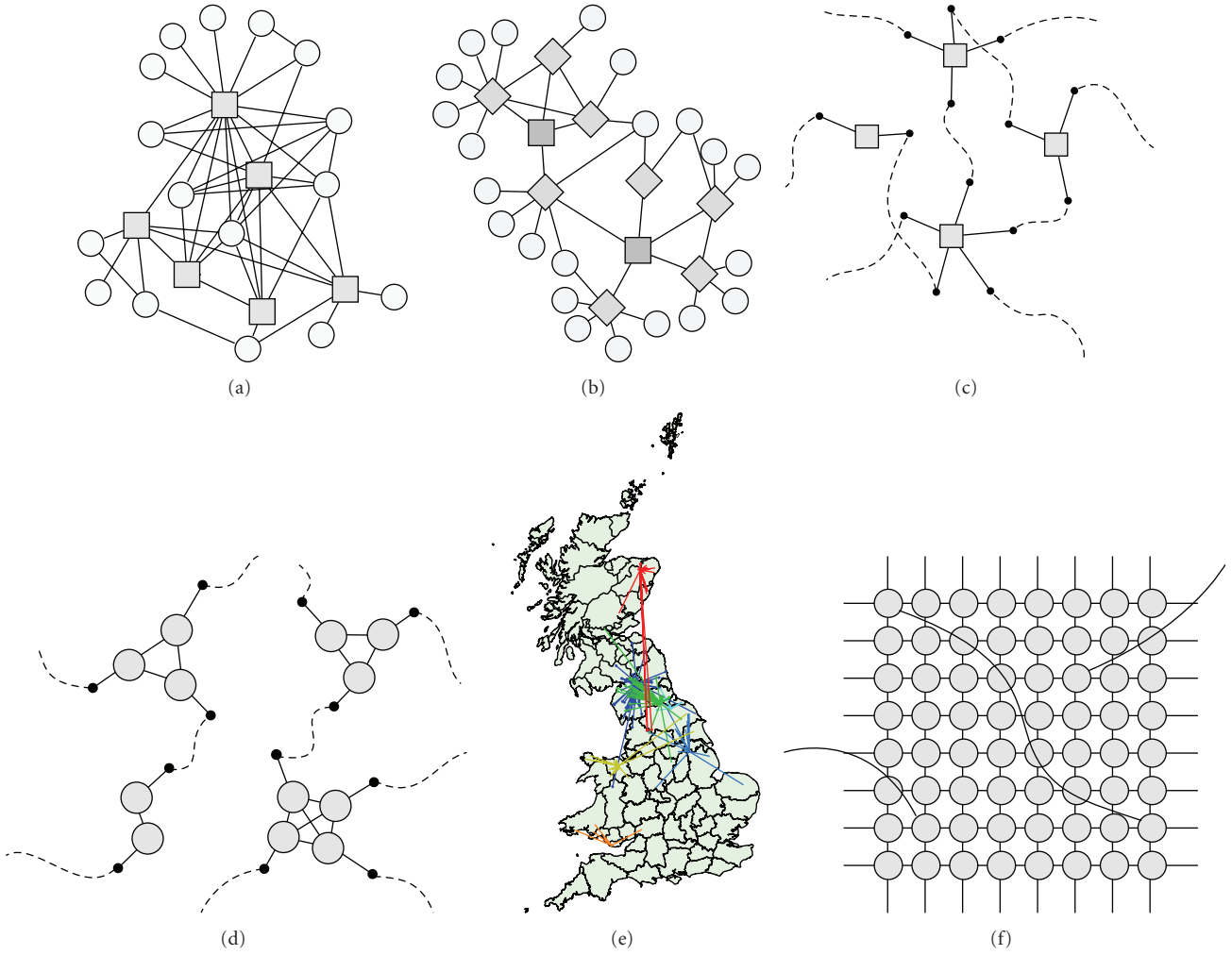

Figure 1: Examples of networks used in epidemiology. (a) Contacts between 22 intravenous drug users, as recorded in [3]; squares refer to primary contacts. Given that the identity of contacts is known, they can be interlinked. (b) Caricature of a snowball sampling algorithm, squares are primary contacts, diamonds are secondary, and circles are tertiary contacts. Given that the identity of contacts is known they can be linked. (c) Example of a configuration model network. Each individual has a prescribed degree distribution, which gives rise to "half-links" that are connected at random. (d) A household configuration network, consisting of completely interconnected households (cliques) with each individual also having one random link to another household. (e) Map showing Great Britain, together with the movements of cattle from six farms (each represented in a separate colour). Notice the heterogeneity between farms and the generally localised nature of movements. (f) Example of a small-world model based on a 2D lattice with nearest neighbor connections. The small-world property is given by the presence of rare random links that can connect distant parts of the network.

tracing was generally only performed for a single iteration although many initial participants in high-risk groups were enrolled, while in the Manitoba study, tracing was performed as part of the routine information gathered by public health nurses. Therefore, while both provide a vast amount of information on sexual contacts, it is not clear if the results are truly a comprehensive picture of the network and sampling biases may corrupt the resulting network [9]. In addition, compared to the ideal network, these sexual contact networks lack any form of temporal information; instead, they provide an integration of the network over a fixed time period and generally lack information on the potential strength of a contact between individuals. Despite these difficulties, they continue to provide an invaluable source of information on human sexual networks and the potential transmission routes of STIs. In particular, they point to the extreme levels of heterogeneity in the number of sexual contacts over a given period—and the variance in the number of contacts has been shown to play a significant role in early transmission dynamics [10].

One of the few early examples of the simulation of disease transmission on an observed network comes from a study of a small network of 22 injection drug users and their sexual partners [3] (Figure 1(a)). In this work, the risk of transmission between two individuals in the network was imputed based on the frequency and types of risk behaviour connecting those two individuals. HIV transmission was modelled using a monthly time step and single index case,

and simulations were run for varying lengths of (simulated) time. This enabled a node's position in the network (as characterised by a variety of measures) to be compared with how frequently it was infected during simulations, and how many other nodes it was typically responsible for infecting.

A different approach to gathering social network and behavioural data was initiated by the Human Dynamics group at MIT and illustrates how modern technology can assist in the process of determining transmission networks. One of the first approaches was to take advantage of the fact that most people carry mobile phones [11]. In 2004, 100 Nokia 6600 smart-phones preinstalled with software were given to MIT students to use over the course of the 2004-2005 academic year. Amongst other things, data were collected using Bluetooth to sense other mobile phones in the vicinity. These data gave a highly detailed account of individuals behaviour and contact patterns. However, a limitation of this work was that Bluetooth has a range of up to 25 meters, and as such networks inferred from these data may not be epidemiological meaningful.

A more recent study into the encounters between wild Tasmanian devils in the Narawntapu National Park in northern Tasmania utilised a similar technological approach [12]. In this work, 46 Tasmanian devils were fitted with proximity loggers that could detect and record the presence of other loggers within a 30 cm range. As such, these loggers were able to provide detailed temporal information on the potential interaction between these 46 animals. This study was initiated to understand the spread of Tasmanian devil facial tumour disease, which causes usually fatal tumours that can be transmitted between devils if they fight and bite each other. Although only 27 loggers with complete data were recovered, and although the methodology only recorded interaction between the 46 devils in the study, the results were highly informative (generating a network that was far from random, heterogeneous, and of detailed temporal resolution). Analyses based on the structure of this network suggested that targeted measures, that focus on the most highly connected ages or sex, were unlikely to curtail the spread of this infection. Of perhaps greater relevance is the potential this method illustrates for determining the contact networks of other species (including humans)—the only limitation being the deployment of a suitable number of proximity loggers.

2.3. Inferred Encounter Networks. Given the huge logistical difficulties of capturing the full network of interactions between individuals within a population, a variety of methods have been developed to generate synthetic networks from known attributes. Generally, such methods fall into two classes: those that utilise egocentric information and those that attempt to simulate the behaviour of individuals.

Egocentric data generally consists of information on a number of individuals (the egos) and their contacts (the alters). As such the information gathered is very similar to that collected in the sexual contact network studies in Manitoba and Colorado Springs, but with only the initial step of the snowball sampling was performed; the difference is that for the majority of egocentric data the identity of partners (alters) is unknown and therefore connections between egos cannot be inferred (Figure 1(c)). The data, therefore exists as multiple independent "stars" linking the egos to the alters, which in itself provides valuable information on heterogeneities within the network. Two major studies have attempted to gather such egocentric information: the NATSAL studies of sexual contacts in the UK [13–16], and the POLYMOD study of social interactions within 8 European countries [17]. The key to generating a network from such data is to probabilistically assign each alter a set of contacts drawn from the information available from egos; in essence, using the ego data to perform the next step in the snowball sampling algorithm. The simplest way to do this is to generate multiple copies of all the egos and to consider the contacts from each ego to be "half-links"; the half-links within the network can then be connected at random generating a configuration network [18–20]; if more information is available on the status (age, gender, etc.) of the egos and alters then this can also be included and will reduce the set of half-links that can be joined together. However, in the vast majority of modelling studies, the egocentric data have simply been used to construct WAIFW (who-acquires-infection-from-whom) matrices [15, 17, 21] that inform about the relative levels of transmission between different groups (e.g., based on sexual activity or age) but neglect the implicit network properties. This matrix-based approach is often reliable: for STIs it is the extreme heterogeneity in the number of contacts (which are close to being power-law or scale-free distributed; see Section 3.2) that drives the infection dynamics [22] although larger-scale structure does play a role [23]; for social interactions, it is the assortativity between (age-) groups that controls the behaviour, with the number of contacts being distributed as a negative binomial [17]. The POLYMOD matrices have therefore been extensively used in the study of the H1N1 pandemic in 2009, providing important information about the cost-effective vaccination of different age-classes [21, 24].

The general configuration model approach of randomly linking together "half-links" from each ego [18, 19] has been adopted and modified to consider the spread of STIs. In particular, simulations have been used to consider the importance of concurrency in sexual networks [25, 26], where concurrency is defined as being in two active sexual partnerships at the same time. A dynamic sexual network was simulated, with partnerships being broken and reformed such that the network density remained constant over time. The likelihood of two nodes forming a partnership depended on their degree, but this relationship could be tuned to make concurrency more or less common and to make the mixing assortative or disassortative based on the degrees of the two nodes. Transmission of an STI (such as gonorrhoea and chlamydia [25] or HIV [26]) was then simulated upon this dynamic network, showing that increasing concurrency substantially increased the growth rate during the early phase of an epidemic (and, therefore, its size after a given period of time). This greater growth rate was related to the increase in giant component size (see Section 3.1) that was caused by increased concurrency.

A slightly more general approach to the generation of model sexual networks was employed by Ghani et al. [27]. In their network model, individuals had a preferred number of concurrent partners and duration of partnerships, and their level of assortativity was tunable. A gonorrhoea-like infection was simulated on the resulting dynamic network. Regression models were used to consider the association between network structures (either snapshots of the state of the network at the end of simulation or accumulated over the last 90 days of simulation) and prevalence of infection. These simulations showed that increasing levels of concurrent partnerships made invasion of the network more likely and also that the mixing patterns of the most sexually active nodes were most important in determining the final prevalence of infection within the population [27]. The same model was later used to consider the importance of different structural measures and sampling strategies, showing that it was important to endeavour to identify infected individuals with a high number of sexual partners in order to correctly define the high-risk group for interventions [23].

The alternative approach of simulating the behaviour of individuals is obviously highly complex and fraught with a great deal of uncertainty. Despite these problems, three groups have attempted just such an approach: Longini's group at Emory [28–31], Ferguson's group at Imperial [32, 33], and Eubank's group at Los Alamos/Virginia Tech [34, 35]. The models of both Longini and Ferguson are primarily agent-based models, where individuals are assigned a home and work location within which they have frequent infection-relevant contacts together with more random transmission in their local neighbourhood. The Longini models separate the entire population into subunits of 2000 individuals (for the USA) or 13000 individuals (for South-East Asia) who constitute the local population where random transmission can operate; in contrast, the Ferguson models assign each individual a spatial location and random transmission occurs via a spatial kernel. In principle, both of these models could be used to generate an explicit network model of possible contacts. The Eubank model is also agent-based aiming to capture the movements of 1.5 million people in Portland, Oregon, USA; but these movements are then used to define a network based on whether two individuals occur in the same place (there are 180 thousand places represented in the model) at the same time. It is this network that is then used to simulate the spread of infection. While in principle this Eubank model could be used to define a temporally varying and real-valued network (where the strength of connection would be related to the type of mixing in a location and the number of people in the location); in the epidemiological publications [35], the network is considered as a static contact network in which extreme heterogeneity in numbers of contacts is again predicted, and the network has "small world" like properties (see below). A similar approach of generating artificial networks of individuals for stochastic simulations of respiratory disease has been recently applied to influenza at the scale of the United States, and the software made generally available [36]. This software took a more realistic dynamic network approach and incorporated flight data within the United States, but was sufficiently resource-intensive to require specialist computing facilities (a single simulation taking around 192 hours of CPU time). All three models have been used to consider optimal control strategies, determining the best deployment of resources in terms of limiting transmission associated with different routes. The predicted success of various control strategies, therefore, critically depends on the strength of contacts within home, at work, within social groups, and that occuring at random.

Whilst smallpox has been eradicated, concern remains about the possibility of a deliberate release of the disease. The stochastic simulation models of the Longini group have predominantly focused on methods of controlling this infection [28, 31]. Their early work utilised networks of two thousand people with realistic age, household size, and school attendance distributions, with the likelihood of each individual becoming infected being derived from the number and type of contacts with infectious individuals [28]. This paper focused on the use of vaccination to contain a small-scale outbreak of smallpox and concluded that early mass-vaccination of the entire population was more effective than targeted vaccination if there was little or no immunity in the population. Later models [31] combined these subnetworks of two thousand people into a larger network of fifty thousand people (with one hospital), and the adult population were able to contact each other through workplaces and high schools. Here, the focus was on surveillance and containment which were generally concluded to be sufficient to control an outbreak. The epidemiological work of the Eubank group has also focused on a release of smallpox although these simulations showed that encouraging people to stay at home as soon as they began to feel unwell was more important than choice of vaccination protocol [35]; this may in part be attributed to the scale-free structure of the network and hence the superspreading nature of some individuals.

The Ferguson models have primarily been used to consider the spread and control of pandemic influenza, examining its potential spread from an initial source in South-East Asia [32] and its spread in mainland USA and Great Britain [33]. The models of South-East Asia were primarily based on Thailand, and included demographic information and satellite-based spatial measures of population density. It focused on containment by the targeted use of antiviral drugs and suggested that as long as the reproductive ratio (R_0) of a novel strain was below 1.8, it could be contained by the rapid use of targeted antivirals and social distancing. However, such a strategy could require a stockpile of around 3 million antiviral doses. The models based on the USA and Great Britain, considered a wider range of control measures, including school closures, household prophylaxis using antiviral drugs, and vaccination, and predicted the likely impact of different policies.

2.4. Movement Networks. An alternative source of network information comes from the recorded movements of individuals. Such data frequently describe a relatively large network as information on movements is often collected by national or international bodies. The network of movements,

therefore, has nodes representing locations (rather than individuals) and edges weighted to capture the number of movements from one location to another—as such the network is rarely symmetric. Four main forms of movement network have played important roles in understanding the spread of infectious diseases: the airline transportation network [37, 38], the movement of individuals to and from work [39, 40], the movement of dollar bills (from which the movement of people can be inferred) [41], and the movement of livestock (especially cattle) [30, 42]. While the structure of these networks has been analysed in some detail, to develop an epidemiological model requires a fundamental assumption about how the epidemic progresses within each locations. All the examples considered in this section make the simplifying assumption that the epidemic dynamics within each location are defined by random (mean-field) interactions, with the network only informing about the flow of individuals or just simply the flow of infection between populations—such a formulation is known as a metapopulation model [43].

Probably the earliest work using detailed movement data to drive simulations comes from the spread of 1918 pandemic influenza in the Canadian Subarctic, based on records kept by the Hudson's Bay Company [44]. A conventional SIR metapopulation model was combined with a network model (the nodes being three fur trading posts in the region: God's Lake, Norway House, and Oxford House), where some individuals remained in their home locations whilst others moved between locations, based on records of arrivals and departures recorded in the post journals. Whilst this model described only a small population, it was able to be parameterised in considerable detail due to the quality of demographic and historical data available and showed that the movement patterns observed interacted with the starting location of a simulated epidemic to change the relative timings of the epidemics in the three communities, but not the overall impact of the disease.

The movement of passenger aircraft as collated by the International Air Transport Association (IATA) provides very useful information about the long-distance movement of individuals and hence how rapidly infection is likely to travel around the globe [37, 45, 46]. Unlike many other network models which are stochastic individual-level simulations, the work of Hufnagel et al. [37] and Colizza et al. [45] was based on stochastic Langevin equations (effectively differential equations with noise included). The early work by Hufnagel et al. [37] focused on the spread of SARS and showed a remarkable degree of similarity between predictions and the global spread of this disease. This work also showed that extreme sensitivity to initial conditions arises from the structure of the network, with outbreaks starting in different locations generating very different spatial distributions of infection. The work of Colizza was more focused towards the spread of H5N1 pandemic influenza arising in South-East Asia and its potential containment using antiviral drugs. However, it was H1N1 influenza from Mexico that initiated the 2009 pandemic, but again, the IATA flight data provided a useful prediction of the early spread [47, 48]. While such global movement networks are obviously highly important in understanding the early spread of pathogens, they unfortunately neglect more localised movements [49] and individual-level transmission networks. However, recent work has aimed to overcome this first issue by including other forms of local movement between populations [40, 50]. This work has again focused on the spread of influenza, mixing long-distance air travel with shorter range commuter movements and with the model predictions by Viboud et al. [40] showing good agreement with the observed patterns of seasonal influenza. An alternative form of movement network has been inferred from the "Where's George" study of the circulation of dollar bills in the USA [38]; this provided far more information about short-range movements, but again did not really inform about the interaction of individuals.

A wide variety (and in practice the vast majority) of movements are not made by aircraft but are regular commuter movements to and from work. The network of such movements has also been studied in some detail for both the UK and USA [39, 40, 51]. The approaches adopted parallel the work done using the network of passenger aircraft, but operate at a much smaller scale, and again, influenza and smallpox have been the considered pathogens. As with the aircraft network certain locations act as major hubs attracting lots of commuters every day; however, unlike the aircraft network, there is the tendency for the network to have a strong daily signature with commuters moving to work during the day but travelling home again in the evening [52]. As such the commuter network can be thought of as heterogeneous, locally clustered, temporal, and with each contact having different strengths (according to the number of commuters making each journey); however, to provide a complete description of population movement, and hence disease transmission requires other causes of movement to be included [51] and requires strong assumptions to be made about individual-level interactions. The key question that can be readily addressed from these commuter-movement models is whether a localised outbreak can be contained within a region or whether it is likely to spread to other nodes on the network [39].

Undoubtedly, one of the largest and most comprehensive data sets of movements between locations comes from the livestock tracing schemes run in Great Britain and being adopted in other European countries. The Cattle Tracing Scheme in particular is spectacularly detailed, containing information of the movements of all cattle between farms in Great Britain; as such, this scheme generates daily networks of contacts between over 30,000 working farms in Great Britain [42, 53–56] (Figure 1(f)). Similar data also exist for the movement of batches of sheep and pigs [57] although here the identity of individual animals making each movement is not recorded. This data source has several key advantages over other movement networks: it is dynamic, in that movements are recorded daily; the movement of livestock is one of the major mechanisms by which many infections are transferred between farms, and the metapopulation assumption that cattle mix homogeneously within a farm is highly plausible. In principle, the information in the Cattle Tracing Scheme can be used to form an even more

comprehensive network, treating each cow as a node and creating an edge if two cows occur within the same farm on the same day—this would generate an individual-level network for each day which can then be used to simulate the spread of infection [52].

The early spread of foot and mouth disease (FMD) in 2001 was primarily due to livestock movements, particularly of sheep [58]. Motivated by this epidemic, Kiss et al. [57] conducted short simulated outbreaks of FMD on both the sheep movement network based on 4 weeks' movements starting on 8 September 2004 and simulated synthetic networks with the same degree distribution. Due to the short time-scales considered (the aim being to model spread of FMD before it had been detected), nodes were susceptible, exposed or infected but never recovered, and network connections remained static. Simulated epidemics were smaller on the sheep movement network than the random networks, most likely due to disassortative mixing in the sheep movement network. Similarly, Natale et al. [59] employed a static network simulation of Italian cattle farms. Here, farms were not merely represented as nodes, but a deterministic SI system of ODEs was used to model infection on each node essentially generating a metapopulation model. The only stochastic part of the model was the number of infectious individuals moved between connected farms in each time step. This simulation model highlighted the impact of the centrality of seed nodes (measured in several different ways) upon the subsequent epidemics' course.

The use of static networks to model the very dynamic movement of livestock is questionable. Expanding on earlier work, Green et al. [53] simulated the early spread of FMD through movement of cattle, sheep, and pigs. Here, the livestock network was treated dynamically, with infection only able to propagate along edges on the day when that edge occurred; additional to this network spread, local transmission could also occur. These simulations enabled regional patterns of risk to a new FMD incursion to be assessed, as well as identifying markets as suitable targets for enhanced surveillance. Vernon and Keeling [55] considered the relationship between epidemics predicted from dynamic cattle networks and their static counterparts in more detail. They compared different network representations of cattle movement in the UK in 2004, simulating epidemics across a range of infectivity and infectious period parameters on the different network representations. They concluded that network representations other than the fully dynamic one (where the movement network changes every day) fail to reproduce the dynamics of simulated epidemics on the fully dynamic network.

2.5. Contact Tracing Networks. Contact tracing and hence the networks generated by this method can take two distinct forms. The first is when contact-tracing is used to initiate proactive control. This is often the case for STIs, where identified cases are asked about their recent sexual partners, and these individuals are traced and tested; if found to be infected, then contact tracing is repeated for these secondary cases. Such a process is related to the snowball sampling that was discussed earlier, with the notable exception that tracing is only performed from known cases. Similar contact-tracing may operate for the early stages of an airborne epidemic (as was seen for the 2009 H1N1 pandemic), but here, the tracing is not generally iterative as contacts are generally traced and treated so rapidly that they are unlikely to have generated secondary cases. An alternative form of contact-tracing is when a transmission pathway is sought between all identified cases [1, 60, 61]. This form of contact tracing is likely to become of ever-increasing importance in the future when improved molecular techniques and statistical inference allow infection trees to be determined from genetic differences between samples of the infecting pathogen [62].

These forms of network have two main advantages but one major disadvantage. The network is often accompanied by test results for the individuals within the network, as such we not only have information on the contact process but also on the resultant transmission of infection. In addition, when contact tracing is only performed to define an infection tree, there is the added advantage that the infection process itself defines the network of contacts, and hence there is no need for human interpretation of which forms of contact may be relevant. Unfortunately, the reliance on the infection process to drive the tracing means that the network only reflects one realisation of the epidemic process and, therefore, may ignore contacts that are of potential importance and would be needed if the epidemic was to be simulated; therefore, while they can inform about past outbreaks, they have little predictive power.

2.6. Surrogate Networks. Obtaining large-scale and reliable information on who contacts whom is obviously very difficult; therefore, there is a temptation to rely on alternative data sets, where network information can be extracted far more easily, and where the data is already collected. As such the movement networks and contact tracing networks discussed above are examples of such surrogate networks although their connection to the physical processes of infection transmission are far more clear. Other examples of networks abound [22, 63–65]; while these are not directly relevant for the spread of infection, they do provide insights into how networks form and grow—structures that are commonly seen in surrogate networks are likely to arise in the types of network associated with disease transmission. One source of network information that would be fantastically rich and also highly informative (if not immediately relevant) is the network of friendships and contacts on social networking sites (such as Facebook); some sites have made data on their social networks available, and these data have been used to examine a range of sociological questions about online interactions [66].

2.7. Theoretical Constructs. Given the huge complexity involved in obtaining large-scale and reliable data on real-transmission networks many researchers have instead relied on theoretically constructed networks. These networks are usually highly simplified but aim to capture some of

the known (or postulated) features of real-transmission networks—often the simplifications are so extreme that some analytical traction can be gained. Here, we briefly outline some of the commonly used theoretical networks and identify which features they capture; some of the results of how infection spreads on such networks are discussed more fully in Section 4.2.

2.7.1. Configuration Networks. One of the simplest forms of network is to allow each individual to have a set of contacts that it wishes to make (in more formal language each node has a set of half-links), these contacts are then made at random with other individuals based on the number of contacts that they wish to make (half-links are randomly connected) [19]. This obviously creates a network of contacts (Figure 1(c)). The advantage of these configuration networks is that because they are formed from many randomly connected individuals, there are no short loops within the network and a range of theoretical results can be proved ranging from conditions for invasion [18, 67, 68] to descriptions of the temporal dynamics [69]. Unfortunately, the elements that make these networks amenable to theoretical analysis—the lack of assortativity, short loops or clustering—are precisely factors that are thought to be important features of real networks.

An alternative formulation that offers a compromise between tractability and realism occurs when individuals that exist in fully interconnected cliques have randomly assigned links within the entire population [69, 70] (Figure 1(d)). As such, these networks mimic the strong interactions within families and the weaker contacts between them. While such models offer a significant improvement over configuration networks and capture the known importance of the household in transmission, they make no allowance for clustering between households due to spatial proximity. Hierarchical metapopulation models [71] allow for this form of additional structure, where households (or other groupings) are themselves grouped in an ascending hierarchy of clustering.

2.7.2. Lattices and Small Worlds. Both lattice networks and small world networks begin with the same formulation: individuals are regularly spaced on a grid (usually in just one or two dimensions), and each individual is connected to their k nearest neighbours—these connections define a lattice. The advantage of such networks is that they retain many elements of the initial spatial arrangement of points, and hence contain both many short loops as well as the property that infection tends to spread locally. There is a clear link between such lattice-based networks and the field of probabilistic cellular automata [72, 73]. The fundamental difficulty with such lattice models is that the presence of short loops and localised spread means that is it difficult (if not impossible) to prove exact results, and hence large-scale multiple simulations are required.

Small world networks improve upon the rigid structure of the lattice by allowing a low number of random contacts across the entire space (Figure 1(e)). Such long range contacts allow infection to spread rapidly though the population and vastly reduce the shortest path length between individuals [74]—this is popularly known as six degrees of separation from the concept that any two individuals on the planet are linked through at most six friends or contacts [75]. Therefore, small world networks offer a step towards reality, capturing the local nature of transmission and the potential for long-range contacts [76, 77]; however, they suffer from neglecting heterogeneity in the number of contacts and the tight clustering of contacts within households or social settings.

2.7.3. Spatial Networks. Spatial networks, as the name suggests, are generated using the spatial location of all individuals in the population, as such lattices and small worlds are a particular form of spatial network. The general methodology initially positions each individual i at a specific location $\underline{x}_i$, usually; these locations are chosen at random, but clustered spatial distributions have also been used [78]. Two individuals (say i and j) are then probabilistically connected based upon the distance between them; the probability is given by a connection kernel which usually decays with distance such that connections are predominantly localised. These spatial networks (especially when the underlying distribution of points is clustered) have many features that we expect from disease networks although it is unclear if such simple formulations can be truly representative.

2.7.4. Exponential Random Graphs. In recent years, there has been growing interest in exponential random graph models (ERGMs) for social networks, also called the p^* class of models. ERGMs were first introduced in the early 1980s by Holland and Leinhardt [79] based on the work of Besag [80]. More recently, Frank and Strauss studied a subset of those that have the simple property that the probability of connection between two nodes is independent of the connection between any other pair of distinct nodes. [81]. This allows the likelihood of any nodes being connected to be calculated conditional on the graph having certain network properties. Techniques such as Markov Chain Monte Carlo can then be used to create a range of plausible networks that agree with a wide variety of information collected on network structures even if the complete network is unknown [82, 83]. Due to their simplicity, ERGMs are widely used by statisticians and social network analysts [84]. Despite significant advances in recent years (e.g., [85]), ERGMs still suffer from problems of degeneracy and computational intractability for large network sizes, which has limited their use in epidemic modelling.

2.8. Expected Network Properties. Here, we have shown that a wide variety of network structures have been measured or synthesised to understand the spread of infectious diseases. Clearly, with such a range of networks, no clear consensus can be drawn on the types of underlying network structures that are generally present; in part, this is because different studies have focused on different infectious diseases and different diseases require different transmission routes.

However, three factors emerge that are key components of epidemiological networks: heterogeneity in the number of contacts such that some individuals are at a higher risk of both catching and transmitting infection, clustering of contacts such that groups of individuals are often highly interconnected, and some reflection of spatial separation such that contacts usually form locally, but occasional long-range connections do occur.

Three fundamental problems still exist in the study of networks. Firstly, are there relatively low-dimensional ways of capturing key aspects of a network's structure? What constitutes a key aspect will vary with the problem being studied, but for epidemiological applications, it should be hoped that a universal set of network characteristics may emerge. There is then the task of assessing reasonable and realistic ranges for these key variables based on values computed for known transmission networks—unfortunately very few transmission networks have been recorded in any degree of detail although modern electronic devices may simplify the process in the future. Secondly, there is the related statistical problem of inferring plausible complete networks from the partial information collected by methods such as contact tracing. This is equivalent to seeking an underlying model for the network connections that is consistent with the known partial information, and hence, has strong resonance with the more mechanistically motivated models in Section 2.3. Even when the network is fully realised (and an epidemic observed), there is considerable statistical difficulty in attributing risk to particular contact types. Finally, there are the key questions of predicting the dynamics of infection on any given network—and while for many complex networks, direct simulation is the only approach, for other simplified networks some analytical traction can be achieved, which helps to provide more generic insights into which elements of network structure are most important. These three key areas are discussed below.

3. Network Properties

Real networks can exhibit staggering levels of complexity. The challenge faced by researchers is to try and make sense of these structures and reduce the complexity in a meaningful way. In order to make any sense of the complexities present, researchers over several decades have defined a large variety of measurable properties that can be used to characterise certain key aspects [63, 65, 86]. Here, we describe the definitions of the most important characterisations of complex networks (in our view), and outline their impact on disease transmission models.

3.1. Components. In general, networks are not necessarily connected; in other words, all parts of the network are not reachable from all others. The component to which a node belongs is that set of nodes that can be reached from it by paths running along edges of the network. A network is said to have a *giant* component if a single component contains the majority of nodes in the network. In directed networks (one in which each edge has an associated direction), a node has both an in-component from which the node can be reached and an out-component that can be reached from that node. A strongly connected component (SCC) is the set of nodes in the network in which each node is reachable from every other node in the component.

The concept of a giant component is central when considering disease propagation in networks. The extent of the epidemic is necessarily limited to the number of nodes in the component that it begins in, since there are no paths to nodes in other components. In directed networks, in the case of a single initial infected individual, only the out-component of that node is at risk from infection. More generally, the strongly connected component contains those nodes that can be reached from each other. Members of the strongly connected component are most at risk from infection imported at a random node, since a single introduction of infection will be able to reach all nodes in the component.

3.2. Degrees, Distributions, and Correlations. The *degree* is defined as the *number of neighbours* that a node has and is most often denoted as k. In directed graphs, the degree has two components, the number of incoming edges k^{in}, (in-degree), and the number of outgoing edges k^{out}, (out-degree). The degree distribution is defined as the set of probabilities, $P(k)$, that a node chosen at random will have degree k. Plotting the distribution of degrees of nodes is one of the most basic and important ways of characterising a given network (Figure 2). In addition, useful characterisations are obtained by calculating the moments of the degree distribution. The nth moment of $P(k)$ is defined as

$$\langle k^n \rangle = \sum_k k^n P(k), \tag{1}$$

with the first moment, $\langle k \rangle$, being the average degree, the second, $\langle k^2 \rangle$ allowing us to calculate the variance $\langle k^2 \rangle - \langle k \rangle^2$, and so on.

The degree distribution is one of the most important ways of characterising a network as it naturally captures the heterogeneity in individuals' potential to become infected as well as cause further infection. Intuitively, the higher the number of edges a node has, the more likely it is to be a neighbour of an already infected node. Also, the more neighbours a node has, the more likely it is to cause a large number of onward cases. Thus, knowing the form of $P(k)$ is crucial for the understanding of the spread of disease. In random networks of the type studied by Erdös and Rényi, $P(k)$ follows a binomial distribution, which is effectively Poisson in the case of large networks. Most real social networks have distributions that are significantly different from the random case.

For the extreme case of $P(k)$ following an unbounded power law and assuming equal transmission across all edges, Pastor-Satorras and Vespignani [87] showed that the classic result of the epidemic threshold from mean field theory [10] breaks down. In real-transmission networks, the distribution of degree is often heavily skewed, and occasionally follows a power law [22], but is always bounded, leading to

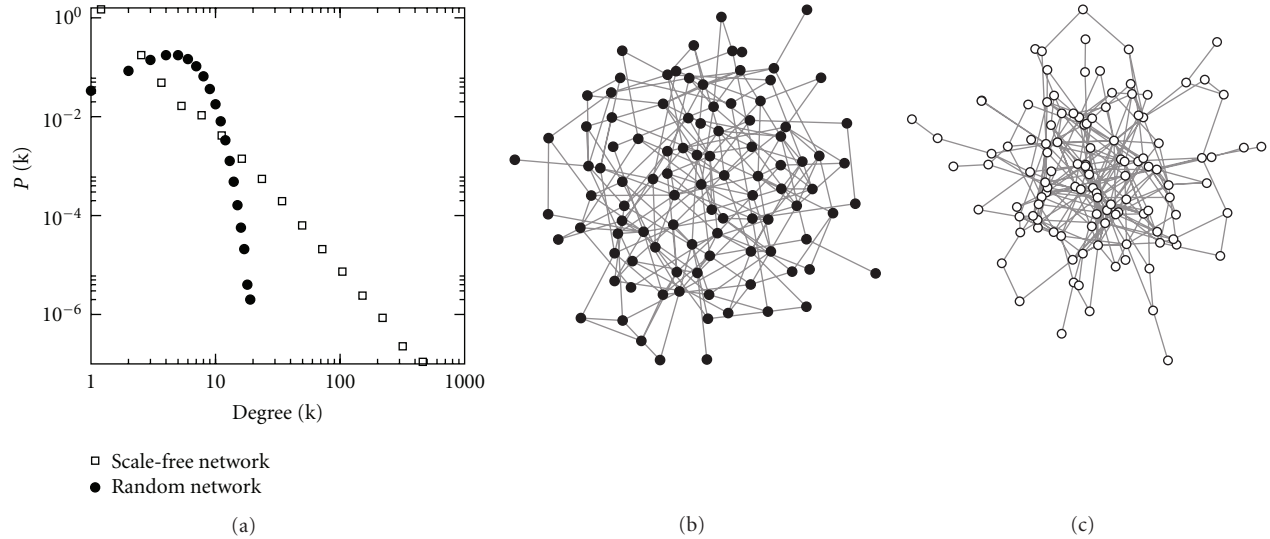

Figure 2: Comparison of random and scale-free networks. (a) Degree distributions for two classes of networks: scale free and random networks. (b) Example random network with 100 nodes and 300 links. All nodes have similar numbers of links. (c) Example scale-free network with 100 nodes and 300 links. Most nodes have few links, with a few nodes having many links.

the recovery of epidemic threshold, but one which is much lower than expected in evenly mixed populations [88].

The degree distribution provides very useful information on uncorrelated networks such as those produced by configuration models. However, real networks are in general correlated with respect to degree; that is, the probability of finding a node with given degree, k, is dependent on the degree of the neighbours of that node, k', which is captured by the conditional probability $P(k' \mid k)$. To characterise this behaviour, several measurements have been proposed. The most straightforward, and probably most useful measure, is to consider the average degree of the neighbours of a node

$$k_{nn,i} = \frac{1}{k_i} \sum_{j \in \mathrm{Nbrs}_i} k_j, \tag{2}$$

where the sum of degrees is made over the neighbours (Nbrs) of i. One can then calculate the average of k_{nn} over all nodes with degree k which is a direct measure of the conditional probability $P(k' \mid k)$, since

$$k_{nn}(k) = \sum_{k'} k' P(k' \mid k). \tag{3}$$

When $k_{nn}(k)$ increases with k, the network is said to be assortative on the degree; that is, high-degree nodes have a tendency to link to other high degree nodes, a behaviour often observed in social networks. Other types of networks, such as the internet at router level, show the converse behaviour; that is, nodes of high degree tend to link to nodes with low degree [63, 89].

Characterising degree correlations is important for understanding disease spread. The classic example is the existence of strong correlations in sexual networks which were shown to be a key factor in understanding HIV spread [90]. More recently, mean field solutions of the SIS model on networks have shown that both the speed and extent of an epidemic are dependent on the correlation pattern of the substrate network [91, 92].

3.3. Distances. In a network, the *shortest path* between two nodes i and j, is the path requiring the smallest number of steps to reach j from i, following edges in the network. There may be (and often there is) more than one shortest path between a pair of nodes. The distance between any pair of nodes $d_{i,j}$ is the minimal number of steps required to reach j from i, that is, the number of steps in the shortest path. The average distance, $\langle d \rangle$ is the mean of the distances between all pairs of nodes and measures the typical distance between nodes

$$\langle d \rangle = \frac{1}{N(N+1)} \sum_{i \neq j} d_{i,j}, \tag{4}$$

where N is the number of nodes in the network. The diameter of the network is defined as the maximum shortest path distance between a pair of nodes in the network, $\max(d_{i,j})$, which measures the most extreme separation of any two nodes in the network.

Characterising networks in terms of the number of steps needed to reach any node from any other is also important. Real networks frequently display the small-world property; that is, the vast majority of nodes are reachable in a small number of steps. This has clear implications for disease spread and its control. Percolation approaches have shown that the effects of the small-world phenomenon can be profound [93]. If it only takes a short number of steps to reach everyone in the population, diseases are able to spread much more rapidly.

The notion of shortest distance through a network can be used to quantify how central a given node is in the network. Many measures have been used [94], but the most relevant of

these is *betweenness* centrality. Betweenness captures the idea that the more shortest paths pass through a node, the more central it is in the network. So, betweenness is simply defined as the *proportion* of shortest paths that pass through a single node

$$B_i = \frac{\#\text{ shortest paths through } i}{N(N-1)}, \tag{5}$$

where N is the number of nodes in the network and the denominator quantifies the total number of shortest paths in the network. In terms of disease spread, identifying those nodes with high betweenness will be important. Central nodes are likely to become infected early on in the epidemic, and are also key targets for intervention [3].

3.4. Clustering. An important example of an observable property of any network is the *clustering coefficient*, ϕ, a measure of the *local density* of a graph. In social network terms, this quantifies the likelihood that the friend of your friend is also your friend. It is defined as the probability that two neighbours of a node will also be neighbours of each other and can be expressed as follows:

$$\phi = \frac{3 \times \#\text{ of triangles in the network}}{\#\text{ of connected triples}}, \tag{6}$$

where a *connected triple* means a single node with edges to a pair of others. ϕ measures the fraction of triples that also form part of a triangle. The factor of three accounts for the fact that each triangle is found in three triples and guarantees that $0 \leq \phi \leq 1$ (and its inclusion depends on the way that triangles in the network are counted).

Locally, the clustering coefficient for each node, i, can be defined as the fraction of triangles formed through the immediate neighbours of i [74]

$$\phi_i = \frac{\#\text{ triangles centered on } i}{\#\text{ triples centered on } i}. \tag{7}$$

The clustering property of networks is essential to the understanding of transmission processes. In clustered networks, rapid local depletion of susceptible individuals plays a hugely important role in the dynamics of spread [95, 96]; for a more analytic treatment of this, see Section 4.2 below.

3.5. Subgraphs. Degree and clustering characterise some aspects of network structure at an individual level. Considering distances between nodes provides information about the global organisation of the network. Intermediate scales are also present, and characterising these can help in our understanding of network structure and therefore the dynamics of spread.

At the simplest level, networks can be thought of being comprised of a collection of subgraphs. The simplest subgraph, the *clique*, is defined as a group of more than two nodes where all the nodes are connected to each other by means of edges in both directions. In other words, a clique is a fully connected subgraph, with the smallest example being a triangle. This is a strong definition and one which is only fulfilled in a limited number of cases, most notably households (see Figure 1(d), Section 4.2 and House and Keeling [70]). *n-cliques* relax the above constraint while retaining its basic premise. The shortest path between all the nodes in a clique is one. Allowing this distance to take higher values, one arrives at the definition of *n-cliques*, which are defined as a subgroups of the graph containing more than two nodes where the maximum shortest path distance between any two nodes in the group is n. Over the years, many variants of these basic ideas have been formalised in the social network literature and a good summary can be found in Wasserman and Faust [94].

Considering higher order structures can be very informative but is more involved. Milo and coworkers began by looking for specific patterns of connections between nodes in small subgraphs, dubbed *motifs*. Given a connected subgraph of size 3, for example, there are 13 possible motifs. Statistically, some of these appear more often and are found to be overrepresented in certain real networks compared to random networks [97]. Understanding the motif composition of a complex network has been shown to improve the predictive power of deterministic models of transmission when motifs are explicitly modelled (see Section 4.2 and House et al. [98]).

In the above definitions, a subgraph has been defined only in reference to itself. A different approach is to compare the number of internal edges to the number of external edges, arising from the intuitive notion that a *community* will be denser in terms of edges than its surroundings. One such definition, the definition of community in the *strong* sense, is defined as a subgraph in which each node has more edges to other nodes within the subgraph than to any other nodes in the network. Again, this definition is quite restrictive, and in order to relax these constraints, the most commonly used (and most intuitive) definition of communities is groups of nodes that have a high density of edges within them and a lower density of edges between groups. This intuitive definition is behind the most widely used approach for studying community structure in networks. Newman and Girvan formalised this in terms of the *modularity* measure Q [99]. Given a particular network which is partitioned into communities, the modularity measure compares the expected number of edges within communities to the actual number of edges within communities.

Although the impact of communities in transmission processes has not been fully explored, a few studies have shown it can have a profound impact on disease dynamics [100, 101]. An alternative measure of how "well-knit" a graph is, named conductance [102], most widely used in the computer science literature has also been found to be important in a range of networks [103].

3.6. Higher Dimensional Networks. All of the above definitions have concentrated on networks where the edges remain unchanged over time and all edges have equal weight. Both of these constraints can naturally be relaxed, but generally, this calls for a higher-dimensional characterisation of the edges within the network. It is a matter of common experience that

social interactions which can lead to infection do change, with some contacts being repeated regularly, while others are more sporadic. The frequency, intensity, and duration of contacts are all time-varying. How these inherently dynamic networks are represented for the purposes of modelling can have a significant impact on the model outcomes [55, 104]. However, capturing the structure of such dynamic networks in a parsimonious manner remains a substantial challenge. More work has been done on weighted networks, as these are a more straightforward extension of the classical presence-absence networks [105, 106]. In terms of disease spread, the movement networks discussed in Section 2.4 are often considered as weighted [37, 40, 107].

In the sections that follow, we discuss how these network properties can be inferred statistically and the improvements in our understanding of the transmission of infection in networks that have come as a result.

4. Model Formulation

4.1. Techniques for Simulation. One of the key advantages of the simulation of disease processes on networks is that it enables the study of systems that are too complex for analytical approaches to be tractable. With that in mind, it is worth briefly considering efficient approaches to disease simulation on networks.

There are two main types of simulation model for infectious diseases on networks: discrete-time and continuous-time models; of these, discrete-time simulations are more common, so we discuss them first. In a discrete-time simulation, at every time step, disease may be transmitted along every edge from an infectious node to a susceptible node with a particular probability (which may be the same for all extant edges or may vary according to properties of the two nodes or the edge). Also, nodes may recover (becoming immune, or reverting to being susceptible) during each time-step. Within a time-step, every infection and recovery event is assumed to occur simultaneously. In a dynamic network simulation, the network is typically updated every time step—for example, in a livestock movement network, during time-step x, infection could only transmit down edges that occurred during time-step x. Clearly, in a directed network, infection may only transmit in the direction of an edge.

Whilst algorithms for discrete-time simulations are not complex, some simple implementation techniques (arising from the observation that most networks of epidemiological interest are sparse) can significantly enhance software performance. In a directed network with N nodes, there are $N(N-1)$ possible edges; in a sparse network with mean node degree k, there are $Nk \ll N(N-1)$ edges. Accordingly, rather than representing the network as an N by N array, where the element in each array is 0 if the edge is absent, nonzero otherwise, it is usually more efficient to maintain a list of the neighbours of each node. Then, if a list of infected nodes is maintained during a simulation run, it is straightforward to consider each susceptible neighbour of an infected node in turn and test if infection is transmitted to that node. Additionally, a fast high-quality pseudorandom number generator such as the Mersenne Twister should be used [108]. The "contagion" software package implements these techniques (amongst others) and is freely available [109].

The alternative approach to simulating disease processes on networks is to simulate a series of stochastic Markovian events—the continuous-time approach. Essentially, given the state of the system, it is possible to calculate the probability distributions of when possible subsequent events (i.e., recovery of an infectious node or infection of a susceptible node) will occur. Random draws from these distributions are then made to determine which event occurs next, the state of the system updated, and the process repeated. This approach was pioneered by Gillespie to study the dynamics of chemical reactions [110]; it is, however, computationally intensive, so approximations have been developed. The τ-leap method [111], where multiple events are allowed to occur during a time period τ, is clearly related to the discrete-time formulation discussed above. However, the ability to allow τ to vary during a simulation to account for the processes involved [112] has potential benefits.

The continuous-time approach is clearly in closer agreement with the ideal of standard disease models; however, utilising this method may be computationally prohibitive especially when large networks are involved. Discrete-time models may provide a viable alternative for three main reasons. Firstly, as the time steps involved in the discrete-time model become sufficiently small, we would expect the two models to converge. Secondly, inaccuracies due to the discrete-time formulation are likely to be less substantial in network models compared to random-mixing models, providing two events do not occur in the same neighbourhood during the same time step. Finally, the daily cycle of contacts that regulate most of our lives means that using time steps of less than 24 hours may falsely represent the temporal accuracy that can be attributed to any simulation of the real world.

4.2. Analytic Methods. In this section, we use the word "analytic" broadly, to imply models that are directly numerically integrable, without the use of Monte Carlo simulation methods, rather than systems for which all results can be written in terms of fundamental functions, of which there are very few in epidemiology. Analytic approaches to transmission of infection on networks fall into three broad categories. Firstly, there are approaches that calculate exact invasion thresholds and final sizes for special networks. Secondly, there are approaches for calculating exact transient dynamics, including epidemic peak heights and times, but again, these only hold in special networks. Finally, there are approaches based on moment closure that are give approximately correct dynamics for a wide class of networks.

Before considering these approaches on networks, it is worth considering what is meant by nonnetwork mixing and showing explicitly how this can derive the standard transmission terms from familiar differential equation models. Nonnetwork mixing can be taken to have one of two meanings: either that every individual in the population is weakly

connected to every other (the mean-field assumption), or that an Erdös-Rényi random graph defines the transmission network, depending on context. To see how this determines the epidemic dynamics, we consider a population of N individuals, with a homogeneous independent probability q that any pair of individuals is linked on the network, which gives each individual a mean number of edges $\overline{n} = q(N-1)$. We then assume that the transmission rate for infection across an edge is τ and that the proportion of the population infectious at a time t is $I(t)$; then, the force of infection experienced by an average susceptible in the population is $\overline{n}\tau I(t) \equiv \beta I(t)$. The quantity β, therefore, defines a population-level transmission rate that can be interpreted in one of two ways as $N \to \infty$. In the case where the population is assumed to be fully connected, the limit is that q is held at unity, and so τ is reduced to as N is increased to hold $q(N-1)\tau$ constant. In the case where the population is connected on a random graph, q is reduced as N is increased to hold $\overline{n}$ constant.

In either case, having defined an appropriate population-level transmission rate, a stochastic susceptible-infectious model of transmission is defined through a Markov chain, in which a population with X susceptible individuals and Y infectious individuals transitions stochastically to a population with $X-1$ susceptible individuals and $Y+1$ infectious individuals at rate $\beta XY/(N-1)$. Then, the exact mean behaviour of such a system in the limit $N \to \infty$ then has its transmission behaviour captured by

$$\dot{S} = -\beta S(t)I(t), \tag{8}$$

where S, I are the proportion of individuals susceptible and infectious, respectively. The mathematical formalism behind deriving such sets of ordinary differential equations from Markov chains is given by Kurtz [113], and a summary of the application of this methodology to infectious disease modelling is given in Diekmann and Heesterbeek [114]. However, it should be clear that (8) is familiar as the basis of all random-mixing epidemiological models.

In the case of exponentially distributed infectious periods and recovery from infection offering long-lasting immunity, the standard *SIR* equations provide an exact description of the mean behaviour of this system. Nevertheless, the existence of waning immunity, a latent period between an individual becoming infected and being able to transmit infection, and nonexponentially distributed recovery periods are also important for epidemiological applications [10, 42, 115]. These can often be incorporated into analytical approaches through the addition of extra disease compartments, which necessitates extra algebraic and computational effort but typically does not require a fundamental conceptual reevaluation. Sometimes, significant additional complexity does not even modify quantitative epidemiological results—for example, regardless of the rate of waning immunity, length of latent period, or infectious period distribution, if the mean infectious period is T, then the basic reproductive ratio is

$$R_0 = \beta T. \tag{9}$$

The estimation of this quantity for complex disease histories, from data likely to be available, is considered by Wallinga and Lipsitch [116]. We, therefore, focus on the transmission process, since this is most affected by network structure, and other elements of biological realism typically act at the individual level. An important caveat to this, however, is when an infected individual's level of transmissibility varies over the course of their infectious period, which sets up correlations between the processes of transmission and recovery that pose a particular challenge for analytic work, especially in structured populations, as noted by for example Ball et al. [117].

4.2.1. Exact Invasion. For nonnetwork mixing, the threshold for invasion is given by the basic reproductive ratio R_0, defined as the expected number of secondary infectious cases created by an average primary infectious case in an otherwise wholly susceptible population. In structured populations, this verbal definition is typically altered to be the secondary cases caused by a typical primary case once the dynamical system has settled into its early asymptotic behaviour. As such, the threshold for invasion is $R_0 = 1$: for values above this, an infection can grow in the population and the disease can successfully invade; for values below it, each chain of infection is doomed to eventual extinction. Values of R_0 can be measured directly during the course of an epidemic by detailed contact tracing; however, there are considerable statistical issues concerning censoring and data quality.

Provided there are no short closed loops in the network, R_0 can be defined through a next-generation matrix

$$K_{km} = \frac{[km](m-1)}{m[m]}p, \tag{10}$$

where K_{km} defines the number of cases in individuals with k contacts from an individual with m contacts during the early stages of the epidemic. Here and elsewhere in this section we use square brackets to represent the numbers of different types on the network; hence, $[m]$ is the number of individuals with m edges in the network and $[km]$ is the number of edges between individuals with k and m contacts, respectively. In addition, p is the probability of infection eventually passing across the edge between a susceptible-infectious pair (for Markovian recovery rate γ and transmission rate τ this is given by $p = \tau/(\tau+\gamma)$). The basic reproductive ratio is given by the dominant eigenvalue of the next-generation matrix

$$R_0 = \|(K_{km})\|. \tag{11}$$

This quantity corresponds to the standard verbal definition of the basic reproductive ratio, and correspondingly the invasion threshold is at $R_0 = 1$.

Once an appreciable number of short closed loops are present in the network, exact threshold parameters can still sometimes be defined, but these typically depart from the standard verbal definition of R_0. For example, Ball et al. [117] consider a branching process on cliques (households) connected to each other through configuration-model edges—cliques are connected to each other at random (Figure 1(d)).

By considering the number of secondary cliques infected by a clique with one initial infected individual, a threshold called R_* can be defined. (For the configuration-model of households where each household is of the same size and each individual has the same number of random connections outside the household, the threshold R_* is given later as (20); however, the methodology is far more general). The calculation of the invasion threshold for the recently defined triangular configuration model [118, 119] involves calculating both the expected number of secondary infectious individuals and triangles rather than just working at the individual level. Trapman [120] deals with how these sort of results can be related to more general networks through bounding. A general feature of clustered networks for which exact thresholds have been derived so far is that there is a local-global distinction in transmission routes, with a general theory of this given by Ball and Neal [121], where an "overlapping groups" and "great circle" model are also analysed. Nevertheless, care still has to be taken in which threshold parameters are mathematically well behaved and easily calculated (e.g [122]).

4.2.2. Exact Final Size. The most sophisticated and general way to obtain exact results for the expected final size of a major outbreak on a network is called the *susceptibility set* argument and the most general version is currently given by Ball et al. [117]. We give an example of these kind of arguments from Diekmann et al. [123], who consider the simpler case of a network in which each individual has n contacts. Where there is a probability p of infection passing across a given network link (so for transmission and recovery at rates τ and γ, resp., $p = \tau/(\tau+\gamma)$), the probability that an individual avoids infection is given by

$$\begin{aligned} S_\infty &= \left(1 - p + \widetilde{S}p\right)^n, \\ \widetilde{S} &= \left(1 - p + \widetilde{S}p\right)^{n-1}. \end{aligned} \tag{12}$$

Here, a two-step process is needed because in an unclustered, regular graph two generations of infection are needed to stabilise the network correlations and so the auxiliary variable $\widetilde{S}$ must also be solved for. Once this and S_∞ are known, the expected attack rate is $R_\infty = 1 - S_\infty$.

4.2.3. Approximate Final Size. The main way to calculate approximate final sizes is given by percolation-based methods. These were reviewed by Bansal et al. [124] and also in [125]. Suppose that we remove a fraction φ of links from the network and can derive an expression for the fraction of nodes remaining in the giant component of the network, $f(\varphi)$. Then,

$$R_\infty \approx f(1-p), \tag{13}$$

and an invasion threshold is given by the value of p for which this final size becomes nonzero in the "thermodynamic limit" of very large network size. This approach is not exact for clustered graphs, but for unclustered graphs exact results like (12) are reproduced.

4.2.4. Exact Dynamics. Some of the earliest work on infectious diseases involved the exact solution of master equations (where the probability of the population being in each possible configuration is calculated) on small, fully connected graphs as summarised in Bailey [126]. The rate at which the complexity of the system of master equations grows means that these equations quickly become too complex to integrate for the most general network. The presence of symmetries in the network, however, does mean that automorphism-driven lumping is one way to manipulate the master equations (whilst preserving the full stochastic information about the system) for solution [127]. At present, this technique has only been applied to relatively simple networks; however, there are no other highly general methods of deriving exact lower-dimensional systems of equations from the master equations.

Nevertheless, other specific routes do exist that allow exact systems of equations of lower dimensionality to be derived for special networks. For static networks constructed using the configuration model (where individuals have heterogeneous degree but connections are made at random such that the presence of short loops can be ignored in a large network, see Figure 1(c)), an exact system of equations for *SIR* dynamics in the limit of large network size was provided by Ball and Neal [69]. This construction involves attributing to each node an "effective degree", which starts the epidemic at its actual degree, and measures connections still available as routes of infection and is, therefore, reduced by transmission and recovery. Using notation consistent with elsewhere in this paper (and ignoring the global infection terms that were included by Ball and coworkers) this yields the relatively parsimonious set of equations

$$\begin{aligned} \dot{S}_k &= -\rho((\tau+\gamma)kS_k - \gamma(k+1)S_{k+1}), \\ \dot{I}_k &= \tau((k+1)I_k - kI_k) - \gamma I_k \\ &\quad + \rho((k+1)(\tau(S_{k+1}+I_{k+1}) + \gamma I_{k+1}) - k(\tau+\gamma)I_k), \\ \rho &:= \frac{\sum_k kI_k}{\sum_l l(S_l+I_l)}. \end{aligned} \tag{14}$$

Here, S_k, I_k are the proportion of effective degree k susceptible and infectious individuals, respectively. Hence, for a configuration-network where the maximum degree is K, we require just $2K$ equations to retrieve the exact dynamics.

While R_0 can be derived using expressions like (11), calculation of the asymptotic early growth rate r requires systems of ODEs like (14). If we assume that transmission and recovery are Markovian processes with rates τ and γ, respectively, two measures of early behaviour are

$$\begin{aligned} R_0^{\mathrm{CM}} &= \frac{\langle n(n-1)\rangle}{\langle n\rangle}\frac{\tau}{\tau+\gamma}, \\ r^{\mathrm{CM}} &= \frac{\langle n(n-2)\rangle}{\langle n\rangle}\tau - \gamma, \end{aligned} \tag{15}$$

where $\langle\cdot\rangle$ informs about the average over the degree distribution. These quantities tell us that the susceptibility to invasion of a network increases with both the mean and the variance of the degree distribution. This closely echos the results for risk-structured models [10] but with an extra term of -1 due to the network, representing the fact that the route through which an individual acquired infection is closed off for future transmission events.

For more structured networks with a local-global distinction, there are two limits in which exact dynamics can also be derived. If the network is composed of m communities of size $n_1, \ldots, n_m$, with the between-community (global) mixing determined by a Poisson process with rate $\overline{n}_G$ and the within-community (local) mixing determined by a Poisson process with rate $\overline{n}_L$, then in the limit as the communities become large, $n_i \to \infty$, the epidemic dynamics on the system are

$$\begin{aligned} \dot{S}_a &= -S_a\left(\beta_L I_a + \alpha \sum_{b \neq a} I_b\right), \\ \dot{I}_a &= S_a\left(\beta_L I_a + \alpha \sum_{b \neq a} I_b\right) - \gamma I_a. \end{aligned} \tag{16}$$

where S_a and I_a are the proportion of individuals susceptible and infectious in community a, and

$$\alpha = \frac{\overline{n}_G \tau}{(m-1)}, \qquad \beta_L = \overline{n}_L \tau. \tag{17}$$

Hence, we have a classic metapopulation model [43], defined in terms of Poisson local and global connections and large local community sizes.

In the limit where $\overline{n}_L \to (n-1)$ and $m \to \infty$—such that there are infinitely many communities of equal size and each community forms a fully interconnected clique— "self-consistent" equations such as in Ghoshal et al. [128] and House and Keeling [70] are exact. These equations evolve the proportion of cliques with x susceptibles and y infecteds, $P_{x,y}$, as well as the proportion of infecteds in the population, I, as follows:

$$\begin{aligned} I &= \frac{1}{n}\sum_{x,y} y P_{x,y}, \\ \dot{P}_{x,y} &= \gamma\left(-yP_{x,y} + (y+1)P_{x,y+1}\right) \\ &\quad + \tau\left(-xyP_{x,y} + (x+1)(y-1)P_{x+1,y-1}\right) \\ &\quad + \beta_G I\left(-xP_{x,y} + (x+1)P_{x+1,y-1}\right), \end{aligned} \tag{18}$$

where $\beta_G = \overline{n}_G \tau$.

Both of these two local-global models, the metapopulation model (16) and the small cliques model (18), are reasonably numerically tractable for modern computational resources, provided the relevant finite number (m or n, resp.) is not too large. The basic reproduction number for the first system is clearly

$$R_0 = \frac{1}{\gamma}(\beta_L + (m-1)\alpha), \tag{19}$$

while for the second, household model, invasion is determined by

$$R_* = \overline{n}_G \frac{\tau}{\tau+\gamma} Z_\infty^n(\tau, \gamma), \tag{20}$$

where $Z_\infty^n(\tau, \gamma)$ is the expected final size of an epidemic in a household of size n with one initial infected. Of course, the within- and between-community mixing for real networks is likely to be much more complex than may be captured by a Poisson process, but these two extremes can provide useful insights. These models show that network structure of the form of communities reduces the potential for an infectious disease to spread, and hence, greater transmission rates are required for the disease to exceed the invasion threshold.

4.2.5. Approximate Dynamics. While all the exact results above are an important guide to intuition, they only hold for very specialised networks. A large class of models exists that form a bridge between "mean-field" models and simulation by using spatial or network moment closure equations. These are highly versatile models. In general, invasion thresholds and final sizes can be calculated rigorously, but exact calculation of transient dynamics is only possible for very special networks. If one wants to calculate transient effects in general network models—most importantly, peak heights and times—then moment closure is really the only versatile way of calculating desired quantities without relying on full numerical simulation.

It is also worth noting that there are many results derived through these "approximate" approaches that are the same as exact results or are numerically indistinguishable from exact results and simulation. We give some examples below and also note that the dynamical PGF approach [129] is numerically indistinguishable from the exact model (14) above for certain parameter values [130]. What is currently lacking is a rigorous mathematical proof of exactness for ODE models other than those outlined in Section 4.2.4 above. While for many practical purposes the absence of such a proof will not matter, we preserve here the conceptual distinction between results that are provably exact, and those that are numerically exact in all cases tested so far.

The idea of moment closure is to start with an exact but unclosed set of equations for the time evolution of different units of structure. Here, we show how these can be derived by considering the rates of change of both types of individual and types of connected pair. Such pairwise moment closure model are a natural extension to the standard

(random-mixing) models, given that infection is passed between pairs of infected individuals

$$\begin{aligned}
[\dot{S_\kappa}] &= -\tau[S_\kappa \longleftarrow I],\\
[\dot{I_\kappa}] &= \tau[S_\kappa \longleftarrow I] - \gamma[I_\kappa],\\
[\dot{S_\kappa S_\lambda}] &= -\tau[S_\kappa S_\lambda \longleftarrow I] + [S_\lambda S_\kappa \longleftarrow I],\\
[\dot{S_\kappa I_\lambda}] &= \tau([S_\kappa S_\lambda \longleftarrow I] - [I \longrightarrow S_\kappa I_\lambda] - [S_\kappa \longleftarrow I_\lambda]) - \gamma[S_\kappa I_\lambda],\\
[\dot{I_\kappa I_\lambda}] &= \tau([I \longrightarrow S_\kappa I_\lambda] + [I \longrightarrow S_\lambda I_\kappa] + [S_\kappa \longleftarrow I_\lambda] + [S_\lambda \longleftarrow I_\kappa])\\
&\quad - 2\gamma[I_\kappa I_\lambda],\\
[\dot{S_\kappa R_\lambda}] &= -\tau[I \longrightarrow S_\kappa R_\lambda] + \gamma[S_\kappa I_\lambda],\\
[\dot{I_\kappa R_\lambda}] &= \tau[I \longrightarrow S_\kappa R_\lambda] + \gamma([I_\kappa I_\lambda] - [I_\kappa R_\lambda]).
\end{aligned} \tag{21}$$

Here, we use square brackets to represent the prevalence of different species within the network. We also use some nonstandard notation to present several diverse approaches in a unified framework: generalised indices κ, λ represent any property of a node (such as its degree), while arrows represent the direction of infection (and so for a directed network, the necessity that an edge in the appropriate direction be present), see Table 1.

Clearly, the system (21) is not closed as it relies on the number of connected triples, and so some form of approximate closure must be introduced to relate the triples to pairs and nodes, which will depend on underlying properties of the network. Most commonly, these closure assumptions deal with heterogeneity in node degree, assortativity, and clustering at the level of triangles. Examples include Keeling [95] and Eames and Keeling [96], where the generalised variables κ, λ above stand for node degrees (k, l), the triple closure is symmetric with respect to the direction of infection, and the network is assumed to be static and nondirected. A general way to write the closure assumption is

$$[A_k B_l C_m] \approx \frac{(l-1)}{l}\left((1-\phi)\frac{[A_k B_l][B_l C_m]}{[B_l]} + \phi\frac{\overline{n}N}{km}\frac{[A_k B_l][B_l C_m][C_m A_k]}{[A_k][B_l][C_m]}\right). \tag{22}$$

where $\overline{n} \equiv \langle n \rangle$ is again the average degree distribution and ϕ measures the ratio of triangles to triples as a means of capturing clustering within the network (see Section 3.4). The typical way to analyse the closed system is direct numerical integration; however, some analytic traction can be gained. One example is the use of a linearising Ansatz to derive the early asymptotic behaviour of the dynamical system. Interestingly, when this is done for $\phi = 0$ (such that there are no triangular loops in the network) as in Eames and Keeling [96], the result for the early asymptotic growth rate agrees with the exact result of (10). In [95], the differential equations for an n-regular graph were also manipulated to give an expression for final size that agreed with the exact result (12)

Equation (22), however, is not the only possible network moment closure regime: Boots and Sasaki [131] and Bauch [132] considered regimes in which closure depended on the disease state (i.e., triples composed of different arrangements of susceptibles and infecteds close differently) to deal with spatial lattice-based systems and early disease invasion respectively. For example Boots and Sasaki [131] use a closure where

$$\begin{aligned}
[SOO] &\approx \varepsilon\frac{\overline{n}-1}{\overline{n}}\frac{[SO][OO]}{[O]},\\
[IOO] &\approx \varepsilon\frac{\overline{n}-1}{\overline{n}}\frac{[IO][OO]}{[O]},\\
[SOS] &\approx [OS]\frac{\overline{n}-1}{\overline{n}}\left(1-\varepsilon\frac{[OO]}{[O]}-\frac{[IO]}{[O]}\right),\\
[ABC] &\approx \frac{\overline{n}-1}{\overline{n}}\frac{[AB][BC]}{[B]} \quad \text{for all other triples,}
\end{aligned} \tag{23}$$

where O represents empty sites within the network that are not currently occupied by individuals, and the parameter $\varepsilon = 0.8093$ accounts for the clustering within lattice-based networks. House and Keeling [133] considered a model of infection transmission and contact tracing on a network, where the closure scheme for $[ABC]$ triples was asymmetric in A and C—this allowed the natural conservation of quantities in a highly clustered system.

The work on dynamical PGF models [129] can be seen as an elegant simplification of this pairwise approach that is valid for SIR-type infection dynamics on configuration model networks. The equations can be reformulated as

$$\begin{aligned}
S &= g(\theta),\\
\dot{I} &= \tau p_I \theta g'(\theta) - \gamma I,\\
\dot{p}_I &= \tau p_S p_I \theta\frac{g''(\theta)}{g'(\theta)} - \tau p_I(1-p_I) - \gamma p_I,\\
\dot{p}_S &= \tau p_S p_I\left(1-\theta\frac{g''(\theta)}{g'(\theta)}\right),\\
\dot{\theta} &= -\tau p_I \theta,
\end{aligned} \tag{24}$$

where g is the probability generating function for the degree distribution, p_S and p_I correspond to the number of contacts of a susceptible that are susceptible or infected, respectively, and θ is defined as probability that a link randomly selected from the entire network has not been associated with the transmission of infection. Here, the closure assumption is implicit in the definition of S; that is, an individual only remains susceptible if all of its links have not seen the transmission of infection, and that the probability is independent for each link, which is comparable to the assumptions underlying the formulation by Ball and Neal [69], equation (14). The precise link between this PGF formulation and the pairwise approach is discussed more fully in House and Keeling [134].

There are many other extensions of this general methodology that are possible. Writing ODEs for the time evolution of triples and closing at a higher order allows

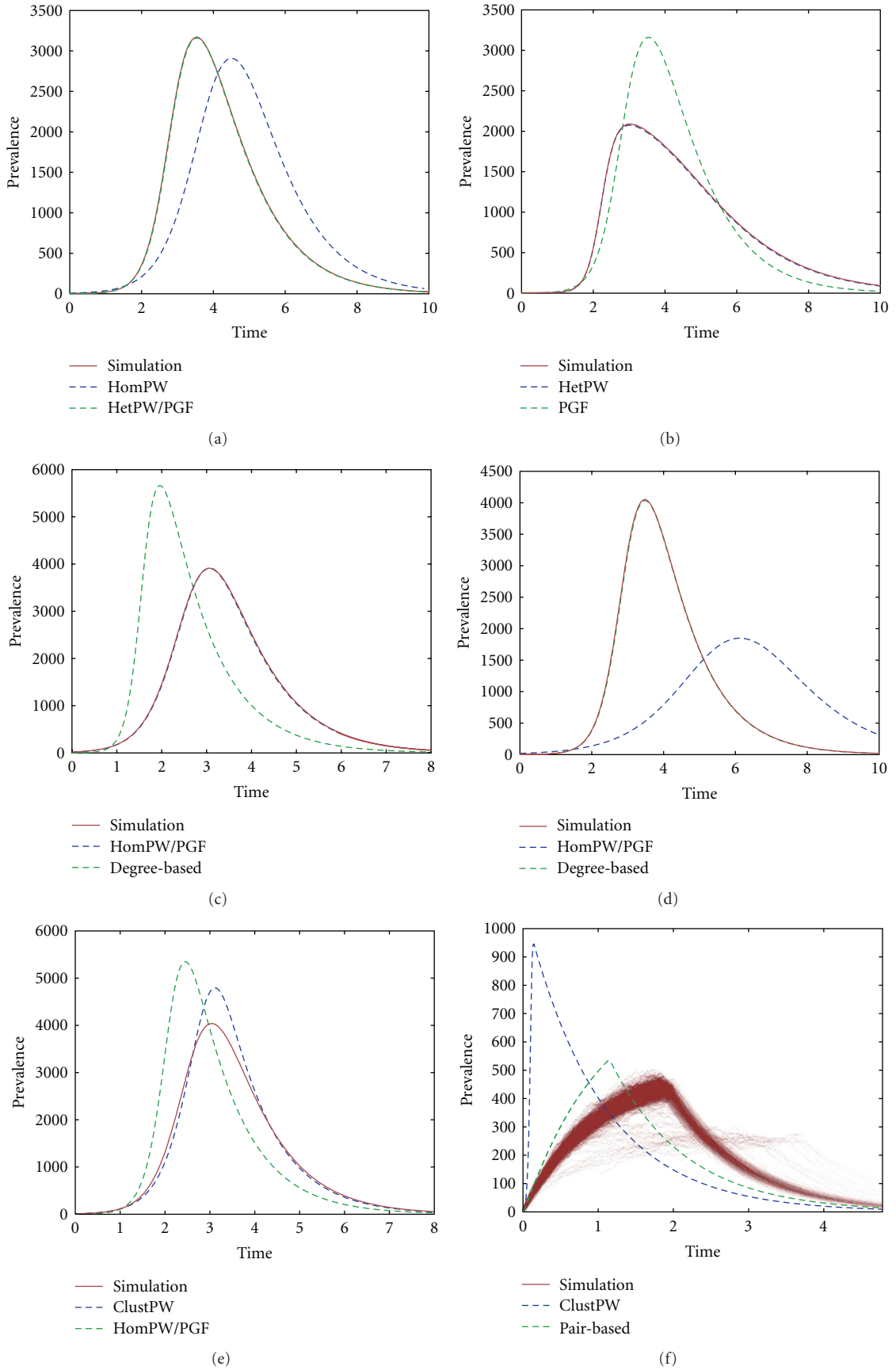

Figure 3: Comparison of simulation and deterministic models for six networks. (a) Two-group configuration model network. (b) Two-group assortative network. (c) Static regular network. (d) Dynamical regular network. (e) Regular clustered network. (f) One-dimensional lattice.

Table 1: Common notation.

Concept/Measure	Other common names	Our notation	Other common notation
Network	Graph	G	
Node	Vertex, point, site, actor	n	v
Edge	Link, tie, bond	l	e
Adjacency matrix	Connectivity matrix	G_{ij}	a_{ij}, A_{ij}
Number of nodes	Size of network	N	n, S
Number of edges	Graph size	L	e, l
Centrality		C	
Degree	Connectivity	k	d, C_d
Betweenness		B_i	bet_i, C_b
Degree distribution	Connectivity distribution	$P(k)$	P_k,p_k
Shortest path distance	Geodesic distance	$D_{i,j}$	$d_{i,j}$
Clustering	transitivity	ϕ	c, Φ
Number of nodes of type A		$[A]$	n_A, N_A
Number of $A-B$ pairs		$[AB]$	n_{AB}, N_{AB}
Diameter	Maximal shortest path	$\text{Diam}(G)$	$\max(D_{i,j})$

the consideration of the epidemiological consequences of varying motif structure [98]. Sharkey et al. [135] considered closure at triple level on directed networks, which involved a more sophisticated treatment of third-order clustering due to the larger repertoire of three-motifs in directed (as compared to undirected) networks. It is also possible to combine stochastic and network moment closure [136]. Time-varying, dynamical networks, particularly applied to sexually transmitted infections where partnerships vary over the course of an epidemic, were considered using approximate ODE-based models by Eames and Keeling [137] and Volz and Meyers [138]. Sharkey [139] considered models appropriate for local networks with large shortest path lengths, where the generic indices μ, λ in (21) stand for node numbers i, j rather than node degrees k, l.

Another approach is to approximate the transmission dynamics in the standard (mean-field) differential equations models. Essentially, this is a form of moment closure at the level of pairs rather than triples. For example, in Roy and Pascual [140] the transmission rate takes the polynomial form

$$\text{Transmission rate to } S_k \text{ from } I_l \propto kl(S_k)^p(I_l)^q, \quad (25)$$

where the exponents, p and q, are typically fitted to simulated data but are thought to capture the spatial arrangement of susceptible and infected nodes. Also, Kiss et al. [141] suggest

$$\text{Transmission rate to } S_k \text{ from } I_l \propto k(l-1)(S_k)(I_l), \quad (26)$$

as a way of accounting for each infected "losing" an edge to its infectious parent.

Finally, a very recent work [142] presents a dynamical system to capture epidemic dynamics on triangular configuration model networks; the relationship between this and other ODE approaches is likely to be an active topic for future work.

This diversity of approaches leads to some important points about methods based on moment closure. These methods are extremely general and can be applied to consider almost any aspect of network structure or disease natural history; they can be applied to populations not currently amenable to direct simulation due to their size, and they do not require a complete description of the network to run—only certain statistical properties. However, there are currently no general methods for the proposal of appropriate closure regimes nor any derivation of the limits on dynamical biases introduced by closure. Therefore, closure methods sit somewhere in between exact results for highly specialised kinds of network and stochastic simulation, where intuitive understanding and general analysis are more difficult.

4.3. Comparison of Analytic Models with Simulation. In the papers that introduced them, the differential-equation-based approximate dynamical systems above were compared to stochastic simulations on appropriate networks. Two recent papers making a comparison of different dynamical systems with simulation are Bansal et al. [124] and Lindquist et al. [130]. There are, however, several issues with attempts to compare deterministic models with simulation and also with each other.

Firstly, it is necessary to define what is meant by agreement between a smooth, deterministic epidemic curve and the rough trajectories produced by simulation. Limiting results about the exactness of different ODE models assume that both the number of individuals infectious and the network size are large, and so the early behaviour of simulations, when there are few infectious individuals, is often dominated by stochastic effects. There are different ways to address this issue, but even after this has been done, there are two sources of deviation of simulations from their deterministic limit. The first of these is the number of simulations realised. If there is a summary statistic such as the mean number of infectious individuals over time, then the confidence interval in such a statistic can be made arbitrarily small by running additional simulations, but agreement between the deterministic limit and a given

realisation may still be poor. The second source of deviation is the network size. By increasing the number of nodes, the prediction interval within which the infection curve will fall can be made arbitrarily small; however, the computational resources needed to simulate extremely large networks can quickly become overwhelming.

More generally, each approximate model is designed with a different application in mind. Models that perform well in one context will often perform poorly in another, and this means that "performance" of a given model in terms of agreement with simulation will primarily be determined by the discrete network system on which simulations are performed.

The above considerations motivate the example comparisons with simulation that we show in Figure 3. This collection of plots is intended to show a variety of different example networks, and the dynamical systems intended to capture their behaviour.

In Figures 3(a)–3(e), continuous-time simulations have their temporal origin shifted so that they agree on the time at which a cumulative incidence of 200 is reached, and then confidence intervals in the mean prevalence of infection are achieved through bootstrapping. The 95% confidence interval is shown as a red shaded region (although typically, this is sufficiently narrow it resembles a line). Six different deterministic models are compared to simulations: HomPW is the pairwise model of Keeling [95] with zero clustering, HetPW is the heterogeneous pairwise model of Eames and Keeling [96], ClustPW is the improved clustered pairwise closure of House and Keeling [133], PGF is the model of Volz [129], Pair-based is the model of Sharkey [139], integrated using the supplementary code from Sharkey [143], and Degree-based is the model of Pastor-Satorras and Vespignani [87].

Figure 3(a) shows a heterogeneous network composed of two risk groups, constructed according to the configuration model [18]. In this case, models that incorporate heterogeneity like HetPW and PGF (which are numerically indistinguishable in this case and several others) are in very close agreement with simulation, while just taking the average degree as in HomPW is a poor choice. In Figure 3(b), assortativity is added to the two group model following the approach of Newman [89], and HetPW outperforms PGF. Figures 3(c) and 3(d) show regular graphs with four links per node, but while Figure 3(c) is static in Figure 3(d) the rate of making and breaking links is much faster than the epidemic process. Models like HomPW and PGF are therefore better for the former and degree-based models are better for the latter—in reality the ratio of the rate of network change to the rate of transmision may not be either large or small and so a more sophisticated method may be best [137, 138]. Figure 3(e) shows a graph with four links per node where clustering has been introduced by the rewiring method of Bansal et al. [144] sometimes called the "big V" [133]. In this case, ClustPW performs better than HomPW and PGF, but clearly there is significant inaccuracy around the region of peak prevalence and so this model captures qualitatively the effects of clustering without appearing to be exact for this precise network. Finally, Figure 3(f) considers the case of a one-dimensional next-nearest-neighbour lattice (so there are four links per node). This introduces long path lengths between nodes in addition to clustering, meaning that the system does not converge onto a period of asymptotic early growth and so realisations are shown as a density plot rather than a confidence interval. ClustPW accounts for clustering but not long path lengths and so is in poor agreement with simulation while the pair-based curve captures the qualitative behaviour of an epidemic on this lattice whilst being quantitatively a reasonable approximation.

5. Inference on Networks

In order to be predictive, epidemic models rely on valid values for parameters governing outbreak dynamics, conditional on the population structure. However, obtaining these parameters is complicated by the fact that even when knowing the underlying contact network structure, infection events are censored—it is only when disease is detected either from symptoms or laboratory tests that a case becomes apparent. In attempting to surmount this difficulty, parameter estimates are often obtained by making strong assumptions as to the infectious period or through ad hoc methods with unknown certainty. Measuring the uncertainty in such estimates is as important as obtaining the estimates themselves in providing an honest risk prediction. Given these difficulties, inference for epidemic processes has perhaps received little attention in comparison to its simulation counterpart.

The presence of contact network data for populations provides a unique opportunity to estimate the importance of various modes of disease transmission from disease incidence or contact tracing data. For example, given knowledge of the rate of contact between two individuals, it is possible to infer the probability that a contact results in an infection. If data on mere connectivity (i.e., a 1 if the individuals are connected and 0 otherwise) is available, then it is still possible to infer a rate of infection between connected individuals. Thus, the detail of the inference is determined to a large extent by the available detail in the network data [145].

5.1. Availability of Data. Epidemic models are defined in terms of times of transitions between infection states, for example a progression from susceptible, to infected, to removed (i.e., recovered with lifelong immunity or dead) in the so-called "SIR" model. Statistical inference requires firstly that observations of the disease process are made: at the very least, this comprises the times of case detections, remembering that infection times are always censored (you only ever know you have a cold a few days after you caught it). In addition, covariate data on the individuals provides structure to the population and begins to enable the statistician to make statements about the importance of individuals' relationships to one another in terms of disease transmission. Therefore, any covariate data, however slight, effectively implies a network structure upon which disease transmission can be superimposed.

As long as populations are relatively small (e.g., populations of farms in livestock disease analysis), it is common for models to operate at the individual level, providing detailed information on case detection times and perhaps even information on epidemiologically significant historical contact events [146–148]. In other populations, however, such detailed data may not be available due to practical and ethical reasons. Instead, data is supplied on an aggregated spatial and/or temporal basis. For the purposes of inference, therefore, this can be regarded as a household model, with areas constituting households.

In a heterogeneous population, the behaviour of an epidemic within any particular locality is governed by the relationship between infected and susceptible individuals. For inference in the early stages of an epidemic, it is important to quantify the amount of uncertainty in the underlying contact networks as the early growth of the epidemic is known to be subexponential due to the depletion of the local susceptible population. This contrasts markedly to the exponential growth observed in a large homogeneously mixing population [10]. When the network is known and details of individual infections are available, contact tracing data may be used to infer the network; this data could also be used for inference on the epidemic parameters [116, 149]. Conversely, if the network is completely unknown, it would be useful if estimation of both the epidemic parameters and parameters specifying the structure of the network was possible. This is a difficult problem because the observed epidemic contains very limited information about the underlying network, as demonstrated by Britton and O'Neill [150]. However, with appropriate assumptions, some results can be obtained; the limited amount of existing work in this area is described in Section 5.3.1 below although clearly the problem is worthy of further study.

5.1.1. Inference on Homogeneous Models. For homogeneous models the basic reproduction number, or R_0, has several equivalent definitions and can be defined in terms of the transmission rate β and removal rate γ. For nonhomogeneous models, the definitions are not equivalent; see for example [122].

Although inference for β and γ is difficult for real applications (see below), it turns out that making inference on R_0 (as a function of β and γ) is rather more straightforward. Heffernan et al. [151] summarise various methods for estimating R_0 from epidemiological data based on endemic equilibrium, average age at infection, epidemic final size, and intrinsic growth rate [114, 152, 153]. However, these methods all rely on observing a complete epidemic, and hence for real-time analysis during an epidemic, we must make strong assumptions concerning the number of currently undetected infections. An example of inference for R_0 based upon complete epidemic data is provided by Stegeman et al. [154], where data from the 2003 outbreak of High Pathogenicity Avian Influenza H7N7 is fitted to a chain-binomial model using a generalised linear model.

Obviously, complete or near-complete epidemic data is rare and hence it is desirable to perform inference based upon partial observation. This is particularly relevant for real time estimation of R_0. For example, Cauchemez et al. [155] attempt to estimate R_0 in real-time by constructing a discrete-time statistical model that imputes the number of secondary cases generated by each primary case. This is based on the method of Wallinga and Teunis [156] who formulate a likelihood function for inferring who infected whom from dates of symptom onset

$$L(i \text{ infected } j) = \frac{w\left(t_j - t_i\right)}{\sum_{j \neq k} w\left(t_j - t_k\right)}, \tag{27}$$

where $w(\cdot)$ is the probability density function for the *generation interval* $t_j - t_i$, that is, the time between infector i's infection time and infectee j's infection time. Of course, infection times are never observed in practice so symptom onset times are used as a proxy, with the assumption that the distribution of infection time to symptom onset time is the same for every individual. Bayesian methods are used to infer "late-onset" cases from known "early-onset" cases, but large uncertainty of course remains when inferring the reproductive ratio close to the current time as there exists large uncertainty about the number of cases detected in the near future. Additionally, a model for $w(\cdot)$ must be chosen (see, [157]).

The tradeoff in the simplicity of estimating R_0 in these ways, however, is that although a population wide R_0 gives a measure of whether an epidemic is under control on a wide-scale, it give no indication as to regional-level, or even individual-level, risk. Moreover, the two examples quoted above do not even attempt to include population heterogeneity into their models though the requirement for its inclusion is difficult to ascertain in the absence of model diagnostics results. It is postulated, therefore, that a simple measure of R_0, although simple to obtain, is not sufficient in order to make tactical control-policy decisions. In these situations, knowledge of both the transmission rate and removal rate are required.

5.2. Inference on Household Models. Inference for households models is well developed in comparison to inference for other "network" models. In essence, this is for three main reasons: firstly, it is a reasonable initial approximation to assume that infection either occurs within the home or from a random source in the population. Secondly, entire households can be serologically sampled following an epidemic, such that the distribution of cases in households of given sizes can be ascertained. Finally, it is often a reasonable approximation that following introduction of infection into the household, the within-household epidemic will go extinct before any further introductions—which dramatically simplifies the mathematics.

The first methods proposed for such inference are maximum likelihood procedures based upon chain-binomial models, such as the Reed-Frost model, or the stochastic formulation of the Kermack-McKendrick model considered by Bartlett [158]. These early methods are summarised by Bailey [126]. They, and the significant majority of

methods proposed for household inference to date, use final-size data which can be readily obtained from household serology results. A simplifying assumption to facilitate inference in most methods is that the epidemics within the various households evolve independently (e.g., see the martingale method of Becker [159], which requires the duration of a latent period to be substantial for practical implementation).

Additionally, fixed probabilities p_C and p_H, corresponding to a susceptible individual escaping community-acquired infection during the epidemic and escaping infection when exposed to a single infected household member, respectively, were initially assumed [160]. Two important, realistic extensions to this framework are to incorporate different levels of risk factors for individuals [161] and to introduce dependence of p_H on an infectious period [162]. The latter inclusion was enabled by appealing to results of Ball et al. [163]. These types of methods are largely based upon the ability to generate closed form formulae for the final size distribution of the models.

The ability to relax assumptions further has been predominately due to use of Markov chain Monte Carlo (MCMC) methods as first considered by O'Neill et al. [162] for household models following earlier studies of Gibson and Renshaw [164] and O'Neill and Roberts [165] who focused on single, large outbreaks. This methodology has been used to in combination with simulation and data augmentation approaches to tailor inference methods for specific data sets of interest; for example, Neal and Roberts [166] consider a model with a spatial component of distance between households and data containing details of dates of symptoms and appearance of rash and has also resulted in a growing number of novel methods for inference, for example Clancy and O'Neill [167] consider a rejection sampling procedure and Cauchemez et al. [168] introduce a constrained simulation approach. Even greater realism can be captured within household models by considering the different compositions of households and, therefore, the weighted nature of contacts within households. For example, Cauchemez et al. [169] considered household data from the Epigrippe study of influenza in France 1999-2000 and showed that children play a key role in the transmission of influenza and the risk of bringing infection into the household.

Whilst new developments are appearing at an increasing rate, the significant majority of methods are based upon final size data and are developed for SIR disease models, perhaps due in part to the simplification of arguments for deriving final size distributions. One key, but still unanswered question from these analyses of household epidemics is how the transmission rate between any two individuals in the household scales with the total number of individuals in the household (compare Longini and Koopman [160] and Cauchemez et al. [169]). Intuition would suggest that in larger households the mixing between any two individuals is decreased, but the precise form of this scaling is still unclear, and much more data on large household sizes is required to provide a definitive answer.

5.2.1. Inference on Fully Heterogeneous Populations. Perhaps the holy grail of statistical inference on epidemics is to make use of an individual-level model to describe heterogeneous populations at the limit of granularity. In this respect, Bayesian inference on stochastic mechanistic models using MCMC have perhaps shown the most promise, allowing inference to be made on both transmission parameters and using data augmentation to estimate the infectious period.

An analysis of the 1861 outbreak of measles in Hagelloch by Neal and Roberts [166] demonstrates the use of a reversible jump MCMC algorithm to infer disease transmission parameters and infectious period, whilst additionally allowing formal comparisons to be made between several nested models. With the uncertainty surrounding model choice, such methodology is vital to enable accurate understanding and prediction. This approach has since been combined with the algorithm of O'Neill and Roberts [165] and used to analyse disease outbreaks such as avian influenza and foot and mouth disease in livestock populations [146, 147, 170] and MRSA outbreaks in hospital wards [171].

Whilst representing the cutting edge of inference on infectious disease processes, these approaches are currently limited by computing power, with their algorithms scaling by the number of infectives multiplied by the number of susceptibles. However, with advances in computer technology expected at an increasing rate, and small approximations made in the calculation of the statistical likelihoods needed in the MCMC algorithms, these techniques may well form the mainstay of epidemic inference in the future.

5.3. Inference from Contact Tracing. In livestock diseases, part of the standard response to a case detection is to gather contact tracing information from the farmer. The resulting data are a list of contacts that have been made in and out of the infected farm during a stipulated period prior to the notification of disease [172]. In terms of disease control on a local level, this has the aim of identifying both the source of infection and any presumed susceptibles that might have been infected as a result of the contact. It has been shown that providing the efficiency of following up any contacts to look for signs of disease is high; this is a highly effective method of slowing the spread of an epidemic and finally containing it.

Much has been written on how contact tracing may be used to decrease the time between infection and detection (notification) during epidemics. However, this focuses on the theoretical aspects of how contact tracing efficiency is related to both epidemic dynamics and population structure (see, e.g., Eames and Keeling [173] Kiss et al. [174], Klinkenberg et al. [175]). In contrast, the use of contact tracing data in inferring epidemic dynamics does not appear to have been well exploited although it was used by the Ministry of Agriculture, Fisheries, and Food (now Defra) to directly infer a spatial risk kernel for foot and mouth disease in 2001. This assumed that the source of infection was correctly identified by the field investigators, thereby giving an empirical estimate of the probability of infection as a function of distance [148, 176, 177]. Strikingly, this shows a high degree of similarity to spatial kernel estimates based

on the statistical techniques of Diggle [178] and Kypraios [179] without using contact tracing information. However, Cauchemez et al. [155] make the point that the analysis of imperfect contact tracing data requires more complex statistical approaches, although they abandoned contact tracing information altogether in their analysis of the 2003 SARS epidemic in China. Nevertheless, recent unpublished work has shown promise in assimilating imperfect contact tracing data and case detection times to greatly improve inference, and hence the predictive capability of simulation techniques.

5.3.1. Inference from Distributions over Families of Networks. Qualitative results from simulations indicate that epidemics on networks, for some parameter values, show features that distinguish them from homogeneous models. The principal features are a very variable length slow-growth phase, followed by a rapid increase in the infection rate and a slower decline after the peak [180]. However, in quantitative terms, there is usually very limited information about the underlying network and parameters are often not identifiable. When the details of the network are unknown, but something is known or assumed about its formation, estimation of both the epidemic parameters and parameters for the network itself are in principle possible using MCMC techniques. All the stochastic models for generating networks described in Section 2.7 above realise a distribution over all or some of the $2^{N(N-1)/2}$ possible networks. In most cases, this distribution is not tractable; MCMC techniques are in principle still possible but in practice would be too slow without careful design of algorithms.

However, with appropriate assumptions some results can be obtained, which provide some insight into what more could be achieved. When the network is taken to be an Erdös-Rényi graph with unknown parameter p and the epidemic is a Markovian SIR, Britton and O'Neill [150] showed that it is possible to estimate the parameters, although they highlight the ever-present challenge of disentangling epidemiological from network parameters. The MCMC algorithm was improved by Neal and Roberts [181] and the extension from SIR to SEIR has been developed by Groendyke et al. [182]. However, the extension to more realistic families of networks remains a challenging problem and will undoubtedly be the subject of exciting future research.

6. Discussion

The use of networks is clearly a rapidly growing field in epidemiology. By assessing (and quantifying) the potential transmission routes between individuals in a population, researchers are able to both better understand the observed distribution of infection as well as create better predictive models of future prevalence. We have shown how many of the structural features in commonly used contact networks can be quantified and how there is an increasing understanding of how such features influence the propagation of infection. However, a variety of challenges remain.

6.1. Open Questions. Several open problems remain if networks are to continue to influence predictive epidemiology. The majority of these stem from the difficulty in obtaining realistic transmission networks for a range of pathogens. Although some work has been done to elucidate the interconnected structure of sexual encounters (and hence the sexual transmission network), these are still relatively small-scale compared to the population size and suffer from a range of potential biases. Determining comparable networks for airborne infections is a far greater challenge due to the less precise definition of a potential contact.

One practical issue is therefore whether new techniques can be developed that allow contact networks to be assessed remotely. Proximity loggers, such as those used by Hamede and colleagues [12], provide one potential avenue although it would require the technology to become sufficiently robust, portable and cheap that a very large proportion of a population could be convinced to carry one at all times. For many human populations, where the use of mobile phones (which can detect each other via Bluetooth) is sufficiently widespread, there is the potential to use them to gather network information—although the challenges of developing sufficiently generic software should not be underestimated. While these remotely sensed networks would provide unparalleled information that could be obtained with the minimum of effort, there would still be some uncertainty surrounding the nature of each contact.

There is now a growing set of diary-based studies that have attempted to record the personal contacts of a large number of individuals; of these, POLYMOD is currently the most comprehensive [17]. While such egocentric data obviously provides extensive information on individual behaviour, due to the anonymity of such surveys it is not clear how the alters should be connected together. The configuration method of randomly connecting half-links provides one potential solution, but what is ideally required is a more comprehensive method that would allow clustering, spatially localised connections and assortativity between degree distributions to be included and specified.

Associated with the desire to have realistic contact networks for entire populations, comes the need to characterise such networks in a relatively parsimonious manner that provides important insights into the types of epidemiological dynamics that could be realised. Such a characterisation would allow for different networks (from different times or different locations) to be compared in a manner that is epidemiologically significant and would allow artificial networks to be created that matched particular known network features. This clearly relies on both existing measures of network structure (as outlined in Section 3) together with a robust understand of how such features influence the transient epidemic dynamics (as outlined in Section 4.2). However, such a generic understanding of all network features is unlikely to arise for many years. A more immediate challenge is to understand ways in which local network structure (clustering, cliques, and spatially localised connections) influence the epidemiological dynamics.

To date the vast majority of the work into disease transmission on networks has focused on static networks

where all links are of equal strength and, therefore, associated with the same basic rate of transmission. However, it is clear that contact networks change over time (both on the short-time scale of who we meet each day, and on the longer time-scale of who our main work and social contacts are), and that links have different weights (such that some contacts are much more likely to lead to the transmission of infection than others). While the simulation of infection on such weighted time-varying networks is feasible, it is unclear how the existing sets of network properties or the existing literature of analytical approaches can be extended to such higher-dimensional networks.

For any methodology to have any substantive use in the field, it is important both to have effective data gathering protocols in place and to have the statistical techniques in place to analyse it. Here, three issues are perhaps most critical. Firstly, data gathering resources are almost always limited. Therefore, carefully designed randomised sampling schemata should be employed to maximise the power of the statistical techniques used to analyse data, rather than having to reply on data augmentation techniques to work around the problems present in ad hoc datasets. This aspect is particularly important when working on network data derived from population samples. Secondly, any inference on both network and infectious disease models should be backed up by a careful analysis of model fit. Although recent advances in statistical epidemiology have given us an unprecedented ability to measure population/disease dynamics based on readily available field data, epidemic model diagnostics are currently in their infancy in comparison to techniques in other areas of statistics. Therefore, it is expected that with the growth in popularity of network models for analysing disease spread, much research effort will be required in designing such methodology.

6.2. Conclusions. We have highlighted that the study of contact networks is fundamentally important to epidemiology and provides a wealth of tools for understanding and predicting the spread of a range of pathogens. As we have outlined above, many challenges still exist, but with growing interest in this highly interdisciplinary field and ever increasing sophistication in the mathematical, statistical and remote-sensing tools being used, these problems may soon be overcome. We conclude, therefore, that now is an exciting time for research into network epidemiology as many of the practical difficulties are surmounted and theoretical concepts are translated into results of applied importance in infection control and public health.

Acknowledgments

This work is funded by the Medical Research Council (L. Danon, M. J. Keeling, M. C. Venon), the Biotechnology and Biological Sciences Research Council (C. P. Jewell, M. J. Keeling, G. O. Roserts), the Engineering and Physical Sciences Research Council (T. House, A. Ford, M. J. Keeling), the Centre for Research in Statistical Methodology funded by the Engineering and Physical Sciences Research Council (GOR), the Research and Policy for Infectious Disease Dynamics (RAPIDD) program of the Science and Technology Directorate (M. J. Keeling), and the Australian Research Council's Discovery Projects funding scheme, Project no. DP110102893 (J. V. Ross). We would like to thank Kieran Sharkey for use of pre-publication MATLAB code and two anonymous reviewers for their comments. All authors contributed equally to this manuscript.

References

[1] A. S. Klovdahl, "Social networks and the spread of infectious diseases: the AIDS example," *Social Science and Medicine*, vol. 21, no. 11, pp. 1203–1216, 1985.

[2] R. M. May and R. M. Anderson, "Transmission dynamics of HIV infection," *Nature*, vol. 326, no. 6109, pp. 137–142, 1987.

[3] D. C. Bell, J. S. Atkinson, and J. W. Carlson, "Centrality measures for disease transmission networks," *Social Networks*, vol. 21, no. 1, pp. 1–21, 1999.

[4] H. L. Goodman, "Snowball sampling," *Annals of Mathematical Statistics*, vol. 32, pp. 148–170, 1961.

[5] D. D. Heckathorn, "Respondent-driven sampling: a new approach to the study of hidden populations," *Social Problems*, vol. 44, no. 2, pp. 174–199, 1997.

[6] A. M. Jolly and J. L. Wylie, "Sampling individuals with large sexual networks: an evaluation of four approaches," *Sexually Transmitted Diseases*, vol. 28, no. 4, pp. 200–207, 2001.

[7] J. L. Wylie and A. Jolly, "Patterns of chlamydia and gonorrhea infection in sexual networks in Manitoba, Canada," *Sexually Transmitted Diseases*, vol. 28, no. 1, pp. 14–24, 2001.

[8] A. S. Klovdahl, J. J. Potterat, D. E. Woodhouse, J. B. Muth, S. Q. Muth, and W. W. Darrow, "Social networks and infectious disease: the Colorado Springs Study," *Social Science and Medicine*, vol. 38, no. 1, pp. 79–88, 1994.

[9] A. C. Ghani, C. A. Donnelly, and G. P. Garnett, "Sampling biases and missing data in explorations of sexual partner networks for the spread of sexually transmitted diseases," *Statistics in Medicine*, vol. 17, no. 18, pp. 2079–2097, 1998.

[10] R. M. Anderson and R. M. May, *Infectious Diseases of Humans*, Oxford University Press, Oxford, UK, 1992.

[11] N. Eagle and A. Pentland, "Reality mining: sensing complex social systems," *Personal and Ubiquitous Computing*, vol. 10, no. 4, pp. 255–268, 2006.

[12] R. K. Hamede, J. Bashford, H. McCallum, and M. Jones, "Contact networks in a wild Tasmanian devil (*Sarcophilus harrisii*) population: using social network analysis to reveal seasonal variability in social behaviour and its implications for transmission of devil facial tumour disease," *Ecology Letters*, vol. 12, no. 11, pp. 1147–1157, 2009.

[13] A. M. Johnson, J. Wadsworth, K. Wellings, S. Bradshaw, and J. Field, "Sexual lifestyles and HIV risk," *Nature*, vol. 360, no. 6403, pp. 410–412, 1992.

[14] A. Johnson, J. Wadsworth, K. Wellings, and J. Field, *Sexual Attitudes and Lifestyles*, Blackwell Scientific Publications, Oxford, UK, 1994.

[15] A. M. Johnson, C. H. Mercer, B. Erens et al., "Sexual behaviour in Britain: partnerships, practices, and HIV risk behaviours," *Lancet*, vol. 358, no. 9296, pp. 1835–1842, 2001.

[16] A. J. Copas, K. Wellings, B. Erens et al., "The accuracy of reported sensitive sexual behaviour in Britain: exploring the extent of change 1990–2000," *Sexually Transmitted Infections*, vol. 78, no. 1, pp. 26–30, 2002.

[17] J. Mossong, N. Hens, M. Jit et al., "Social contacts and mixing patterns relevant to the spread of infectious diseases," *PLoS Medicine*, vol. 5, no. 3, article e74, pp. 381–391, 2008.

[18] M. Molloy and B. Reed, "A critical-point for randomgraph-swith a given degree sequence," *Random Structures and Algorithms*, vol. 6, pp. 161–179, 1995.

[19] M. Molloy and B. Reed, "The size of the giant component of a random graph with a given degree sequence," *Combinatorics Probability and Computing*, vol. 7, no. 3, pp. 295–305, 1998.

[20] J. M. Read, K. T.D. Eames, and W. J. Edmunds, "Dynamic social networks and the implications for the spread of infectious disease," *Journal of the Royal Society Interface*, vol. 5, no. 26, pp. 1001–1007, 2008.

[21] M. Baguelin, A. J. V. Hoek, M. Jit, S. Flasche, P. J. White, and W. J. Edmunds, "Vaccination against pandemic influenza A/H1N1v in England: a real-time economic evaluation," *Vaccine*, vol. 28, no. 12, pp. 2370–2384, 2010.

[22] F. Liljeros, C. R. Edling, L. Amaral, H. E. Stanley, and Y. Åberg, "The web of human sexual contacts," *Nature*, vol. 411, no. 6840, pp. 907–908, 2001.

[23] A. C. Ghani and G. P. Garnett, "Risks of acquiring and transmitting sexually transmitted diseases in sexual partner networks," *Sexually Transmitted Diseases*, vol. 27, no. 10, pp. 579–587, 2000.

[24] J. Medlock and A. P. Galvani, "Optimizing influenza vaccine distribution," *Science*, vol. 325, no. 5948, pp. 1705–1708, 2009.

[25] M. Kretzschmar and M. Morris, "Measures of concurrency in networks and the spread of infectious disease," *Mathematical Biosciences*, vol. 133, no. 2, pp. 165–195, 1996.

[26] M. Morris and M. Kretzschmar, "Concurrent partnerships and the spread of HIV," *AIDS*, vol. 11, no. 5, pp. 641–648, 1997.

[27] A. C. Ghani, J. Swinton, and G. P. Garnett, "The role of sexual partnership networks in the epidemiology of gonorrhea," *Sexually Transmitted Diseases*, vol. 24, no. 1, pp. 45–56, 1997.

[28] M. E. Halloran, I. M. Longini, A. Nizam, and Y. Yang, "Containing bioterrorist smallpox," *Science*, vol. 298, no. 5597, pp. 1428–1432, 2002.

[29] I. M. Longini, A. Nizam, S. Xu et al., "Containing pandemic influenza at the source," *Science*, vol. 309, no. 5737, pp. 1083–1087, 2005.

[30] T. C. Germann, K. Kadau, I. M. Longini, and C. A. Macken, "Mitigation strategies for pandemic influenza in the United States," *Proceedings of the National Academy of Sciences of the United States of America*, vol. 103, no. 15, pp. 5935–5940, 2006.

[31] I. M. Longini Jr., M. E. Halloran, A. Nizam et al., "Containing a large bioterrorist smallpox attack: a computer simulation approach," *International Journal of Infectious Diseases*, vol. 11, no. 2, pp. 98–108, 2007.

[32] N. M. Ferguson, D. A. T. Cummings, S. Cauchemez et al., "Strategies for containing an emerging influenza pandemic in Southeast Asia," *Nature*, vol. 437, no. 7056, pp. 209–214, 2005.

[33] N. M. Ferguson, D. A. T. Cummings, C. Fraser, J. C. Cajka, P. C. Cooley, and D. S. Burke, "Strategies for mitigating an influenza pandemic," *Nature*, vol. 442, no. 7101, pp. 448–452, 2006.

[34] G. Chowell, J. M. Hyman, S. Eubank, and C. Castillo-Chavez, "Scaling laws for the movement of people between locations in a large city," *Physical Review E*, vol. 68, no. 6, Article ID 066102, pp. 661021–661027, 2003.

[35] S. Eubank, H. Guclu, V. S. A. Kumar et al., "Modelling disease outbreaks in realistic urban social networks," *Nature*, vol. 429, no. 6988, pp. 180–184, 2004.

[36] D. L. Chao, M. E. Halloran, V. J. Obenchain, and I. M. Longini, "FluTE, a publicly available stochastic influenza epidemic simulation model," *PLoS Computational Biology*, vol. 6, no. 1, article e1000656, 2010.

[37] L. Hufnagel, D. Brockmann, and T. Geisel, "Forecast and control of epidemics in a globalized world," *Proceedings of the National Academy of Sciences of the United States of America*, vol. 101, no. 42, pp. 15124–15129, 2004.

[38] R. Guimerà, S. Mossa, A. Turtschi, and L. A. N. Amaral, "The worldwide air transportation network: anomalous centrality, community structure, and cities' global roles," *Proceedings of the National Academy of Sciences of the United States of America*, vol. 102, no. 22, pp. 7794–7799, 2005.

[39] I. M. Hall, J. R. Egan, I. Barrass, R. Gani, and S. Leach, "Comparison of smallpox outbreak control strategies using a spatial metapopulation model," *Epidemiology and Infection*, vol. 135, no. 7, pp. 1133–1144, 2007.

[40] C. Viboud, O. N. Bjørnstad, D. L. Smith, L. Simonsen, M. A. Miller, and B. T. Grenfell, "Synchrony, waves, and spatial hierarchies in the spread of influenza," *Science*, vol. 312, no. 5772, pp. 447–451, 2006.

[41] D. Brockmann, L. Hufnagel, and T. Geisel, "The scaling laws of human travel," *Nature*, vol. 439, no. 7075, pp. 462–465, 2006.

[42] S. E. Robinson, M. G. Everett, and R. M. Christley, "Recent network evolution increases the potential for large epidemics in the British cattle population," *Journal of the Royal Society Interface*, vol. 4, no. 15, pp. 669–674, 2007.

[43] I. Hanski and O. Gaggiotti, *Ecology, Genetics, and Evolution of Metapopulations*, Elsevier, New York, NY, USA, 2004.

[44] L. Sattenspiel and D. A. Herring, "Structured epidemic models and the spread of influenza in the central Canadian Subarctic," *Human Biology*, vol. 70, no. 1, pp. 91–115, 1998.

[45] V. Colizza, A. Barrat, M. Barthélemy, and A. Vespignani, "The role of the airline transportation network in the prediction and predictability of global epidemics," *Proceedings of the National Academy of Sciences of the United States of America*, vol. 103, no. 7, pp. 2015–2020, 2006.

[46] V. Colizza, A. Barrat, M. Barthelemy, A. J. Valleron, and A. Vespignani, "Modeling the worldwide spread of pandemic influenza: baseline case and containment interventions," *PLoS Medicine*, vol. 4, no. 1, article 13, pp. 0095–0110, 2007.

[47] K. Khan, W. Hu, P. Raposo et al., "Spread of a novel influenza A (H1N1) virus via global airline transportation," *New England Journal of Medicine*, vol. 361, no. 2, pp. 212–214, 2009.

[48] D. Balcan, H. Hu, B. Goncalves et al., "Seasonal transmission potential and activity peaks of the new influenza A(H1N1): a Monte Carlo likelihood analysis based on human mobility," *BMC Medicine*, vol. 7, article 45, 2009.

[49] C. Viboud, M. A. Miller, B. T. Grenfell, O. N. Bjørnstad, and L. Simonsen, "Air travel and the spread of influenza: important caveats," *PLoS Medicine*, vol. 3, no. 11, pp. 2159–2160, 2006.

[50] D. Balcan, V. Colizza, B. Gonçalves, H. Hud, J. J. Ramasco, and A. Vespignani, "Multiscale mobility networks and the spatial spreading of infectious diseases," *Proceedings of the National Academy of Sciences of the United States of America*, vol. 106, no. 51, pp. 21484–21489, 2009.

[51] L. Danon, T. House, and M. J. Keeling, "The role of routine versus random movements on the spread of disease in Great Britain," *Epidemics*, vol. 1, no. 4, pp. 250–258, 2009.

[52] M. J. Keeling, L. Danon, M. C. Vernon, and T. A. House, "Individual identity and movement networks for disease metapopulations," *Proceedings of the National Academy of Sciences of the United States of America*, vol. 107, no. 19, pp. 8866–8870, 2010.

[53] D. M. Green, I. Z. Kiss, and R. R. Kao, "Modelling the initial spread of foot-and-mouth disease through animal movements," *Proceedings of the Royal Society B*, vol. 273, no. 1602, pp. 2729–2735, 2006.

[54] M. F. Heath, M. C. Vernon, and C. R. Webb, "Construction of networks with intrinsic temporal structure from UK cattle movement data," *BMC Veterinary Research*, vol. 4, article 11, 2008.

[55] M. C. Vernon and M. J. Keeling, "Representing the UK's cattle herd as static and dynamic networks," *Proceedings of the Royal Society B*, vol. 276, pp. 469–476, 2009.

[56] E. Brooks-Pollock and M. Keeling, "Herd size and bovine tuberculosis persistence in cattle farms in Great Britain," *Preventive Veterinary Medicine*, vol. 92, no. 4, pp. 360–365, 2009.

[57] I. Z. Kiss, D. M. Green, and R. R. Kao, "The network of sheep movements within Great Britain: network properties and their implications for infectious disease spread," *Journal of the Royal Society Interface*, vol. 3, no. 10, pp. 669–677, 2006.

[58] J. C. Gibbens, C. E. Sharpe, J. W. Wilesmith et al., "Descriptive epidemiology of the 2001 foot-and-mouth disease epidemic in Great Britain: the first five months," *Veterinary Record*, vol. 149, no. 24, pp. 729–743, 2001.

[59] F. Natale, A. Giovannini, L. Savini et al., "Network analysis of Italian cattle trade patterns and evaluation of risks for potential disease spread," *Preventive Veterinary Medicine*, vol. 92, no. 4, pp. 341–350, 2009.

[60] D. T. Haydon, M. Chase-Topping, D. J. Shaw et al., "The construction and analysis of epidemic trees with reference to the 2001 UK foot-and-mouth outbreak," *Proceedings of the Royal Society B*, vol. 270, no. 1511, pp. 121–127, 2003.

[61] S. Riley, C. Fraser, C. A. Donnelly et al., "Transmission dynamics of the etiological agent of SARS in Hong Kong: impact of public health interventions," *Science*, vol. 300, no. 5627, pp. 1961–1966, 2003.

[62] E. M. Cottam, J. Wadsworth, A. E. Shaw et al., "Transmission pathways of foot-and-mouth disease virus in the United Kingdom in 2007," *PLoS Pathogens*, vol. 4, no. 4, Article ID e1000050, 2008.

[63] M. E. J. Newman, "The structure and function of complex networks," *SIAM Review*, vol. 45, no. 2, pp. 167–256, 2003.

[64] S. Boccaletti, V. Latora, Y. Moreno, M. Chavez, and D.-U. Hwang, "Complex networks: structure and dynamics," Physics Reports, 2006.

[65] M. Newman, A. Barabasi, and D. Watts, *The Structure and Dynamics of Networks*, Princeton University Press, Princeton, NJ, USA, 2006.

[66] D. M. Boyd and N. B. Ellison, "Social network sites: definition, history, and scholarship," *Journal of Computer-Mediated Communication*, vol. 13, no. 1, article 11, pp. 210–230, 2007.

[67] M. E. Fisher and J. Esam, "Some cluster size and percolation problems," *Journal of Mathematical Physics*, vol. 2, pp. 609–619, 1961.

[68] B. Nickel and D. Wilkinson, "Invasion percolation on the Cayley tree: exact solution of a modified percolation model," *Physical Review Letters*, vol. 51, no. 2, pp. 71–74, 1983.

[69] F. Ball and P. Neal, "Network epidemic models with two levels of mixing," *Mathematical Biosciences*, vol. 212, no. 1, pp. 69–87, 2008.

[70] T. House and M. J. Keeling, "Deterministic epidemic models with explicit household structure," *Mathematical Biosciences*, vol. 213, no. 1, pp. 29–39, 2008.

[71] D. J. Watts, R. Muhamad, D. C. Medina, and P. S. Dodds, "Multiscale, resurgent epidemics in a hierarchical metapopulation model," *Proceedings of the National Academy of Sciences of the United States of America*, vol. 102, no. 32, pp. 11157–11162, 2005.

[72] J. L. Lebowitz, C. Maes, and E. R. Speer, "Statistical mechanics of probabilistic cellular automata," *Journal of Statistical Physics*, vol. 59, no. 1-2, pp. 117–170, 1990.

[73] C. J. Rhodes and R. M. Anderson, "Epidemic thresholds and vaccination in a lattice model of disease spread," *Theoretical Population Biology*, vol. 52, no. 2, pp. 101–118, 1997.

[74] D. J. Watts and S. H. Strogatz, "Collective dynamics of "small-world" networks," *Nature*, vol. 393, no. 6684, pp. 440–442, 1998.

[75] J. Travers and S. Milgram, "An experimental study of the small world problem," *Sociometry*, vol. 32, no. 4, pp. 425–443, 1969.

[76] M. Boots and A. Sasaki, ""Small worlds" and the evolution of virulence: infection occurs locally and at a distance," *Proceedings of the Royal Society B*, vol. 266, no. 1432, pp. 1933–1938, 1999.

[77] M. Boots, P. J. Hudson, and A. Sasaki, "Large shifts in pathogen virulence relate to host population structure," *Science*, vol. 303, no. 5659, pp. 842–844, 2004.

[78] J. Badham, H. Abbass, and R. Stocker, "Parameterisation of Keeling's network generation algorithm," *Theoretical Population Biology*, vol. 74, no. 2, pp. 161–166, 2008.

[79] P. W. Holland and S. Leinhardt, "An exponential family of probability distributions for directed graphs," *Journal of the American Statistical Association*, vol. 76, no. 373, pp. 33–50, 1981.

[80] J. Besag, "Spatial interaction and the statistical analysis of lattice systems," *Journal of the Royal Statistical Society. Series B*, vol. 36, no. 2, pp. 192–236, 1974.

[81] O. Frank and D. Strauss, "Markov graphs," *Journal of the American Statistical Association*, vol. 81, no. 395, pp. 832–842, 1986.

[82] M. S. Handcock and J. H. Jones, "Likelihood-based inference for stochastic models of sexual network formation," *Theoretical Population Biology*, vol. 65, no. 4, pp. 413–422, 2004.

[83] G. Robins, P. Pattison, and J. Woolcock, "Missing data in networks: exponential random graph (p*) models for networks with non-respondents," *Social Networks*, vol. 26, no. 3, pp. 257–283, 2004.

[84] G. Robins, T. Snijders, P. Wang, M. Handcock, and P. Pattison, "Recent developments in exponential random graph (p*) models for social networks," *Social Networks*, vol. 29, no. 2, pp. 192–215, 2007.

[85] S. M. Goodreau, "Advances in exponential randomgraph (p*)models applied to a large social network," *Social Networks*, vol. 29, no. 2, pp. 231–248, 2007.

[86] R. Albert and A. L. Barabási, "Statistical mechanics of complex networks," *Reviews of Modern Physics*, vol. 74, no. 1, pp. 47–97, 2002.

[87] R. Pastor-Satorras and A. Vespignani, "Epidemic spreading in scale-free networks," *Physical Review Letters*, vol. 86, no. 14, pp. 3200–3203, 2001.

[88] A. L. Lloyd and R. M. May, "How viruses spread among computers and people," *Science*, vol. 292, no. 5520, pp. 1316–1317, 2001.

[89] M. E. J. Newman, "Assortative mixing in networks," *Physical Review Letters*, vol. 89, no. 20, Article ID 208701, 4 pages, 2002.

[90] S. Gupta, R. M. Anderson, and R. M. May, "Networks of sexual contacts: implications for the pattern of spread of HIV," *AIDS*, vol. 3, no. 12, pp. 807–817, 1989.

[91] M. Boguna and R. Pastor-Satorras, "Epidemic spreading in correlated complex networks," *Physical Review E*, vol. 66, no. 4, Article ID 047104, pp. 1–4, 2002.

[92] V. M. Eguiluz and K. Klemm, "Epidemic threshold in structured scale-free networks," *Physical Review Letters*, vol. 89, no. 10, Article ID 108701, pp. 1–4, 2002.

[93] C. Moore and M. E. J. Newman, "Epidemics and percolation in small-world networks," *Physical Review E*, vol. 61, no. 5, pp. 5678–5682, 2000.

[94] S. Wasserman and K. Faust, *Social Network Analysis: Methods and Applications*, Cambridge University Press, Cambridge, UK, 1994.

[95] M. J. Keeling, "The effects of local spatial structure on epidemiological invasions," *Proceedings of the Royal Society B*, vol. 266, no. 1421, pp. 859–867, 1999.

[96] K. T. D. Eames and M. J. Keeling, "Modeling dynamic and network heterogeneities in the spread of sexually transmitted diseases," *Proceedings of the National Academy of Sciences of the United States of America*, vol. 99, no. 20, pp. 13330–13335, 2002.

[97] R. Milo, S. Shen-Orr, S. Itzkovitz, N. Kashtan, D. Chklovskii, and U. Alon, "Network motifs: simple building blocks of complex networks," *Science*, vol. 298, no. 5594, pp. 824–827, 2002.

[98] T. House, G. Davies, L. Danon, and M. J. Keeling, "A motif-based approach to network epidemics," *Bulletin of Mathematical Biology*, vol. 71, no. 7, pp. 1693–1706, 2009.

[99] M. E. J. Newman and M. Girvan, "Finding and evaluating community structure in networks," *Physical Review E*, vol. 69, no. 2, Article ID 026113, 15 pages, 2004.

[100] C. Buckee, L. Danon, and S. Gupta, "Host community structure and the maintenance of pathogen diversity," *Proceedings of the Royal Society B*, vol. 274, no. 1619, pp. 1715–1721, 2007.

[101] M. Salathé and J. H. Jones, "Dynamics and control of diseases in networks with community structure," *PLoS Computational Biology*, vol. 6, no. 4, article e1000736, 2010.

[102] R. Kannan, S. Vempala, and A. Vetta, "On clusterings: good, bad and spectral," *Journal of the ACM*, vol. 51, no. 3, pp. 497–515, 2004.

[103] J. Leskovec, K. J. Lang, A. Dasgupta, and M. W. Mahoney, "Community structure in large networks: natural cluster sizes and the absence of large welldefined clusters," *Internet Mathematics*, vol. 6, no. 1, pp. 29–123, 2009.

[104] R. R. Kao, L. Danon, D. M. Green, and I. Z. Kiss, "Demographic structure and pathogen dynamics on the network of livestock movements in Great Britain," *Proceedings of the Royal Society B*, vol. 273, no. 1597, pp. 1999–2007, 2006.

[105] A. Barrat, M. Barthélemy, R. Pastor-Satorras, and A. Vespignani, "The architecture of complex weighted networks," *Proceedings of the National Academy of Sciences of the United States of America*, vol. 101, no. 11, pp. 3747–3752, 2004.

[106] M. Newman, "The architecture of complex weighted networks," *Physical Review E*, vol. 70, no. 5, Article ID 056131, 9 pages, 2004.

[107] J. V. Ross, T. House, and M. J. Keeling, "Calculation of disease dynamics in a population of households," *PLoS One*, vol. 5, article e9666, 2010.

[108] M. Matsumoto and T. Nishimura, "Mersenne twister: a 623-dimensionally equidistributed uniform pseudo-random number generator," *ACM Transactions on Modeling and Computer Simulation*, vol. 8, no. 1, pp. 3–30, 1998.

[109] M. C. Vernon, "Contagion: free software for network analysis & generation, and disease simulation," 2007, http://contagion.principate.org/.

[110] D. T. Gillespie, "Exact stochastic simulation of coupled chemical reactions," *Journal of Physical Chemistry*, vol. 81, no. 25, pp. 2340–2361, 1977.

[111] D. T. Gillespie, "Approximate accelerated stochastic simulation of chemically reacting systems," *Journal of Chemical Physics*, vol. 115, no. 4, pp. 1716–1733, 2001.

[112] Y. Cao, D. T. Gillespie, and L. R. Petzold, "Efficient step size selection for the tau-leaping simulation method," *Journal of Chemical Physics*, vol. 124, no. 4, Article ID 044109, pp. 1–11, 2006.

[113] T. Kurtz, "Solutions of ordinary differential equations as limits of pure jump Markov processes," *Journal of Applied Probability*, vol. 7, no. 1, pp. 49–58, 1970.

[114] O. Diekmann and J. Heesterbeek, *Mathematical Epidemiology of Infectious Diseases: Model Building, Analysis and Interpretation*, John Wiley & Sons, New York, NY, USA, 2000.

[115] M. J. Keeling and P. Rohani, *Modeling Infectious Diseases in Humans and Animals*, Princeton University Press, Princeton, NJ, USA, 2007.

[116] J. Wallinga and M. Lipsitch, "How generation intervals shape the relationship between growth rates and reproductive numbers," *Proceedings of the Royal Society B*, vol. 274, no. 1609, pp. 599–604, 2007.

[117] F. Ball, D. Sirl, and P. Trapman, "Threshold behavior and final outcome of an epidemic on a random network with household structure," *Advances in Applied Probability*, vol. 41, no. 3, pp. 765–796, 2009.

[118] J. Miller, "Percolation and epidemics in random clustered networks," *Physical Review E*, vol. 80, no. 2, pp. 1–4, 2009.

[119] M. Newman, "Random graphs with clustering," *Physical Review Letters*, vol. 103, no. 5, pp. 1–4, 2009.

[120] P. Trapman, "On analytical approaches to epidemics on networks," *Theoretical Population Biology*, vol. 71, no. 2, pp. 160–173, 2007.

[121] F. Ball and P. Neal, "A general model for stochastic SIR epidemics with two levels of mixing," *Mathematical Biosciences*, vol. 180, pp. 73–102, 2002.

[122] L. Pellis, N. M. Ferguson, and C. Fraser, "Threshold parameters for a model of epidemic spread among households and workplaces," *Journal of the Royal Society Interface*, vol. 6, no. 40, pp. 979–987, 2009.

[123] O. Diekmann, M. C. M. De Jong, and J. A. J. Metz, "A deterministic epidemic model taking account of repeated contacts between the same individuals," *Journal of Applied Probability*, vol. 35, no. 2, pp. 448–462, 1998.

[124] S. Bansal, B. T. Grenfell, and L. A. Meyers, "When individual behaviour matters: homogeneous and network models in epidemiology," *Journal of the Royal Society Interface*, vol. 4, no. 16, pp. 879–891, 2007.

[125] M. E. J. Newman, *Networks: An Introduction*, Oxford University Press, Oxford, UK, 2010.

[126] N. Bailey, *The Mathematical Theory of Infectious Diseases and Its Applications*, Charles Griffin and Company, London, UK, 1975.

[127] P. L. Simon, M. Taylor, and I. Z. Kiss, "Exact epidemic models on graphs using graph automorphism driven lumping," *Journal of Mathematical Biology*. In press.

[128] G. Ghoshal, L. M. Sander, and I. M. Sokolov, "SIS epidemics with household structure: the self-consistent field method," *Mathematical Biosciences*, vol. 190, no. 1, pp. 71–85, 2004.

[129] E. Volz, "SIR dynamics in random networks with heterogeneous connectivity," *Journal of Mathematical Biology*, vol. 56, no. 3, pp. 293–310, 2008.

[130] J. Lindquist, J. Ma, P. van den Driessche, and F. H. Willeboordse, "Effective degree network disease models," *Journal of Mathematical Biology*. In press.

[131] M. Boots and A. Sasaki, "Parasite-driven extinction in spatially explicit host-parasite systems," *American Naturalist*, vol. 159, no. 6, pp. 706–713, 2002.

[132] C. T. Bauch, "The spread of infectious diseases in spatially structured populations: an invasory pair approximation," *Mathematical Biosciences*, vol. 198, no. 2, pp. 217–237, 2005.

[133] T. House and M. J. Keeling, "The impact of contact tracing in clustered populations," *PLoS Computational Biology*, vol. 6, no. 3, article e1000721, 2010.

[134] T. A. House and M. J. Keeling, "Insights from unifying modern approximations to infections on networks," *Journal of the Royal Society Interface*, vol. 8, no. 54, pp. 67–73, 2011.

[135] K. J. Sharkey, C. Fernandez, K. L. Morgan et al., "Pair-level approximations to the spatio-temporal dynamics of epidemics on asymmetric contact networks," *Journal of Mathematical Biology*, vol. 53, no. 1, pp. 61–85, 2006.

[136] C. E. Dangerfield, J. V. Ross, and M. J. Keeling, "Integrating stochasticity and network structure into an epidemic model," *Journal of the Royal Society*, vol. 6, no. 38, pp. 761–774, 2009.

[137] K. T. D. Eames and M. J. Keeling, "Monogamous networks and the spread of sexually transmitted diseases," *Mathematical Biosciences*, vol. 189, no. 2, pp. 115–130, 2004.

[138] E. Volz and L. A. Meyers, "Susceptible-infected-recovered epidemics in dynamic contact networks," *Proceedings of the Royal Society B*, vol. 274, no. 1628, pp. 2925–2933, 2007.

[139] K. J. Sharkey, "Deterministic epidemiological models at the individual level," *Journal of Mathematical Biology*, vol. 57, no. 3, pp. 311–331, 2008.

[140] M. Roy and M. Pascual, "On representing network heterogeneities in the incidence rate of simple epidemic models," *Ecological Complexity*, vol. 3, no. 1, pp. 80–90, 2006.

[141] I. Z. Kiss, D. M. Green, and R. R. Kao, "The effect of contact heterogeneity and multiple routes of transmission on final epidemic size," *Mathematical Biosciences*, vol. 203, no. 1, pp. 124–136, 2006.

[142] E. M. Volz, "Dynamics of infectious disease in clustered networks with arbitrary degree distributions," In press, http://arxiv.org/abs/1006.0970.

[143] K. Sharkey, "Deterministic epidemic models on contact networks: correlations and unbiological terms," Preprint.

[144] S. Bansal, S. Khandelwal, and L. A. Meyers, "Exploring biological network structure with clustered random networks," *BMC Bioinformatics*, vol. 10, article 405, 2009.

[145] C. Jewell, T. Kypraios, P. Neal, and G. Roberts, "Bayesian analysis for emerging infectious diseases," *Bayesian Analysis*, vol. 4, pp. 465–496, 2009.

[146] C. P. Jewell, M. J. Keeling, and G. O. Roberts, "Predicting undetected infections during the 2007 foot-and-mouth disease outbreak," *Journal of the Royal Society Interface*, vol. 6, no. 41, pp. 1145–1151, 2009.

[147] C. P. Jewell, T. Kypraios, R. M. Christley, and G. O. Roberts, "A novel approach to real-time risk prediction for emerging infectious diseases: a case study in avian influenza H5N1," *Preventive Veterinary Medicine*, vol. 91, no. 1, pp. 19–28, 2009.

[148] M. J. Keeling, M. E. J. Woolhouse, D. J. Shaw et al., "Dynamics of the 2001 UK foot and mouth epidemic: stochastic dispersal in a heterogeneous landscape," *Science*, vol. 294, no. 5543, pp. 813–817, 2001.

[149] J. Wallinga, P. Teunis, and M. Kretzschmar, "Using data on social contacts to estimate age-specific transmission parameters for respiratory-spread infectious agents," *American Journal of Epidemiology*, vol. 164, no. 10, pp. 936–944, 2006.

[150] T. Britton and P. D. O'Neill, "Bayesian inference for stochastic epidemics in populations with random social structure," *Scandinavian Journal of Statistics*, vol. 29, no. 3, pp. 375–390, 2002.

[151] J. M. Heffernan, R. J. Smith, and L. M. Wahl, "Perspectives on the basic reproductive ratio," *Journal of the Royal Society Interface*, vol. 2, no. 4, pp. 281–293, 2005.

[152] "The structure of epidemic models," in *Epidemic Models: Their Structure and Relation to Data*, D. Mollison, Ed., CUP, 1995.

[153] H. W. Hethcote, "Mathematics of infectious diseases," *SIAM Review*, vol. 42, no. 4, pp. 599–653, 2000.

[154] A. Stegeman, A. Bouma, A. R. W. Elbers et al., "Avian influenza a virus (H7N7) epidemic in the Netherlands in 2003: course of the epidemic and effectiveness of control measures," *Journal of Infectious Diseases*, vol. 190, no. 12, pp. 2088–2095, 2004.

[155] S. Cauchemez, P. Y. Boëlle, C. A. Donnelly et al., "Real-time estimates in early detection of SARS," *Emerging Infectious Diseases*, vol. 12, no. 1, pp. 110–113, 2006.

[156] J. Wallinga and P. Teunis, "Different epidemic curves for severe acute respiratory syndrome reveal similar impacts of control measures," *American Journal of Epidemiology*, vol. 160, no. 6, pp. 509–516, 2004.

[157] M. Lipsitch, T. Cohen, B. Cooper et al., "Transmission dynamics and control of severe acute respiratory syndrome," *Science*, vol. 300, no. 5627, pp. 1966–1970, 2003.

[158] M. Bartlett, "Some evolutionary stochastic processes," *Journal of the Royal Statistical Society B*, vol. 11, pp. 211–229, 1949.

[159] N. Becker, "An estimation procedure for household disease data," *Biometrika*, vol. 66, no. 2, pp. 271–277, 1979.

[160] I. M. Longini and J. S. Koopman, "Household and community transmission parameters from final distributions of infections in households," *Biometrics*, vol. 38, no. 1, pp. 115–126, 1982.

[161] I. M. Longini, J. S. Koopman, M. Haber, and G. A. Cotsonis, "Statistical inference for infectious diseases. Risk-specific household and community transmission parameters," *American Journal of Epidemiology*, vol. 128, no. 4, pp. 845–859, 1988.

[162] P. D. O'Neill, D. J. Balding, N. G. Becker, M. Eerola, and D. Mollison, "Analyses of infectious disease data from household outbreaks by Markov chain Monte Carlo methods," *Journal of the Royal Statistical Society. Series C*, vol. 49, no. 4, pp. 517–542, 2000.

[163] F. Ball, D. Mollison, and G. Scalia-Tomba, "Epidemics with two levels of mixing," *Annals of Applied Probability*, vol. 7, no. 1, pp. 46–89, 1997.

[164] G. J. Gibson and E. Renshaw, "Estimating parameters in stochastic compartmental models using Markov chain methods," *IMA Journal of Mathemathics Applied in Medicine and Biology*, vol. 15, no. 1, pp. 19–40, 1998.

[165] P. D. O'Neill and G. O. Roberts, "Bayesian inference for partially observed stochastic epidemics," *Journal of the Royal Statistical Society. Series A*, vol. 162, no. 1, pp. 121–129, 1999.

[166] P. J. Neal and G. O. Roberts, "Statistical inference and model selection for the 1861 Hagelloch measles epidemic," *Biostatistics*, vol. 5, no. 2, pp. 249–261, 2004.

[167] D. Clancy and P. D. O'Neill, "Exact Bayesian inference and model selection for stochastic models of epidemics among a community of households," *Scandinavian Journal of Statistics*, vol. 34, no. 2, pp. 259–274, 2007.

[168] S. Cauchemez, A. J. Valleron, P. Y. Boëlle, A. Flahault, and N. M. Ferguson, "Estimating the impact of school closure on influenza transmission from Sentinel data," *Nature*, vol. 452, no. 7188, pp. 750–754, 2008.

[169] S. Cauchemez, F. Carrat, C. Viboud, A. J. Valleron, and P. Y. Boëlle, "A Bayesian MCMC approach to study transmission of influenza: application to household longitudinal data," *Statistics in Medicine*, vol. 23, no. 22, pp. 3469–3487, 2004.

[170] I. Chis Ster and N. M. Ferguson, "Transmission parameters of the 2001 foot and mouth epidemic in Great Britain," *PloS One*, vol. 2, no. 6, article e502, 2007.

[171] T. Kypraios, P. D. O'Neill, S. S. Huang, S. L. Rifas-Shiman, and B. S. Cooper, "Assessing the role of undetected colonization and isolation precautions in reducing Methicillin-Resistant Staphylococcus aureus transmission in intensive care units," *BMC Infectious Diseases*, vol. 10, article 29, 2010.

[172] Defra, Defra's framework response plan for exotic animal diseases, 2007.

[173] K. T. D. Eames and M. J. Keeling, "Contact tracing and disease control," *Proceedings of the Royal Society B*, vol. 270, no. 1533, pp. 2565–2571, 2003.

[174] I. Z. Kiss, D. M. Green, and R. R. Kao, "Disease contact tracing in random and clustered networks," *Proceedings of the Royal Society B*, vol. 272, no. 1570, pp. 1407–1414, 2005.

[175] D. Klinkenberg, C. Fraser, and H. Heesterbeek, "The effectiveness of contact tracing in emerging epidemics," *PloS One*, vol. 1, no. 1, article e12, 2006.

[176] N. M. Ferguson, C. A. Donnelly, and R. M. Anderson, "The foot-and-mouth epidemic in Great Britain: pattern of spread and impact of interventions," *Science*, vol. 292, no. 5519, pp. 1155–1160, 2001.

[177] N. J. Savill, D. J. Shaw, R. Deardon et al., "Topographic determinants of foot and mouth disease transmission in the UK 2001 epidemic," *BMC Veterinary Research*, vol. 2, article 3, 2006.

[178] P. J. Diggle, "A partial likelihood for spatio-temporal point processes.," *Statistical Methods in Medical Research*, vol. 15, no. 4, pp. 325–336, 2006.

[179] T. Kypraios, *Efficient Bayesian inference for partially observed stochastic epidemics and a new class of semi-parametric time series models*, Ph.D. thesis, Department of Mathematics and Statistics, Lancaster University, Lancaster, UK, 2007.

[180] M. Keeling, "The implications of network structure for epidemic dynamics," *Theoretical Population Biology*, vol. 67, no. 1, pp. 1–8, 2005.

[181] P. Neal and G. Roberts, "A case study in non-centering for data augmentation: stochastic epidemics," *Statistics and Computing*, vol. 15, no. 4, pp. 315–327, 2005.

[182] C. Groendyke, D. Welch, and D. Hunter, "Bayesian inference for contact networks given epidemic data," Tech. Rep., Department of Statistics, Pennsylvania State University, 2010.

Hindawi Publishing Corporation
Interdisciplinary Perspectives on Infectious Diseases
Volume 2011, Article ID 543520, 13 pages
doi:10.1155/2011/543520

Research Article

Epidemic Percolation Networks, Epidemic Outcomes, and Interventions

Eben Kenah[1] and Joel C. Miller[2,3]

[1] *Department of Biostatistics, School of Public Health, University of Washington, Seattle, WA 98195-7232, USA*
[2] *Center for Communicable Disease Dynamics, Department of Epidemiology, Harvard School of Public Health, Boston, MA 02115, USA*
[3] *Fogarty International Center, National Institutes of Health, Bethesda, MD 20892, USA*

Correspondence should be addressed to Eben Kenah, eek4@u.washington.edu

Received 17 July 2010; Revised 3 November 2010; Accepted 23 December 2010

Academic Editor: Lauren Meyers

Epidemic percolation networks (EPNs) are directed random networks that can be used to analyze stochastic "Susceptible-Infectious-Removed" (SIR) and "Susceptible-Exposed-Infectious-Removed" (SEIR) epidemic models, unifying and generalizing previous uses of networks and branching processes to analyze mass-action and network-based S(E)IR models. This paper explains the fundamental concepts underlying the definition and use of EPNs, using them to build intuition about the final outcomes of epidemics. We then show how EPNs provide a novel and useful perspective on the design of vaccination strategies.

1. Introduction

With the continual improvement of computing power, individual-based models of infectious disease spread have become more popular. These models allow us to incorporate stochastic effects, and individual-scale detail in ways that cannot be captured in more traditional models. In this paper, we review a framework based on directed random networks that unifies a range of individual-based models in closed populations, simplifying their analysis. We then show how this framework provides a new and potentially useful perspective on the design of vaccination strategies.

Directed random networks that we call *epidemic percolation networks* (EPNs) can be used to understand the final outcomes of stochastic "Susceptible-Infected-Removed" (SIR) and "Susceptible-Exposed-Infectious-Removed" (SEIR) epidemic models. In these models, susceptible persons are infected upon infectious contact with an infectious person. Once infected, they either become infectious immediately (in SIR models) or become infectious after a *latent period* (in SEIR models). Infectious persons eventually recover, after which they can neither infect others nor be infected. The number of persons infected in an epidemic is called the *size* of the epidemic, and the proportion of the population infected is called the *attack rate*. The average number of persons infected by a typical infectious person in the early stages of an epidemic is called the *basic reproductive number* and denoted by R_0.

For simplicity, we assume the entire population is susceptible to infection at the beginning of an epidemic. When one or more persons are infected, there are two possible outcomes. In a *minor epidemic* or *outbreak*, the attack rate is negligible and transmission ceases because infected persons fail to make any infectious contacts. A *major epidemic* has a higher attack rate and transmission ceases because infected persons make infectious contact with previously infected persons. When $R_0 \leq 1$, major epidemics have probability zero. When $R_0 > 1$, both major and minor epidemics can occur, and the probability and attack rate of a major epidemic both increase as R_0 increases. (Mathematically, the distinction between major and minor epidemics is exact only in the limit of an infinite population size. In a finite population, there is a bimodal distribution of epidemic sizes when $R_0 > 1$.) This pattern was first recognized in

the 1950s [1], and it has proven to hold for almost all stochastic S(E)IR epidemic models, including mass-action and network-based models.

The idea of using networks to represent the final outcomes of stochastic epidemic models developed separately for *mass-action* models and *network-based* models. In a mass-action model, an infectious person i can make infectious contact with any other person, but the probability of infectious contact from i to any given $j \neq i$ is inversely proportional to the population size. In a network-based model, infection is transmitted across the edges of a *contact network*. An infectious person i can make infectious contact with $j \neq i$ only if there is an edge connecting i and j in the contact network. The number of neighbors of i and the probabilities of infectious contact from i to his or her neighbors when i is infectious are independent of the population size. Both mass-action and network-based models can be analyzed using EPNs. Related concepts have been used previously [2–7], generally as a theoretical tool for proving rigorous results. In fact, this approach deserves more attention as a general framework for exploring S(E)IR epidemics: it provides a powerful theoretical tool, efficient numerical methods, and a guide to vaccination strategy design. In this paper, we review the fundamental concepts underlying the definition and use of EPNs and give examples of their use in designing efficient vaccination strategies for both mass-action and network-based epidemic models.

2. Epidemic Percolation Networks

Informally, a single realization of the EPN is generated by considering each individual i separately, imagining i is infected, and drawing an arrow from i to all persons with whom he or she makes infectious contact. This gives us four possible edges in each unordered pair of nodes i and j:

(1) no edge between i and j,

(2) a directed edge from i to j ($i \rightarrow j$),

(3) a directed edge from j to i ($i \leftarrow j$),

(4) an undirected edge between i and j ($i \leftrightarrow j$).

An outgoing or undirected edge from i to j indicates that i will make infectious contact with j if i is ever infected. If i is infected and j is at the end of one of the outgoing or undirected edges from i, then j is either infected by i or infected from another source prior to receiving infectious contact from i. In either case, j is infected before i recovers from infection. If person j is infected, then all persons at the end of an outgoing or undirected edge starting from j will be infected before j recovers from infection, and so on. Eventually, all persons connected to i by a series of outgoing or undirected edges will be infected.

In the rest of this section, we formally define a general stochastic SEIR model, define its EPN, and describe the epidemic threshold in terms of the emergence of giant components in the EPN.

2.1. General Stochastic SEIR Model. Consider a closed population of n individuals assigned indices $1, \ldots, n$. Each individual is in one of four possible states: susceptible (S), exposed (E), infectious (I), or removed (R). Person i moves from S to E at his or her *infection time* t_i, with $t_i = \infty$ if i is never infected. After infection, i has a *latent period* of length ε_i, during which he or she is infected but not infectious. At time $t_i + \varepsilon_i$, i moves from E to I, beginning an *infectious period* of length ι_i. At time $t_i + r_i$, where $r_i = \varepsilon_i + \iota_i$ is the *recovery period*, i moves from I to R. Once in R, i can no longer infect others or be infected. The latent period is a nonnegative random variable with cumulative distribution function (cdf) $F_i^{\mathrm{E}}(\varepsilon)$ and the infectious period is a strictly positive random variable with cdf $F_i^{\mathrm{I}}(\iota)$. The recovery period is finite with probability one. An SIR model is an SEIR model where $\varepsilon_i = 0$ with probability one for all i.

An epidemic begins with one or more persons infected from outside the population, which we call *initial infections*. After becoming infectious at time $t_i + \varepsilon_i$, person i makes infectious contact with $j \neq i$ at time $t_{ij} = t_i + \varepsilon_i + \tau_{ij}^*$, where the *infectious contact interval* τ_{ij}^* is a strictly positive random variable with $\tau_{ij}^* = \infty$ if infectious contact never occurs. Since infectious contact must occur while i is infectious or never, $\tau_{ij}^* \in (0, \iota_i]$ or $\tau_{ij}^* = \infty$. We define infectious contact to be sufficient to cause infection in a susceptible person, so the infection time $t_j \leq t_{ij}$. Let $F_{ij}^*(\tau \mid \iota_i)$ denote the conditional cdf of τ_{ij}^* given ι_i. $F_{ij}^*(\tau \mid \iota_i)$ may depend on properties of i and j (such as age, immune status, contact intensity, etc.).

The general stochastic SEIR model can be turned into almost any standard epidemic model by choosing appropriate $F_i^{\mathrm{E}}(\varepsilon)$, $F_i^{\mathrm{I}}(\iota)$, and $F_{ij}^*(\tau \mid \iota_i)$.

Example 1. In the stochastic Kermack-McKendrick SIR model for a population of size n, infectious persons have a constant hazard μ of recovery and there is a constant hazard $\beta(n-1)^{-1}$ of infectious contact in every infectious-susceptible pair. This model can be obtained by taking

$$F_i^{\mathrm{I}}(\iota) = 1 - e^{-\mu\iota},$$
$$F_{ij}^*(\tau \mid \iota_i) = \begin{cases} 1 - e^{-\beta\tau/(n-1)} & \text{if } \tau \in (0, \iota_i], \\ 1 - e^{-\beta\iota_i/(n-1)} & \text{if } \tau \in (\iota_i, \infty). \end{cases} \quad (1)$$

Example 2. In the network-based analogue of the Kermack-McKendrick model, infection is transmitted across the edges of a contact network. It has the same infectious period distribution as the mass-action model but a constant hazard β of infectious contact that does not depend on n. Thus,

$$F_{ij}^*(\tau \mid \iota_i) = \begin{cases} 1 - e^{-\beta\tau} & \text{if } \tau \in (0, \iota_i], \\ 1 - e^{-\beta\iota_i} & \text{if } \tau \in (\iota_i, \infty), \end{cases} \quad (2)$$

whenever i and j are connected in the contact network. When i and j are not connected, $\tau_{ij}^* = \infty$ with probability one.

2.2. Time Homogeneity and the EPN. The general stochastic epidemic model is *time-homogeneous*, which means that the latent period, infectious period, and infectious contact interval distributions are specified *a priori*. This gives us two equivalent ways to run the model.

(1) First, we can sample "on the fly" for each new infection i by generating a latent period ε_i and an infectious period ι_i and then sampling τ_{ij}^* from its conditional distribution given ι_i for each $j \neq i$.

(2) Second, we can sample *a priori* by generating ε_i and ι_i for each i and then sampling τ_{ij}^* from the appropriate conditional distribution for each ordered pair ij before starting the epidemic. We then look up these values as we need them to run the model.

Sampling on the fly is more efficient if the goal is to produce just a single epidemic realization, but sampling *a priori* provides information about many possible epidemics and leads to the definition of the EPN. A single realization of the EPN can be generated as follows.

(1) For each individual i,

   (a) sample a latent period ε_i from $F_i^{\mathrm{E}}(\varepsilon)$,
   (b) sample an infectious period ι_i from $F_i^{\mathrm{I}}(\iota)$,
   (c) for each $j \neq i$, sample an infectious contact interval τ_{ij}^* from $F_{ij}^*(\tau \mid \iota_i)$.

(2) For each pair of individuals i and j,

   (a) if $\tau_{ij}^* < \infty$ and $\tau_{ji}^* < \infty$, draw an undirected edge between i and j,
   (b) if $\tau_{ij}^* < \infty$ and $\tau_{ji}^* = \infty$, draw a directed edge from i to j,
   (c) if $\tau_{ij}^* = \infty$ and $\tau_{ji}^* < \infty$, draw a directed edge from j to i,
   (d) if $\tau_{ij}^* = \infty$ and $\tau_{ji}^* = \infty$, draw no edge between i and j.

The time homogeneity assumption guarantees that ε_i, ι_i, and each τ_{ij}^* are chosen from the correct distributions regardless of when node i actually becomes infected. For a population of size n, there are up to $2^{n(n+1)}$ possible realizations of the EPN, each with a different edge set. The probability of each possible edge set is determined by the underlying SEIR model.

2.3. Degrees, Components, and Epidemics. The most important properties of the EPN are its degree distribution and its component size distributions. The *indegree*, *outdegree*, and *undirected degree* of node i are the number of incoming, outgoing, and undirected edges incident to i. The degree distribution of the EPN is the joint distribution of these degrees over the nodes in the network. The *in-component* of node i is the set of nodes from which i can be reached by following a series of edges in the correct direction. The *out-component* of node i is the set of nodes that can be reached from i by following a series of edges in the correct direction. In both definitions, undirected edges can be crossed in either direction and the in- and out-components of node i include i itself. If any node in the in-component of i is infected, then i will be infected eventually. If i is infected, then every node in the out-component of i will be infected eventually. Since the EPN is a random network, each node does not have fixed in-, out-, or undirected degrees or fixed in- and out-components (though these are fixed in any single realization of the EPN). However, the distribution of the out-component sizes of node i is exactly the same as the distribution of epidemic sizes obtained in repeated runs of the corresponding S(E)IR model with i as the initial infection [8, 9].

This property of the EPN has several useful consequences. The epidemic threshold of an S(E)IR model corresponds to the emergence of *giant components* in the EPN. A *strongly connected component* is a group of nodes in which each node can be reached from every other node by following a series of edges. The nodes in a strongly connected component all have the same in-component and the same out-component. The EPN for a model below the epidemic threshold consists of many small strongly connected components. The EPN for a model above the epidemic threshold consists of a single *giant strongly connected component* (GSCC) and many small strongly connected components. The in- and out-components of nodes in the GSCC are called the *giant in-component* (GIN) and the *giant out-component* (GOUT). A schematic diagram of the giant components is in Figure 1. If all initial infections occur outside the GIN, a minor epidemic occurs because the out-components of all initial infections are small. If an initial infection occurs in the GIN, infection spreads to the GSCC and to the rest of the GOUT, so there is a major epidemic. If a single initial infection is chosen randomly, the distribution of outbreak sizes is equal to the distribution of small out-component sizes and the probability of a major epidemic is equal to the proportion of the network contained in the GIN. No matter where a major epidemic starts, its attack rate is equal to the proportion of the network contained in the GOUT.

3. Analysis of Stochastic SEIR Models

In the limit of large n, almost all realizations of the EPN have the same degree distribution and the same distribution of in-, out-, and strongly connected component sizes, so a great deal of information is contained in a single realization of the EPN for an S(E)IR model with a large population. For many models, the asymptotic distribution of small component sizes and the proportion of the network contained in each of the giant components—and hence the outbreak size distribution and the asymptotic probability and attack rate of a major epidemic—can be calculated using probability generating functions [8–10]. In this section, we show how the analysis of mass-action and network-based SEIR models using EPNs and probability generating functions is a generalization of earler methods. We also show that EPNs are a useful theoretical tool and a powerful numerical tool for simulating S(E)IR epidemics in closed populations.

To demonstrate the accuracy of the EPN framework, we compare theoretical predictions of the probability and attack rate of a major epidemic based on EPNs with observations from a series of simulations of mass-action and network-based models. These simulations were implemented in Python (http://www.python.org/)

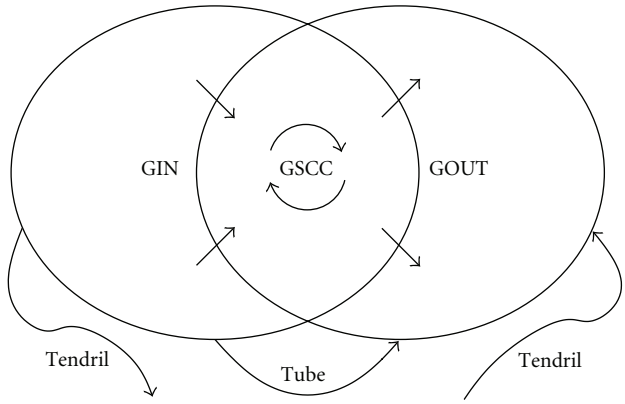

Figure 1: Schematic diagram of the giant components of an EPN. Note that the GIN and GOUT both include the GSCC. Tendrils are directed paths out of the GIN or into the GOUT that do not enter or leave the GSCC; a tube is a tendril that goes from the GIN to the GOUT. An initial infection in the GIN will lead to the infection of the entire GOUT (including the GSCC). If the initial infection is outside the GSCC, it will also infect a few tendrils or tubes and a few nodes in the GIN outside the GSCC. Since these are small components, their existence does not affect the calculation of the asymptotic probability and attack rate of a major epidemic. Adapted from [19].

using the SciPy (http://www.scipy.org/) [11] and NetworkX (http://networkx.lanl.gov/) [12] packages. The code is available as online supplementary material (see Supplementary Material available online at doi:10.1155/2011/543520).

3.1. EPNs for Mass-Action Models. In mass-action SEIR models like Example 1, infectious contact is possible between any two individuals, but the probability of infectious contact is inversely proportional to the population size. (Mathematically, the cumulative hazard of infectious contact is inversely proportional to the population size, but the cumulative hazard and the probability are approximately equal for very small probabilities.) There is a long tradition of approximating the initial spread of infection using a branching process [1, 13–15]. In a branching process, one or more initial nodes have offspring, where the number of offspring is a random sample from a given discrete distribution. Their offspring have offspring according to the same distribution, and so on. The *total size* of the branching process is the total number of individuals produced. When the mean number of offspring is greater than one, there is a positive probability that the branching process "explodes," continuing forever and producing an infinite population. The total size distribution and the explosion probability can be calculated using probability generating functions.

For mass-action models with independent infectiousness and susceptibility, the outbreak size distribution and the probability and attack rate of a major epidemic can be predicted using branching process approximations that become exact in the limit of large n [14]. In the "forward" branching process, the offspring of each infection are the people he or she infects. In the "backward" branching process, the offspring of each infection are the people who would have infected the parent had they been infected. Asymptotically, the outbreak size distribution is equal to the distribution of finite total sizes in the forward branching process, and the probability of an epidemic is equal to the probability that the forward branching process explodes. The attack rate of a major epidemic is asymptotically equal to the probability that the backward branching process explodes. For these models, the out-component size distribution in the EPN is identical to the total size distribution of the forward branching process and the in-component size distribution of the EPN is identical to the total size distribution of the backward branching process. Thus, the EPN predicts the same outbreak size distribution and probability and attack rate of a major epidemic as the branching process approximations. When infectiousness and susceptibility are not independent, the branching process approximations break down but the EPN predictions remain correct [9]. In this case, the probability generating functions in the EPN approach are similar to those of a branching process, but they allow the number of offspring in the first generation (i.e., the initial infections) to have a different distribution than the number of offspring in all subsequent generations.

Figure 2 shows the observed and predicted probabilities and attack rates of a major epidemic in a series of mass-action SIR models. Each model had a population of 50,000. The observed probability of a major epidemic was the number of epidemics with a final size $\geq$250 out of 1,000 runs. The observed final size of an epidemic was based on a single major epidemic, which was defined as an epidemic with a final size $\geq$250. All models have a mean infectious period of one. There are three series of models: one with a fixed infectious period, one with an exponentially distributed infectious period, and one where the infectious period has a Weibull distribution with shape parameter 0.5. At each R_0, these distributions produce different probabilities of a major epidemic but the same attack rate. The predicted probability and attack rate of a major epidemic are equal only when the infectious period is fixed.

3.2. EPNs for Network-Based Models. In a network-based SEIR model, infection is transmitted across the edges of a contact network. For network-based models, analysis via EPNs can be seen as a generalization of analysis via bond percolation models, first used to calculate the attack rate of a major epidemic [16] and later extended to the size distribution of minor epidemics and the probability of a major epidemic [17]. In this approach, each edge in the contact network is erased with probability $1 - T$, where T is the marginal probability of infectious contact from an infected node to a neighbor. When infectiousness and susceptibility are constant, the distribution of minor epidemic sizes is equal to the distribution of small component sizes, the epidemic threshold corresponds to the emergence of a giant component in the posterasure contact network, and the probability and attack rate of a major epidemic are both equal to the proportion of the network contained in the giant component.

To illustrate this approach and its limitations, we generalize the network-based Kermack-McKendrick model from

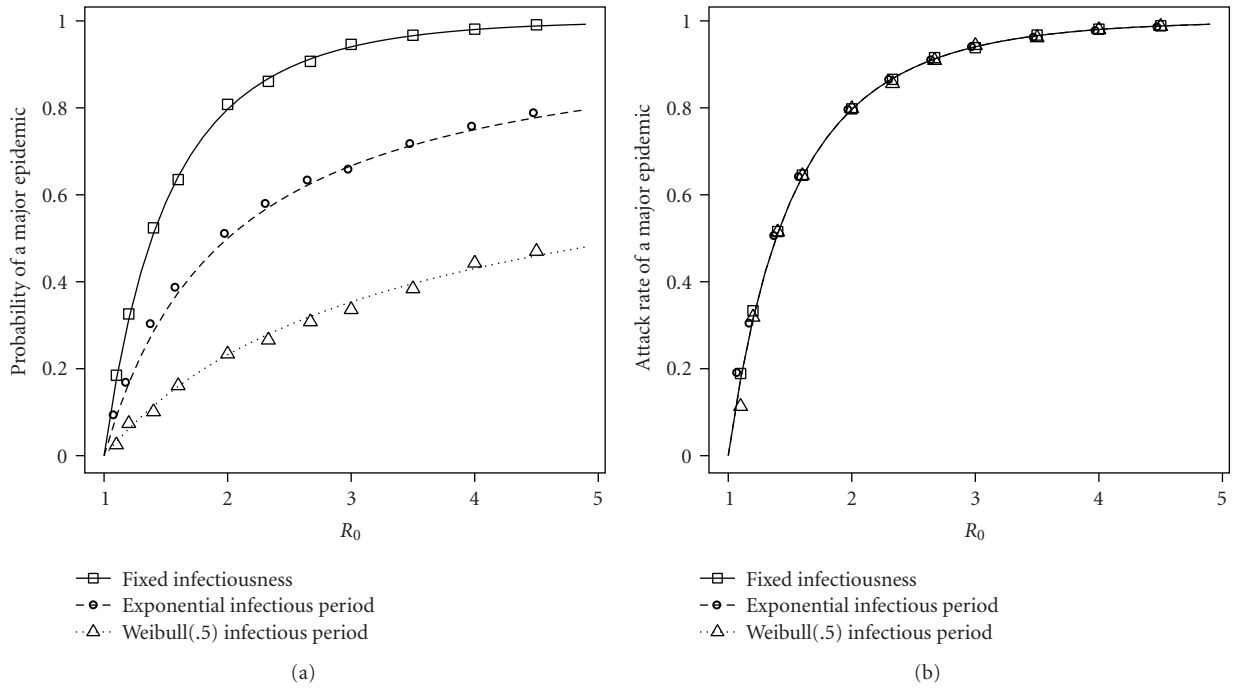

Figure 2: Major epidemic probabilities and attack rates in the mass-action models from Section 3.1. Lines represent theoretical predictions based on EPNs, and symbols represent observed probabilities and attack rates in simulations. The observed probability of a major epidemic is based on 1,000 runs of each model, where a major epidemic was defined as an epidemic with a final size ≥250. The observed attack rate is based on a single major epidemic. All models have a population of size 50,000. The predicted probability and attack rate of a major epidemic are equal only when the infectious period is fixed.

Example 2 by allowing it to have an arbitrary infectious period distribution. In the corresponding bond percolation model, each edge in the contact network would be retained independently with probability

$$T = \int_0^\infty 1 - e^{-\beta\iota} \mathrm{d}F^{\mathrm{I}}(\iota), \tag{3}$$

where $1-\exp(-\beta\iota)$ is the conditional probability of infectious contact given an infectious period of ι and $\mathrm{d}F^{\mathrm{I}}(\iota)$ represents integration or summation over the infectious period distribution. When the infectious period is fixed, the bond percolation model and the EPN predict exactly the same distribution of outbreak sizes and the same probability and attack rate of a major epidemic (which are equal in this case). However, the bond percolation model does not predict the correct outbreak size distribution or probability of an epidemic if the infectious period is variable.

Example 3. Consider a network-based Kermack-McKendrick model that has an exponential infectious period with mean one. The probability that a single initial infection with 2 neighbors fails to transmit infection is

$$\int_0^\infty e^{-(2\beta+1)\iota}\, d\iota = \frac{1}{2\beta+1}, \tag{4}$$

which is the probability that the corresponding node has an out-component of size one in the EPN. In the bond percolation model, (3) gives us $T = \beta(\beta+1)^{-1}$, so the probability that both edges incident to the initial infection get erased is

$$(1-T)^2 = \frac{1}{\beta^2+2\beta+1} < \frac{1}{2\beta+1}. \tag{5}$$

Thus, the bond percolation model underestimates the probability of an outbreak of size one. The bond percolation model treats infection of the two neighbors as independent events, but they are positively correlated because both are affected by the infectious period of the initial node. This limitation of the bond percolation model also affects contact networks that include directed edges, as considered in [18]. To see this, replace the undirected edges in this example with any combination of outgoing and undirected edges.

In this class of models, the bond percolation model overestimates the probability of a major epidemic whenever there is a variable infectious period [8, 10]. To demonstrate this, we conducted a series of simulations on Erdős-Rényi networks with mean degree 5. Each model had a population of 50,000. The observed probability of a major epidemic was the number of epidemics with a final size ≥250 out of 1,000 runs. The observed final size of an epidemic was based on a single major epidemic, defined as an epidemic with a final size ≥250. One series of simulations had a fixed infectious period of one, the second series had an exponentially distributed infectious period with mean one, and the third series had infectious persons transmit to all or none of their contacts. The first and last models define

the upper and lower bounds, respectively, of the epidemic probability for models with independent infectiousness and susceptibility [10].

For a given R_0, all three models have the same T, so they should have identical major epidemic probabilities and attack rates according to the bond percolation framework. In addition, the bond percolation framework implies that the probability and attack rate are always equal. However, Figure 3 clearly shows that the three models produce different major epidemic probabilities but equal attack rates. The probability and attack rate are equal only in models with a fixed infectious period. In models with variable infectiousness, the probabilities are lower than the attack rates. The EPN predictions of probability and attack rate are accurate for all of these models.

In these examples and the models considered in [17], there is variable infectiousness but constant susceptibility. When models have variable infectiousness and susceptibility, the bond percolation approach can predict the wrong attack rate for a major epidemic in addition to the wrong outbreak size distribution and probability of a major epidemic [10]. The EPN is very similar to the "locally dependent random graph" [4] for SIR epidemics on lattices, which was used to show that SIR models on lattices reduce to bond percolation processes if and only if the infectious period is constant [20]. In these and all other time-homogeneous S(E)IR models on networks, an analysis based on EPNs predicts the correct minor epidemic size distribution and the correct probability and attack rate of a major epidemic.

3.3. EPNs as a Theoretical Tool. Most stochastic simulations of epidemic spread provide dynamic information about the spread of an epidemic. In contrast, a realization of an EPN is a static object, so many more mathematical tools are available to analyze it. To calculate the probability of a major epidemic, it suffices to calculate the proportion of nodes in the GIN. To calculate the attack rate, it suffices to calculate the proportion in the GOUT. In the infinite population limit, this is equivalent to calculating the probability that the EPN has an infinite path directed into or out of a randomly chosen node. This justifies the branching process approximation for mass-action models, and a similar approach is appropriate in networks without short cycles. These lead to analyses based on probability generating functions for the bond percolation model [17] and for EPNs [8–10].

More generally, however, we cannot use probability generating functions when the branches of the initial spread of infection intersect with asymptotically nonzero probability. Thus, we need different approaches to calculate the size and probability of an epidemic on a network with short cycles. This can be done numerically with EPNs as described below, but we can also use EPNs to make rigorous statements about the disease spread.

For example, if we want to analyze the impact a single individual has on an epidemic, a standard stochastic model would require many simulations. With an EPN approach, we are able to generate a realization of the EPN, including edges between all other nodes, and then consider the impact of each possible edge involving the targeted individual. This approach was used in [21] to investigate the impact of heterogeneity in the population. This paper compared two different random rules (with identical average) for assigning each node's infectiousness and susceptibility (independently of other nodes and each other), showing that the rule which provides a more homogeneous population results in larger and more probable epidemics. The approach was to choose a node u and consider any EPN realization created without edges involving u. Then the infectiousness and susceptibility of u would be assigned and the edges involving u chosen. It was then proven that regardless of how the remainder of the EPN was assigned, the size of in- and out-components would be maximized by the more homogeneous assignment rule.

3.4. EPNs as a Numerical Tool. EPNs are a powerful numerical tool for the simulation and analysis of epidemics. Traditionally, the probability and attack rate of a major epidemic in an S(E)IR model are estimated by running the model repeatedly. For each run, we record whether a major epidemic occurred and, if so, we record the attack rate. Whether a major epidemic occurs is a binomial process where each run of the model is like a single coin flip. When an epidemic occurs, the size has only a small variation. Thus, repeated simulation produces an accurate estimate of the attack rate much faster than the probability. In a model with a sufficiently large population, the probability and attack rate of a major epidemic can be calculated with equal precision from a single realization of the EPN. Tarjan's algorithm [22] can be used to identify the GSCC, GIN, and GOUT in a time that is linear in the population size n. The sizes of the giant components vary by an amount of order $\ln n$, so the proportional error is small for large n.

In Figure 4, we compare the result from a single EPN and the results from 50 simulations with the exact calculations in the infinite population limit. We consider three different models for the spread of a disease: exponentially distributed infectious periods, all-or-nothing infectiousness, and all-or-nothing susceptibility. In all-or-nothing infectiousness, a proportion of the population infects every susceptible neighbor, while the remainder infect none. In all-or-nothing susceptibility, a proportion become infected if any neighbor is ever infected, while the remainder are never infected. In the simulations, a single initial infection was chosen at random. At each R_0, the calculations of a single EPN took approximately 1/3 the time of simulating 50 epidemics. We find that either approach does very well at predicting the attack rate. However, the probability of an epidemic is poorly predicted by the simulations because the convergence of a binomial process is relatively slow. If the population had short cycles, the exact calculations used to predict the probability and attack rate would fail. In that case, a single EPN would provide an accurate numerical prediction of the probability of a major epidemic much faster than repeated simulations.

Although our attention has focused on static quantities such as the probability or size of major epidemics, EPNs can also be used to calculate the dynamic spread of an epidemic. Returning to the generation algorithm described in Section 2.2, we can assign a latent period ε_i to each node i.

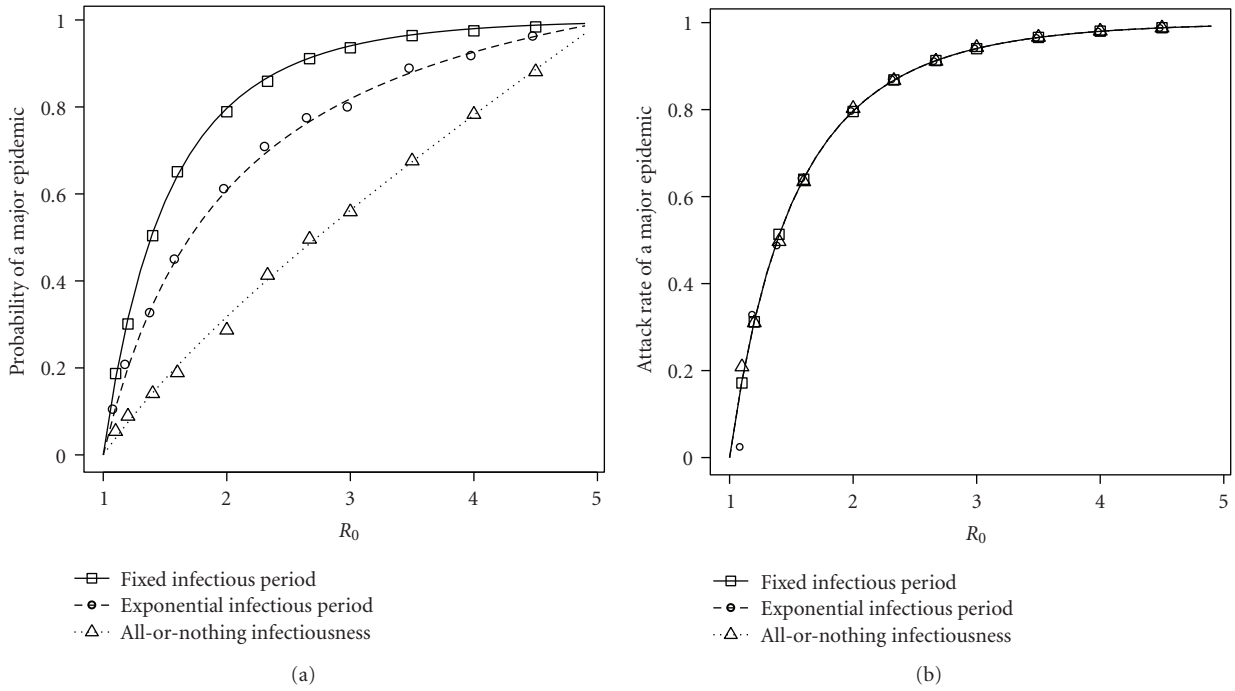

FIGURE 3: Major epidemic probabilities and attack rates in network-based models from Section 3.2. Lines represent theoretical predictions based on EPNs and symbols represent observed probabilities and attack rates in simulations. The observed probability of a major epidemic is based on 1,000 runs of each model, where a major epidemic was defined as having a final size ≥250. The observed attack rate is based on a single major epidemic. All models have a population of size 50,000 and an Erdős-Rényi contact network with mean degree 5. The predicted probability and attack rate of a major epidemic are equal only when the infectious period is fixed.

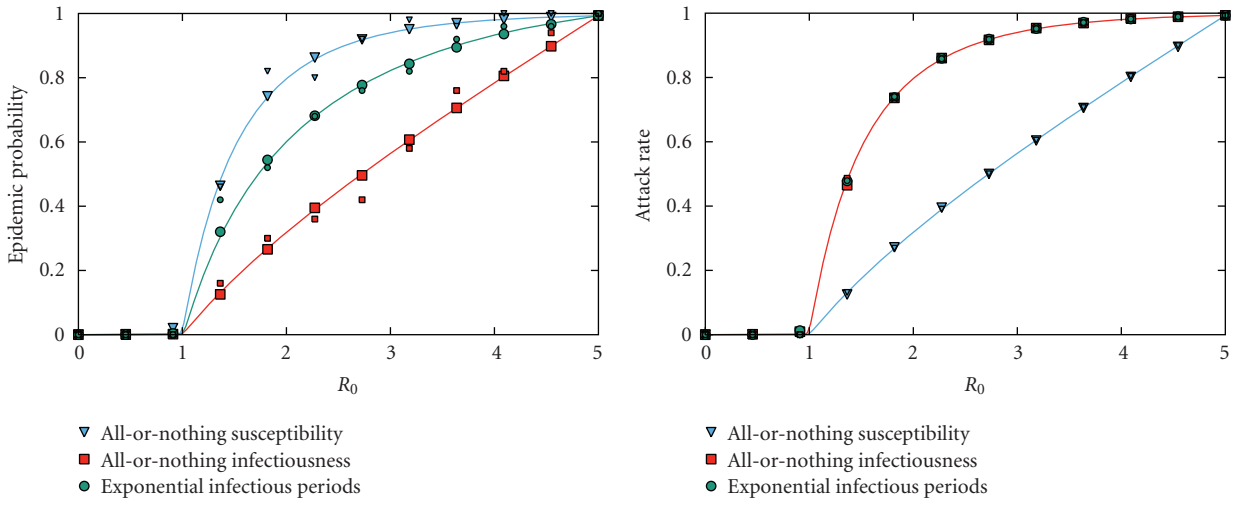

FIGURE 4: A comparison of the predictions from a single EPN with 50 simulations for three different epidemic processes on an Erdős-Rényi network of 50,000 nodes with average degree 5. The EPN results (large symbols) closely match the calculated predictions in the asymptotic limit. The simulated results (small symbols) compare well for size but poorly for probability. Generating an EPN is a much more efficient numerical method for estimating the probability of a major epidemic than simulation.

For each ordered pair with $\tau_{ij}^* < \infty$, we can assign a time of $\varepsilon_i + \tau_{ij}^*$ to the edge from i to j in the EPN (similarly, if $\tau_{ji}^* < \infty$, assign a time of $\varepsilon_j + \tau_{ji}^*$ to the opposite direction). The time associated with eamch edge can be thought of as the "length" of the edge. If an epidemic begins with a single initial infection at time zero, the infection time of node i is simply the total length of the shortest path from the initial infection to node i. If no such path exists, i is never infected. These paths and their lengths can be found in time proportional to $n \ln n$ using Dijkstra's algorithm [23]. Thus, EPNs provide an

extremely efficient way to get complete runs of an epidemic model, including time dynamics as well as the final outcome. By choosing a different initial infection each time, many nearly independent runs of the SEIR model can be obtained from a single EPN.

4. Vaccination Strategies

In this section, we show how EPNs provide a useful guide to the design of efficient vaccination strategies in mass-action and network-based SEIR models. For simplicity, we assume that we have a perfect vaccine that makes its recipients immune to infection. The effect of the vaccine can be represented by erasing all incoming, outgoing, and undirected edges incident to each vaccinated node in the EPN. Since a major epidemic is possible if and only if there is a GSCC, we hypothesized that vaccine should be targeted to nodes with a high probability of inclusion in the GSCC and a high number of connections to nodes in GSCC.

4.1. Vaccination in Mass-Action Models. To test the effect of this targeting strategy in a mass-action model, we created a mass-action model with three subpopulations, A, B, and C, of equal size. Subpopulation A had high infectiousness but low susceptibility, subpopulation B had average infectiousness and susceptibility, and subpopulation C had low infectiousness but high susceptibility. Within subpopulation A, each node had a relative susceptibility that was exponentially distributed with mean one. Within subpopulation C, each node had a relative infectiousness that was exponentially distributed with mean one. Subpopulation A had the highest probability of being in the GIN, subpopulation B had the highest probability of being in the GSCC, and subpopulation C had the highest probability of being in the GOUT. With no vaccination, $R_0 = 2.14$ and the probability and attack rate of a major epidemic are both equal to .72. The EPN for this model is summarized in Table 1. Calculations of R_0 and the probability and attack rate of a major epidemic at different vaccination fractions in each subpopulation were done using probability generating functions [9, 10].

Results. The results of the three vaccination strategies are shown in Figures 5 and 6. Vaccinating subpopulation A was optimal for reducing the probability of an epidemic because its members were the most infectious and the most likely to be in the GIN. Vaccinating subpopulation C was optimal for reducing the attack rate of an epidemic because its members were the most susceptible and the most likely to be in the GOUT. Vaccinating subpopulation B was nearly optimal for reducing both the probability and attack rate of a major epidemic because its members had the right combination of infectiousness and susceptibility to make them the most likely to be in the GSCC. Vaccinating any of the three subpopulations produced exactly the same effect on R_0, but vaccinating subpopulation B was most effective in reducing the overall risk of infection given a single initial infection. The theory of EPNs gives us intuitive explanations for all of these effects.

Table 1: Summary of the mass-action model from Section 4.1. Subpopulation A has high infectiousness but low susceptibility, subpopulation B has average infectiousness and susceptibility (by both arithmetic and geometric mean), and subpopulation C has low infectiousness but high susceptibility. Nodes in subpopulation B have the highest probability of being in the GSCC and the highest expected number of edges connecting them to other nodes in the GSCC.

Subpopulation	A	B	C
Mean outdegree (infectiousness)	5	2.5	1.25
Mean indegree (susceptibility)	1.25	2.5	5
. Pr (causes epidemic)	.951	.779	.430
Pr (infected in epidemic)	.430	.779	.951
Pr (in GSCC)	.409	.607	.409
Mean degree within GSCC	.835	.942	.835

4.2. Vaccination in Network-Based Models. The standard approach to vaccination targeting in network-based models is to target nodes with high degree in the contact network [24, 25]. However, this approach ignores all information about the disease other than the contact network itself. An approach based on the EPN uses information about both the contact network and the epidemiological characteristics of the disease. In a series of epidemic models, we compared two vaccine-targeting strategies, each represented by a ranked list of nodes to vaccinate. For the first strategy, we ranked the nodes by degree in the contact network. For the second, we generated a single realization of the EPN and ranked nodes in the GSCC by the number of edges connecting them to other nodes in the GSCC, ignoring direction. Nodes outside the GSCC were placed in random order at the bottom of the list. For a vaccination fraction of v, the first nv nodes on each list would be vaccinated, where $n = 100{,}000$ was the population size.

To compare the two vaccination strategies, we estimated the probability and attack rate of a major epidemic as a function of the vaccination fraction v. For each v, we generated ten independent realizations of the EPN and estimated the probability and attack rate of an epidemic by calculating the mean proportion of the population in the GIN and the GOUT, respectively. We compared strategies on two different types of contact networks: an Erdős-Rényi network with mean degree five and a scale-free network with $\alpha = 2$ and an exponential cutoff around 50. If p_k denotes the probability that node has degree k, then $p_k \propto 5^k/k!$ in the Erdős-Rényi network and $p_k \propto k^{-2} \exp -k/50$ in the scale-free network.

When all nodes have the same infectiousness and susceptibility, we expect to see no difference between the two strategies because degree in the contact network is the only determinant of a node's probability of being in the GSCC. To represent the effects of variation in susceptibility and infectiousness, we allowed the transmission probability from node i to node j to be

$$p_{ij} = 1 - e^{-100 \times \inf_i \times \sus_j}, \tag{6}$$

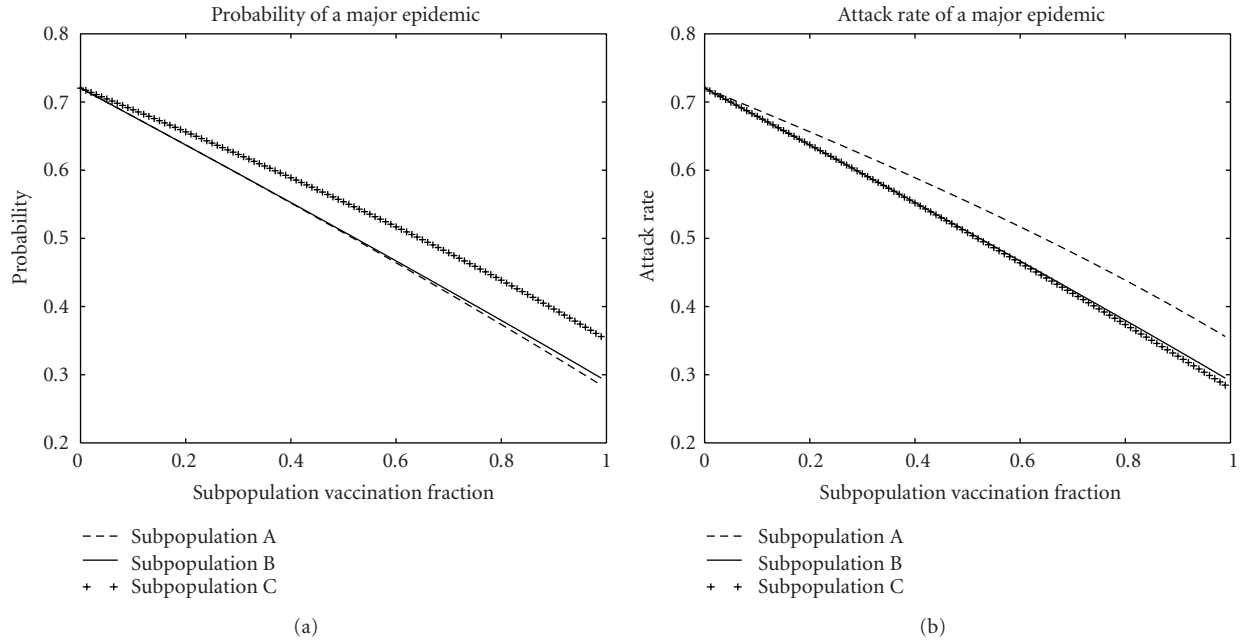

Figure 5: Effects of vaccination on the probability and attack rate of a major epidemic in the mass-action model from Section 4.1. Vaccinating subpopulation A, the most infectious and least susceptible, is optimal for reducing the probability. Vaccinating subpopulation C, the most susceptible and least infectious, is optimal for reducing the attack rate. Vaccinating subpopulation B, of average infectiousness and susceptibility, is nearly optimal for both.

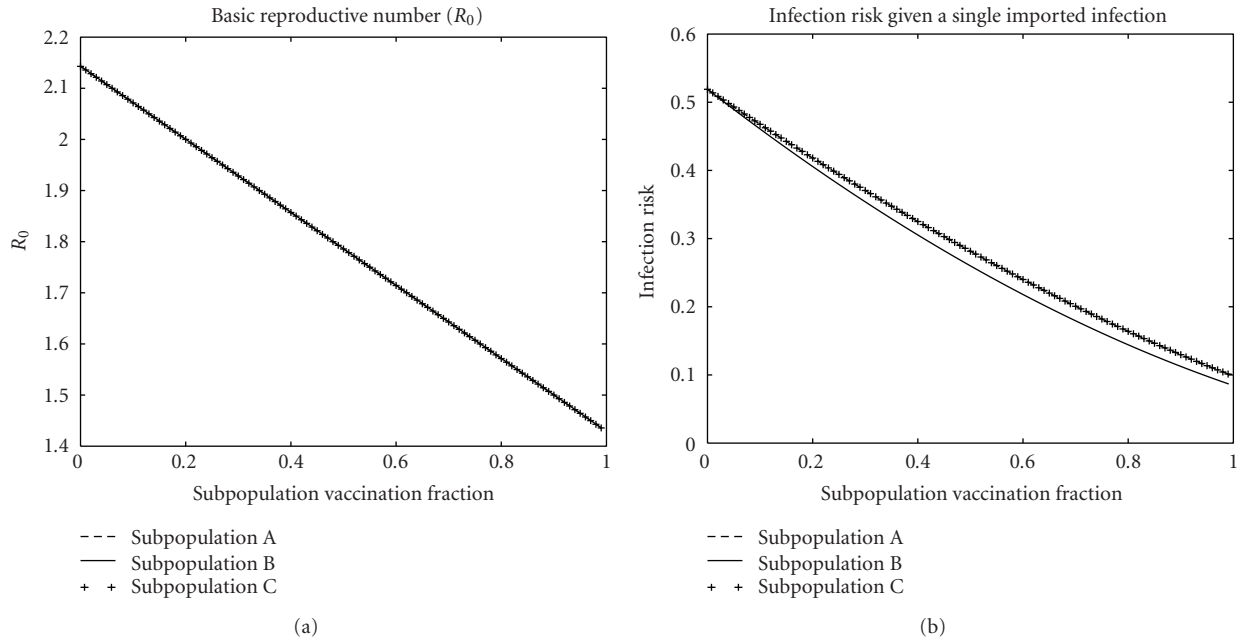

Figure 6: Effects of vaccination on R_0 and the risk of infection given a single randomly chosen initial infection (the probability of a major epidemic times the attack rate) in the mass-action models from Section 4.1. Though all three vaccination strategies have the same effect on R_0, vaccinating subpopulation B is optimal for reducing the overall risk of infection.

where $0 < \text{inf}_i < 1$ represents the infectiousness of i and $0 < \text{sus}_j < 1$ represents the susceptibility of node j. We allowed inf_i and sus_i to have different beta distributions. A beta(2, 2) distribution has a single peak at 0.5, so there is little variation in infectiousness and susceptibility. A beta(.25, .25) distribution has peaks near zero and one, so most nodes have either very high or very low infectiousness (or susceptibility). In our primary models, inf_i and sus_i were chosen independently from the specified beta distribution. To look at the effects of positive and negative correlations

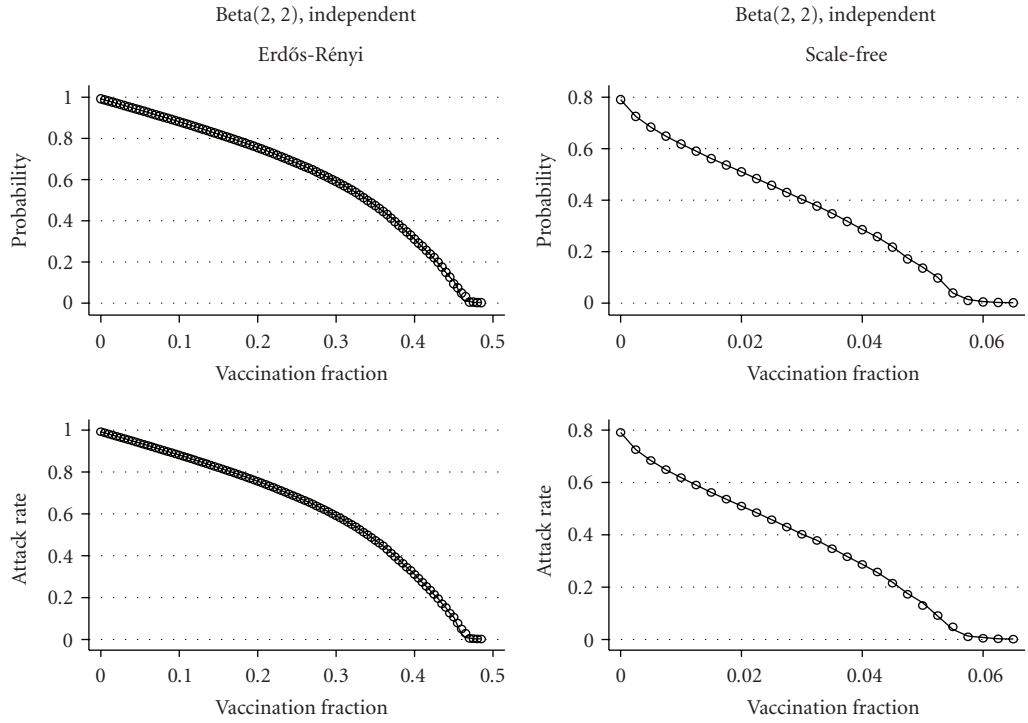

(a)

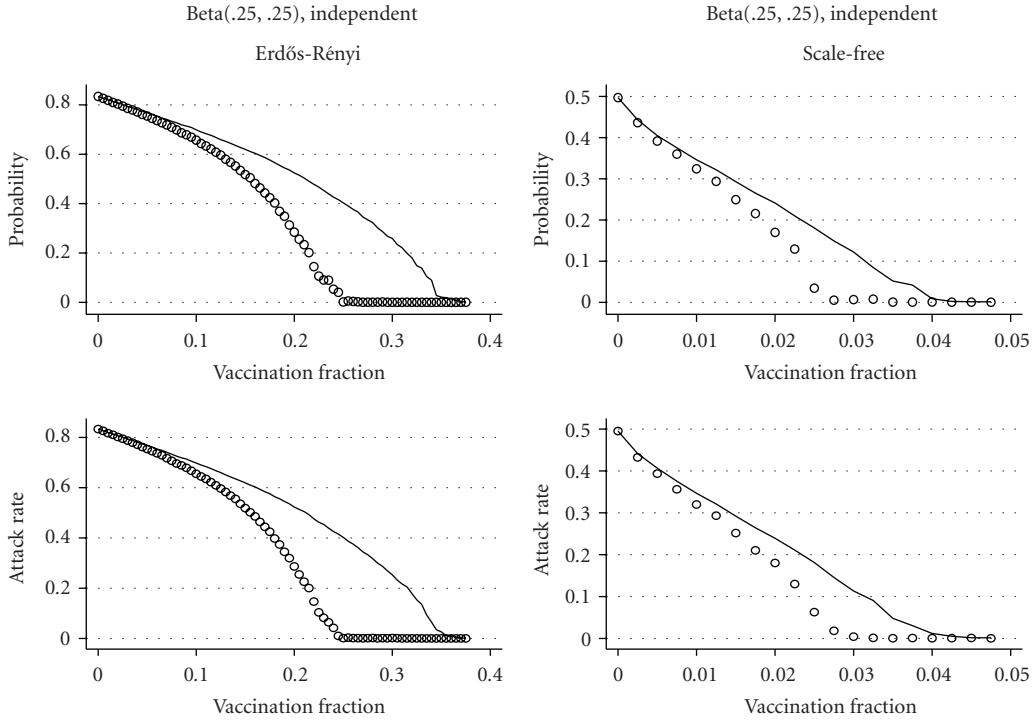

(b)

Figure 7: Comparison of targeting by contact network degree (lines) and targeting the GSCC (circles) in the network-based model from Section 4.2 with independent susceptibility and infectiousness. When infectiousness and susceptibility have beta(2, 2) distributions, the two strategies produce nearly identical results. When they have beta(.25, .25) distributions, targeting the GSCC is more effective in reducing both the probability and attack rate of major epidemics on both Erdős-Rényi and scale-free networks.

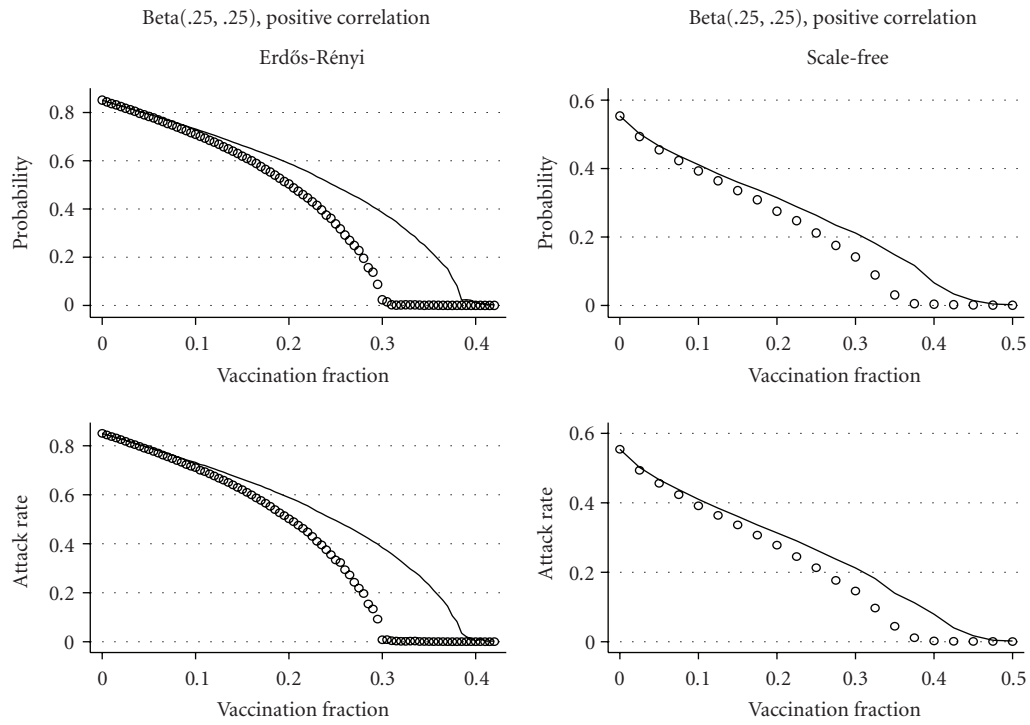

(a)

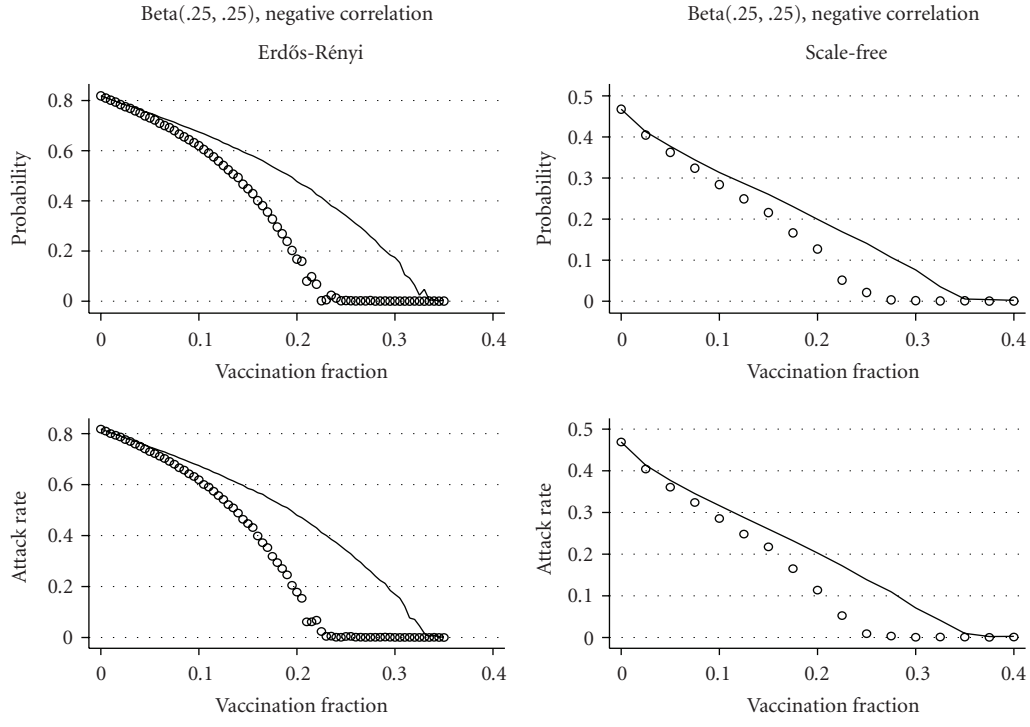

(b)

Figure 8: Comparison of targeting by contact network degree (lines) and targeting the GSCC (circles) in the network-based models from Section 4.2 with beta(.25, .25) distributions of infectiousness and susceptibility and positive or negative correlations. In both cases, targeting the GSCC is more effective in reducing the probability and attack rate of an epidemic on both Erdős- Rényi and scale-free networks. In the corresponding models with beta(2, 2) distributions of infectiousness and susceptibility, targeting the GSCC and targeting by contact network degree had identical effects (not shown).

of infectiousness and susceptibility, we also compared the strategies in positively correlated models, where $\text{inf}_i = \text{sus}_i$, and negatively correlated models, where $\text{inf}_i = 1 - \text{sus}_i$.

Results. The results of the comparison for a model with independent infectiousness and susceptibility are shown in Figure 7. As expected, we see almost no difference in the effectiveness of the two strategies when inf and sus have beta(2, 2) distributions. When inf_i and sus_i have beta(.25, .25) distributions, targeting vaccination to the GSCC is much more effective in reducing both the probability and attack rate of a major epidemic than targeting nodes with high degree in the contact network. Figure 8 shows similar results for models with positive and negative correlations between infectiousness and susceptibility. Targeting vaccination to the GSCC of the EPN takes advantage of information about the epidemiology of the disease that targeting to nodes with high degree in the contact network does not, and this makes a substantial difference in the effectiveness of the vaccination strategy.

5. Discussion

EPNs provide a very useful intuitive point of view when thinking about the behavior of stochastic SEIR epidemic models. The "bow-tie" diagram in Figure 1 provides a simple visual explanation for the following basic facts.

(i) The ultimate outcome of an epidemic does not depend on where it starts.

(ii) The probability and attack rate of an epidemic must be both zero or both positive, so there is a single epidemic threshold.

(iii) In general, vaccinating the highly infectious (i.e., those likely to be in the GIN) will reduce the probability of a major epidemic, and vaccinating the highly susceptible (i.e., those likely to be in the GOUT) will reduce its attack rate. Vaccinating those likely to be in the GSCC will reduce both.

The ideal vaccination targets are not necessarily the most infectious or the most susceptible individuals. Instead, they are those individuals with the right combination of infectiousness and susceptibility to be effective receivers and transmitters of infection. It is precisely these nodes that hold together the GSCC of the EPN. In Section 4, we showed that targeting vaccine to nodes likely to be in the GSCC and highly connected within the GSCC was an efficient intervention strategy for both mass-action and network-based models. The correspondence between the epidemic threshold in an SEIR model and the emergence of the GSCC in its EPN makes elimination of the GSCC a necessary and sufficient condition for the elimination of disease transmission in a population.

The primary limitation of EPNs is that they are defined only for time-homogeneous SEIR models. They cannot accurately represent the final outcomes of complex, time-dependent SEIR models and interventions. For example, they cannot accurately represent seasonality, the effects of changing behavior or demographics, or the effects of an intervention that is implemented only when a certain prevalence of infection is reached. The vaccination strategies in Section 4 were all prevaccination strategies, where the population was vaccinated prior to the beginning of disease spread. If vaccination began after an epidemic had already started, as was the case in the recent influenza A(H1N1) pandemic, its effects could not be represented accurately using an EPN.

Nonetheless, EPNs generalize earlier approaches to the analysis of mass-action and network-based models, providing a simple unified framework for the analysis and implementation of time-homogeneous S(E)IR models. They are powerful theoretical and practical tools, and they represent an important application of networks in infectious disease epidemiology.

Acknowledgments

The authors thank Aric Hagberg and Leon Arriola for their comments on the vaccination strategy research, which was done primarily at the Los Alamos Mathematical Modeling and Analysis Summer Institute in 2007 at Los Alamos National Laboratory (LANL). E. Kenah was supported by National Institutes of Health (NIH) cooperative agreement 5U01GM076497 at the Harvard School of Public Health and National Institute of General Medical Sciences (NIGMS) grant F32GM085945 at the University of Washington. Office space and administrative support for E. Kenah was provided by the Fred Hutchinson Cancer Research Center. J. C. Miller was supported by the Department of Energy (DOE) at LANL under contract DE-AC52-06NA25397 and the DOE office of the ASCR programme in Applied Mathematical Sciences, by the RAPIDD programme of the Science and Technology Directorate, Department of Homeland Security and the Fogarty International Center, National Institutes of Health, and by the Center for Communicable Disease Dynamics, Department of Epidemiology, Harvard School of Public Health under NIGMS award Number U54GM088558. The content is solely the responsibility of the authors and does not necessarily represent the official views of NIGMS or NIH.

References

[1] D. G. Kendall, "Deterministic and stochastic epidemics in closed populations," in *Proceedings of the 3rd Berkeley Symposium on Mathematical Statistics and Probability*, J. Neyman, Ed., vol. 4 of *Contributions to Biology and Problems of Health*, pp. 149–165, 1956.

[2] D. Ludwig, "Final size distributions for epidemics," *Mathematical Biosciences*, vol. 23, no. 1-2, pp. 33–46, 1975.

[3] B. von Bahr and A. Martin-Löf, "Threshold limit theorems for some epidemic processes," *Advances in Applied Probability*, vol. 12, no. 12, pp. 319–349, 1980.

[4] K. Kuulasmaa, "The spatial general epidemic and locally dependent random graphs," *Mathematical Biosciences*, vol. 19, no. 4, pp. 745–758, 1982.

[5] P. Picard and C. Lefèvre, "A unified analysis of the final size and severity distribution in collective Reed-Frost epidemic

processes," *Advances in Applied Probability*, vol. 22, pp. 269–294, 1990.

[6] O. Diekmann, M. C. M. De Jong, and J. A. J. Metz, "A deterministic epidemic model taking account of repeated contacts between the same individuals," *Journal of Applied Probability*, vol. 35, no. 2, pp. 448–462, 1998.

[7] F. Ball and P. Neal, "Poisson approximations for epidemics with two levels of mixing," *Annals of Probability*, vol. 32, no. 1 B, pp. 1168–1200, 2004.

[8] E. Kenah and J. M. Robins, "Second look at the spread of epidemics on networks," *Physical Review E*, vol. 76, no. 3, Article ID 036113, 2007.

[9] E. Kenah and J. M. Robins, "Network-based analysis of stochastic SIR epidemic models with random and proportionate mixing," *Journal of Theoretical Biology*, vol. 249, no. 4, pp. 706–722, 2007.

[10] J. C. Miller, "Epidemic size and probability in populations with heterogeneous infectivity and susceptibility," *Physical Review E*, vol. 76, no. 1, Article ID 010101(R), 2007.

[11] E. Jones, T. Oliphant, P. Peterson et al., "SciPy: open source scientific tools for Python," 2001.

[12] A. A. Hagberg, D. A. Schult, and P. J. Swart, "Exploring network structure, dynamics, and function using Network X," in *Proceedings of the 7th Python in Science Conference (SciPy '08)*, pp. 11–15, CAUSA, Pasadena, Calif, USA, August 2008.

[13] F. Ball and P. Donnelly, "Strong approximations for epidemic models," *Stochastic Processes and their Applications*, vol. 55, no. 1, pp. 1–21, 1995.

[14] O. Diekmann and J. A. P. Heesterbeek, *Mathematical Epidemiology of Infectious Diseases: Model Building, Analysis, and Interpretation*, Wiley Series in Mathematical and Computational Biology, John Wiley & Sons, Chichester, UK, 2000.

[15] H. Andersson and T. Britton, *Stochastic Epidemic Models and Their Statistical Analysis*, vol. 151 of *Lecture Notes in Statistics*, Springer, New York, NY, USA, 2000.

[16] H. Andersson, "Limit theorems for a random graph epidemic model," *Annals of Applied Probability*, vol. 8, no. 4, pp. 1331–1349, 1998.

[17] M. E. J. Newman, "Spread of epidemic disease on networks," *Physical Review E*, vol. 66, no. 1, Article ID 016128, 2002.

[18] L. A. Meyers, M. E. J. Newman, and B. Pourbohloul, "Predicting epidemics on directed contact networks," *Journal of Theoretical Biology*, vol. 240, no. 3, pp. 400–418, 2006.

[19] S. N. Dorogovtsev, J. F. F. Mendes, and A. N. Samukhin, "Giant strongly connected component of directed networks," *Physical Review E*, vol. 64, no. 2, Article ID 025101(R), 2001.

[20] K. Kuulasmaa and S. Zachary, "On spatial general epidemics and bond percolation processes," *Journal of Applied Probability*, vol. 21, no. 4, pp. 911–914, 1984.

[21] J. C. Miller, "Bounding the size and probability of epidemics on networks," *Journal of Applied Probability*, vol. 45, no. 2, pp. 498–512, 2008.

[22] R. Tarjan, "Depth-first search and linear graph algorithms," *SIAM Journal on Computing*, vol. 1, no. 2, pp. 146–160, 1972.

[23] E. W. Dijkstra, "A note on two problems in connexion with graphs," *Numerische Mathematik*, vol. 1, no. 1, pp. 269–271, 1959.

[24] R. Albert, H. Jeong, and A. L. Barabási, "Error and attack tolerance of complex networks," *Nature*, vol. 406, no. 6794, pp. 378–382, 2000.

[25] R. Cohen, K. Erez, D. Ben-Avraham, and S. Havlin, "Resilience of the internet to random breakdowns," *Physical Review Letters*, vol. 85, no. 21, pp. 4626–4628, 2000.

Hindawi Publishing Corporation
Interdisciplinary Perspectives on Infectious Diseases
Volume 2011, Article ID 238743, 9 pages
doi:10.1155/2011/238743

Research Article

Contact Heterogeneity and Phylodynamics: How Contact Networks Shape Parasite Evolutionary Trees

Eamon B. O'Dea[1] and Claus O. Wilke[1, 2, 3]

[1] *Section of Integrative Biology, The University of Texas at Austin, Austin, TX 78712, USA*
[2] *Center for Computational Biology and Bioinformatics, The University of Texas at Austin, Austin, TX 78712, USA*
[3] *Institute for Cellular and Molecular Biology, The University of Texas at Austin, Austin, TX 78712, USA*

Correspondence should be addressed to Eamon B. O'Dea, ebo@mail.utexas.edu

Received 4 June 2010; Accepted 15 October 2010

Academic Editor: Katia Koelle

The inference of population dynamics from molecular sequence data is becoming an important new method for the surveillance of infectious diseases. Here, we examine how heterogeneity in contact shapes the genealogies of parasitic agents. Using extensive simulations, we find that contact heterogeneity can have a strong effect on how the structure of genealogies reflects epidemiologically relevant quantities such as the proportion of a population that is infected. Comparing the simulations to BEAST reconstructions, we also find that contact heterogeneity can increase the number of sequence isolates required to estimate these quantities over the course of an epidemic. Our results suggest that data about contact-network structure will be required in addition to sequence data for accurate estimation of a parasitic agent's genealogy. We conclude that network models will be important for progress in this area.

1. Introduction

Epidemiology is a data-driven field, and it is currently being infused at an increasing rate with molecular sequence data. This new and growing data source has led to a call for multilevel models of the relationship between sequence data and infectious disease dynamics [1, 2], dubbed phylodynamic models.

By allowing for additional data to be used and integrated, phylodynamic modeling may lead to improvements in the accuracy and quality of the surveillance of infectious diseases. For example, the number of norovirus outbreaks reported increased in 2002. It was not clear, however, whether the higher reported numbers were a sign of more outbreaks or more frequent reporting of outbreaks. Case-reporting bias does not affect molecular data, however. So coalescent analysis of molecular data [3] provided a valuable and largely independent line of evidence that the increase in outbreaks was real. Of course, coalescent analysis will have its own biases, and here we examine those that result from host heterogeneity in contact.

To model heterogeneity in contact, we represent individuals in a population as nodes, and we represent the potential for two hosts to infect each other as an edge that links two nodes. Researchers call the resulting networks contact networks. Contact-network structure necessarily affects the genealogy of any replicating infectious agent that is spreading through a host population. In this paper, we use the term parasite to refer to all such infectious agents, including bacteria and viruses. The genealogy of these parasites must fit inside the tree of infections that forms as the parasite spreads from host to host, and this tree of infections must fit inside the host population's contact network. While more elaborate elements of contact-network structure may be important, we here focus simply on variation in the number of edges coming out of nodes, which corresponds to heterogeneity in contact rates.

Contact heterogeneity has often not been discussed as a possible bias in coalescent analyses (e.g., [4–6]). Researchers performing coalescent analyses have considered contact heterogeneity in a variety of other ways. Hughes et al. [7] linked it to the phylogenetic clustering of sequence isolates. Biek et al. [8] mentioned that it may have contributed to changes in an estimation of R_0 (the expected number of new cases that a single case produces in a susceptible population). Nakano et al. [9] discussed how iatrogenic transmission may have been an important type of transmission in the spread of hepatitis C. Bennett et al. [10] pointed out that population-size estimates from coalescent analyses are more accurately interpreted as ratios of population size to reproductive variance. But researchers have rarely quantitatively considered how contact heterogeneity might be directly influencing the results of their coalescent analyses. Volz et al. [11] did account for contact heterogeneity in their coalescent model with a saturation parameter, but this application does not provide a general illustration of how contact-network structure can affect genealogies.

Our primary goal here is to assess how contact heterogeneity affects the relationship between coalescent reconstructions and the reality of parasite population dynamics. First, we build contact networks with different levels of heterogeneity. Then, we simulate the spread of parasites through the networks, generating epidemic dynamics and a genealogy of the parasite with each simulation. Then, we use the BEAST software package [12] to produce Bayesian skyride [13] reconstructions of parasite population dynamics based on the simulated genealogies. We also use the framework of Volz et al. [11] to predict the skyride reconstructions based on the simulated epidemic dynamics. We explain how the contact-network structure affects the epidemic dynamics that, in turn, affect the predicted reconstructions. The close agreement between the predicted skyrides and the skyride reconstructions validates this explanation. We also examine how much of the simulated genealogy the skyride reconstruction requires as input in order to produce a reconstruction that agrees with the theoretical prediction.

2. Materials and Methods

We simulated infectious disease progression on networks. The nodes of the networks represented hosts and had states of being susceptible, infectious, or recovered. The edges of the network determined the set of possible transmission events; infectious hosts transmitted infection across edges shared with susceptible hosts until the infectious hosts recovered. The number of nodes in the network was kept at 10,000, and the mean degree (degree is the number of edges coming out of a node) was kept at 4. The networks were built to be either regular, meaning that all nodes have the same degree, or with degree distributions sampled from Poisson, exponential, or Pareto distributions. The minimum degree in the Pareto networks was 1. The regular networks served as models with zero heterogeneity, Poisson networks as models with heterogeneity similar to a Poisson process, exponential networks as models with heterogeneity similar to a variety of social networks [14], and Pareto networks (scale-free networks) as models with the extreme levels of heterogeneity that might be found in sexual contact networks [15]. We used the Erdös-Rényi algorithm [16] to generate Poisson networks and an edge-shuffling algorithm [17] to generate the regular, exponential, and Pareto networks.

We simulated epidemics and genealogies in continuous time using a method based on the Stochastic Simulation Algorithm [18, 19]. Epidemics began with one node infectious and the rest of the nodes being susceptible. Infectious nodes recovered at a set rate and transmitted infection to susceptible neighbors (nodes sharing an edge) at a set rate. We drew the time to the next event from an exponential distribution with a rate equal to the sum of the rates of all possible events. We then selected an event with probability proportional to its rate, updated the state of the network accordingly, and drew the time until the next event. This process was iterated until either the time evolution of the epidemic reached a set time point or no more events were possible.

Simulation source code is available from the authors upon request. The code made use of the GNU scientific library [20, version 1.13+dsfg-1] to generate random numbers and the igraph library [21, version 0.5.3-6] to construct networks.

The output of a simulation included a time series of prevalence, that is, the count of infected nodes (given a fixed population of 10,000 nodes), and incidence, that is, the sum of the rates of all possible transmissions. Simulations also generated infection trees in which each transmission was a bifurcating node, each recovery was a terminal node, and branch lengths were equal to the time between events. We sampled from the full infection trees to generate the trees for input in the skyride coalescent analyses. We sampled by selecting a set of nodes uniformly at random from the full infection tree to become tip branches of an infection subtree. To generate the subtree, we cut the branches of the full infection tree at the subset of randomly selected nodes that had no descendants in the set of randomly selected nodes, and we pruned off any paths that did not terminate in this subset of nodes.

Using the sampled infection trees as genealogies, we obtained a posterior distribution for the skyride population sizes with the time-aware method of Minin et al. [13], implemented in BEAST [12, version 1.5.4]. The MCMC chain lengths were 100,000 states, and every 10th state was written to a log file. We discarded the first 10,000 states as burn in. In all cases, effective sample sizes were well above 200. Thus, convergence had occurred. Examples of BEAST XML input files are available from the authors upon request.

Using the posterior skyride population-size distributions, we obtained the skyride trajectories with Tracer [22, version 1.5]. Using the framework of Volz et al. [11], we calculated a predicted skyride as described next in the Results.

To plot time series from different stochastic simulations on a common time scale, we used the time at which growth

became nearly deterministic in each simulation as time zero for that simulation.

3. Results

3.1. Theory. Coalescent theory is an area of population genetics that models the structure of genealogies backward in time from a set of lineages sampled from a large population. A simple coalescent process turns out to be a good model for the genealogies of a wide range of scenarios in population genetics [23]. In the coalescent process, each pair of lineages in the sample coalesces into a common ancestral lineage at a constant rate. When time is measured in units of generations, this rate is the reciprocal of the effective population size. So the rate at which any of the pairs coalesces is equal to the number of pairs of lineages divided by the effective population size.

The skyride uses this simple relationship between effective population size and the expected time before coalescence to estimate population size from the length of intracoalescent intervals in a genealogy. The median of a skyride reconstruction y_{rec} at time t within an intracoalescent interval is approximately

$$y_{\text{rec}} = N_e\tau = \binom{n}{2}u, \tag{1}$$

where N_e is the effective population size, τ is the generation time, $\binom{n}{2}$ is the average number of pairs of lineages in the sample within the intracoalescent interval, and u is the length of the intracoalescent interval.

Predicting a skyride from the dynamics of an epidemic model is simply a matter of calculating the rate at which a pair of lineages will coalesce, that is, the rate at which two chains of infection merge into a single chain. Volz et al. [11] have described how coalescence rates follow from prevalence and incidence. Prevalence, given a fixed population size, refers to the count of cases of infection, and so we denote it by I. Incidence refers to the rate at which new cases are occurring, and so we denote it by r_i. The rate of coalescence of a single pair of cases is

$$r_iP, \tag{2}$$

where P is the probability that we can trace a particular pair of cases back to a single case before the last transmission event. We have

$$P = 1/\binom{I}{2}, \tag{3}$$

making the approximation that the last transmission event was equally likely to have taken place between any pair of current cases. Therefore, the predicted skyride y_{pred} satisfies

$$y_{\text{pred}} = \frac{1}{r_iP} = \binom{I}{2}/r_i. \tag{4}$$

The similarity of (4) and (1) reflects the similarity of the coalescent process to the transmission process in a continuous-time epidemic model. N_e and τ, however, are often considered as parameters of a discrete-time population model that has nonoverlapping generations. The coalescent process describes the genealogy in such a model when we sample a small fraction of the lineages in a population. So how do we interpret N_e and τ in the terms of a continuous-time epidemic model that has overlapping generations? Following Frost and Volz [24] and the general theory of Wakeley and Sargsyan [25], we say that generation time τ is equal to the expected time before an infected individual transmits infection:

$$\tau = \frac{I}{r_i}. \tag{5}$$

Then from (1) and (4) and $y_{\text{rec}} = y_{\text{pred}}$, we have

$$N_e = \frac{I-1}{2} \approx \frac{I}{2}. \tag{6}$$

3.2. Simulation. To determine the effect of sampling on the ability of the skyride to reconstruct prevalence history, we simulated genealogies and pruned off a variable number of branches from the genealogies. We found that small amounts of pruning rapidly reduced the number of coalescent events in the sampled genealogy that occurred in the peak and late phases of the epidemic, thereby restricting accurate reconstruction to the early phase of the epidemic (Figure 1).

To demonstrate the effect of network structure on the reconstruction of prevalence history, epidemics were simulated on networks with varying heterogeneity. Keeping the extent of sampling equal and increasing heterogeneity compressed the coalescent events in the sampled genealogy into the beginning of the epidemic. Figure 2 shows a representative example of this general trend that holds across intermediate levels of sampling. Consequently, increasing heterogeneity has a similar effect to reducing the proportion of nodes sampled: the time at which the prediction of the skyride based on prevalence and incidence diverges from the estimated skyride based on the genealogy occurs earlier.

Figure 3 shows how differences in the scaling of prevalence of the skyride follows from differences in trajectories of prevalence and incidence. The ratio of prevalence to incidence is the expected time until an infected host transmits infection, and we here define it as the generation time (5). In Figure 3, we see that generation times are at, or quickly reach, a minimum after an epidemic begins and then gradually increase until the epidemic ends. In the regular networks, the decline in the number of susceptible hosts over the course of the epidemic causes this increase to happen. In the other networks, which have hosts of varying degree, infection first moves to the high-degree hosts and then to progressively lower- and lower-degree hosts [26–28]. Because the degree of a host determines how much his/her infection increases incidence, this movement of infection from high- to low-degree hosts translates into generation times being at first shorter and then longer in heterogeneous networks relative to regular networks (Figure 3).

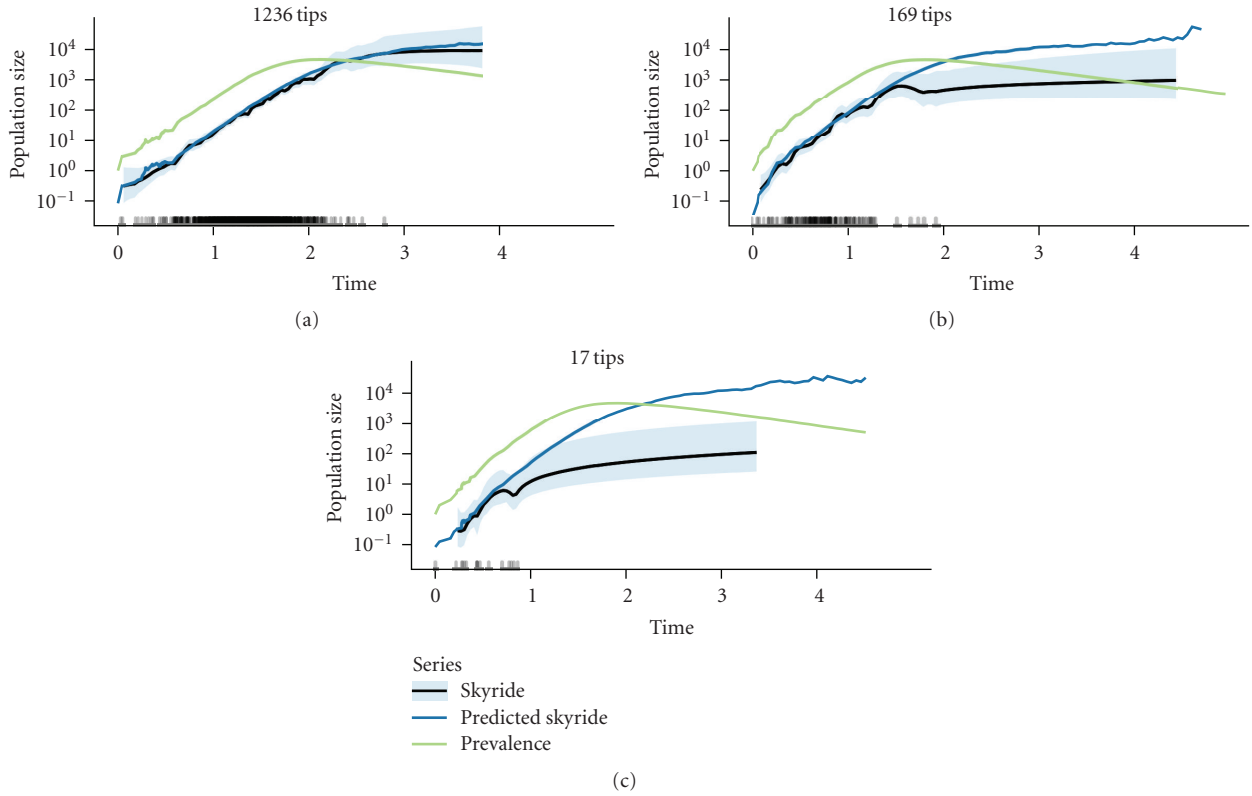

Figure 1: Low levels of proportional sampling may prevent accurate reconstruction of prevalence during and after the epidemic peak. We consider reconstruction to be accurate when the skyride and the predicted skyride match. The light-blue ribbons are the middle 95% of the posterior density of the skyride reconstruction. The small bars on the x-axis represent the times of coalescent events in the sampled genealogy. Labels above the Panels indicate the number of tips in the sampled genealogy. Parameters: contact-network size = 10,000, Poisson degree distribution with mean = 4, transmission rate = 2, recovery rate = 1, proportion of nodes sampled = {0.1, 0.01, 0.001} ((a), (b), and (c)).

4. Discussion

The effects of contact heterogeneity can be important in relating the structure of genealogies to infectious disease dynamics (Figure 3). The strength of the effect will vary from system to system, and for some systems other aspects of contact-network structure such as the frequency of short paths [29] and the dynamics of edge formation [30–33] may also be important. More generally, models may also require more detailed models of the course of infection within hosts (including incubation periods, e.g.), the effects of natural selection [34, 35], and other additions before they can make precise predictions in real-world systems.

But are the data requirements of these more complex models feasible? To begin answering this question, we next discuss the implications of obtaining the equivalent of our simulated data from a real-world system.

We knew the true infection tree in our simulations. In typical coalescent analyses of an infectious disease (e.g., [13, 36]), we do not know the true genealogy and so we must infer it along with the dynamics of the effective population size. Although there is a large set of methods for the inference of trees from sequences [37–39], the variety of methods available reflects the difficulty of the task. Additionally, as is well known by practitioners of phylogenetics, substitution rates set fundamental limits on the amount of phylogenetic information that sequences may contain. Sequences with common ancestors that are very recent may not have any polymorphic sites that could suggest the structure of the branching of the tree connecting them. Sequences with common ancestors that are too distant similarly contain little information about the true genealogy [40].

It may be possible to work around the second problem by collecting sequences over time such that there are no branching points in the tree that are too far from every pair of tips. For the first problem, there is simply no information that the sequences alone can provide, and additional knowledge of events in the chain of infection is necessary to determine the infection tree. The panels labeled "Time to coalescence" in Figure 3 show that this additional information is most likely to be needed early in the epidemic and when there is a large amount of variance in the contact network. It is then perhaps fortunate that contact-tracing methods are practiced by many health departments for sexually transmitted diseases (STDs) [41, 42], which are thought to have higher contact heterogeneity than airborne diseases [15]. However, we probably need more widespread practice of contact tracing for large genealogies

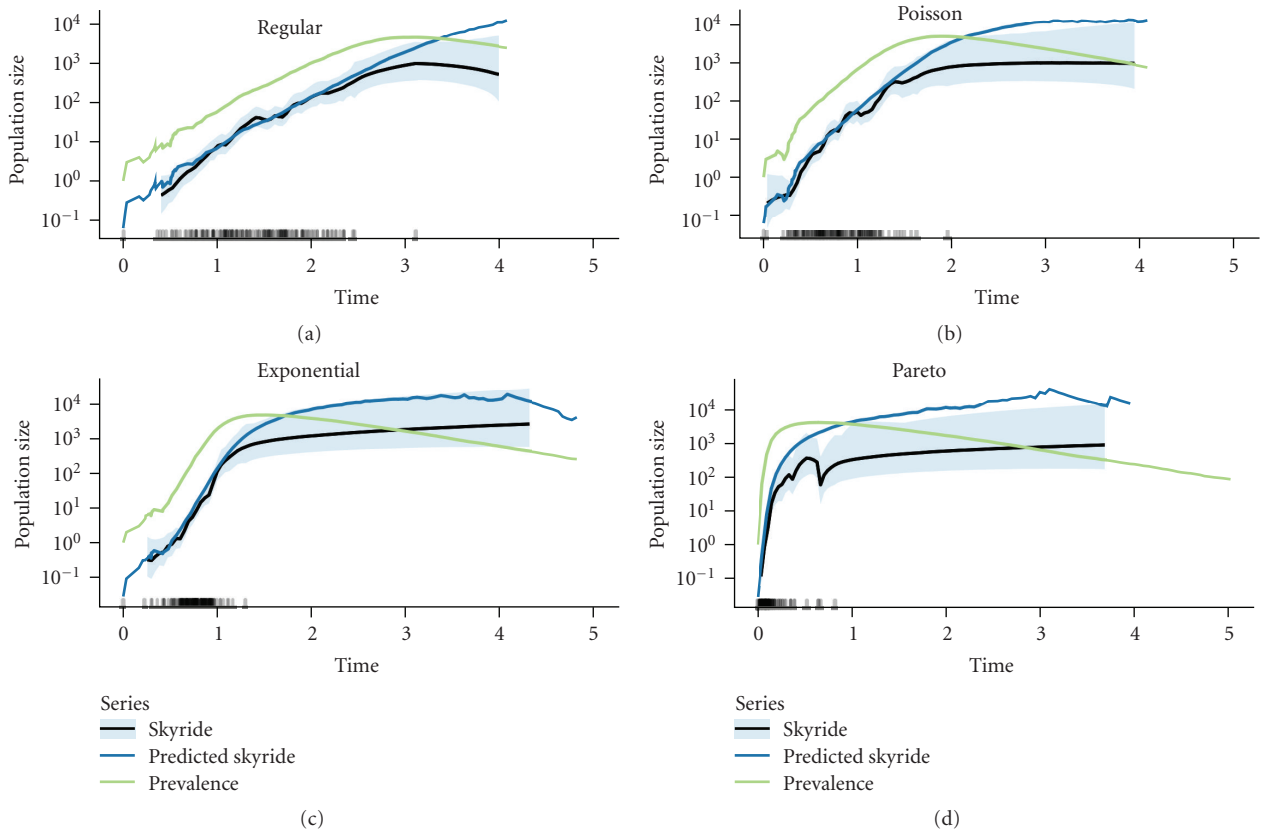

Figure 2: Contact heterogeneity determines the amount of time over which the skyride estimated from the genealogy is informative of the skyride predicted by prevalence and incidence. Contact heterogeneity also affects the relationship between the skyride and prevalence trajectories. The light-blue ribbons are the middle 95% of the posterior density of the skyride reconstruction. The small bars on the x-axis represent the times of coalescent events in the sampled genealogy. Labels above the Panels indicate the approximate degree distribution of the contact networks. The variance of the degree distributions increases from (a) to (d). Parameters: contact-network size = 10,000, degree distribution mean = 4, transmission rate = 2, recovery rate = 1, proportion of nodes sampled = 0.01.

to be assembled. A recent survey of physicians in the United States [43] found that less than one-third of physicians routinely screen patients for STDs and many physicians relied on patients to notify health departments and partners, and similar surveys in other countries [42, 44, 45] likewise indicate that contact tracing is not a routine in general medical care of STDs.

There also may be a need for contact tracing to establish the genealogy for airborne infections because many airborne transmissions may occur in a single day during which a single strain may be dominant in a host, as the super-spreading events in the 2003 SARS-coronavirus outbreak demonstrated [46]. Contact tracing is also practiced for airborne diseases. It has been used to help contain the SARS-coronavirus outbreak [47], smallpox [48], and tuberculosis [49]. Given that contacts for airborne diseases can be quite transient, it seems that, even with the addition of contact-tracing data, we may generally know less about parasite genealogies for airborne diseases compared to STDs. On the upside, our results suggest that the ability to reconstruct early parts of the epidemic is robust to much pruning of the full genealogy (Figure 1). However, this robustness may depend on our sampling scheme. Using discrete-time simulations, Stack et al. [50] found that the difference between reconstructed prevalence and simulated prevalence depended largely on how the samples were distributed over the course of the epidemic. Also, it is unclear how any of our sampling levels might compare to realistic amounts of contact tracing and molecular data for a specific infectious disease.

In addition to being necessary to fill gaps in molecular data, contact tracing may be necessary because genealogies do not always match infection trees. Such discordance is likely to occur when there is relatively little time between transmissions. When there is little time for a mutant to become fixed between transmissions, the order in which alleles at loci of a sequence appear in transmitting inocula (or sequence isolates) need not match the order in which the alleles appeared in the within-host population. Measures of within-host viral load and sequence diversity may be informative of the chance of such discordance. If populations tend to be large and diverse, then sequence data may be useless for reconstructing the recent details of chains of infection but still useful in reconstructing deeper branches in the tree. Sequence data from diverse within-host populations could also be useful in parameter estimation for coalescent models (e.g., [51]) that include the within-host dynamics

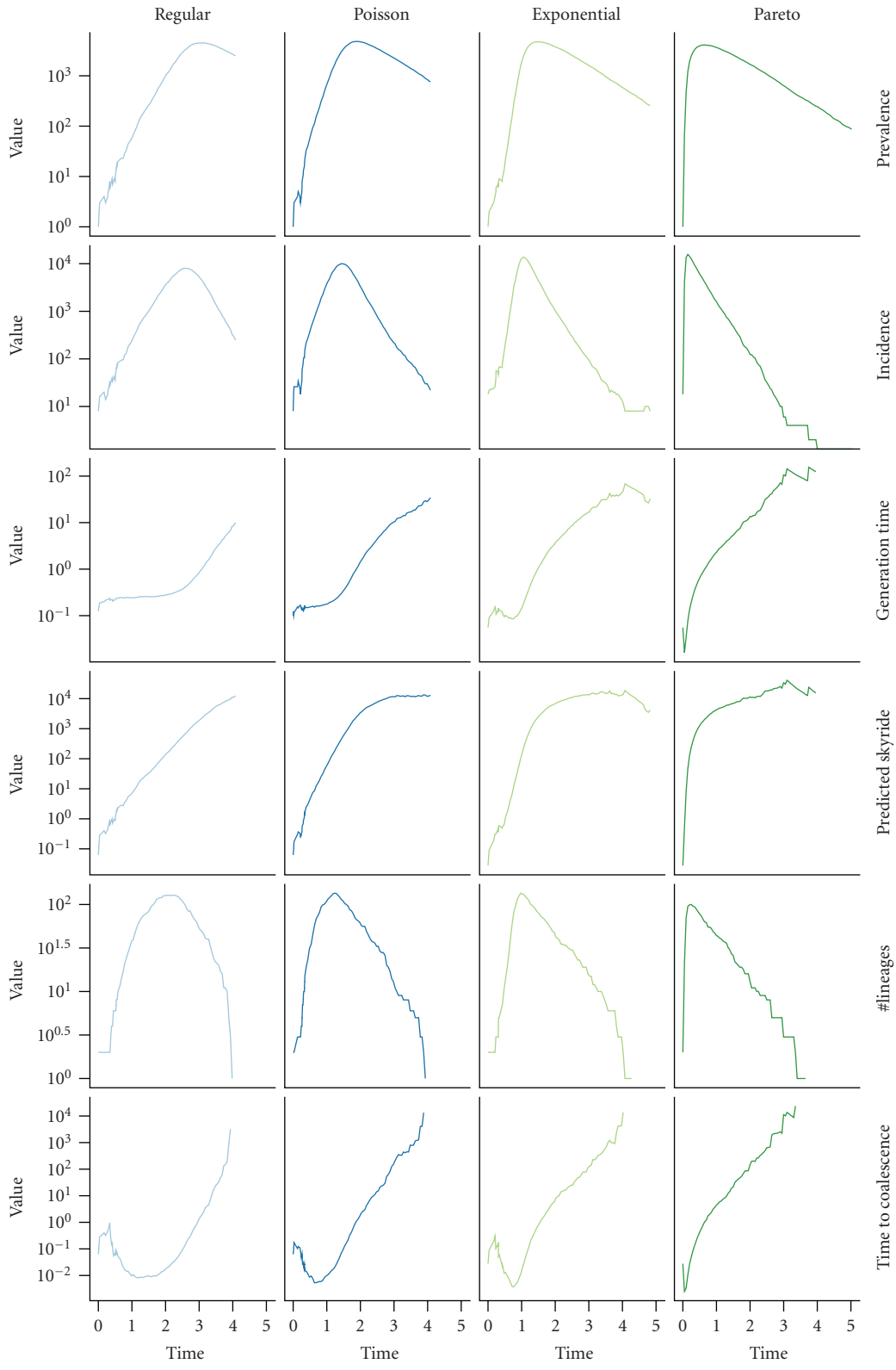

Figure 3: Contact-network structure, infectious disease dynamics, and genealogical structure interact. The ratio of prevalence to incidence is the generation time, which scales prevalence of the predicted skyride (up to a constant factor). Dividing the predicted skyride by the number of pairs of lineages backs out a smoothed expected length of intracoalescent intervals in the genealogy. Panel labels on the top indicate the approximate degree distribution of the contact networks. The variance of the degree distributions increase from left to right. Parameters: contact-network size = 10,000, degree distribution mean = 4, transmission rate = 2, recovery rate = 1, proportion of nodes sampled = 0.01.

of the parasite. Two properties that parasites may have that would help increase the chance that infection trees and genealogies match are a low level of diversity in transmitting inocula (i.e., a strong bottleneck effect at transmission) and reduction of diversity in an incubation period that precedes all transmission.

In our simulations, we also knew the variance of the degree distribution. We do have some data about the structure of contact networks for some systems. We have survey data about human sexual-contact networks (e.g., [52, 53]) and survey data about networks of close, but not sexual, human contacts [54–56]. Researchers have used field data to construct hypothetical contact networks for wildlife and vector-borne diseases (e.g., [57, 58]), and researchers have also used census data to construct hypothetical contact networks for human diseases (e.g., [59, 60]). It seems likely, however, that in the analysis of real sequence data the heterogeneity of the contact network will be at least as uncertain as disease incidence and prevalence. Thus, estimation of contact heterogeneity may be an important goal of the analysis. We note that previous work (e.g., [61]) has also discussed the potential use of sequence data to estimate contact heterogeneity.

5. Conclusions

Contact heterogeneity is well known to have a strong effect on infectious disease dynamics. We have shown how the relationship between infectious disease dynamics and genealogies is similarly sensitive to the contact heterogeneity specified by a network. We have argued that direct knowledge of the tree of infections is likely needed in addition to sequence data for the accurate inference of prevalence from sequence data. Thus, it seems that understanding the structure of the contact networks for various diseases will be important for progress in phylodynamics.

Acknowledgments

This work was supported by NSF Grant EF-0742373. The Texas Advanced Computing Center at UT provided computing resources.

References

[1] B. T. Grenfell, O. G. Pybus, J. R. Gog et al., "Unifying the epidemiological and evolutionary dynamics of pathogens," *Science*, vol. 303, no. 5656, pp. 327–332, 2004.

[2] E. C. Holmes and B. T. Grenfell, "Discovering the phylodynamics of RNA viruses," *PLoS Computational Biology*, vol. 5, no. 10, Article ID e1000505, 2009.

[3] J. J. Siebenga, P. Lemey, S. L. Kosakovsky Pond, A. Rambaut, H. Vennema, and M. Koopmans, "Phylodynamic reconstruction reveals norovirus GII.4 epidemic expansions and their molecular determinants," *PLoS Pathogens*, vol. 6, no. 5, Article ID e1000884, 2010.

[4] C. Fraser, C. A. Donnelly, S. Cauchemez et al., "Pandemic potential of a strain of influenza A (H1N1): early findings," *Science*, vol. 324, no. 5934, pp. 1557–1561, 2009.

[5] G. J. D. Smith, D. Vijaykrishna, J. Bahl et al., "Origins and evolutionary genomics of the 2009 swine-origin H1N1 influenza a epidemic," *Nature*, vol. 459, no. 7250, pp. 1122–1125, 2009.

[6] A. Rambaut and E. C. Holmes, "The early molecular epidemiology of the swine-origin A/H1N1 human inuenza pandemic," *PLoS Currents: Influenza*, vol. 1, article RRN1003, 2009.

[7] G. J. Hughes, E. Fearnhill, D. Dunn, S. J. Lycett, A. Rambaut, and A. J. Leigh Brown, "Molecular phylodynamics of the heterosexual HIV epidemic in the United Kingdom," *PLoS Pathogens*, vol. 5, no. 9, Article ID e1000590, 2009.

[8] R. Biek, J. C. Henderson, L. A. Waller, C. E. Rupprecht, and L. A. Real, "A high-resolution genetic signature of demographic and spatial expansion in epizootic rabies virus," *Proceedings of the National Academy of Sciences of the United States of America*, vol. 104, no. 19, pp. 7993–7998, 2007.

[9] T. Nakano, L. Lu, Y. He, Y. Fu, B. H. Robertson, and O. G. Pybus, "Population genetic history of hepatitis C virus 1b infection in China," *Journal of General Virology*, vol. 87, no. 1, pp. 73–82, 2006.

[10] S. N. Bennett, A. J. Drummond, D. D. Kapan et al., "Epidemic dynamics revealed in dengue evolution," *Molecular biology and evolution*, vol. 27, no. 4, pp. 811–818, 2010.

[11] E. M. Volz, S. L. Kosakovsky Pond, M. J. Ward, A. J. Leigh Brown, and S. D.W. Frost, "Phylodynamics of infectious disease epidemics," *Genetics*, vol. 183, no. 4, pp. 1421–1430, 2009.

[12] A. J. Drummond and A. Rambaut, "BEAST: Bayesian evolutionary analysis by sampling trees," *BMC Evolutionary Biology*, vol. 7, no. 1, article 214, 2007.

[13] V. N. Minin, E. W. Bloomquist, and M. A. Suchard, "Smooth skyride through a rough skyline: Bayesian coalescent-based inference of population dynamics," *Molecular Biology and Evolution*, vol. 25, no. 7, pp. 1459–1471, 2008.

[14] S. Bansal, B. T. Grenfell, and L. A. Meyers, "When individual behaviour matters: homogeneous and network models in epidemiology," *Journal of the Royal Society Interface*, vol. 4, no. 16, pp. 879–891, 2007.

[15] F. Liljeros, C. R. Edling, and L. A. N. Amaral, "Sexual networks: implications for the transmission of sexually transmitted infections," *Microbes and Infection*, vol. 5, no. 2, pp. 189–196, 2003.

[16] P. Erdős and A. Renyi, "On random graphs. I," *Publicationes Mathematicae*, vol. 6, pp. 290–297, 1959.

[17] F. Viger and M. Latapy, "Efficient and simple generation of random simple connected graphs with prescribed degree sequence," in *Computing and Combinatorics*, pp. 440–449, Springer, Berlin, Germany, 2005.

[18] D. T. Gillepsie, "A general method for numerically simulating the stochastic time evolution of coupled chemical reactions," *Journal of Computational Physics*, vol. 22, no. 4, pp. 403–434, 1976.

[19] D. T. Gillespie, "Stochastic simulation of chemical kinetics," *Annual Review of Physical Chemistry*, vol. 58, pp. 35–55, 2007.

[20] M. Galassi, J. Davies, J. Theiler et al., *GNU Scientific Library Reference Manual*, Network Theory Ltd., 3rd edition, 2009.

[21] G. Csardi and T. Nepusz, "The igraph software package for complex network research," *InterJournal*, vol. Complex Systems, p. 1695, 2006.

[22] A. Rambaut and A. J. Drummond, "Tracer v1.5," 2009, http://beast.bio.ed.ac.uk/Tracer.

[23] J. F. C. Kingman, "On the genealogy of large populations," *Journal of Applied Probability*, vol. 19, pp. 27–43, 1982.

[24] S. D.W. Frost and E. M. Volz, "Viral phylodynamics and the search for an effective number of infections," *Philosophical Transactions of the Royal Society B*, vol. 365, no. 1548, pp. 1879–1890, 2010.

[25] J. Wakeley and O. Sargsyan, "Extensions of the coalescent effective population size," *Genetics*, vol. 181, no. 1, pp. 341–345, 2009.

[26] M. Barthélemy, A. Barrat, R. Pastor-Satorras, and A. Vespignani, "Velocity and hierarchical spread of epidemic outbreaks in scale-free networks," *Physical Review Letters*, vol. 92, no. 17, Article ID 178701, 2004.

[27] M. Barthélemy, A. Barrat, R. Pastor-Satorras, and A. Vespignani, "Dynamical patterns of epidemic outbreaks in complex heterogeneous networks," *Journal of Theoretical Biology*, vol. 235, no. 2, pp. 275–288, 2005.

[28] E. Volz, "SIR dynamics in random networks with heterogeneous connectivity," *Journal of Mathematical Biology*, vol. 56, no. 3, pp. 293–310, 2008.

[29] J. C. Miller, "Spread of infectious disease through clustered populations," *Journal of the Royal Society Interface*, vol. 6, no. 41, pp. 1121–1134, 2009.

[30] E. Volz and L. A. Meyers, "Susceptible-infected-recovered epidemics in dynamic contact networks," *Proceedings of the Royal Society B*, vol. 274, no. 1628, pp. 2925–2933, 2007.

[31] M. Altmann, "Susceptible-infected-removed epidemic models with dynamic partnerships," *Journal of Mathematical Biology*, vol. 33, no. 6, pp. 661–675, 1995.

[32] M. Morris and M. Kretzschmar, "A microsimulation study of the effect of concurrent partnerships on the spread of HIV in Uganda," *Mathematical Population Studies*, vol. 8, pp. 109–133, 2000.

[33] E. Volz and L. A. Meyers, "Epidemic thresholds in dynamic contact networks," *Journal of the Royal Society Interface*, vol. 6, no. 32, pp. 233–241, 2009.

[34] B. D. O'Fallon, J. Seger, and F. R. Adler, "A continuous-state coalescent and the impact of weak selection on the structure of gene genealogies," *Molecular Biology and Evolution*, vol. 27, no. 5, pp. 1162–1172, 2010.

[35] D. Welch, G. K. Nicholls, A. Rodrigo, and W. Solomon, "Integrating genealogy and epidemiology: the ancestral infection and selection graph as a model for reconstructing host virus histories," *Theoretical Population Biology*, vol. 68, no. 1, pp. 65–75, 2005.

[36] A. J. Drummond, A. Rambaut, B. Shapiro, and O. G. Pybus, "Bayesian coalescent inference of past population dynamics from molecular sequences," *Molecular Biology and Evolution*, vol. 22, no. 5, pp. 1185–1192, 2005.

[37] Z. Yang, *Computational Molecular Evolution*, Oxford Series in Ecology and Evolution, Oxford University Press, Oxford, Miss, USA, 2006.

[38] J. Felsenstein, *Inferring Phylogenies*, Sinauer Associates, 2nd edition, 2003.

[39] P. Lemey, M. Salemi, and A.-M. Vandamme, Eds., *The Phylogenetic Handbook: A Practical Approach to Phylogenetic Analysis and Hypothesis Testing*, Cambridge University Press, Cambridge, Mass, USA, 2nd edition, 2009.

[40] G. I. Hagstrom, D. H. Hang, C. Ofria, and E. Torng, "Using Avida to test the effects of natural selection on phylogenetic reconstruction methods," *Artificial Life*, vol. 10, no. 2, pp. 157–166, 2004.

[41] T. Stokes and P. Schober, "A survey of contact tracing practice for sexually transmitted diseases in GUM clinics in England and Wales," *International Journal of STD and AIDS*, vol. 10, no. 1, pp. 17–21, 1999.

[42] M. McCarthy, L. J. Haddow, V. Furner, and A. Mindel, "Contact tracing for sexually transmitted infections in New South Wales, Australia," *Sexual Health*, vol. 4, no. 1, pp. 21–25, 2007.

[43] J. S. St. Lawrence, D. E. Montaño, D. Kasprzyk, W. R. Phillips, K. Armstrong, and J. S. Leichliter, "STD screening, testing, case reporting, and clinical and partner notification practices: a national survey of US physicians," *American Journal of Public Health*, vol. 92, no. 11, pp. 1784–1788, 2002.

[44] R. K. W. Chan, H. H. Tan, M. T. W. Chio, P. Sen, K. W. Ho, and M. L. Wong, "Sexually transmissible infection management practices among primary care physicians in Singapore," *Sexual Health*, vol. 5, no. 3, pp. 265–271, 2008.

[45] C. Heal and R. Muller, "General practitioners' knowledge and attitudes to contact tracing for genital Chlamydia trachomatis infection in North Queensland," *Australian and New Zealand Journal of Public Health*, vol. 32, no. 4, pp. 364–366, 2008.

[46] Y. Ruan, C. L. Wei, L. A. Ee et al., "Comparative full-length genome sequence analysis of 14 SARS coronavirus isolates and common mutations associated with putative origins of infection," *Lancet*, vol. 361, no. 9371, pp. 1779–1785, 2003.

[47] C. A. Donnelly, A. C. Ghani, G. M. Leung et al., "Epidemiological determinants of spread of causal agent of severe acute respiratory syndrome in Hong Kong," *Lancet*, vol. 361, no. 9371, pp. 1761–1766, 2003.

[48] F. Fenner, D. A. Henderson, I. Arita, Z. Jezek, and I. D. Ladnyi, *Smallpox and Its Eradication*, vol. 6 of *History of International Public Health*, World Health Organization, Geneva, Switzerland, 1988.

[49] R. B. Rothenberg, P. D. McElroy, M. A. Wilce, and S. Q. Muth, "Contact tracing: comparing the approaches for sexually transmitted diseases and tuberculosis," *International Journal of Tuberculosis and Lung Disease*, vol. 7, no. 12, pp. S342–S348, 2003.

[50] J. C. Stack, J. D. Welch, M. J. Ferrari, B. U. Shapiro, and B. T. Grenfell, "Protocols for sampling viral sequences to study epidemic dynamics," *Journal of the Royal Society Interface*, vol. 7, no. 48, pp. 1119–1127, 2010.

[51] C. T. T. Edwards, E. C. Holmes, D. J. Wilson et al., "Population genetic estimation of the loss of genetic diversity during horizontal transmission of HIV-1," *BMC Evolutionary Biology*, vol. 6, article no. 28, 2006.

[52] J. J. Potterat, L. Phillips-Plummer, S. Q. Muth et al., "Risk network structure in the early epidemic phase of HIV transmission in Colorado Springs," *Sexually Transmitted Infections*, vol. 78, no. 1, pp. i159–i163, 2002.

[53] R. B. Rothenberg, D. M. Long, C. E. Sterk et al., "The Atlanta urban networks study: a blueprint for endemic transmission," *AIDS*, vol. 14, no. 14, pp. 2191–2200, 2000.

[54] J. Wallinga, P. Teunis, and M. Kretzschmar, "Using data on social contacts to estimate age-specific transmission parameters for respiratory-spread infectious agents," *American Journal of Epidemiology*, vol. 164, no. 10, pp. 936–944, 2006.

[55] N. Hens, N. Goeyvaerts, M. Aerts, Z. Shkedy, P. Van Damme, and P. Beutels, "Mining social mixing patterns for infectious disease models based on a two-day population survey in Belgium," *BMC Infectious Diseases*, vol. 9, article no. 5, 2009.

[56] J. Mossong, N. Hens, M. Jit et al., "Social contacts and mixing patterns relevant to the spread of infectious diseases," *PLoS Medicine*, vol. 5, no. 3, article no. e74, 2008.

[57] M. E. Craft, E. Volz, C. Packer, and L. A. Meyers, "Distinguishing epidemic waves from disease spillover in a wildlife

population," *Proceedings of the Royal Society B*, vol. 276, no. 1663, pp. 1777–1785, 2009.

[58] D. J. Salkeld, M. Salathé, P. Stapp, and J. H. Jones, "Plague outbreaks in prairie dog populations explained by percolation thresholds of alternate host abundance," *Proceedings of the National Academy of Sciences of the United States of America*, vol. 107, no. 32, pp. 14247–14250, 2010.

[59] L. A. Meyers, B. Pourbohloul, M. E. J. Newman, D. M. Skowronski, and R. C. Brunham, "Network theory and SARS: predicting outbreak diversity," *Journal of Theoretical Biology*, vol. 232, no. 1, pp. 71–81, 2005.

[60] S. Eubank, "Network based models of infectious disease spread," *Japanese Journal of Infectious Diseases*, vol. 58, no. 6, pp. S9–S13, 2005.

[61] L. M. Sander, C. P. Warren, I. M. Sokolov, C. Simon, and J. Koopman, "Percolation on heterogeneous networks as a model for epidemics," *Mathematical Biosciences*, vol. 180, pp. 293–305, 2002.

Hindawi Publishing Corporation
Interdisciplinary Perspectives on Infectious Diseases
Volume 2011, Article ID 194507, 9 pages
doi:10.1155/2011/194507

Research Article

Assortativity and the Probability of Epidemic Extinction: A Case Study of Pandemic Influenza A (H1N1-2009)

Hiroshi Nishiura,[1,2] Alex R. Cook,[3] and Benjamin J. Cowling[4]

[1] *PRESTO, Japan Science and Technology Agency, Saitama 332-0012, Japan*
[2] *Theoretical Epidemiology, University of Utrecht, Yalelaan 7, 3584 CL Utrecht, The Netherlands*
[3] *Department of Statistics and Applied Probability, National University of Singapore, Singapore 117546*
[4] *School of Public Health, The University of Hong Kong, Hong Kong Special Administrative Region, Hong Kong*

Correspondence should be addressed to Hiroshi Nishiura, nishiurah@gmail.com

Received 26 May 2010; Accepted 29 November 2010

Academic Editor: Ben Kerr

Unlike local transmission of pandemic influenza A (H1N1-2009), which was frequently driven by school children, most cases identified in long-distance intranational and international travelers have been adults. The present study examines the relationship between the probability of temporary extinction and the age-dependent next-generation matrix, focusing on the impact of assortativity. Preferred mixing captures as a good approximation the assortativity of a heterogeneously mixing population. We show that the contribution of a nonmaintenance host (i.e., a host type which cannot sustain transmission on its own) to the risk of a major epidemic is greatly diminished as mixing patterns become more assortative, and in such a scenario, a higher proportion of non-maintenance hosts among index cases elevates the probability of extinction. Despite the presence of various other epidemiological factors that undoubtedly influenced the delay between first importations and the subsequent epidemic, these results suggest that the dominance of adults among imported cases represents one of the possible factors explaining the delays in geographic spread observed during the recent pandemic.

1. Introduction

Since it was first identified in early 2009, a novel strain of influenza A (H1N1-2009) has caused a global pandemic. Although the rapid international spread created various epidemiological challenges, such as quantifying the strain's transmission potential and virulence during the very early stages of the pandemic [1, 2], many key insights have been obtained to date [3]. Prior to the pandemic, the importance of contact networks in elucidating the epidemiological dynamics of infectious diseases has been emphasized with applications to severe acute respiratory syndrome (SARS), sexually transmitted infections and other directly transmitted diseases [4, 5]. The age specificity in the transmission of the H1N1-2009 indicates the relevance of contact heterogeneity [6–9]. Although the differential attack rates in different age groups by H1N1-2009 have multiple explanatory factors, including age-specific susceptibility and pre-existing immunity [10–12], age-dependent contact is also thought to be associated with a higher susceptibility to infection and greater infectiousness once infected in children [13]. The consequences of this are that community-wide epidemics have been frequently driven by school outbreaks [7], while attack rates of H1N1-2009 were highest among school-age children in various parts of the world [8, 11]. A network model was used to describe the temporal variations in the age-specific composition of cases during the course of the pandemic and found that attack rates for a novel strain of influenza tend to be initially biased towards children and then shift towards adults [14].

A parsimonious simplification of the complexity of an age-structured contact network can be obtained by approximating the network by an appropriately quantified age-dependent next-generation matrix. This is accomplished by using the next-generation matrix, the square matrix with generic entry R_{ij}, the average number of secondary

cases in age-group i generated by a single primary case in age-group j in a fully susceptible population. Discretizing chronological age into a small number of age groups, the matrix, $\mathbf{K} = \{R_{ij}\}$, for H1N1-2009 has been quantified using age-stratified epidemic data [2, 6, 7, 15]. The age-dependent $\mathbf{K}$ has two important properties in understanding epidemiological dynamics. First, the dominant eigenvalue of $\mathbf{K}$ corresponds to the basic reproduction number, R_0 [16], which frequently yields a threshold condition, that is, a major epidemic is possible if and only if $R_0 > 1$. Second, the final proportion of hosts of type i that become infected, z_i, is given by the solution to $1 - z_i = \exp(-\sum_j R_{ij} z_j)$ [17]. One important use of R_{ij} is to the development of optimal vaccination strategies before a pandemic [18, 19] and during a pandemic [20].

The present study investigates the relationship between the age-dependent next-generation matrix, $\mathbf{K}$, and the invasion of a novel virus into a large population, which has not been well clarified to date. Whereas this subject has been partly explored via percolation theory [5], it is important from an epidemiological perspective to address this using a simpler model that can more readily be fitted to observational data from the outbreak in question. More specifically, we examine the impact of assortativity, that is, preferential mixing of different host types (here, age), on the probability of epidemic extinction, because age-dependent human contact networks have been shown to be highly assortative in contact surveys [21, 22]. Such an assortative network is known to allow disease percolation more easily than disassortative ones [23], echoed by the finding that increasing the preferential mixing component of simpler models such as ours tends to allow an epidemic to grow more easily [24].

In addition to these issues, the present study investigates the role of the age of cases importing infection to a local area by long-distance travel either intranationally or internationally on the resulting growth of a local epidemic. As a practical example, the age-dependent transmission of the H1N1-2009 pandemic is considered, and we first present our study motivations in the next section.

2. Materials and Methods

2.1. Study Motivation. Figure 1(a) shows the time delay from the introduction of first imported case on 1 May 2009 to the subsequent increase in local transmission in Hong Kong [25]. Despite the number of imported cases, it took 39 days to observe the first locally acquired case. The interpretation of Figure 1(a) is affected by several factors, such as case ascertainment, ecological factors such as seasonality, and disease control [27], but as with many other countries exponential growth in the local epidemic did not start for some time after the first imported case. Hong Kong instigated particularly stringent quarantine measures, but a recent study comparing the time delay in local transmission between countries with and without entry screening has shown that the entry screening measures were not associated with a substantial delay in the start of local transmission [28].

Figure 1(b) shows weekly hospitalization rates due to H1N1-2009 in three coastal areas in the Netherlands [26]. A surge in hospitalizations is first seen in Amsterdam followed by Rotterdam. The peak hospitalization rate in Zeeland occurs three weeks later than that in Amsterdam. There may be various interpretations for the delay before exponential growth, and, in particular, the spatial heterogeneity in Figure 1(b) is likely to have been associated with differing inflows of infected individuals and intrinsically differing patterns of spread within each region. Despite the presence of various possible factors explaining Figure 1(b), it is clear that the spatio-temporal dynamics are not synchronized even in this geographically limited country, and thus, Figure 1(b) at least indicates that stochastic effects may not have been insignificant for the intranational spread. A similar substantial delay in interregional spread has also been seen in the results of seroepidemiological study in England [29].

Both Figures 1(a) and 1(b) indicate a delay in causing international or interregional spread, but from a sufficiently high number of homogeneous index cases that repeated stochastic extinction is unlikely as an explanation. A more plausible reason is the contrast in age distributions between local and imported cases: whereas imported cases have been predominantly adults [30], local transmissions are frequently driven by school children. That is, adults were more likely to travel than children, and those aged 25 years and older accounted for more than half of the imported cases in Japan [30]. Similarly, adults may also more likely be the source of spread within a country, especially as the movement distance becomes longer. However, adults are less likely to cause secondary transmissions than children in a local setting [2, 6, 13, 15], making it critically important to understand the differential probability of extinction of the infection tree emerging from a typical child index and a typical adult index case. Because assortativity regulates the frequencies of within- and between-group transmissions, examining the effects of assortativity provides a natural avenue for assessing this. Accordingly, in this paper we use a simple stochastic model to clarify the different roles of children and adults in causing a major epidemic and its relevance to assortativity.

2.2. A Model for Clade Extinction. We employ a multitype branching process to approximate the probability of extinction of the clade of infection emanating from a single index case [31]. Consider a large population which is fully susceptible, and let there be two subpopulations, that is, children and adults. For simplicity, we ignore pre-existing immunity among adults. Throughout this paper, we label children as type 1 and adults as type 2. Let γ_i $(i = 1, 2)$ be the recovery rate of infectious individuals of type i and $\beta_{ij} (1 \leq i, j \leq 2)$ be the birth rate (i.e., the rate of new infection) of type i infected individuals caused by a single type j infected individual during the initial stage of an epidemic. We consider the case when a small number of a_i infected individuals of type i invades a fully susceptible large population. Given the large and (assumed) fully susceptible population, and the small initial number of infectives, depletion of the susceptible stock can be ignored and the initial

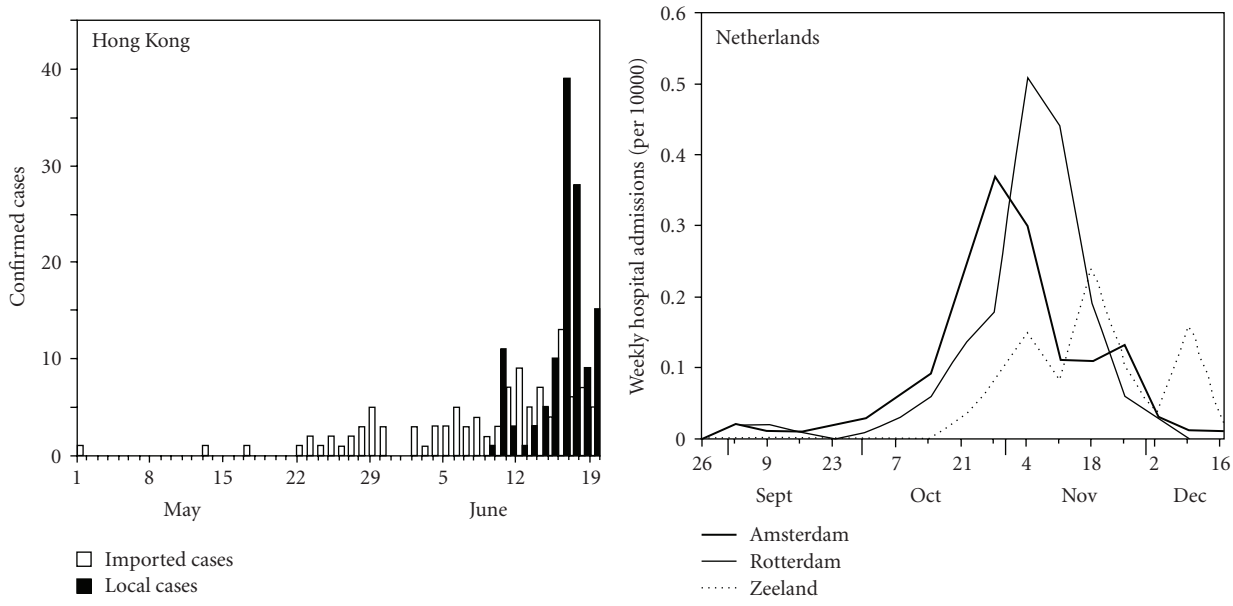

Figure 1: Epidemiology of the pandemic influenza A (H1N1-2009) in Hong Kong and the Netherlands. (a) Introduction of imported confirmed cases in Hong Kong followed by an increase in local (indigenous) confirmed cases from May–June, 2009 [25]. (b) The hospitalization rates of the influenza A (H1N1-2009) in Amsterdam, Rotterdam and Zeeland from August–December, 2009 [26]. Weekly numbers of hospitalizations are divided by the population size in each locality.

stages of the outbreak interpreted as a multivariate birth-and-death process [32]. For mathematical convenience, we assume that the generation time is exponentially distributed, and thus, $R_{ij} = \beta_{ij}/\gamma_j$. This assumption is common to many compartmental models, although its realism is dubious. The proposed approach considers a linearized system for the early epidemic period with a crude approximation of host types, but the similar approach of mapping next generation with the use of a square matrix can be employed for explicit network models [33]. In addition to the aforementioned assumptions, we assume that the age-specificity of R_{ij} is fully attributable to the infection rate β_{ij}, and thus the infectious period γ_j is assumed to be a constant γ, independent of host type. Consequently, if we further ignore the age-specific susceptibility and infectiousness, R_{ij} is determined only by the frequency of contact within- and between-age groups.

Letting the random vector $\mathbf{X}_n = (X_{1n}, X_{2n})$ represent the number of child and adult infected individuals in the population in the nth generation, we consider the process $\{\mathbf{X}_n\}$ as a multitype branching process. Assuming that an individual of type j has probability $p_j(\mathbf{x})$ of infecting, in the next generation, x_1 children and x_2 adults, we define the probability generating function as

$$F_j(s_1, s_2) = \sum_{\mathbf{x}} p_j(x_1, x_2) s_1^{x_1} s_2^{x_2}, \quad j = 1, 2. \tag{1}$$

Following foregoing studies [32, 34], the generating function $F_j(\mathbf{s})$ with an exponentially distributed generation time is known to be given by

$$F_j(\mathbf{s}) = \frac{\gamma_j}{\gamma_j + \sum_{k=1}^{2} \beta_{kj}(1 - s_k)} \tag{2}$$

for $j = 1, 2$. Since γ_j is assumed to be independent of host type j, $R_{ij} = \beta_{ij}/\gamma$, (2) simplifies to

$$F_j(\mathbf{s}) = \frac{1}{1 + R_{1j}(1 - s_1) + R_{2j}(1 - s_2)}. \tag{3}$$

The clade of infections, $\{\mathbf{X}_n\}$, emanating from the initial index cases becomes extinct with probability 1 if and only if the dominant eigenvalue of $\mathbf{K}$ is less than or equal to unity, that is, $\rho(\mathbf{K}) \leq 1$ [34].

Let π_i be the probability of extinction given that a single infected individual of type i is introduced to the population. The extinction probability is the nonnegative root of the equations

$$\pi_j = F_j(\boldsymbol{\pi}), \quad j = 1, 2. \tag{4}$$

As is standard in branching process models, each of the secondary cases of type i generated by a primary case becomes an ancestor of an independent subprocess (which restarts with a type i individual) behaving identically among the same type i [31, 35]. Because of this multiplicative nature, we have the probability of extinction

$$p(\mathbf{a}) = \prod_{j=1}^{2} \left\{ \pi_j^{a_j} \right\} \tag{5}$$

of the entire clade with initial vector $\mathbf{a} = (a_1, a_2)$.

In the two-host population, that is, a population consisting of children and adults, the probabilities of extinction

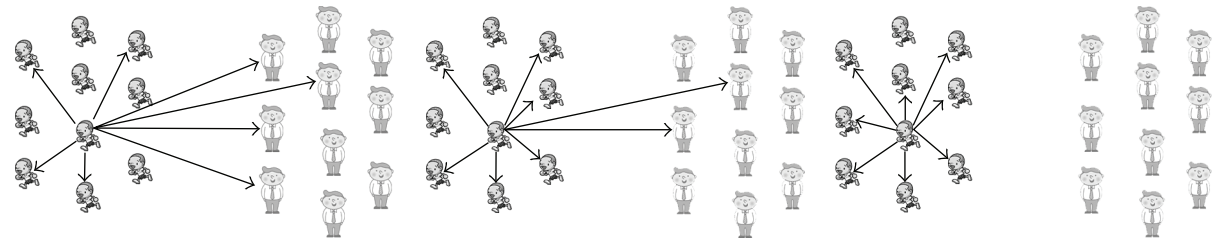

Figure 2: Preferential mixing given a single child index case. The hypothetical population consists of 10 children (left) and 10 adults (right) with equal susceptibility and infectiousness. We consider an introduction of a single child index case who has a potential to cause 8 secondary transmissions. Panels (a)–(c) illustrate contacts generated by the child index case with different θ, proportion of within-group contacts, being 0, 0.5 and 1.0, respectively. With $\theta = 0$ (i.e., random mixing), four edges extend to child susceptibles and the other four to adult susceptibles. Nevertheless, with $\theta = 0.5$, additional two edges are reserved for within-child mixing and only the remaining two are connected to adult susceptibles. With $\theta = 1$ (i.e., fully assortative mixing), all edges are connected with child susceptibles.

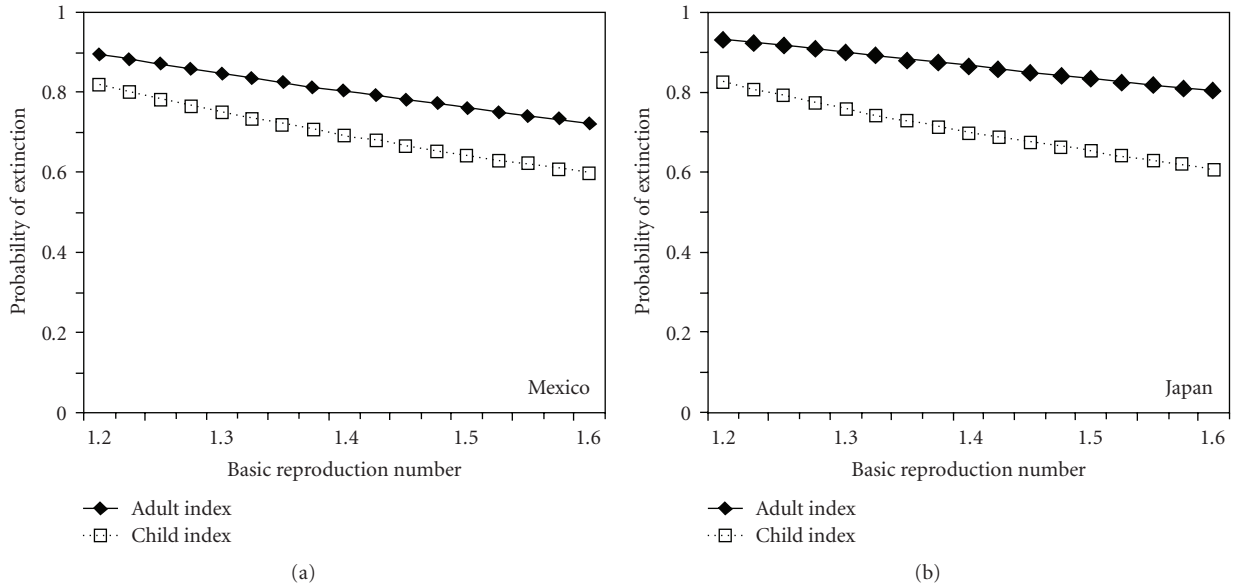

Figure 3: Probability of extinction given an introduction of single child or adult index case. The probabilities of extinction are calculated, assuming that a single child or adult index case is introduced into a fully susceptible large population. The probability approximately accounts for heterogeneous transmission among and between child and adult populations. The estimates of the next-generation matrices are extracted from A. Fraser et al. [6] based on an analysis in Mexico and B. Nishiura et al. [2] in Japan. The basic reproduction numbers in the original studies in Mexico and Japan are estimated at $R_0 = 1.58$ and 1.22, respectively, and both panels rescales the next-generation matrix by multiplying each entry with R/R_0 where R measures the horizontal axis.

given a single child or adult infected individual, π_1 and π_2, satisfy

$$\pi_1 = \frac{1}{1 + R_{11}(1-\pi_1) + R_{21}(1-\pi_2)},$$
$$\pi_2 = \frac{1}{1 + R_{12}(1-\pi_1) + R_{22}(1-\pi_2)}. \quad (6)$$

In other words, given that the next-generation matrix R_{ij} is known, the problem of calculating the probability of extinction given a certain number of infected individuals of host i and j in the zero generation is replaced by the problem of solving two quadratic equations with two unknown parameters. There are four possible combinations of the solutions for (6) including complex numbers, but we iteratively find the only nonnegative real numbers in the range of $0 \leq \pi_1, \pi_2 \leq 1$ (see [31, page 18]), except for a combination $(\pi_1, \pi_2) = (1, 1)$.

2.3. Quantitative Illustrations. The probability of extinction is investigated for the following three different scenarios. First, to gain an overview of the extinction probabilities π_1 and π_2 for the H1N1-2009, (6) are solved using published

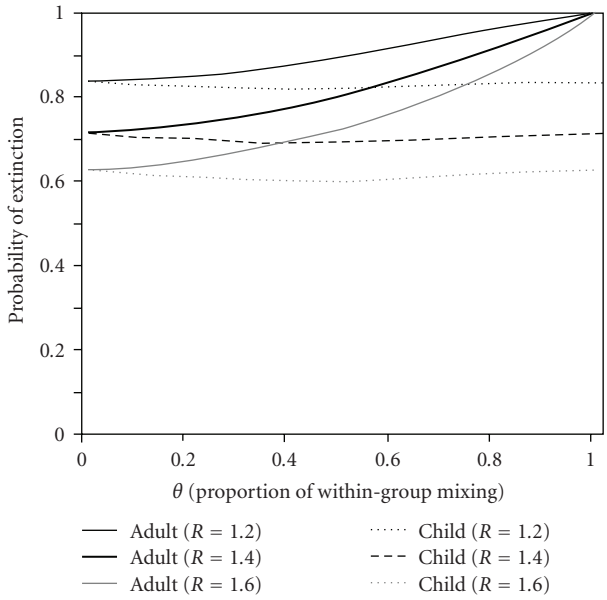

Figure 4: Assortativity and the probability of extinction. The probability of extinction in a fully susceptible population given a single adult or child index case is measured as a function of θ, the proportion of within-group mixing. The next-generation matrix, parameterized by Fraser et al. [6] with the dominant eigenvalue $R_0 = 1.58$, is rescaled by multiplying each entry with R/R_0 where R is set to be 1.2, 1.4 and 1.6, respectively.

estimates of $\mathbf{K}$ from Mexico [6] and Japan [2]. Approximating the original $\mathbf{K}$ into a two-host population, we use

$$\mathbf{K}_a = \begin{pmatrix} 1.41 & 0.34 \\ 0.35 & 0.87 \end{pmatrix} \tag{7}$$

for Mexico, and

$$\mathbf{K}_b = \begin{pmatrix} 1.14 & 0.25 \\ 0.21 & 0.45 \end{pmatrix} \tag{8}$$

for Japan. The originally estimated dominant eigenvalues are 1.58 and 1.22, respectively. It should be noted that the child group in Mexico is assumed to be up to age 14 years while that in Japan is up to age 19 years. Assuming that the reproduction number, R possibly ranges from 1.2–1.6 [2, 36], we rescale the next-generation matrices by

$$\mathbf{K}_q' = \frac{R}{\rho\left(\mathbf{K}_q\right)}\mathbf{K}_q, \quad q = a, b, \tag{9}$$

where R is the reproduction number to be examined.

Second, $\mathbf{K}_a$ in Mexico is further examined in relation to the assortativity. The element R_{ij} of $\mathbf{K}_a$ has been parameterized as

$$R_{ij} \sim \begin{cases} (1-\theta)\alpha_i\beta_j n_i, & \text{for } i \neq j, \\ \theta\alpha_i\beta_j + (1-\theta)\alpha_i\beta_j n_i, & \text{for } i = j, \end{cases} \tag{10}$$

where n_i is the relative size of the subpopulation i (i.e., $n_1 + n_2 = 1$). α_j and β_j are originally described as the age-specific susceptibility and infectiousness [6], and these can also be regarded as the so-called proportionate mixing components. The biological interpretation of proportionate mixing is that irrespective of its own type, an individual can acquire infection from any given individual (i.e., the secondary transmission from host j to i is determined by host j). Introduction of the most important parameter in the present study, θ is classically referred to as "preferred" or "preferential" mixing [37, 38]. Although the original definition of the term preferred mixing has a broader meaning, θ in (10) represents the proportion of contacts reserved for within-group mixing, and $(1-\theta)$ represents the proportion of contacts subject to proportionate mixing. If $\theta = 1$, the mixing is referred to as fully assortative (Figure 2). If $\theta = 0$, the mixing corresponds to random mixing (though it should be noted that the mixing matrix still includes a proportionate mixing component). An empirical estimate of θ from Mexico is 0.50, although the 95% confidence interval is broad: 0–0.72 [6]. Therefore, we examine the sensitivity of the probabilities of extinction, π_1 and π_2, to different θ in the range of 0-1 and R in the range of 1.2–1.6. Other parameters are fixed at $n_1 = 0.32$, $\alpha_1 = 2.06$, $\alpha_2 = \beta_1 = \beta_2 = 1$ [6].

Third, to clarify the practical implications of the predomination of adults among travelers, we examine the sensitivity of the probability of extinction to the proportion of adult travelers over various θ and R. Specifically, we consider the probability of extinction given a small importation of ten cases in the zero generation independently entering a large susceptible population at their infection-age 0 (i.e., immediately after their own infections: for simplicity, we ignore the infection-age distribution of imported cases at the time of invasion in the present study, because its realistic incorporation enforces us to account for the epidemic dynamics in exporting countries and thus, the exporting country and travel distance for each imported case would be required [39]). Among the 10 cases, we vary the number of adult cases from 0 to 10, and examine the probability of extinction given by (5).

3. Results

Figure 3 shows the probabilities of extinction, π_1 and π_2, using published estimates of $\mathbf{K}_a$ and $\mathbf{K}_b$ in (7) and (8). In both panels, using estimates from Mexico and Japan, π_2, the probability of extinction given a single adult case, always appeared to be higher than π_1, and thus the clade of infections resulting from the introduction of an adult index case is more likely to be self-limiting than from a child index case. The estimates of π_1 and π_2 using the published estimates of R_0 were 61 and 73%, respectively, for Mexico (with $R_0 = 1.58$) and 81 and 93%, respectively, for Japan (with $R_0 = 1.22$), indicating that the reproduction number R in the range of 1.2–1.6 is not far from the critical level and the impact of variations in R_0 on epidemic extinction is large. The reader should note the crudeness of the dichotomization of the population into two subpopulations,

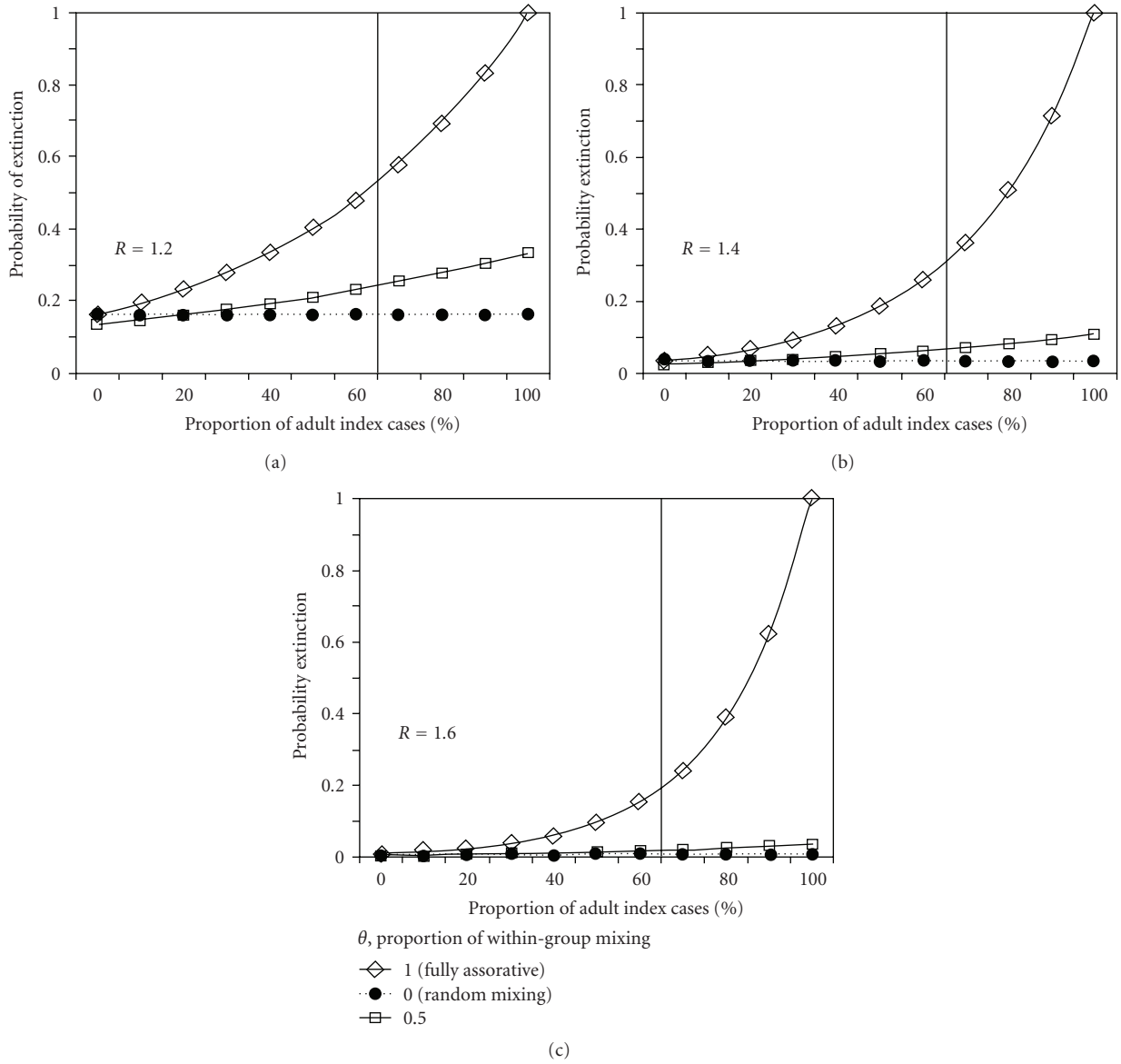

Figure 5: The impact of the age specificity of index cases on the probability of extinction. All panels, (a)–(c), examine the sensitivity of the probability of extinction in a fully susceptible large population given 10 index cases with $R = 1.2$, 1.4 and 1.6, respectively, with different θ, the proportion of within-group mixing and the proportion of adult index cases. Vertical grey bold line represents the empirically observed proportion of adult imported cases in Japan (i.e., 63.4% were aged <15 years). The horizontal axis measures the proportion of adult index cases among the total number of 10 index cases. The next-generation matrix, parameterized by Fraser et al. [6] with the dominant eigenvalue $R_0 = 1.58$, is rescaled by multiplying each entry with R/R_0,.

and that incorporating more detailed network structure (e.g., by dividing the population into many more types of host) tends to yield higher probability of extinction [2, 5]. Moreover, whereas the present study assumes an exponentially distributed generation time, a more realistic depiction, for example, gamma-distributed generation time, tends to capture overdispersion of the offspring distribution more appropriately [40, 41], and thus, again yields a higher probability of extinction than is shown herein.

Figure 4 examines the probabilities of extinction, π_1 and π_2, as a function of θ, the proportion of within-group mixing and R. As expected from the randomly mixing interpretation, π_1 and π_2 were equal to $1/R$ with $\theta = 0$. However, for populations with more within-group mixing, clades from adults were more likely to go extinct, reaching 100% with $\theta = 1$. This is attributable to the next-generation matrices (7) and (8) involving the typical reservoir dynamics [42]: children act as a maintenance host ($R_{11} > 1$), among whom transmission can be maintained by themselves, while adults constitute a nonmaintenance host group ($R_{22} < 1$), and thus, with little relative mixing between the two groups, an adult index case would never lead to a major epidemic.

The probability of extinction, π_1, given a single child index case, reached a minimum with θ in the range of 0.4-0.5, although this probability was not very sensitive to θ. Such θ may lead to a "well-mixed" population, thereby allowing the child index case to involve both child and adult secondary cases effectively.

Figure 5 examines the probability of extinction given 10 index cases as a function of θ and the proportion of adult index cases. With random mixing, the probability of extinction given a single index case is $(100/R)\%$ (e.g., 71% with $R = 1.4$). The extinction probability given 10 index cases in the randomly mixing population was independent of the proportion of adults, $(1/R)^{10} = 0.035$ (with $R = 1.4$), indicating that a major epidemic is almost unavoidable without any intervention. However, as assortativity increased, the increase in the proportion of adult index cases promoted extinction. The vertical reference line of 63% indicates the empirically observed proportion of adults (i.e., those aged $\geq$15 years in (7) as defined by [6]) among all imported cases in Japan [30]. At around that proportion, the probability of extinction was estimated to be 1%–58% over the full range of θ from 0 to 1, for 10 index cases. Given 10 index cases with $\theta = 1$, the results were independent of the proportion of adult index cases, because $a_1 + a_2 = 10$ and $\pi_2 = 1$ (for $\theta = 1$), whatever the number of adults, a_2, the extinction probability is

$$p(a_1, a_2) = \pi_1^{a_1} \pi_2^{a_2} = \pi_1^{a_1}. \tag{11}$$

That is, as mixing becomes more and more assortative, the contribution of the initial number of adults, a_2 to the risk of a major epidemic becomes less important, and moreover, an increase in the proportion of adults indirectly reduces a_1, leading to an increase in the probability of extinction. Even when we divide the entire population into many more subpopulations, this argument holds as long as the host type of interest i is incapable of maintaining disease by itself, that is, when the host-specific reproduction number, $R_{ii} < 1$ [42]. Of course, if $a_2 = 10$, $p(0, 10) = 1$ for $\theta = 1$.

4. Discussion

The present study investigated the relationship between the next-generation matrix and the probability of extinction, employing a simple model that may be viewed as an approximation to a full network model. The modelled heterogeneous mixing accounted for assortativity via an assumption of preferred mixing, and the probability of extinction was derived from a multidimentional branching process model. As a practical example, the age dependency in the transmission of pandemic influenza A (H1N1-2009) was considered, dividing the population into children and adults. Through quantitative illustrations, it has been shown that the probability of extinction given an adult index case increases with θ, at least for diseases with similar transmissibility as influenza. Although this exercise employed several simplifying assumptions, a formal hypothesis can be developed for explaining a slow interregional and international spread of the H1N1-2009 even in today's highly mobile world population. That is, whereas empirically observed delays in local transmission can be influenced by a large number of factors including pre-existing immunity, public health interventions and seasonality, the dominance of adults among travelers is one possible explanation for the high probability of extinction, and may play an important role in describing the underlying reason (Figure 1). Since the present study adopted three simplifying assumptions (i.e., (1) the crude dichotomization of hosts into two different types, (2) the adoption of exponentially distributed generation times, and (3) ignorance of infection-age among imported cases), the probability of extinction is likely to have been underestimated. The extinction probabilities become higher with more precise network structure (e.g., due to localized burnout of susceptible individuals) and more detailed natural history of infection [5, 40, 41].

Three practical implications are drawn from our exercise. First, the importance of assortativity in appropriately capturing the probability of extinction highlights a critical need to account for this aspect when quantifying the next-generation matrix in an approximately modelled heterogeneous population. Whenever the statistical inference of the next-generation matrix is made for directly transmitted diseases, the estimation framework should ideally account for assortative mixing. Whereas the social contact survey revealed that the age-dependent contact pattern is highly assortative [20, 21], the definition of a contact can be too broad to be practical for all diseases, and more realistic incorporation of assortative mixing and its precise estimation should be the subject of future studies.

Second, as was highlighted with an application, accounting for the age specificity in the surveillance of international and interregional mobility patterns and its use for statistical inference of epidemic dynamics are of utmost importance. For example, global airline transportation is one of the most well-studied networks, and this has been analyzed for H1N1-2009 [43], but a full description of global dynamics should better account for age-specific travel patterns. In addition, whereas imported cases from Mexico have been utilized to make statistical inference (e.g., spatial backcalculation) of the incidence in Mexico [6, 44, 45], the present study emphasizes a critical need to examine age-specificity in relevant frameworks, so that ultimately, the global dynamics can be described by a multihost metapopulation model [46, 47].

Third, as a disease control implication, although adults dominate imported cases, it should be remembered that the more important target host is still children. If stringent border control measures, for example, travel reduction and movement restrictions among all incoming passengers [48], are adopted as containment strategies against a highly virulent novel virus, the target host to promote radical reductions in travel-induced illness would be children, at least for diseases with a similar next-generation matrix to that of the recent pandemic.

Although the role of heterogeneously mixing population in the spread of infectious diseases has been examined using stochastic modelling approaches, past studies tended to focus on final epidemic size and its relevance to disease

control policy [49, 50]. Moreover, a limited number of studies examining the probability of extinction took an average of the probabilities over different types of host (e.g., by weighting the relative population size to the type specific probability of extinction) [24, 49]. The present study emphasized the importance of capturing type-specificity of index cases in estimating the probability of extinction and examining the impact of assortativity on extinction. In conclusion, we believe our simple exercise successfully illustrated the diminished role of nonmaintenance hosts in causing a major epidemic when assortativity is high, indicating a critical need to capture the assortativity in modelling the initial invasion of an epidemic disease.

5. Conclusions

Unlike local transmission of the H1N1-2009 which was frequently driven by school children, imported cases were predominantly adults. This study examined the relationship between the age-dependent next-generation matrix and the probability of extinction, focusing on the role of nonmaintenance hosts and the impact of assortativity on the epidemic extinction. The preferred mixing assumption captures assortativity in a much simpler way than full contact network models, allowing analysis in place of Monte Carlo calculations. The contribution of nonmaintenance hosts to the risk of a major epidemic is diminished as the mixing pattern becomes more assortative, so that an increase in the proportion of nonmaintenance hosts among index cases increases the probability of extinction, if temporary in the face of repeat importations. These results helped us to formulate a hypothesis that the dominance of adults in imported cases was one of the possible causes of observing substantial delay in interregional and international spread of the 2009 influenza pandemic. The importance of capturing the assortativity in estimating the next-generation matrix was highlighted.

Acknowledgments

The work of H. Nishiura is supported by the Japan Science and Technology Agency (JST) PRESTO program. A. R. Cook is grateful to the National University of Singapore for supporting his research. B. J. Cowling is supported by the Harvard Center for Communicable Disease Dynamics from the US National Institutes of Health Models of Infectious Disease Agent Study program (grant no. 1 U54 GM088558).

References

[1] Anonymous, "Mathematical modelling of the pandemic H1N1 2009," *Weekly Epidemiological Record*, vol. 84, no. 34, pp. 341–348, 2009.

[2] H. Nishiura, G. Chowell, M. Safan, and C. Castillo-Chavez, "Pros and cons of estimating the reproduction number from early epidemic growth rate of influenza A (H1N1) 2009," *Theoretical Biology and Medical Modelling*, vol. 7, no. 1, article 1, 2010.

[3] D. Butler, "Portrait of a year-old pandemic," *Nature*, vol. 464, no. 7292, pp. 1112–1113, 2010.

[4] L. A. Meyers, B. Pourbohloul, M. E. J. Newman, D. M. Skowronski, and R. C. Brunham, "Network theory and SARS: predicting outbreak diversity," *Journal of Theoretical Biology*, vol. 232, no. 1, pp. 71–81, 2005.

[5] M. E. J. Newman, "Spread of epidemic disease on networks," *Physical Review E*, vol. 66, no. 1, Article ID 016128, pp. 1–11, 2002.

[6] C. Fraser, C. A. Donnelly, S. Cauchemez et al., "Pandemic potential of a strain of influenza A (H1N1): early findings," *Science*, vol. 324, no. 5934, pp. 1557–1561, 2009.

[7] H. Nishiura, C. Castillo-Chavez, M. Safan, and G. Chowell, "Transmission potential of the new influenza A(H1N1) virus and its age-specificity in Japan," *Eurosurveillance*, vol. 14, no. 22, p. 19227, 2009.

[8] D. N. Fisman, R. Savage, J. Gubbay et al., "Older age and a reduced likelihood of 2009 H1N1 virus infection," *New England Journal of Medicine*, vol. 361, no. 20, pp. 2000–2001, 2009.

[9] A. L. Greer, A. Tuite, and D. N. Fisman, "Age, influenza pandemics and disease dynamics," *Epidemiology and Infection*, vol. 138, no. 11, pp. 1542–1549, 2010.

[10] Y. Itoh, K. Shinya, M. Kiso et al., "In vitro and in vivo characterization of new swine-origin H1N1 influenza viruses," *Nature*, vol. 460, no. 7258, pp. 1021–1025, 2009.

[11] T. Reichert, G. Chowell, H. Nishiura, R. A. Christensen, and J. A. McCullers, "Does Glycosylation as a modifier of Original Antigenic Sin explain the case age distribution and unusual toxicity in pandemic novel H1N1 influenza?" *BMC Infectious Diseases*, vol. 10, article 5, 2010.

[12] M. I. C. Chen, V. J. M. Lee, W. Y. Lim et al., "2009 Influenza A(H1N1) seroconversion rates and risk factors among distinct adult cohorts in Singapore," *Journal of the American Medical Association*, vol. 303, no. 14, pp. 1383–1391, 2010.

[13] B. J. Cowling, K. H. Chan, V. J. Fang et al., "Comparative epidemiology of pandemic and seasonal influenza A in households," *New England Journal of Medicine*, vol. 362, no. 23, pp. 2175–2184, 2010.

[14] S. Bansal, B. Pourbohloul, N. Hupert, B. Grenfell, and L. A. Meyers, "The shifting demographic landscape of pandemic influenza," *PLoS ONE*, vol. 5, no. 2, Article ID e9360, 2010.

[15] Y. Yang, J. D. Sugimoto, M. Elizabeth Halloran et al., "The transmissibility and control of pandemic influenza a (H1N1) virus," *Science*, vol. 326, no. 5953, pp. 729–733, 2009.

[16] O. Diekmann, J. A. Heesterbeek, and J. A. Metz, "On the definition and the computation of the basic reproduction ratio R0 in models for infectious diseases in heterogeneous populations," *Journal of Mathematical Biology*, vol. 28, no. 4, pp. 365–382, 1990.

[17] F. Ball and D. Clancy, "The final size and severity of a generalised stochastic multitype epidemic model," *Advances in Applied Probability*, vol. 25, no. 4, pp. 721–736, 1993.

[18] I. M. Longini, E. Ackerman, and L. R. Elveback, "An optimization model for influenza A epidemics," *Mathematical Biosciences*, vol. 38, no. 1-2, pp. 141–157, 1978.

[19] J. Medlock and A. P. Galvani, "Optimizing influenza vaccine distribution," *Science*, vol. 325, no. 5948, pp. 1705–1708, 2009.

[20] J. Wallinga, M. Van Boven, and M. Lipsitch, "Optimizing infectious disease interventions during an emerging epidemic," *Proceedings of the National Academy of Sciences of the United States of America*, vol. 107, no. 2, pp. 923–928, 2010.

[21] J. Mossong, N. Hens, M. Jit et al., "Social contacts and mixing patterns relevant to the spread of infectious diseases," *PLoS Medicine*, vol. 5, no. 3, article e74, pp. 0381–0391, 2008.

[22] J. Wallinga, P. Teunis, and M. Kretzschmar, "Using data on social contacts to estimate age-specific transmission parameters for respiratory-spread infectious agents," *American Journal of Epidemiology*, vol. 164, no. 10, pp. 936–944, 2006.

[23] M. E. J. Newman, "Assortative mixing in networks," *Physical Review Letters*, vol. 89, no. 20, Article ID 208701, pp. 1–4, 2002.

[24] I. C. Marschner, "The effect of preferential mixing on the growth of an epidemic," *Mathematical Biosciences*, vol. 109, no. 1, pp. 39–67, 1992.

[25] The Government of the Hong Kong Special Administrative Region, "Update on human swine influenza (July 2009)," The Government of the Hong Kong Special Administrative Region, Hong Kong, 2009.

[26] Rijksinstituut voor volksgezondheid en milieu (RIVM), "The Netherlands, Ziekenhuisopnamen Nieuwe Influenza A (H1N1)," RIVM, Bilthoven, 2010.

[27] J. T. Wu, B. J. Cowling, E. H. Y. Lau et al., "School closure and mitigation of pandemic (H1N1) 2009, Hong Kong," *Emerging Infectious Diseases*, vol. 16, no. 3, pp. 538–541, 2010.

[28] B. J. Cowling, L. L. H. Lau, P. Wu et al., "Entry screening to delay local transmission of 2009 pandemic influenza A (H1N1)," *BMC Infectious Diseases*, vol. 10, article 82, 2010.

[29] E. Miller, K. Hoschler, P. Hardelid, E. Stanford, N. Andrews, and M. Zambon, "Incidence of 2009 pandemic influenza A H1N1 infection in England: a cross-sectional serological study," *The Lancet*, vol. 375, no. 9720, pp. 1100–1108, 2010.

[30] H. Nishiura, "Travel and age of influenza A (H1N1) 2009 virus infection," *Journal of Travel Medicine*, vol. 17, no. 4, pp. 269–270, 2010.

[31] C. J. Mode, "Multitype branching processes: theory and applications," in *Modern Analytic and Computational Methods in Science and Mathematics*, R. Bellman, Ed., American Elsevier, New York, NY, USA, 1971.

[32] D. A. Griffiths, "Multivariate birth-and-death processes as approximations to epidemic processes," *Journal of Applied Probability*, vol. 10, no. 1, pp. 15–26, 1973.

[33] M. Boguñá and R. Pastor-Satorras, "Epidemic spreading in correlated complex networks," *Physical Review E - Statistical, Nonlinear, and Soft Matter Physics*, vol. 66, no. 4, Article ID 047104, pp. 1–4, 2002.

[34] F. Ball, "The threshold behaviour of epidemic models," *Journal of Applied Probability*, vol. 20, no. 2, pp. 227–241, 1983.

[35] T. E. Harris, *The Theory of Branching Processes*, Springer, Berlin, Germany, 1963.

[36] Anonymous, "Transmission dynamics and impact of pandemic influenza A (H1N1) 2009 virus," *Weekly Epidemiological Record*, vol. 84, no. 46, pp. 481–484, 2009.

[37] J. A. Jacquez, C. P. Simon, J. Koopman, L. Sattenspiel, and T. Perry, "Modeling and analyzing HIV transmission: the effect of contact patterns," *Mathematical Biosciences*, vol. 92, no. 2, pp. 119–199, 1988.

[38] H. W. Hethcote, "Modelling heterogeneous mixing in infectious disease dynamics," in *Models for Infectious Human Diseases: Their Structure and Relation to Data*, V. S. Isham and G. F. Medley, Eds., pp. 215–238, Cambridge University Press, Cambridge, UK, 1996.

[39] P. Mukherjee, P. L. Lim, A. Chow et al., "Epidemiology of travel-associated pandemic (H1N1) 2009 infection in 116 patients, Singapore," *Emerging Infectious Diseases*, vol. 16, no. 1, pp. 21–26, 2010.

[40] T. Garske and C. J. Rhodes, "The effect of superspreading on epidemic outbreak size distributions," *Journal of Theoretical Biology*, vol. 253, no. 2, pp. 228–237, 2008.

[41] J. O. Lloyd-Smith, S. J. Schreiber, P. E. Kopp, and W. M. Getz, "Superspreading and the effect of individual variation on disease emergence," *Nature*, vol. 438, no. 7066, pp. 355–359, 2005.

[42] H. Nishiura, B. Hoye, M. Klaassen, S. Bauer, and H. Heesterbeek, "How to find natural reservoir hosts from endemic prevalence in a multi-host population: a case study of influenza in waterfowl," *Epidemics*, vol. 1, no. 2, pp. 118–128, 2009.

[43] K. Khan, J. Arino, W. Hu et al., "Spread of a novel influenza A (H1N1) virus via global airline transportation," *New England Journal of Medicine*, vol. 361, no. 2, pp. 212–214, 2009.

[44] M. Lipsitch, M. Lajous, J. J. O'Hagan et al., "Use of cumulative incidence of novel influenza A/H1N1 in foreign travelers to estimate lower bounds on cumulative incidence in Mexico," *PLoS ONE*, vol. 4, no. 9, Article ID e6895, 2009.

[45] D. Balcan, H. Hu, B. Goncalves et al., "Seasonal transmission potential and activity peaks of the new influenza A(H1N1): a Monte Carlo likelihood analysis based on human mobility," *BMC Medicine*, vol. 7, article 45, 2009.

[46] J. Arino, J. R. Davis, D. Hartley, R. Jordan, J. M. Miller, and P. van den Driessche, "A multi-species epidemic model with spatial dynamics," *Mathematical Medicine and Biology*, vol. 22, no. 2, pp. 129–142, 2005.

[47] J. Arino, R. Jordan, and P. van den Driessche, "Quarantine in a multi-species epidemic model with spatial dynamics," *Mathematical Biosciences*, vol. 206, no. 1, pp. 46–60, 2007.

[48] H. Nishiura, N. Wilson, and M. G. Baker, "Quarantine for pandemic influenza control at the borders of small island nations," *BMC Infectious Diseases*, vol. 9, article 27, 2009.

[49] N. Becker and I. Marschner, "The effect of heterogeneity on the spread of disease," in *Stochastic Processes in Epidemic Theory*, J. P. Gabriel, C. Lefevre, and P. Picard, Eds., vol. 86 of *Lecture Notes in Biomathematics*, pp. 90–103, Springer, New York, NY, USA, 1990.

[50] H. Andersson and T. Britton, "Heterogeneity in epidemic models and its effect on the spread of infection," *Journal of Applied Probability*, vol. 35, no. 3, pp. 651–661, 1998.

Hindawi Publishing Corporation
Interdisciplinary Perspectives on Infectious Diseases
Volume 2011, Article ID 267049, 10 pages
doi:10.1155/2011/267049

Research Article

Pathogens, Social Networks, and the Paradox of Transmission Scaling

Matthew J. Ferrari,[1] Sarah E. Perkins,[1,2] Laura W. Pomeroy,[1,3] and Ottar N. Bjørnstad[4]

[1] *Center for Infectious Disease Dynamics, Department of Biology, The Pennsylvania State University, University Park, PA 16802, USA*
[2] *Cardiff School of Biosciences, Cardiff University, Biomedical Sciences Building, Museum Avenue, Room C7.29, Cardiff CF10 3AX, UK*
[3] *Department of Veterinary Preventative Medicine, The Ohio State University, Columbus, OH 43210, USA*
[4] *Center for Infectious Disease Dynamics, Departments of Biology and Entomology, The Pennsylvania State University, University Park, PA 16802, USA*

Correspondence should be addressed to Matthew J. Ferrari, mferrari@psu.edu

Received 24 September 2010; Revised 26 December 2010; Accepted 15 January 2011

Academic Editor: Katia Koelle

Understanding the scaling of transmission is critical to predicting how infectious diseases will affect populations of different sizes and densities. The two classic "mean-field" epidemic models—either assuming density-dependent or frequency-dependent transmission—make predictions that are discordant with patterns seen in either within-population dynamics or across-population comparisons. In this paper, we propose that the source of this inconsistency lies in the greatly simplifying "mean-field" assumption of transmission within a fully-mixed population. Mixing in real populations is more accurately represented by a network of contacts, with interactions and infectious contacts confined to the local social neighborhood. We use network models to show that density-dependent transmission on heterogeneous networks often leads to apparent frequency dependency in the scaling of transmission across populations of different sizes. Network-methodology allows us to reconcile seemingly conflicting patterns of within- and across-population epidemiology.

1. Introduction

Transmission is the driver of host-pathogen interactions and the most important determinant of disease dynamics. The patterns and dynamics of transmission within any given host population depend on how infectious and susceptible hosts interact, both spatially and socially [1]. Ultimately, pathogen transmission at the population level is determined by patterns of mixing at the individual level. Network science has highlighted that the mean and variance in transmission among individuals is key to the dynamics of spread within a given population network [2–5]. Predictions of disease dynamics, however, often require that we make projections from one population to another. Population size (i.e., counts), and possibly density, is a common metric with which to characterize differences among populations. Thus, a central challenge in infectious disease ecology is to understand how the distribution of contacts scales across populations of varying size.

Classically, the complex biology of host mixing has been characterized using select formulations from a small number of candidate mathematical models (e.g., [6–11]). If we consider only the increase in infected individuals (i.e., due to disease transmission), then the rate of increase in the number of infected individuals (I), dI/dt, is given by the number of susceptible hosts, S, times the force of infection (the per capita rate of infection). The force of infection, in turn, is the product of the rate of contacts among individuals, the probability of a contact being with an infectious host, and the probability of that contact giving rise to an infection. The first and third terms are commonly combined into a transmission term, β. In the simplest case, the rate of contact among hosts is assumed constant (i.e., independent of both population size and density). In a well-mixed population, the

probability of any given contact being infected is then I/N, where N is the population size (i.e., count), and the rate of increase of infected individuals in the population is given by

$$\frac{dI}{dt} = \beta S \frac{I}{N}. \quad (1)$$

This formulation is commonly referred to as *frequency-dependent transmission* (note that there has been extensive discussion of the appropriate terminology for these models; here, we defer to the derivations and terminology of Begon et al. [10]). Alternatively, if transmission scales linearly with population density (i.e., $\beta = \theta N/A$, where A is area occupied by the population) then we arrive at the *density-dependent transmission* model:

$$\frac{dI}{dt} = \beta SI. \quad (2)$$

Though the derivation of (2) is stated in terms of population density, the dependence on area is commonly suppressed by assuming that area is constant through time [10], and thus population size and density are equivalent measures. Begon et al. [10] caution, however, that this simplification in interpreting the two models leads to challenges in comparing dynamics across different populations that presumably occupy ranges of a different area. The frequency- and density-dependent transmission models are extreme special cases. While a variety of alternative or intermediate models have been proposed on theoretical or empirical grounds (see [9–11]), these remain the dominant archetypes in the literature.

Both models assume homogeneous mixing ("mean field") with no explicit spatial or social structure. While the mechanism of transmission is not explicitly considered in the derivation of (1) and (2), the choice between these two models is often motivated by the mode of transmission. Vector-borne and sexually transmitted diseases are generally assumed to be transmitted in a frequency-dependent manner because the mean number of contacts is independent of population density (if the number of sexual partners or vector attack rates are constant, e.g., [12]). Directly transmitted diseases, in contrast, are typically expected to spread in a density-dependent manner (because the number of encounters may increase with density and/or population size). Alternatively, the density-dependent transmission model has been equated with homogeneous or uniformly random mixing among individuals in contrast to frequency-dependent transmission, which is taken to reflect some degree of local heterogeneity in the population (i.e., in sexual partners) [13]. Begon et al. [10], however, have argued that heterogeneity of the contact structure is orthogonal to the distinction between density- and frequency-dependent transmission.

For host populations of constant size, occupying ranges of constant area, and pathogens that do not cause mortality, the frequency- and density-dependent formulations are equivalent. One may think of both as having a force-of-infection (= *per* susceptible rate of infection) equal to $\beta' I$, where $\beta' = \beta/N$ for the former and $\beta' = \beta$ for the latter. However, they make very different predictions about dynamics and control—such as targets for vaccination coverage and culling [9, 14]—when the host population size varies as a result of extrinsic forces or disease-induced mortality because of their implicit scaling-laws. In the frequency-dependent model, the realized population-level *per capita* (per susceptible-and-infected) transmission rate ($\hat{\beta} = dI/SIdt$) declines with increasing population size (N). As a consequence, the basic reproductive ratio, R_0—which defines the epidemic invasion criterion ($R_0 > 1$)—remains constant across varying population sizes. In contrast, the density-dependent model predicts a constant per capita transmission rate across population density. In this model, $\hat{\beta}$ is independent of population size, so consequently R_0 increases with N. The difference in the predictions of the two models leads to important and divergent predictions for dynamics: the frequency-dependent model has no threshold density for invasion [15] and predicts that moderately infectious pathogens ($R_0 > 2$) that result in lethal infections should lead to extinction of the host and the pathogen [14, 16] while the density-dependent model predicts a critical host density for pathogen invasion and long-term persistence and coexistence of the host and pathogen [17]. Further, for endemic, immunizing pathogens of hosts with a relatively long lifespan, L, the mean age-of-infection is predicted to be approximately L/R_0 [17, 18]. Thus, based on these models, we expect that frequency-dependent pathogens should exhibit constant mean age-of-infection and proportion of the population that is susceptible while, with density-dependent pathogens, mean age-of-infection and susceptible proportion decay with host population size.

Though the theoretical predictions of the frequency- and density-dependent transmission models are clearly distinct, the empirical patterns that emerge when transmission rates (or R_0) have been estimated in real populations are less clear [11]. When reviewing the literature, we find that the patterns do not align with the classic dichotomy between directly transmitted pathogens and sexually or vector transmitted pathogens (Table 1). The different theoretical predictions with respect to the scaling of dynamics with population size are particularly relevant, as we often observe disease processes at one scale (or location) and make inference about the behavior at another. As such, understanding how transmission scales across populations of different sizes are critical to making valid predictions.

Numerous empirical observations have provided direct measures of R_0 and/or $\hat{\beta}$ from collections of host populations that vary in size geographically, or individual populations that vary in size through time (Table 1). For example, two directly transmitted pathogens within the morbilliviridae have had $\hat{\beta}$ estimated for a broad range of population sizes: both measles [19] (Figure 1) and phocine distemper virus [20] found $\hat{\beta}$ to be inversely related to population size, and as a consequence, R_0 to be relatively invariant. These scaling patterns are as predicted by the frequency-dependent model, despite these pathogens being directly transmitted (and not "frequency-dependent" STDs or vector-borne pathogens)

Table 1: Empirical examples from the published literature of beta and R_0 measured in host populations differing in size, indicating the empirical observations and the likely mean-field scaling model.

Host-pathogen system	Empirical observations	Model supported	Reference
Humans-measles Humans-pertussis Humans-diphtheria Humans-scarlet fever	Found R_0 to be relatively invariant across population sizes.	Frequency dependent	[15]
Humans-smallpox	Transmission was inverse of population size	Frequency dependent	[58]
House finches-mycoplasma	Transmission was independent of flock sizes	Frequency dependent	[59]
Pigs-Aujeszky's disease virus (ADV)	R_0 was invariant across different population sizes	Frequency dependent	[21]
Harbor seals-phocine distemper virus (PDV)	Density-dependent scaling did not explain differences in transmission between different-sized seal haul-out sites	Frequency dependent	[20]
Rana mucosa-chytridiomycosis	Transmission rate increases and saturates with density of infected individuals	Frequency dependent	[33]
Tasmanian devil—devil facial tumor disease	Maintenance of high prevalence following population decline	Frequency dependent	[34]
Brushtail possums-leptospira interogans	Density-dependent model fit experimental infection rates	Density dependent	[60]
Elk-brucellosis	Population density was associated with an increase in seroprevalence but could not differentiate among linear and nonlinear effects of host density.	Nonlinear density dependent	[61]
Rodents-cowpox	Both models fit to incidence time series; support for both equivocal.	Frequency and density dependent	[22]
Rodents-cowpox	Transmission term lies between density- and frequency-dependent and varies seasonally.	Model is intermediate	[11]
Indian meal moth-granulosis virus	A decline in transmission with increasing density of infectious cadavers	Neither	[26]
Possum-tuberculosis	Transmission did not fit frequency- or density-dependent models	Neither	[62]
Tiger salamander-*Abystomatigrinum* virus	Transmission was best modeled by a power or negative binomial function, that is, nonlinear density dependence.	Neither	[63]
Badgers-*Mycobacterium bovis*	Negative relationship between host abundance and infection prevalence	Neither	[64]

for which density dependence is normally expected. Other empirical studies are ambiguous in their model support when scaled across populations (Table 1). For example, R_0 was concluded to be invariant across population sizes for Aujeszky's disease virus in pigs [21], supporting a frequency-dependent model; Begon et al. [22] found equal support for frequency- and density-dependent transmission models in cowpox data in rodents; Smith et al. [11] have subsequently found support for model that is intermediate to the density- and frequency-dependent models based on an analysis of long-term time series from the same system. Bucheli and Shykoff [23] argued that support of the density- versus frequency-dependent model depended on the spacing of the host plants in pollinator-vectored anther smut. Klepac et al. [24] found that while the density-dependent model fit the observations of the 2002 phocine distemper virus outbreak in the Dutch Wadden Sea better than a frequency-dependent model, the observed dynamics in juvenile and adult seals (which are less social) was better explained by a frequency-dependent model.

Experimental manipulations of populations and studies of the ensuing scaling patterns are also equivocal in their support for either frequency or density dependence. Knell et al. [25, 26] found that transmission of *Bacillus thuringiensis* and a granulosis virus increased with density of susceptible *Plodia interpunctella* and decreased with density of infectious cadavers, and thus fails to conform to the density-dependent model. Antonovics and Alexander [27] manipulated both host density and frequency of infected *Silene latifolia* and found that deposition of the anther smut fungus *Microbotryum violaceum* by pollinating insects increased with frequency of infection, but not density, supporting the notion that vector-borne pathogens are spread in a frequency-dependent fashion. Ryder et al. [28], however, independently manipulated the density and frequency of two-spot lady birds, *Adalia bipunctata*, parasitized by the mite, *Coccipolipus hippodamiae*, and found that infection

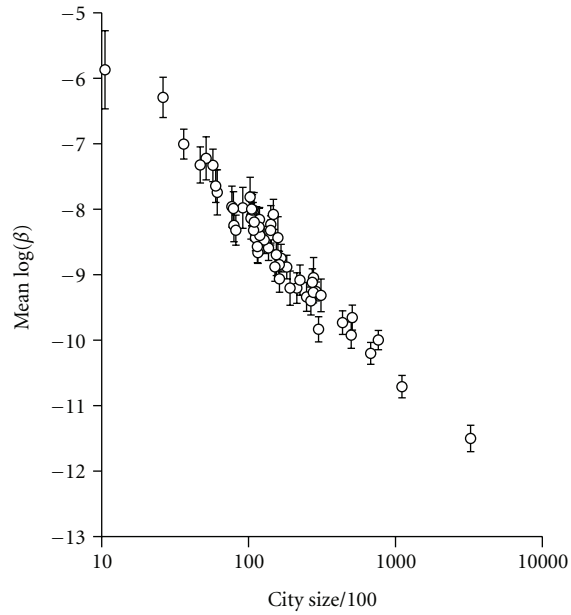

Figure 1: Scaling of measles transmission. The estimated mean transmission rate (β) of measles in England and Wales plotted against increasing city size in thousands. Reproduced from [19].

rates scaled with host density because of increased promiscuity at high density, in contrast to the notion that STDs spread in a frequency-dependent fashion.

Evidence based on serology and age-serology is also difficult to interpret, yet the serological data for a range of directly transmitted human pathogens [17] is to a greater or lesser extent consistent with an invariant R_0 across scales and thus, in accordance with the frequency-dependent model. Edmunds et al. [29] found the median age at infection for Hepatitis B virus to vary from 1–18 years in highly endemic areas (6 African surveys, 3 in south-east Asia, 2 in Oceania, and 1 in South American). These surveys spanned populations ranging in size from a few hundred (an Amerindian village; [30]) to >10 million (Hu et al. [31]) and showed no negative correlation between median age and population size. Metcalf et al. [32] similarly found no correlation between mean age of infection with rubella and population size in the 31 states of Mexico and Mexico City.

On the whole, scaling of $\hat{\beta}$ and R_0 across populations tend to follow predictions consistent with the frequency-dependent model. In contrast, dynamical patterns within populations are often contradictory to this model and favor the density-dependent model. A key distinction between the frequency- and density-dependent models is that the former predicts moderately lethal pathogens can lead to extinction of the host and parasite. Rachowicz and Briggs [33] showed that transmission of *Batrachochytrium dendrobatidis*, which has been implicated in amphibian extinctions, in tadpoles more closely scaled with frequency than density of infected individuals. In general, however, there is little empirical evidence of pathogen-induced host extinction. In a review of 43 empirical papers, de Castro and Bolker [14] found only one study that gives direct evidence of pathogen-induced extinction. McCallum et al. [34] observed the maintenance of high prevalence of the directly transmitted devil facial tumor disease even as populations suffered significant declines, raising the concern that the disease could lead to extinction of the host. Under the density-dependent model, the reduction of the susceptible population below a threshold level drives the effective transmission rate below 1 and leads to extinction of the pathogen only. The successful application of this principle in, for example, rabies [35], smallpox [36], and foot-and-mouth disease [37] is consistent with density-dependent transmission.

Measles and phocine distemper, which have been well studied both within and across populations, are exemplary of the paradoxical predictions of the mixing models; both exhibit scaling of transmission rates across populations that is consistent with frequency dependence but local dynamics that are consistent with density dependence [19]. We believe that this paradox arises from the application of the same mean-field transmission model to describe both the within-population transmission and the implicit scaling between populations. We need to revisit the assumption of random host mixing in the face of the strong social and spatial structuring that may limit the interactions between individuals [1]. The dynamics of within-population transmission depend on both the mode of transmission and the structure of transmission network [2–4]; however, the scaling of transmission across populations hinges on the social and spatial structuring of the host population, somewhat independent of the mode of transmission. Note that this point was already raised by De Jong et al. [15]. In the next section, we use network models to show that the equivocal support of the classical models can be resolved by explicit considerations of the contact networks of social and spatial contact patterns.

2. Epidemics and Social Networks

Network models have become very popular methods to relax the assumption of complete mixing among individuals (see [5] for a general review). In most natural populations and particularly those with strong social or spatial structure, individuals interact with only a small proportion of the population. We first introduce the network formalism to capturing social organization, and then we discuss the emergent scaling of pathogen transmission on three classes of social networks.

Epidemic network models differ from the mean-field models in that individuals only interact within their local social neighborhood. We can use these models to investigate the scaling of the realized *per capita* transmission rate, $\hat{\beta}$, with host population size in relation to both the mean neighborhood size ($\langle k \rangle$ = mean degree) and the heterogeneity of contacts. Cellular automata models have similarly been used to study the distinction between local transmission and global dynamics (e.g., [38–41]). However, the nature of cellular automata models limit the range of social structures that can be studied to those that can be reasonably collapsed to 2 dimensions (i.e., a lattice). Contact network models

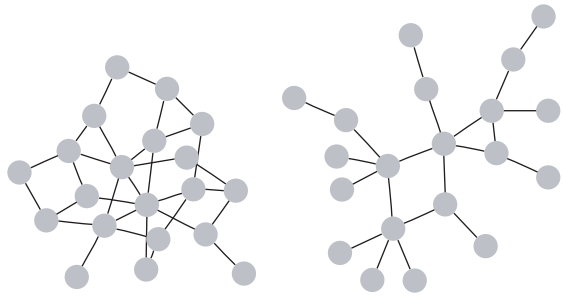

FIGURE 2: Classes of social networks. Two classes of social networks where the node represents an individual and the edge a social connection or epidemiological relevant contact according to edge distributions (i.e., contact networks) that are described by (a) Poisson networks and (b) power law networks.

allow the flexibility to study a wide range of social structures with a complex mix of both local and global interactions [42].

Various characteristics of contact network topology (i.e., clustering, assortativity, etc.) may vary with population size. However, there are few empirical studies of the scaling of network properties on social networks of various sizes. Here, we focus simply on the scaling of the mean number of contacts with network size, both because of its straight forward interpretation and its parallels with the classic formulations of the density- and frequency-dependent mean-field models. The classic mean-field models make explicit assumptions about the way the mean rate of contacts scales with population density, but are restricted by implicit assumptions of how the variance in contacts scales with density. Contact network models make explicit the relationship between the mean and variance of contacts in the choice of the degree distribution. Further, contact network models relax the assumption that population density or size is a proxy for the contact rate, which is implicit in the mean-field models.

Host social organizations that have constraints on group size (e.g., classroom size for school children, harem size for some social mammals) may be adequately represented by a Poisson distribution of social contacts (i.e., a variance to mean ratio near 1, Figure 2(a)) [2]. In contrast, many animal species exhibit skewed social contact networks with few individuals having many contacts, and the majority having few contacts (i.e., a variance to mean ratio $\gg 1$, Figure 2(b)) [43, 44]. Following established theory, these social interactions are commonly characterized by truncated power laws [45, 46].

We generated networks of size $N = 100$, 500, 1000, 2000, 5000, and 10000 nodes (individuals) for which the mean number of contacts scaled in one of 3 ways: (1) the mean number of contacts was independent of population size ($\langle k \rangle = 6$), (2) the mean number of contacts increased slower than linearly with population size ($\langle k \rangle = .6 * \sqrt{N}$), and (3) the mean number of contacts increased linearly with population size ($\langle k \rangle = 0.06 * N$). Note that all networks have the same mean when $N = 100$. The constant and linear scaling functions are analogous to the assumptions of the classic frequency- and density-dependent transmission functions in the mean-field models when area is held constant. The intermediate function represents an intermediate setting where, for example, the number of contacts increases initially with population size (e.g., larger cities lead to larger workplaces), but the total number of contacts is limited by time or typical home range. In these models, we base the scaling of contacts on the population size rather than density. While in many settings it may be reasonable to assume that the probability of a contact depends on spatial proximity [47], the complexity of empirical contact networks has highlighted that space is not always a reasonable proxy for social proximity [48].

We considered the effect of local heterogeneity of contacts by generating networks with Poisson, exponential, and truncated power law contact distributions. The Poisson contact distribution reflects a setting with relatively low variance in the number of contacts and thus approximates the homogeneous contact structure of the mean-field models [10]. The power law contact distributions reflect extreme heterogeneity in local contacts that is seen in many empirical contact networks. The exponential contact distribution represents an intermediate case. Networks were generated using the algorithm described by Molloy and Reed [49]. We approximated a power law degree distribution using a negative binomial distribution with dispersion parameter, $\theta = 0.1$. The presence of highly connected individuals, so-called "super spreaders" [43], has been consistently shown to have large impacts on the threshold conditions and final size of outbreaks [4, 50]. Thus, under the assumption of constant mean contacts for networks of increasing size, we might expect emergent scaling of dynamics for the three degree distributions as larger networks will better sample the degree distribution, which would mean a greater proportion of rare "super spreaders" in the exponential and power law distributed networks.

For all three families of edge distributions, nodes were connected at random with the restriction that self-loops (nodes connected to themselves) and double edges between nodes were disallowed. Thus, individuals cannot infect themselves and cannot infect another in the population more than once.

We simulated epidemics on the contact networks according to a discrete time, stochastic susceptible-infected-removed ("chain-binomial") [51] model. Susceptible hosts become infected in each time step with probability $p_j = 1 - \exp(-\beta \overline{I}_j)$, where $\overline{I}_j$ is the number of infected individuals within the local neighborhood of individual j at a given time point. Thus, infection depends on the local density of infected hosts, where density is relative to the social neighborhood rather than a fixed neighborhood in Euclidean space (i.e., transmission is *locally* density dependent). Infected individuals were removed from the population in each time step with probability $1 - \exp(-\gamma)$, thus leading to a geometrically distributed infectious period—the discrete

time equivalent of the standard SIR assumptions. Removed individuals were assumed to be permanently immune and thus unable to be subsequently infected; in practice, these nodes in the network are "turned off", so while the total number of nodes remains constant, the effective number of nodes in the epidemiologically active portion of the network declines (i.e., thus, for this model equivalent to disease-induced mortality). In an important contrast to the mean-field models, the removal of infected nodes results in reduced contacts for their remaining neighbors. Thus, for structured contact networks (as has been well explored for cellular automata models [38, 39]), the local and global impact of the removal of infected individuals can be quite different. However, in contrast to nonnetwork models (e.g., cellular automata and small-world models for which only local connections are explicit), variance in the distribution of contacts leads to a structured cascade of infection from highly connected individuals to less well-connected individuals, which results in a decline in the per capita realized transmission. This effect is equivalent to the frailty effect discussed in mathematical demography [19]. The rate and magnitude of this decline depends explicitly on the distribution of the underlying transmission network [52].

For each configuration, we generated 30 networks and simulated epidemics seeded by a single infection. In each time step, the probability of transmission across an edge was assumed to be 0.1, and the probability that an infected node recovered was 0.1. We calculated, for each configuration and each time step, the realized per capita (per infected) transmission rate, $\hat{\beta}_t$:

$$\hat{\beta}_t = \frac{I_t - I_{t-1}}{S_t I_t}, \tag{3}$$

where I_t and S_t are the total number of infectious and susceptible nodes on the network at time t. The selective removal of highly connected nodes early in the epidemic results in a decrease in the realized transmission rate as the epidemic progresses [52]. To generate time-weighted realized per capita rates, we, therefore, calculated $\hat{\beta}$ as the intercept of the regression of $\hat{\beta}_t$ on time. Thus, we are describing the scaling of the rate of transmission at the initiation of an epidemic. Calculations using the time-course average yields similar scaling results and are, therefore, not included (Ferrari et al., unpublished results).

We find that the realized *per capita* transmission rate ($\hat{\beta}$) decreased with population size despite local transmission being modeled as a density-dependent process (Figures 3(a), 3(c), and 3(e)). Only when the mean number of contacts is assumed to increase linearly with population size is *per capita* rate ($\hat{\beta}$) constant across networks (Figures 3(a), 3(c), and 3(e)). Social group sizes that increase slower-than-linearly with community size yield intermediate results; $\hat{\beta}$ decays but slower than $1/N$. In all cases, the local scale transmission remains constant across network sizes; that is, the number of new infections per susceptible-infected pair remains constant regardless of network size or configuration (Figures 3(b), 3(d), and 3(f)). Surprisingly, these scaling relationships are remarkably constant across the three classes of networks despite the difference in the variance in local contacts. For a given network size and mean number of contacts, the per capita transmission rate was lowest for the Poisson networks and greatest for the scale-free networks, in agreement with the standard observation that transmission is positively correlated with variance in the contact distribution. The critical finding from our analysis is that we need to distinguish between the *mode* of transmission within-populations (frequency versus density dependent) and the *scaling* of transmission between populations.

3. Discussion

Classically, the choice of model to describe disease dynamics was based on the transmission route of the pathogen, with little regard to empirical patterns. Even though this method may accurately describe local transmission between individual hosts, as evidenced by the wealth of empirical examples and the success of the resultant theory in disease management, it is not evident that these models will scale correctly to describe transmission across socially or spatially distinct populations (see examples in Table 1). In the above example, we have shown that the scaling pattern of pathogen transmission among distinct populations can be determined by the structure and scaling of the local host contact network and that the scaling pattern is independent of the mode of transmission. The scaling relationship depends explicitly on the heterogeneity in contacts and how the average connectivity changes with population size. In general, the scaling of transmission is likely to depend on the particular nature of host mixing and contact network structure—pathogen transmission biology may not play a large role.

In all the models, the heterogeneity in the contact structure leads to a structured cascade of infection from highly connected individuals to less connected individuals [52], which results in a decline in the realized per capita transmission rate that is consistent with the predictions of the mean-field density-dependent model. (Note that the constant, or increasing, per capita transmission rate that is predicted by the mean-field, frequency-dependent model requires that new contacts be formed among individuals remaining in network model to overcome this frailty effect.) However, we only observed density-dependent scaling with population size in network models when the mean number of contacts is proportional to population size. This phenomenon is rarely observed in the literature (Table 1), possibly due to natural constraints on the number of contacts as populations grow, due to limited time or space. Presumably, for some very well-mixed systems such as phages in bacterial emulsions, density-dependent scaling with population size may be possible.

Despite locally density-dependent transmission, the network models predict $\hat{\beta}$ to scale in a pattern consistent with the frequency-dependent mean-field model when the mean number of social contacts is independent of population size or increases at a decelerating rate. We would expect this scaling pattern when social forces place constraints on the number of contacts independently of population size; for

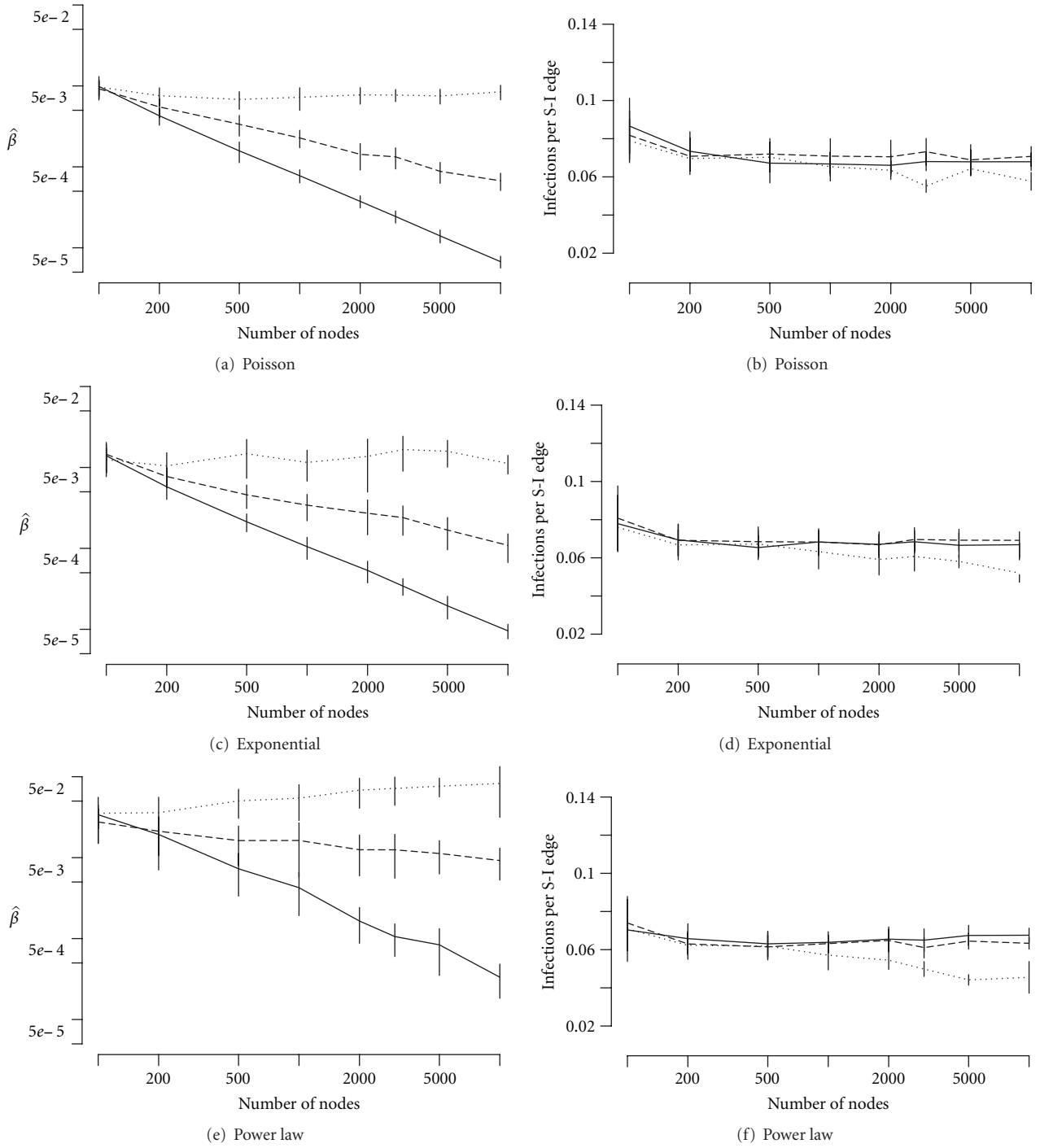

FIGURE 3: Scaling of transmission on Poisson (a, b), exponential (c, d), and scale-free (e, f) networks. Left-hand panels are the mean realized per capita transmission rate, $\hat{\beta}$, plotted against network size. Right-hand panels are the mean number of infections per edge between susceptible and infected nodes. Solid lines indicate a constant mean number of contacts for all population sizes. Dashed lines indicate a mean number of contacts that increase proportional to the square root of population size. Dotted lines indicate a mean number of contacts that increase linearly with the population size. Vertical bars give the standard deviation in observations from 30 simulated networks.

example, measles, for which school classroom sizes tend to be reasonably constrained [19], and phocine distemper virus in harbor seals, for which spatial constraints limit the number of seals on haulouts [18].

We further found that the scaling relationship was independent of the variance in the edge distribution of the contact network. Thus, the choice of the mean-field, density-dependent model to represent populations with

homogeneous mixing [13], is not justified and would impose a scaling relationship that is only consistent with the extreme case where the mean number of contacts scale linearly with population size. As such, this observation corroborates the heuristic argument of Begon et al. [10] that the degree of local heterogeneity in the contact structure is "orthogonal to the distinction between density- and frequency-dependent contact rates and transmission."

The network models we present here are necessarily simplistic in that they presume that epidemic dynamics are fast relative to ecological dynamics, so we can ignore births, nondisease mortality, and the formation of new connections following node removal (i.e., in the event that node removal is interpreted as mortality rather than lasting immunity). In principle, these should not impact our general observations providing that births and deaths are not biased with respect to the connectivity of nodes, an assumption implicit in the mean-field models. In practice, however, it is likely that births and deaths are biased with respect to network characteristics (e.g., [53]) or that connections are dynamic (connections accrue or change as nodes age [54]). Understanding these mechanisms that generate contact processes is an important ecological challenge and the efficient algorithms to incorporate these dynamics into model representations remain an important technical challenge.

The density- and frequency-dependent, mean-field models make explicit assumptions about how the mean contact rate should scale with population density (or size if area is held constant as is the common assumption). As Begon et al. [10] point out, the direct application of these models across populations presents a challenge, as it requires the presumption that either area is comparable among populations of different size, or that the relationship between density and contact rate is consistent across populations. A variety of more flexible mean-field models have been proposed that allow for more intermediate, nonlinear relationships between density and contact rate [11]. However, while these intermediate relationships may provide better fit to observed dynamics, they are difficult to interpret in terms of explicit mechanisms, as there may be a range of candidate explanations for the nonlinear relationship between density and contacts [11].

Contact network models, while occasionally limiting in their complexity, present a useful tool for understanding the role of the social contact structure in generating observed dynamics. The focus on explicit characteristics of the contact structure provides a mechanistic explanation for the resulting dynamics compared with the phenomenological representations of contact rate assumed in the mean-field models. Here, we have shown the flexibility of these models to retain commonly observed within-population dynamics (i.e., the decline in realized transmission due to contact frailty) and a range of scaling patterns across population sizes as a function of the relationship between the contact distribution and the network size. We have presented only relatively simple examples where the mean and variance of the contact distribution scale with network size. However, it is reasonable to presume that a variety of additional, higher-order characteristics of contact networks (i.e., clustering, assortativity) may also scale with population size or density. The challenges of projecting even simple mean-field models across populations highlights the need for a greater understanding of how the characteristics of contact network correlate with more directly measureable metrics such as population size and density in order to make the lessons from contact network epidemiology predictive.

In conclusion, we must understand the local mixing dynamics of the host population rather than assume an implicit mixing structure defined by the pathogen in order to make predictions about epidemic dynamics across scales. Both experimental and theoretical work is needed to resolve the uncertainty about the scaling of transmission with population size and density. Experimentally, proper model systems will permit exploration of the effects of population size and density on mixing behavior and epidemic dynamics. Critically, this may depend strongly on behavioral responses to population size or density at the scale of individuals (e.g., [28]) that give rise to important deviations from the simple scaling models. Theoretically, method development and application will allow the study of contact network properties from field-sampled data on real populations. Network models in physics and epidemiology have provided great insights into the effect of heterogeneities and network topology on epidemic dynamics; however, connecting these insights to dynamics in real systems is challenging because of the need for fully censused populations to recreate contact networks and the assumption that network topology is static (though see [55]). The development of statistical methods to conduct inference on social network models [56] may prove useful to understand network assembly rules and for generating candidate networks for investigation of epidemic dynamics through simulation; in particular, how models of host movement and interaction among individuals give rise to scaling rules—be they network properties or mean-field approximations—for population mixing [57]. Overall, increasing the comprehension of host contact and mixing dynamics—through experimental and theoretical methods—will permit a more complete understanding of epidemic dynamics.

References

[1] S. Altizer, C. L. Nunn, P. H. Thrall et al., "Social organization and parasite risk in mammals: integrating theory and empirical studies," *Annual Review of Ecology, Evolution, and Systematics*, vol. 34, pp. 517–547, 2003.

[2] L. A. Meyers, B. Pourbohloul, M. E. J. Newman, D. M. Skowronski, and R. C. Brunham, "Network theory and SARS: predicting outbreak diversity," *Journal of Theoretical Biology*, vol. 232, no. 1, pp. 71–81, 2005.

[3] M. E. J. Newman, "Spread of epidemic disease on networks," *Physical Review E*, vol. 66, no. 1, Article ID 016128, 11 pages, 2002.

[4] R. Pastor-Satorras and A. Vespignani, "Epidemic spreading in scale-free networks," *Physical Review Letters*, vol. 86, no. 14, pp. 3200–3203, 2001.

[5] S. Bansal, B. T. Grenfell, and L. A. Meyers, "When individual behaviour matters: homogeneous and network models in

epidemiology," *Journal of the Royal Society Interface*, vol. 4, no. 16, pp. 879–891, 2007.

[6] R. M. Anderson and R. M. May, "Regulation and stability of host-parasite population interactions I. Regulatory processes," *Journal of Animal Ecology*, vol. 47, pp. 219–247, 1978.

[7] M. C. M. de Jong, "Mathematical modelling in veterinary epidemiology: why model building is important," *Preventive Veterinary Medicine*, vol. 25, no. 2, pp. 183–193, 1995.

[8] G. Dwyer, J. S. Elkinton, and J. P. Buonaccorsi, "Host heterogeneity in susceptibility and disease dynamics: tests of a mathematical model," *American Naturalist*, vol. 150, no. 6, pp. 685–707, 1997.

[9] H. McCallum, N. Barlow, and J. Hone, "How should pathogen transmission be modelled?" *Trends in Ecology and Evolution*, vol. 16, no. 6, pp. 295–300, 2001.

[10] M. Begon, M. Bennett, R. G. Bowers, N. P. French, S. M. Hazel, and J. Turner, "A clarification of transmission terms in host-microparasite models: numbers, densities and areas," *Epidemiology and Infection*, vol. 129, no. 1, pp. 147–153, 2002.

[11] M. J. Smith, S. Telfer, E. R. Kallio et al., "Host-pathogen time series data in wildlife support a transmission function between density and frequency dependence," *Proceedings of the National Academy of Sciences of the United States of America*, vol. 106, no. 19, pp. 7905–7909, 2009.

[12] P. H. Thrall, J. Antonovics, and D. W. Hall, "Host and pathogen coexistence in sexually transmitted and vector-borne diseases characterized by frequency-dependent disease transmission," *American Naturalist*, vol. 142, no. 3, pp. 543–552, 1993.

[13] A. B. Lockhart, P. H. Thrall, and J. Antonovics, "Sexually transmitted diseases in animals: ecological and evolutionary implications," *Biological Reviews of the Cambridge Philosophical Society*, vol. 71, no. 3, pp. 415–471, 1996.

[14] F. De Castro and B. Bolker, "Mechanisms of disease-induced extinction," *Ecology Letters*, vol. 8, no. 1, pp. 117–126, 2005.

[15] M. C. M. De Jong, O. Diekmann, and H. Heesterbeek, "How does transmission of infection depend on population size?" in *Epidemic Models: Their Structure and Relation to Data*, D. Mollison, Ed., pp. 84–94, Cambridge University Press, Cambridge, UK, 1995.

[16] W. M. Getz and J. Pickering, "Epidemic models: thresholds and population regulation," *The American Naturalist*, vol. 121, pp. 892–898, 1983.

[17] R. M. Anderson and R. M. May, *Infectious Diseases of Humans: Dynamics and Control*, Oxford University Press, Oxford, UK, 1991.

[18] J. Swinton, J. Harwood, B. T. Grenfell, and C. A. Gilligan, "Persistence thresholds for phocine distemper virus infection in harbour seal Phoca vitulina metapopulations," *Journal of Animal Ecology*, vol. 67, no. 1, pp. 54–68, 1998.

[19] O. N. Bjørnstad, B. F. Finkenstädt, and B. T. Grenfell, "Dynamics of measles epidemics: estimating scaling of transmission rates using a Time series SIR model," *Ecological Monographs*, vol. 72, no. 2, pp. 169–184, 2002.

[20] J. Swinton, J. Harwood, and A. Hall, "Scaling of phocine distemper virus transmission with harbor seal community size," *Ecologie*, vol. 30, pp. 231–240, 1999.

[21] A. Bouma, M. C. M. de Jong, and T. G. Kimman, "Transmission of pseudorabies virus within pig populations is independent of the size of the population," *Preventive Veterinary Medicine*, vol. 23, no. 3-4, pp. 163–172, 1995.

[22] M. Begon, S. M. Feore, K. Bown, J. Chantrey, T. Jones, and M. Bennett, "Population and transmission dynamics of cowpox in bank voles: testing fundamental assumptions," *Ecology Letters*, vol. 1, no. 2, pp. 82–86, 1998.

[23] E. Bucheli and J. A. Shykoff, "The influence of plant spacing on density-dependent versus frequency-dependent spore transmission of the anther smut Microbotryum violaceum," *Oecologia*, vol. 119, no. 1, pp. 55–62, 1999.

[24] P. Klepac, L. W. Pomeroy, O. N. Bjørnstad, T. Kuiken, A. D. M. E. Osterhaus, and J. M. Rijks, "Stage-structured transmission of phocine distemper virus in the Dutch 2002 outbreak," *Proceedings of the Royal Society B*, vol. 276, no. 1666, pp. 2469–2476, 2009.

[25] R. J. Knell, M. Begon, and D. J. Thompson, "Transmission dynamics of Bacillus thuringiensis infecting Plodia interpunctella: a test of the mass action assumption with an insect pathogen," *Proceedings of the Royal Society of London B*, vol. 263, no. 1366, pp. 75–81, 1996.

[26] R. J. Knell, M. Begon, and D. J. Thompson, "Transmission of Plodia interpunctella granulosis virus does not conform to the mass action model," *Journal of Animal Ecology*, vol. 67, no. 4, pp. 592–599, 1998.

[27] J. Antonovics and H. M. Alexander, "Epidemiology of Anther-Smut infection of Silene-alba (= S-Latifolia) caused by Ustilago-Violacea—patterns of spore deposition in experimental populations," *Proceedings of the Royal Society of London B*, vol. 250, no. 1328, pp. 157–163, 1992.

[28] J. J. Ryder, K. M. Webberley, M. Boots, and R. J. Knell, "Measuring the transmission dynamics of a sexually transmitted disease," *Proceedings of the National Academy of Sciences of the United States of America*, vol. 102, no. 42, pp. 15140–15143, 2005.

[29] W. J. Edmunds, G. F. Medley, D. J. Nokes, C. J. O'Callaghan, H. C. Whittle, and A. J. Hall, "Epidemiological patterns of hepatitis B virus (HBV) in highly endemic areas," *Epidemiology and Infection*, vol. 117, no. 2, pp. 313–325, 1996.

[30] J. R. Torres and A. Mondolfi, "Protracted outbreak of severe delta hepatitis: experience in an isolated Amerindian population of the Upper Orinoco Basin," *Reviews of Infectious Diseases*, vol. 13, no. 1, pp. 52–55, 1991.

[31] M. Hu, D. Schenzle, F. Deinhardt, and R. Scheid, "Prevalence of markers of hepatitis A and B in the Shanghai area," *Journal of Infectious Diseases*, vol. 147, no. 2, p. 360, 1983.

[32] C. J. E. Metcalf et al., "The epidemiology of rubella in Mexico: seasonality, stochasticity and regional variation," *Epidemiology and Infection*. In press.

[33] L. J. Rachowicz and C. J. Briggs, "Quantifying the disease transmission function: effects of density on Batrachochytrium dendrobatidis transmission in the mountain yellow-legged frog Rana muscosa," *Journal of Animal Ecology*, vol. 76, no. 4, pp. 711–721, 2007.

[34] H. McCallum, M. Jones, C. Hawkins et al., "Transmission dynamics of Tasmanian devil facial tumor disease may lead to disease-induced extinction," *Ecology*, vol. 90, no. 12, pp. 3379–3392, 2009.

[35] R. M. Anderson, H. C. Jackson, R. M. May, and A. M. Smith, "Population dynamics of fox rabies in Europe," *Nature*, vol. 289, no. 5800, pp. 765–771, 1981.

[36] R. N. Basu, Z. Jezek, and N. A. Ward, *The Eradication of Smallpox in India*, World Health Organization, Geneva, Switzerland, 1979.

[37] M. J. Keeling, M. E. J. Woolhouse, R. M. May, G. Davies, and B. T. Grenfell, "Modelling vaccination strategies against foot-and-mouth disease," *Nature*, vol. 421, no. 6919, pp. 136–142, 2003.

[38] C. J. Rhodes and R. M. Anderson, "Epidemic thresholds and vaccination in a lattice model of disease spread," *Theoretical Population Biology*, vol. 52, no. 2, pp. 101–118, 1997.

[39] J. Turner, M. Begon, and R. G. Bowers, "Modelling pathogen transmission: the interrelationship between local and global approaches," *Proceedings of the Royal Society B*, vol. 270, no. 1510, pp. 105–112, 2003.

[40] M. Boots, P. J. Hudson, and A. Sasaki, "Large shifts in pathogen virulence relate to host population structure," *Science*, vol. 303, no. 5659, pp. 842–844, 2004.

[41] S. N. Wood and M. B. Thomas, "Space, time and persistence of virulent pathogens," *Proceedings of the Royal Society B*, vol. 263, no. 1371, pp. 673–680, 1996.

[42] J. M. Read and M. J. Keeling, "Disease evolution on networks: the role of contact structure," *Proceedings of the Royal Society B*, vol. 270, no. 1516, pp. 699–708, 2003.

[43] J. O. Lloyd-Smith, S. J. Schreiber, P. E. Kopp, and W. M. Getz, "Superspreading and the effect of individual variation on disease emergence," *Nature*, vol. 438, no. 7066, pp. 355–359, 2005.

[44] M. E. J. Woolhouse, C. Dye, J. F. Etard et al., "Heterogeneities in the transmission of infectious agents: implications for the design of control programs," *Proceedings of the National Academy of Sciences of the United States of America*, vol. 94, no. 1, pp. 338–342, 1997.

[45] W. Jetz, C. Carbone, J. Fulford, and J. H. Brown, "The scaling of animal space use," *Science*, vol. 306, no. 5694, pp. 266–268, 2004.

[46] M. Sjöberg, B. Albrectsen, and J. Hjältén, "Truncated power laws: a tool for understanding aggregation patterns in animals?" *Ecology Letters*, vol. 3, no. 2, pp. 90–94, 2000.

[47] S. E. Perkins, F. Cagnacci, A. Stradiotto, D. Arnoldi, and P. J. Hudson, "Comparison of social networks derived from ecological data: implications for inferring infectious disease dynamics," *Journal of Animal Ecology*, vol. 78, no. 5, pp. 1015–1022, 2009.

[48] C. Song, Z. Qu, N. Blumm, and A. L. Barabási, "Limits of predictability in human mobility," *Science*, vol. 327, no. 5968, pp. 1018–1021, 2010.

[49] M. Molloy and B. Reed, "A critical-point for random graphs with a given degree sequence," *Random Structures & Algorithms*, vol. 6, no. 2-3, pp. 161–179, 1995.

[50] R. Pastor-Satorras and A. Vespignani, "Epidemic dynamics in finite size scale-free networks," *Physical Review E*, vol. 65, no. 3, Article ID 035108, 4 pages, 2002.

[51] N. T. J. Bailey, *The Mathematical Theory of Epidemics*, Griffin, London, UK, 1957.

[52] M. J. Ferrari, S. Bansal, L. A. Meyers, and O. N. Bjørnstad, "Network frailty and the geometry of herd immunity," *Proceedings of the Royal Society B*, vol. 273, no. 1602, pp. 2743–2748, 2006.

[53] A. L. Barabási and R. Albert, "Emergence of scaling in random networks," *Science*, vol. 286, no. 5439, pp. 509–512, 1999.

[54] S. Bansal et al., "The dynamic nature of contact networks in infectious disease epidemiology," *Journal of Biological Dynamics*, vol. 4, no. 5, pp. 478–489, 2010.

[55] J. Saramäki and K. Kaski, "Modelling development of epidemics with dynamic small-world networks," *Journal of Theoretical Biology*, vol. 234, no. 3, pp. 413–421, 2005.

[56] M. S. Handcock and J. H. Jones, "Likelihood-based inference for stochastic models of sexual network formation," *Theoretical Population Biology*, vol. 65, no. 4, pp. 413–422, 2004.

[57] M. C. González, C. A. Hidalgo, and A. L. Barabási, "Understanding individual human mobility patterns," *Nature*, vol. 453, no. 7196, pp. 779–782, 2008.

[58] N. Becker and J. Angulo, "On estimating the contagiousness of a disease transmitted from person to person," *Mathematical Biosciences*, vol. 54, no. 1-2, pp. 137–154, 1981.

[59] S. Altizer, W. M. Hochachka, and A. A. Dhondt, "Seasonal dynamics of mycoplasmal conjunctivitis in eastern North American house finches," *Journal of Animal Ecology*, vol. 73, no. 2, pp. 309–322, 2004.

[60] P. Caley and D. Ramsey, "Estimating disease transmission in wildlife, with emphasis on leptospirosis and bovine tuberculosis in possums, and effects of fertility control," *Journal of Applied Ecology*, vol. 38, no. 6, pp. 1362–1370, 2001.

[61] P. C. Cross, D. M. Heisey, B. M. Scurlock, W. H. Edwards, M. R. Ebinger, and A. Brennan, "Mapping brucellosis increases relative to elk density using hierarchical bayesian models," *PLoS One*, vol. 5, no. 4, 2010.

[62] N. D. Barlow, "Non-linear transmission and simple models for bovine tuberculosis," *Journal of Animal Ecology*, vol. 69, no. 4, pp. 703–713, 2000.

[63] A. L. Greer, C. J. Briggs, and J. P. Collins, "Testing a key assumption of host-pathogen theory: density and disease transmission," *Oikos*, vol. 117, no. 11, pp. 1667–1673, 2008.

[64] R. Woodroffe, C. A. Donnelly, G. Wei et al., "Social group size affects Mycobacterium bovis infection in European badgers (Meles meles)," *Journal of Animal Ecology*, vol. 78, no. 4, pp. 818–827, 2009.

Hindawi Publishing Corporation
Interdisciplinary Perspectives on Infectious Diseases
Volume 2011, Article ID 676949, 12 pages
doi:10.1155/2011/676949

Review Article

Network Models: An Underutilized Tool in Wildlife Epidemiology?

Meggan E. Craft[1] and Damien Caillaud[2]

[1] *Boyd Orr Centre for Population and Ecosystem Heath, College of Medical, Veterinary and Life Sciences, University of Glasgow, Glasgow G12 8QQ, UK*
[2] *Section of Integrative Biology, University of Texas, Austin, TX 78712, USA*

Correspondence should be addressed to Meggan E. Craft, meggan.craft@gmail.com

Received 20 October 2010; Accepted 14 December 2010

Academic Editor: Lauren Meyers

Although the approach of contact network epidemiology has been increasing in popularity for studying transmission of infectious diseases in human populations, it has generally been an underutilized approach for investigating disease outbreaks in wildlife populations. In this paper we explore the differences between the type of data that can be collected on human and wildlife populations, provide an update on recent advances that have been made in wildlife epidemiology by using a network approach, and discuss why networks might have been underutilized and why networks could and should be used more in the future. We conclude with ideas for future directions and a call for field biologists and network modelers to engage in more cross-disciplinary collaboration.

1. Introduction

Conventional methods for studying infectious disease dynamics include a repertoire of modeling techniques: traditional mean field (or Susceptible-Infected-Recovered (SIR) compartmental), metapopulation, lattice-based, reaction-diffusion, and network models [1]. Many of these modeling approaches have been around for decades. The contact network approach, originally developed for applications in the field of statistical physics, has only recently gained in popularity. In network terminology, individuals, or groups of individuals, are defined as *nodes*, connections between those nodes are *edges*, and the number of edges from one node to another is the *degree* (Figure 1). In network epidemiology, diseases spread from node to node following the edges. If the transmission probability along edges is high enough, an epidemic can occur. A very appealing property of networks is their ability to easily depict the complexity of the real world. In particular, the degree distribution captures heterogeneity in transmission among hosts, allowing the disproportionate role of highly connected individuals—superspreaders—to be easily investigated [2, 3]. Networks also often include lists of attributes to nodes or edges that describe between-edge variation in disease transmission or between-host variation in infectiveness or pathogen excretion patterns.

The network approach is not inherently different from the other modeling tools. It is simply a more general way of representing epidemiological systems. In fact, most alternative models can be considered as particular cases of network model. For example, modeling an epidemic using an SIR compartmental model is equivalent to using a complete network model in which all the nodes are connected to each other (Figure 2(a)). A lattice-based model can also be replaced by a network model in which nodes that are neighbors on the lattice are connected to each other and all nodes have same degree.

Because it offers more flexibility, the network approach can be used to answer new questions and to improve disease control. Since all individuals and all potential transmission paths are represented in the network, it becomes possible to identify individuals or edges that play a key role for disease transmission. Epidemiologists can then propose measures to alter the network in order to prevent or stop disease percolation. For example, vaccinating super-spreading individuals changes the degree distribution, which may be a more efficient way to achieve herd immunity than

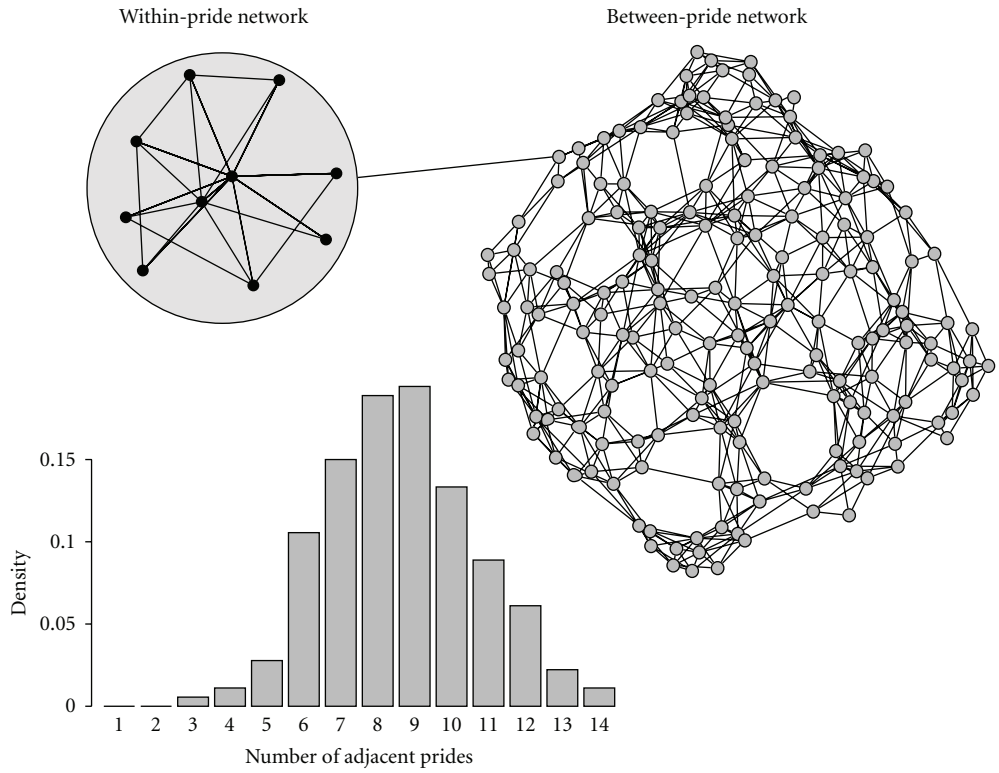

Figure 1: An example of a wildlife network: the Serengeti lion network [4]. In the within-pride network, the nodes (circles) are individuals and edges (lines between circles) are contacts observed on a short time scale (this is a cartoon, not based on data). The between-pride network is derived from behavioral observations of individually known lions as in [4] where nodes represent prides, and edges represent contacts between prides. The histogram represents the degree distribution of the between-pride network.

random vaccination. For these reasons, network techniques have been increasingly used for the study of human diseases [2, 7, 8]. To obtain parameters for these contact network models, populations of humans can rather easily self-report contact data quickly and efficiently through contact tracing or contact diaries [9]; there are also clever ways of using proxies for human disease incidence, such as mining the number of flu-related internet queries [10] or using mobile phone locations as a proxy for human movement or contact-tracing studies [11].

Despite the advantages over traditional disease models, networks are still underused for the study of diseases in wild animal populations. In this paper we describe the state of the art for wildlife network modeling, discuss reasons why network models are an underused tool in wildlife epidemiology, and suggest how contact network epidemiology could become more widespread for biologists. For clarity, we restrict our discussion to microparasites with simple life cycles and focus on between-host disease dynamics.

2. Current Use of Network Models in Wildlife Epidemiology

This section provides an overview of the current state of wildlife network epidemiology. We first present the main reasons why network models are particularly suited to wildlife epidemiology. We then expose a critical particularity of wildlife epidemiology: the type of data that are collected. Finally, we present recent advances made in the field.

2.1. Why Might Network Models Be Preferred to Traditional Modeling Techniques? Traditional compartmental or metapopulation epidemiological models assume that individuals constituting an epidemiological system can be pooled in a small number of functional groups within which the disease incidence rate is simply proportional to the number of susceptible and infectious individuals. These models are often qualified as "mass-action models". Within these functional groups, all the individuals are therefore assumed to be epidemiologically identical. The originality of network models resides in their ability to take into account interindividual or intergroup (i.e., internode) variations in epidemiological properties (e.g., degree, infectiveness, recovery rate). With this high resolution, the role played by each individual in the network can be assessed. Since network models capture more heterogeneity among nodes than traditional models, fitted network models can be used to predict the impact of interventions targeting individuals that are critical for disease percolation.

Network models therefore constitute powerful tools to analyze highly heterogeneous epidemiological systems. For

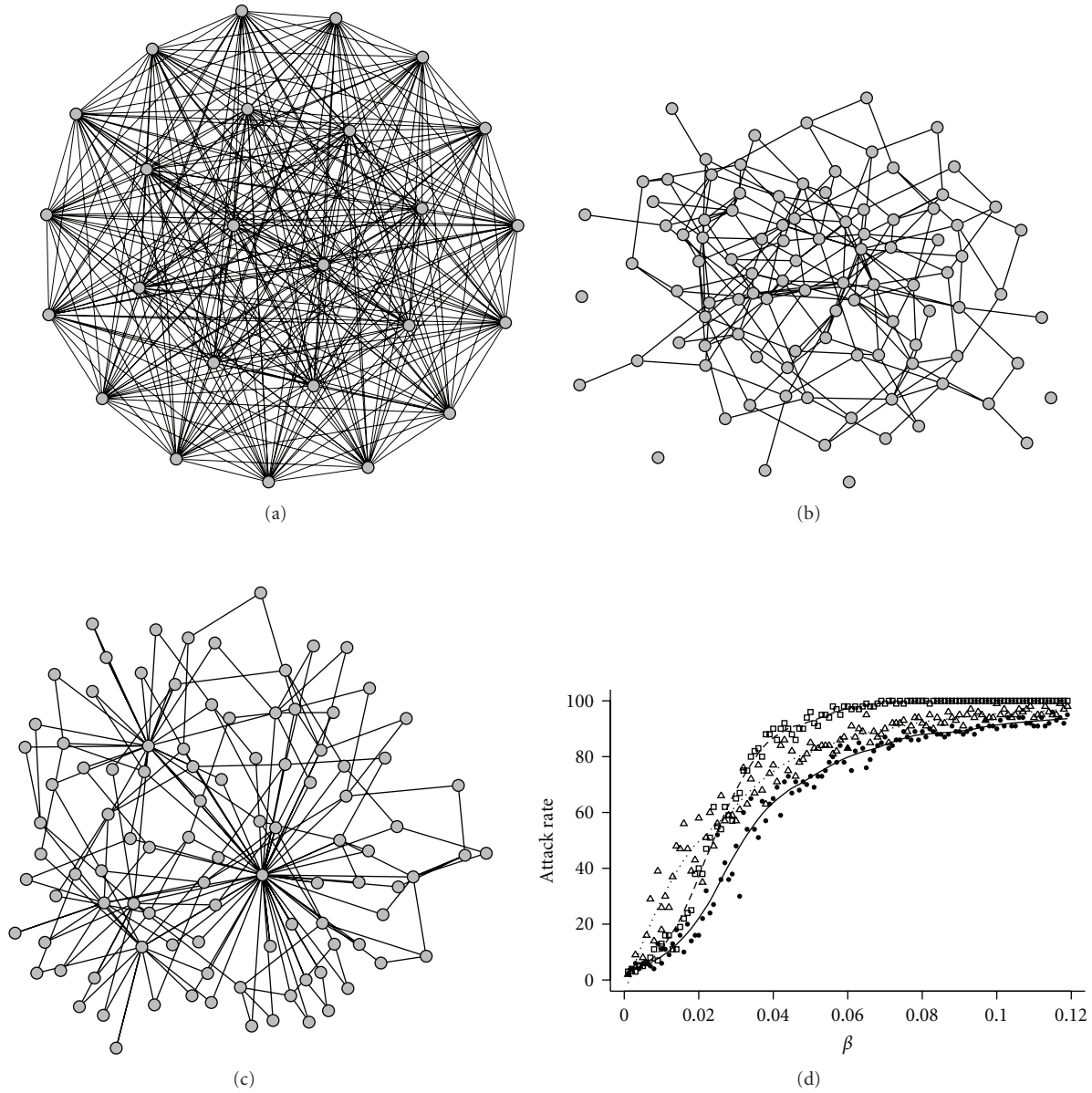

Figure 2: Three examples of contact networks with identical number of nodes (with 100 nodes) and connectedness (where the mean number of effective contacts per node = 4), but different degree distributions. (a) Fully-connected network. Each node has a degree of 99, but a weight of 4/99 = .0404 is applied to each edge to keep the average connectedness of each node equal to four. Diseases spread through this network in an equivalent way as in a mass action model. For clarity, only 25 nodes out of 100 are represented here. (b) Random network with Poisson degree distribution and mean degree = 4, generated following the Erdos and Renyi model [5]. (c) Scale-free network generated using Barbasi-Albert's preferential attachment algorithm [6], with mean degree = 4 and a power law degree distribution. The network is created by starting with one node and no edges. At each time step, a node is added and connected to two other vertices chosen in proportion to their current degree. This network is characterized by a few highly connected nodes, which may act as superspreaders during epidemics. (d) Stochastic SIR simulations of disease dynamics through the three networks (120 runs per network type). Squares, circles and triangles correspond to networks (a), (b), and (c), respectively. The final epidemic size (attack rate) is represented in relation to the intergroup transmission β. The recovery rate is fixed at 0.1. Note that even when the mean connectivity is kept constant, disease impacts vary with network structure.

example, when the degree distribution is strongly right-skewed, the small number of individuals with the highest degree values tend to be infected very early during the epidemic, and subsequently redistribute the disease to a large number of individuals. These "hub" individuals are then responsible for very high incidence rates at the beginning of the epidemic, which traditional models are unable to predict (see Figure 2). If a mass-action model is used to fit prevalence data collected during this epidemic, the associated goodness-of-fit will be poor, and the estimates of epidemiological parameters will be biased. As explained below, wild animal populations are typical examples of heterogeneous

systems and therefore greatly benefit from the network approach.

2.2. How Is Wildlife Data Different from Human Data? From the epidemiological point of view, wildlife systems differ in four important respects from human systems: (i) the underlying structure of the population, (ii) the tools available to collect data on the network structure, (iii) available epidemiological data, and (iv) potential control options.

First, wild animal populations are often highly structured. Numerous species live in groups, which generally interact nonrandomly. And within a given area, several species susceptible to the same disease can also interact. In such a complex system, the global contact network is modular. It can be decomposed into elements corresponding to the different observation scales: within-group networks (level $n = 1$), between-group networks ($n = 2$), and sometimes higher order level networks like between-species network ($n = 3$). Level-n networks (with $n \geq 2$) can then be considered as metanetworks, that is, networks of networks, with the networks of the level n-1 constituting the nodes of the level n (Figure 1). Wildlife epidemiologists need to estimate basic structural parameters of their study population in order to know how these different networks are combined together. Basically they need to answer the following questions: do the animals live in groups? If so, what is the group size distribution? How do individuals interact within a group? How do groups interact? Does the disease of interest likely involve several species in the study area? Are there other potentially relevant hierarchical levels, such as subgroups (groups inside groups) or subpopulations (groups of groups)?

Second, wildlife biologists face multiple challenges when collecting contact data [12–14]. Behavioral observations of animals rarely allow inferring exact, full contact networks, as it is basically impossible to watch all individuals of a population at the same time. The use of indirect measures (through technology) can help this problem, although the number of individuals that can be simultaneously monitored is often limited due to logistical difficulties or the high costs of technology (but see [15] which might have recorded a full network of a study lizard population). More commonly, a representative subset of the study population is generally chosen and then either directly observed using standard behavioral sampling methods or indirectly monitored using biologgers, radio telemetry, mark-recapture, or other methods (for a discussion of methods see Table 1). When choosing a technique to inform a contact model, it is important to take into account whether the species is habituated or not, captive or wild, the local environment of the population (e.g., heavily forested or underwater), the size of the animal, the resolution of the data needed to create a contact network specific to that animal's behavior, the budget, and the sample size needed. It is important not to change the animal's behavior using these techniques, for example through observer presence of timid animals, or heavy tags limiting movement.

There are a few specific challenges in constructing contact networks from empirical data. (i) Contact networks are normally derived from healthy individuals, and an animal's behavior, and hence the topography of the contact network, might change upon infection. Often it is unknown whether infection would alter the network structure by causing more contacts (e.g., "furious" rabies) or fewer contacts ("dumb" rabies). In this case, a sensitivity analysis could be used to hedge against any changes in contact rates due to infection. (ii) It is quite difficult to define a "contact"; clearly the definition of a contact will depend on the transmission of the pathogen of interest. Is the pathogen sexually transmitted? Aerosol borne? Does it persist in the environment? What is an effective contact? (of course, a contact does not necessarily mean a transmission event.) The best way to get answers to these questions is to do controlled transmission experiments, but this can be ethically challenging, especially for wild animals of conservation concern. (iii) Once a definition of "contact" is created, and a technique chosen to capture these contacts, it is then difficult to measure other types of social interactions for which you are not monitoring. (iv) Despite the recent technological advances allowing the collection of biologically relevant contact data for the majority of a population, how to sample a network is still a problem. For example, technological failures can lead to incomplete networks even if the whole population was successfully tagged, and there are often edge effects with other populations [24]. (v) The type of method used to collect the contact data can influence the properties of the network, hence the infectious period of the disease must be taken into account when choosing a method [27]. Because another behavioral variable is normally being used as a proxy for contact (i.e., proximity data), the raw data collected from these indirect measures does not immediately yield a contact network. But, after adequate processing, it becomes possible to reconstruct contact networks that will not exactly match the actual full network, but will rather have the same statistical, and hence epidemiological, properties.

Wild animal contact networks also often, if not always, exhibit temporal variation, creating a dynamic network. For example, individuals or groups can migrate to a different area (e.g., reindeer [40], wildebeest [41], birds [42], monarch butterflies [43]), individuals can transfer to a different group (e.g., [44]), and animal societies can fission-fusion (e.g., hyenas [45], chimpanzees [46], bottlenose dolphins [47], elephants [48], lions [49], and guppies [50]). In addition, contact networks can change over long time scales due to demographic processes such as births and deaths. Theoretical studies have shown that the spread of infectious diseases in dynamic networks differs from static networks [51]. Significant changes in contact patterns during the course of an epidemic need to be accounted for, and this data describing contact network dynamics can be obtained using direct observation or technology as listed above and in Table 1.

Third, epidemiological parameters can also be challenging to collect [52]. Incidence can be recorded through passive surveillance operations or direct observation for only the few diseases where wild animals exhibit overt clinical signs (e.g., rabies [53]). However, the majority of wild animals do not show visual signs of disease and most wild animals simply disappear when they die. In the field it is often

Table 1: Direct and indirect techiques that could be used to collect contact network data on wildlife populations and selected examples using these techniques.

Technique	Useful for which type of species?	Comments	Selected references
Direct			
Behavioral observations of known individuals	Diurnal habituated animals that can be easily observed (not cryptic species)	Potentially a "gold standard" for contact networks (multiple types of social interactions can be recorded); labor intensive	[16–19]
Viewpoint scanning	Visible animals active during the day; open habitat (not cryptic species)	Allows between-species observations at replicable sites; labor intensive yet incomplete observations	[20]
Indirect			
Biologging	Easily captured and handled individuals	Population needs to be saturated with detectors; excellent resolution of proximity data although proximity does not mean contact; continuous time record; cannot distinguish between types of close contacts (e.g., fighting versus mating)	[21]
Biologging: animal-borne acoustic proximity receiver	Marine mammals	Need to handle animal to retrieve device; good between-animal resolution	[22]
Biologging: PIT (Passive Integrated Transponder) tags	Useful for small mammals	Good data on duration of presence/absence of marked individuals at specific places (e.g., supplemented foraging sites) equipped with PIT loggers; approximation of contacts	[23]
Biologging: proximity data loggers/collars	Medium to large animals	measure frequency and duration of contact; complete temporal data; need to recover loggers	[24–26]
Capture-mark-recapture	Easily captured and handled individuals	A contact is defined as occupying same area during same period of time; good for capturing movement/dispersal data, not good at capturing within-group contacts	[27–31]
Direct manipulation	Captive populations of common animals	Great for repeatable experiments on experimentally infected individuals to measure transmission, but does this reflect contact patterns in wild?	[32, 33]
GPS recorders	Easily captured and handled medium to large individuals	Need recorders on all individuals in select area; if recorders are synced well, excellect contact data for the time the GPS takes point (with spotty coverage in between). Maybe local avoidance happens but would be undetected?	[15]
Powder marking	Easily trapped and handled individuals	Gives good contact data if contacts involve direct phyical contact; can only monitor a few indivuals at a time due to contstraints on the number of powder colors	[23]

Table 1: Continued.

Technique	Useful for which type of species?	Comments	Selected references
Radio telemetry	Handled individuals, not good for very small individuals	Contact defined as occupying same area during same period of time. Good indicator of (i) scale of interaction but gives coarse resolution of a "contact", (ii) mixing between groups of animals, but not within groups and (iii) den-sharing contacts. Presence of fieldworkers may alter behavior.	[27, 34–36]
Trapping and bait marking	Easily trapped and handled individuals who use latrines to mark territories	Good data on home range overlap and intergroup movement rates	[37]
Video tracking from animal's perspective	Animal must be able to be caught and wear something like a video backpack	Great contact data from individual perspective	[38]
Video trapping from fixed perspective (automated)	Social insects that can be individually tagged and the group monitored	Great resolution of contact data; software records duration and frequency of contacts	[39]

difficult to detect carcasses, and more worrying, even detect any sort of die-off (e.g., [54]). As another example, out of over 1000 lions suspected to die in a fatal canine distemper virus outbreak in the Serengeti in 1994, only 11 carcasses were recovered from a highly-monitored population [55]. Prevalence data can be collected through active surveillance methods such as serological surveys. Blood can be screened directly for pathogens or indirectly for antibodies to pathogens to provide insight on disease dynamics [56]. Longitudinal surveys are generally the preferred type of serological survey; cross-sectional serological surveys can be misleading because antibodies persist long after the end of the infection [57]. Collecting blood samples is only possible if the study animals can be trapped or darted. It is generally expensive, time-consuming, and potentially risky to the animal. However, in recent years, noninvasive disease screening methods have been developed, such as immunoglobulin dosage in urine and feces (e.g., SIV in chimps [58]) or parasite genotyping in feces (e.g., malaria in great apes [59]).

In contrast to human diseases, multiple hosts are often involved in wildlife diseases. Human outbreaks often involve animals, but generally only at the very beginning; whereas in wildlife, multiple species are often involved during the entire course of the outbreak. This increases the complexity of building a multihost network, and often it is challenging to have accurate assessments of contact networks from multiple hosts, forcing a fall-back strategy on mean field models [60].

Finally, despite constraints to inferring the structure of the contact network and collecting disease data, network models allow us to easily evaluate a wide range of disease control interventions in wildlife populations. In humans, because there are numerous ways to modify human networks, such as school closure, travel warnings, and airport closure in certain cases, public health actions often focus on improving epidemiological surveillance and implementing subsequent vaccination campaigns. In wildlife epidemiology, altering networks is also possible, but in very different ways [61]. For example, oral vaccination baits can occasionally be used with success [62]. Parenteral vaccination can be used for small wild animal populations [63], but is logistically challenging and sometimes considered too invasive. Wildlife contact networks can also be modified by reducing contacts between domestic animals, humans, and wildlife to avoid the spillover to wildlife in the first place—this is a type of quarantine [64–66]. Population density can also be reduced through culling or decreasing birth rates [34, 67]. An important benefit of the network approach is the ability to identify central individuals likely responsible for most transmission events. When those individuals are targeted for intervention purposes, this reduces the number of wildlife needing to be culled or vaccinated, for example.

2.3. Recent Progress in Wildlife Network Epidemiology. In the past 5–10 years, wildlife biologists have made solid progress in characterizing contact networks in wildlife populations. Through the use of these contact networks we have been able to address novel questions relating to wildlife and their diseases. For example, superspreading animals have been found in some populations (e.g., deer mice and possums [23, 28]), while they are not obvious in other systems (e.g., Tasmanian devil and African lion populations [4, 24]). The Tasmanian devil network was found to be one giant component, meaning that the whole endangered population is threatened by a novel infectious cancer [24]. Well-connected individuals were more likely to be infected in some wildlife populations (brushtail possums, sleepy lizards, skinks, and bumble-bees [15, 29, 32, 39]) but not in others (meerkats [16]). In a study of possums, density was found to be uncorrelated

with contact rates [25]. In contrast, abundance thresholds above which disease can spread (percolation thresholds) have been identified in gerbils with plague [68] and in multihost plague systems of mice and prairie dogs [69]. With networks, researchers were able to distinguish spatial patterns of disease spillover from epidemic waves [17]. Temporal changes in contact patterns were also identified as critical for the spread of respiratory diseases in wild chimpanzees [70]. Issues of different spatial scales have been tackled with networks, specifically the relative importance of local versus long range transmission events in driving disease spread [68]. Finally, multilevel network models have been developed and successfully applied to tuberculosis transmission between badgers groups and cows [26]. For a more extensive list of insights we refer to Table 1 of a recent review [71].

3. Despite These Advances, Why Are Network Models Underused in Wildlife Epidemiology?

The network approach might need a public relations campaign in the literature. Networks have been used in other fields like statistical physics for decades, yet have only in the past 10 years really taken off with the human epidemiology literature, and are now at the cutting edge of wildlife epidemiology. Contact networks models are likely *not well-known* in the wildlife community. The number of studies using this approach is still relatively limited, but of those studies combining networks and wildlife, they often get published in high profile journals—potentially indicating that wildlife network epidemiology is still in its infancy.

Second, the network literature, especially in the physics literature, is quite hard to grasp and at first sight, may seem *complicated* for the field biologist. The analytical treatment of network epidemiological models is however only slightly more difficult than solving systems of differential equations of mass action models. A few articles are notable for presenting the mathematics of network models in an accessible way for biologists [72–74]. However, finding analytical solutions is not always necessary. Agent-based stochastic simulations can be good alternatives and are relatively easy to implement. They are particularly interesting to model complex systems that have a lot of parameters and hence cannot be described by closed form equations. Unfortunately there is limited network software with easy-to-use graphical user interfaces implementing these methods, and often people program their own network simulation models (Table 2). Coding using basic programming languages (e.g., R, Python or NetLogo) is often a disparate skill set from a field biologist who successfully collects contact and epidemiological data on wild populations.

Third, networks are indeed *data intensive*, and wildlife systems are unfortunately often data limited. Individual-level data can be expensive and time-consuming to collect [71]. For example, in constructing a contact network for a population of Serengeti lions, only 36 pride-to-pride contacts were observed per 1294 hours of daylight observation over a 3 year time period [4]. In addition, wild animals cannot be continuously observed, and dealing with gaps and missing data is often challenging (see Section 4).

Finally, contact networks are inferred from contact data collected for a specific species, for a specific ecosystem, and for a specific period of time. Therefore it can be *difficult to generalize* epidemiological results obtained with a network model to other circumstances (e.g., [4]).

4. What Can Be Done to Dispel Doubts about Networks?

Network approaches need to become better *known* and more accessible. Wildlife epidemiologists should be encouraged to promote their network approach at meetings and in journals that have not normally embraced a network approach. More training sessions such as SISMID (University of Washington) or INSNA's workshops at Sunbelt would be useful. A formal comparison between network and mean-field models would also help spread the word. Currently, there are few papers comparing the performance of mean-field and network models. Although scientists might have tried multiple modeling approaches during the course of the study, normally only one approach is published. Mass action models normally work "well enough," but we are unaware of any formal quantitative comparison of the pros and cons of using mean-field versus network models for a range of empirical and theoretical systems.

It is likely that network models are only going to get more *complex*: they will include more parameters and variables. "Complexity" is an intrinsic, objective property of a model. It is not necessarily synonymous with "complicated"—a subjective judgment of the difficulty of the modeling task. For example, it is important to note that stochastic agent-based modeling handles very complex models but is generally not complicated. In the last few years, biologists have increasingly used these types of models to investigate respective effects of different variables on biological phenomenon. Several software and user-friendly computer languages are particularly suited to develop network epidemiological agent-based models (Table 2). It has even become possible to fit such models to field data. The recent developments in approximate Bayesian computation (ABC), a set of methods initially developed by population geneticists, greatly facilitate agent-based model fitting [84–86]. We would like to attract the attention of epidemiologist to these methods, which we believe will be used extensively in the future.

Technology is helping to bridge the gap between *data-intensive* network models, and the challenges inherent in collecting contact data. There has been a burst of new technology such as satellite GPS radio telemetry, proximity data loggers, camera and video traps, tracking, proximity data radio collars, powder marking, PIT tags, and antennae, and capture-mark-recapture (Table 1). These methods almost always collect data at discrete time intervals. Ignoring the gaps inherent to these datasets can lead to biased estimates of contact network or epidemiological parameters. For example, if an animal is observed susceptible at time t and reobserved infected 10 days later, should we assume that it became infected on the first day, on the last day, or maybe after five days? The answer is that none of these assumptions is necessary. At least three statistical methods can be used to

Table 2: Selected list of free software packages that can be used in wildlife network epidemiology.

Category name	Type	Programming skills required?	Comments	Ref./Download location
Capture-mark-recapture				
M-Surge	Application	No	Windows platform	[75]/http://www.cefe.cnrs.fr/BIOM/logiciels.htm
MARK	Application	No	Windows platform	[76]/http://warnercnr.colostate.edu/~gwhite/mark/mark.htm
Network simulation/analysis				
Pajek	Application	No	Analysis of large networks	[77]/http://vlado.fmf.uni-lj.si/pub/networks/pajek/
igraph	R Package	Basic	Used for all network visualizations in this article	[78]/http://www.r-project.org/
sna	R package	Basic	Other related R packages available on http://statnet.org/	[79]/http://www.r-project.org/
network	R Package	Basic	Other related R packages available on http://statnet.org/	[80]/http://www.r-project.org/
ClustRNet	Python package	Basic	Simulates network with variable clustering degree	[81]/http://sbansal.com/ClustRNet/
NetLogo	Interpreted language	Basic	Cross-platform	[82]/http://ccl.northwestern.edu/netlogo/
Epidemiological modelling				
EpiFire (GUI)	Application	No	Cross-platform	unpublished/http://sourceforge.net/projects/epifire/
NetLogo	Interpreted language	Basic	Cross-platform	[82]/http://ccl.northwestern.edu/netlogo/
R	Interpreted language	Basic	Cross-platform	[83]/http://www.r-project.org/
Python	Interpreted language	Basic	Cross-platform	http://www.python.org/
EpiFire (API)	C++ library	Yes (C/C++)	Includes network simulation capabilities	unpublished/http://sourceforge.net/projects/epifire/

deal with this uncertainty. First, survival analyses, that were initially developed to estimate survival rates using date-of-last-observation data can also be applied, for example, to estimate rates of seroconversion. One simply has to assume that seroconversion is equivalent to death [87]. Second, multistate capture-mark-recapture (CMR) models have proven very useful to estimate animal migration rates, survival rates, and rates of change of individual state (for example, states S, I or R). Although user-friendly software exists to fit CMR models (Table 2), these models could be more broadly used in wildlife epidemiology, both to estimate network parameters and epidemiological parameters. Third, agent-based models, coupled with ABC fitting procedure, can easily circumvent the problem of missing data [84–86]. Our purpose here is to attract the attention of epidemiologists to these methods rather than to describe them in detail, so we encourage interested readers to consult the references cited.

An exciting and useful push for future directions would be to develop theoretical advances for network models that allow us to develop "universal principles". As stated above, current network models are generally inferred from contact data. But one generally does not know what rules govern the establishment of contact patterns. Understanding these rules, in particular how ecological variables such as food resource distribution, distribution of conspecifics, and climate influence contact patterns, would allow identifying universal principles governing networks' structure. It would then become possible to extrapolate these mechanistic models to other populations, areas, or time periods.

Network epidemiological modeling is by essence interdisciplinary. This is even more pertinent to wildlife network epidemiology, because new fields such as behavioral ecology, capture-mark-recapture, and advanced statistics are combined. Collaborative work is an efficient way to do network modeling. Field biologists know their system, and know how to collect data, while theoreticians can work on the hardcore modeling aspects. We would like to promote better collaboration between modelers and field biologists. Modelers may need to be seen as more approachable by field biologists. Importantly, we believe collaborations should take place at all stages of epidemiological studies, from the design of the data collection protocol to the end of the modeling stage.

5. Conclusion

Network models have promising applications in the field of wildlife epidemiology. Although using this approach requires some substantial training, the learning curve is not as steep as it seems, and several software and interpreted computer languages have been developed that will make this step easier. In any case, we strongly believe that the benefits far outweigh these costs. The number of applications of network models in wildlife epidemiology is already broad, and will keep increasing. New application domains beg to be explored. For example, network models are well-suited to combine network and genetic data, potentially for viral diseases such as feline immunodeficiency virus and simian immunodeficiency virus. Contact network epidemiology using directed networks (where there is stronger transmission in one direction) has been applied to animals using the same resting spots for indirectly transmitted pathogens [15, 29], and could be expanded to fresh water organisms because river networks are easy to map, have a good spatial component, and pathogens might travel downstream.

We feel that developing collaboration between field biologists and network modelers will be a key factor bringing advances to wildlife epidemiology. We need to become more multidisciplinary and cross disciplinary [14, 88].

Acknowledgments

M. Craft is grateful for funding from NSF (OISE-0804186). D. C. is supported by NSF Grant DEB-0749097 to L. A. Meyers. The authors are grateful to L. A. Meyers and Sarah Perkins for helpful improvements to the draft.

References

[1] M. J. Keeling and P. Rohani, *Modeling Infectious Diseases in Humans and Animals*, Princeton University Press, Princeton, NJ, USA, 2008.

[2] L. A. Meyers, B. Pourbohloul, M. E. J. Newman, D. M. Skowronski, and R. C. Brunham, "Network theory and SARS: predicting outbreak diversity," *Journal of Theoretical Biology*, vol. 232, no. 1, pp. 71–81, 2005.

[3] J. O. Lloyd-Smith, S. J. Schreiber, P. E. Kopp, and W. M. Getz, "Superspreading and the effect of individual variation on disease emergence," *Nature*, vol. 438, no. 7066, pp. 355–359, 2005.

[4] M. E. Craft, E. Volz, C. Packer, and L. A. Meyers, "Disease transmission in territorial populations: the small-world network of Serengeti lions," *Journal of the Royal Society Interface*. In press.

[5] P. Erdos and A. Renyi, "On random graphs," *Publicationes Mathematicae*, vol. 6, pp. 290–297, 1959.

[6] A. L. Barabási and R. Albert, "Emergence of scaling in random networks," *Science*, vol. 286, no. 5439, pp. 509–512, 1999.

[7] B. Pourbohloul, L. A. Meyers, D. M. Skowronski, M. Krajden, D. M. Patrick, and R. C. Brunham, "Modeling control strategies of respiratory pathogens," *Emerging Infectious Diseases*, vol. 11, no. 8, pp. 1249–1256, 2005.

[8] S. Bansal, B. Pourbohloul, and L. A. Meyers, "A comparative analysis of influenza vaccination programs," *PLoS Medicine*, vol. 3, no. 10, article e387, pp. 1816–1825, 2006.

[9] M. J. Keeling and K. T. D. Eames, "Networks and epidemic models," *Journal of the Royal Society Interface*, vol. 2, no. 4, pp. 295–307, 2005.

[10] J. Ginsberg, M. H. Mohebbi, R. S. Patel, L. Brammer, M. S. Smolinski, and L. Brilliant, "Detecting influenza epidemics using search engine query data," *Nature*, vol. 457, no. 7232, pp. 1012–1014, 2009.

[11] D. A. King, C. Peckham, J. K. Waage, J. Brownlie, and M. E. J. Woolhouse, "Infectious diseases: preparing for the future," *Science*, vol. 313, no. 5792, pp. 1392–1393, 2006.

[12] T. Wey, D. T. Blumstein, W. Shen, and F. Jordán, "Social network analysis of animal behaviour: a promising tool for the study of sociality," *Animal Behaviour*, vol. 75, no. 2, pp. 333–344, 2008.

[13] J. Krause, D. P. Croft, and R. James, "Social network theory in the behavioural sciences: potential applications," *Behavioral Ecology and Sociobiology*, vol. 62, no. 1, pp. 15–27, 2007.

[14] H. McCallum, "Six degrees of *Apodemus* separation," *Journal of Animal Ecology*, vol. 78, no. 5, pp. 891–893, 2009.

[15] S. T. Leu, P. M. Kappeler, and C. M. Bull, "Refuge sharing network predicts ectoparasite load in a lizard," *Behavioral Ecology and Sociobiology*, vol. 64, pp. 1495–1503, 2010.

[16] J. A. Drewe, "Who infects whom? Social networks and tuberculosis transmission in wild meerkats," *Proceedings of the Royal Society B*, vol. 277, no. 1681, pp. 633–642, 2010.

[17] M. E. Craft, E. Volz, C. Packer, and L. A. Meyers, "Distinguishing epidemic waves from disease spillover in a wildlife population," *Proceedings of the Royal Society B*, vol. 276, no. 1663, pp. 1777–1785, 2009.

[18] J. Altmann, "Observational study of behavior: sampling methods," *Behaviour*, vol. 49, no. 3-4, pp. 227–267, 1974.

[19] M. A. de Menezes, R. W. Baird, D. Lusseau, P. Guimarães, P. R. Guimarães, and S. F. dos Reis, "Vulnerability of a killer whale social network to disease outbreaks," *Physical Review E*, vol. 76, no. 4, Article ID 042901, 2007.

[20] C. Richomme, D. Gauthier, and E. Fromont, "Contact rates and exposure to inter-species disease transmission in mountain ungulates," *Epidemiology and Infection*, vol. 134, no. 1, pp. 21–30, 2006.

[21] S. Prange, T. Jordan, C. Hunter, and S. D. Gehrt, "New radiocollars for the detection of proximity among individuals," *Wildlife Society Bulletin*, vol. 34, no. 5, pp. 1333–1344, 2006.

[22] T. L. Guttridge, S. H. Gruber, J. Krause, and D. W. Sims, "Novel acoustic technology for studying free-ranging shark social behaviour by recording individuals' interactions," *PLoS ONE*, vol. 5, no. 2, Article ID e9324, 2010.

[23] C. A. Clay, E. M. Lehmer, A. Previtali, S. St. Jeor, and M. D. Dearing, "Contact heterogeneity in deer mice: implications for Sin Nombre virus transmission," *Proceedings of the Royal Society B*, vol. 276, no. 1660, pp. 1305–1312, 2009.

[24] R. K. Hamede, J. Bashford, H. McCallum, and M. Jones, "Contact networks in a wild Tasmanian devil (*Sarcophilus harrisii*) population: using social network analysis to reveal seasonal variability in social behaviour and its implications for transmission of devil facial tumour disease," *Ecology Letters*, vol. 12, no. 11, pp. 1147–1157, 2009.

[25] W. Ji, P. C. L. White, and M. N. Clout, "Contact rates between possums revealed by proximity data loggers," *Journal of Applied Ecology*, vol. 42, no. 3, pp. 595–604, 2005.

[26] M. Böhm, M. R. Hutchings, and P. C. L. White, "Contact networks in a wildlife-livestock host community: identifying high-risk individuals in the transmission of bovine TB among badgers and cattle," *PLoS ONE*, vol. 4, no. 4, Article ID e5016, 2009.

[27] S. E. Perkins, F. Cagnacci, A. Stradiotto, D. Arnoldi, and P. J. Hudson, "Comparison of social networks derived from ecological data: implications for inferring infectious disease dynamics," *Journal of Animal Ecology*, vol. 78, no. 5, pp. 1015–1022, 2009.

[28] T. Porphyre, M. Stevenson, R. Jackson, and J. McKenzie, "Influence of contact heterogeneity on TB reproduction ratio R in a free-living brushtail possum Trichosurus vulpecula population," *Veterinary Research*, vol. 39, no. 3, article 31, 2008.

[29] S. S. Godfrey, C. M. Bull, R. James, and K. Murray, "Network structure and parasite transmission in a group living lizard, the gidgee skink, Egernia stokesii," *Behavioral Ecology and Sociobiology*, vol. 63, no. 7, pp. 1045–1056, 2009.

[30] J. D. Lebreton, K. P. Burnham, J. Clobert, and D. R. Anderson, "Modeling survival and testing biological hypotheses using marked animals: a unified approach with case studies," *Ecological Monographs*, vol. 62, no. 1, pp. 67–118, 1992.

[31] K. H. Pollock, J. D. Nichols, C. Brownie, and J. E. Hines, "Statistical inference for capture-recapture experiments," *Wildlife Monographs*, vol. 107, pp. 3–97, 1990.

[32] L. A. L. Corner, D. U. Pfeiffer, and R. S. Morris, "Social-network analysis of Mycobacterium bovis transmission among captive brushtail possums (Trichosurus vulpecula)," *Preventive Veterinary Medicine*, vol. 59, no. 3, pp. 147–167, 2003.

[33] D. Naug, "Structure of the social network and its influence on transmission dynamics in a honeybee colony," *Behavioral Ecology and Sociobiology*, vol. 62, no. 11, pp. 1719–1725, 2008.

[34] D. Ramsey, N. Spencer, P. Caley et al., "The effects of reducing population density on contact rates between brushtail possums: implications for transmission of bovine tuberculosis," *Journal of Applied Ecology*, vol. 39, no. 5, pp. 806–818, 2002.

[35] M. E. Gompper and A. N. Wright, "Altered prevalence of raccoon roundworm (Baylisascaris procyonis) owing to manipulated contact rates of hosts," *Journal of Zoology*, vol. 266, no. 2, pp. 215–219, 2005.

[36] P. C. Cross, J. O. Lloyd-Smith, J. A. Bowers, C. T. Hay, M. Hofmeyr, and W. M. Getz, "Integrating association data and disease dynamics in a social ungulate: bovine tuberculosis in African buffalo in the Kruger National Park," *Annales Zoologici Fennici*, vol. 41, no. 6, pp. 879–892, 2004.

[37] J. Vicente, R. J. Delahay, N. J. Walker, and C. L. Cheeseman, "Social organization and movement influence the incidence of bovine tuberculosis in an undisturbed high-density badger Meles meles population," *Journal of Animal Ecology*, vol. 76, no. 2, pp. 348–360, 2007.

[38] L. A. Bluff and C. Rutz, "A quick guide to video-tracking birds," *Biology Letters*, vol. 4, no. 4, pp. 319–322, 2008.

[39] M. C. Otterstatter and J. D. Thomson, "Contact networks and transmission of an intestinal pathogen in bumble bee (*Bombus impatiens*) colonies," *Oecologia*, vol. 154, no. 2, pp. 411–421, 2007.

[40] S. Sharma, S. Couturier, and S. D. Côté, "Impacts of climate change on the seasonal distribution of migratory caribou," *Global Change Biology*, vol. 15, no. 10, pp. 2549–2562, 2009.

[41] R. M. Holdo, R. D. Holt, and J. M. Fryxell, "Opposing rainfall and plant nutritional gradients best explain the wildebeest migration in the serengeti," *The American Naturalist*, vol. 173, no. 4, pp. 431–445, 2009.

[42] J. H. Rappole, S. R. Derrickson, and Z. Hubálek, "Migratory birds and spread of West Nile virus in the Western Hemisphere," *Emerging Infectious Diseases*, vol. 6, no. 4, pp. 319–328, 2000.

[43] L. P. Brower, "Understanding and misunderstanding the migration of the monarch butterfly (Nymphalidae) in North America: 1857–1995," *Journal - Lepidopterists' Society*, vol. 49, no. 4, pp. 304–385, 1995.

[44] E. H. M. Sterck, D. P. Watts, and C. P. van Schaik, "The evolution of female social relationships in nonhuman primates," *Behavioral Ecology and Sociobiology*, vol. 41, no. 5, pp. 291–309, 1997.

[45] J. E. Smith, J. M. Kolowski, K. E. Graham, S. E. Dawes, and K. E. Holekamp, "Social and ecological determinants of fission-fusion dynamics in the spotted hyaena," *Animal Behaviour*, vol. 76, no. 3, pp. 619–636, 2008.

[46] J. Lehmann and C. Boesch, "To fission or to fusion: effect of community size on wild chimpanzee (Pan troglodytes versus) social organisation," *Behavioral Ecology and Sociobiology*, vol. 56, no. 3, pp. 207–216, 2004.

[47] R. C. Connor, R. Wells, J. Mann, and A. Read, "The bottlenose dolphin: social relationships in a fission-fusion society," in *Cetacean Societies: Field Studies of Whales and Dolphins*, J. Mann, R. Connor, P. Tyack, and H. Whitehead, Eds., pp. 91–126, University of Chicago Press, Chicago, Ill, USA, 2000.

[48] G. Wittemyer, I. Douglas-Hamilton, and W. M. Getz, "The socioecology of elephants: analysis of the processes creating multitiered social structures," *Animal Behaviour*, vol. 69, no. 6, pp. 1357–1371, 2005.

[49] G. B. Schaller, *The Serengeti Lion; A Study of Predator-Prey Relations*, University of Chicago Press, Chicago, Ill, USA, 1972.

[50] D. P. Croft, J. Krause, and R. James, "Social networks in the guppy (Poecilia reticulata)," *Proceedings of the Royal Society B*, vol. 271, no. 6, pp. S516–S519, 2004.

[51] E. Volz and L. A. Meyers, "Epidemic thresholds in dynamic contact networks," *Journal of the Royal Society Interface*, vol. 6, no. 32, pp. 233–241, 2009.

[52] S. Cleaveland, C. Packer, K. Hampson et al., "The multiple roles of infectious diseases in the Serengeti ecosystem," in *Serengeti III: Human Impacts on Ecosystem Dynamics*, A. R. E. Sinclair, S. Mduma, and J. Fryxell, Eds., pp. 209–239, Chicago University Press, Chicago, Ill, USA, 2008.

[53] T. Lembo, K. Hampson, D. T. Haydon et al., "Exploring reservoir dynamics: a case study of rabies in the Serengeti ecosystem," *Journal of Applied Ecology*, vol. 45, no. 4, pp. 1246–1257, 2008.

[54] D. Caillaud, F. Levréro, R. Cristescu et al., "Gorilla susceptibility to Ebola virus: the cost of sociality," *Current Biology*, vol. 16, no. 13, pp. R489–R491, 2006.

[55] M. E. Roelke-Parker, L. Munson, C. Packer et al., "A canine distemper virus epidemic in Serengeti lions (Panthera leo)," *Nature*, vol. 379, no. 6564, pp. 441–445, 1996.

[56] C. Packer, S. Altizer, M. Appel et al., "Viruses of the Serengeti: patterns of infection and mortality in African lions," *Journal of Animal Ecology*, vol. 68, no. 6, pp. 1161–1178, 1999.

[57] S. Cleaveland, T. Mlengeya, M. Kaare et al., "The conservation relevance of epidemiological research into carnivore viral diseases in the Serengeti," *Conservation Biology*, vol. 21, no. 3, pp. 612–622, 2007.

[58] M. L. Santiago, M. Lukasik, S. Kamenya et al., "Foci of endemic simian immunodeficiency virus infection in wild-living eastern chimpanzees (Pan troglodytes schweinfurthii)," *Journal of Virology*, vol. 77, no. 13, pp. 7545–7562, 2003.

[59] F. Prugnolle, P. Durand, C. Neel et al., "African great apes are natural hosts of multiple related malaria species, including Plasmodium falciparum," *Proceedings of the National Academy of Sciences of the United States of America*, vol. 107, no. 4, pp. 1458–1463, 2010.

[60] M. E. Craft, P. L. Hawthorne, C. Packer, and A. P. Dobson, "Dynamics of a multihost pathogen in a carnivore community," *Journal of Animal Ecology*, vol. 77, no. 6, pp. 1257–1264, 2008.

[61] R. J. Delahay, G. C. Smith, and M. R. Hutchings, Eds., *Management of Disease in Wild Mammals*, Springer, New York, NY, USA, 2009.

[62] M. L. Cross, B. M. Buddle, and F. E. Aldwell, "The potential of oral vaccines for disease control in wildlife species," *The Veterinary Journal*, vol. 174, no. 3, pp. 472–480, 2007.

[63] D. T. Haydon, D. A. Randall, L. Matthews et al., "Low-coverage vaccination strategies for the conservation of endangered species," *Nature*, vol. 443, no. 7112, pp. 692–695, 2006.

[64] I. B. Rwego, G. Isabirye-Basuta, T. R. Gillespie, and T. L. Goldberg, "Gastrointestinal bacterial transmission among humans, mountain gorillas, and livestock in Bwindi Impenetrable National Park, Uganda," *Conservation Biology*, vol. 22, no. 6, pp. 1600–1607, 2008.

[65] S. Köndgen, H. Kühl, P. K. N'Goran et al., "Pandemic human viruses cause decline of endangered great apes," *Current Biology*, vol. 18, no. 4, pp. 260–264, 2008.

[66] S. A. Osofsky, S. Cleaveland, W. B. Karesh et al., *Conservation and Development Interventions at the Wildlife/Livestock Interface: Implications for Wildlife, Livestock, and Human Health*, IUCN, Gland, Switzerland, 2005.

[67] G. Caughley, R. Pech, and D. Grice, "Effect of fertility control on a population's productivity," *Wildlife Research*, vol. 19, no. 6, pp. 623–627, 1992.

[68] S. Davis, P. Trapman, H. Leirs, M. Begon, and J. A. P. Heesterbeek, "The abundance threshold for plague as a critical percolation phenomenon," *Nature*, vol. 454, no. 7204, pp. 634–637, 2008.

[69] D. J. Salkeld, M. Salathé, P. Stapp, and J. H. Jones, "Plague outbreaks in prairie dog populations explained by percolation thresholds of alternate host abundance," *Proceedings of the National Academy of Sciences of the United States of America*, vol. 107, no. 32, pp. 14247–14250, 2010.

[70] H. S. Kuehl, C. Elzner, Y. Moebius, C. Boesch, and P. D. Walsh, "The price of play: self-organized infant mortality cycles in chimpanzees," *PLoS ONE*, vol. 3, no. 6, Article ID e2440, 2008.

[71] D. M. Tompkins, A. M. Dunn, M. J. Smith, and S. Telfer, "Wildlife diseases: from individuals to ecosystems," *Journal of Animal Ecology*, vol. 80, no. 1, pp. 19–38, 2011.

[72] M. E. J. Newman, "Spread of epidemic disease on networks," *Physical Review E*, vol. 66, no. 1, Article ID 016128, 11 pages, 2002.

[73] M. E. J. Newman, S. H. Strogatz, and D. J. Watts, "Random graphs with arbitrary degree distributions and their applications," *Physical Review E*, vol. 64, no. 2, Article ID 026118, 7 pages, 2001.

[74] L. A. Meyers, M. E. J. Newman, and B. Pourbohloul, "Predicting epidemics on directed contact networks," *Journal of Theoretical Biology*, vol. 240, no. 3, pp. 400–418, 2006.

[75] R. Choquet, A. M. Reboulet, R. Pradel, O. Gimenez, and J. D. Lebreton, "M-SURGE: new software specifically designed for multistate capture-recapture models," *Animal Biodiversity and Conservation*, vol. 27, no. 1, pp. 207–215, 2004.

[76] G. C. White and K. P. Burnham, "Program MARK: survival estimation from populations of marked animals," *Bird Study*, vol. 46, pp. S120–S139, 1999.

[77] V. Batagelj and A. P. Mrvar, "Analysis and visualization of large networks," in *Graph Drawing Software*, M. Jünger and P. Mutzel, Eds., pp. 77–103, Springer, Berlin, Germany, 2003.

[78] G. Csardi and T. Nepusz, "The igraph software package for complex network research," *InterJournal Complex Systems*, vol. 2006, p. 1695, 2006.

[79] M. S. Handcock, D. R. Hunter, C. T. Butts, S. M. Goodreau, and M. Morris, "statnet: software tools for the representation, visualization, analysis and simulation of network data," *Journal of Statistical Software*, vol. 24, no. 1, pp. 1548–7660, 2008.

[80] C. T. Butts, "network: a package for managing relational data in R," *Journal of Statistical Software*, vol. 24, no. 2, 2008.

[81] S. Bansal, S. Khandelwal, and L. A. Meyers, "Exploring biological network structure with clustered random networks," *BMC Bioinformatics*, vol. 10, article 405, 2009.

[82] U. Wilensky, *NetLogo: Center for Connected Learning and Computer-Based Modeling*, Northwestern University, Evanston, Ill, USA, 1999.

[83] R Development Core Team, *R: A Language and Environment for Statistical Computing*, R Foundation for Statistical Computing, Vienna, Austria, 2010.

[84] T. Toni, D. Welch, N. Strelkowa, A. Ipsen, and M. P. H. Stumpf, "Approximate Bayesian computation scheme for parameter inference and model selection in dynamical systems," *Journal of the Royal Society Interface*, vol. 6, no. 1, pp. 187–202, 2009.

[85] D. Wegmann, C. Leuenberger, and L. Excoffier, "Efficient approximate Bayesian computation coupled with Markov chain Monte Carlo without likelihood," *Genetics*, vol. 182, no. 4, pp. 1207–1218, 2009.

[86] C. Leuenberger and D. Wegmann, "Bayesian computation and model selection without likelihoods," *Genetics*, vol. 184, no. 1, pp. 243–252, 2010.

[87] H. Hagan, H. Thiede, and D. C. Des Jarlais, "Hepatitis C virus infection among injection drug users: survival analysis of time to seroconversion," *Epidemiology*, vol. 15, no. 5, pp. 543–549, 2004.

[88] D. T. Haydon, "Cross-disciplinary demands of multihost pathogens," *Journal of Animal Ecology*, vol. 77, no. 6, pp. 1079–1081, 2008.

Hindawi Publishing Corporation
Interdisciplinary Perspectives on Infectious Diseases
Volume 2011, Article ID 157194, 5 pages
doi:10.1155/2011/157194

Commentary

Empiricism and Theorizing in Epidemiology and Social Network Analysis

Richard Rothenberg[1] and Elizabeth Costenbader[2]

[1] *Institute of Public Health, Georgia State University, 140 Decatur Street, Atlanta, GA 30303, USA*
[2] *Family Health International, Behavioral and Social Sciences Department, 2224 E NC Hwy 54, Durham, NC 27713, USA*

Correspondence should be addressed to Richard Rothenberg, rrothenberg@gsu.edu

Received 24 June 2010; Accepted 6 October 2010

The connection between theory and data is an iterative one. In principle, each is informed by the other: data provide the basis for theory that in turn generates the need for new information. This circularity is reflected in the notion of abduction, a concept that focuses on the space between induction (generating theory from data) and deduction (testing theory with data). Einstein, in the 1920s, placed scientific creativity in that space. In the field of social network analysis, some remarkable theory has been developed, accompanied by sophisticated tools to develop, extend, and test the theory. At the same time, important empirical data have been generated that provide insight into transmission dynamics. Unfortunately, the connection between them is often tenuous and the iterative loop is frayed. This circumstance may arise both from data deficiencies and from the ease with which data can be created by simulation. But for whatever reason, theory and empirical data often occupy different orbits. Fortunately, the relationship, while frayed, is not broken, to which several recent analyses merging theory and extant data will attest. Their further rapprochement in the field of social network analysis could provide the field with a more creative approach to experimentation and inference.

1. Introduction

Theory and empirical data are in principle intimately interwoven. Yet in the practice of social network analysis, there appears to be a disconnect: theorizing and empiricism often seem to occupy separate orbits, and these separate discussions may be difficult to relate to each other. The root of the problem may lie in the different skill sets required by each, or perhaps in the substantial obstacles to collection of human network data. The following exploration of the distance between theory and empiricism suggests that a rapprochement would be of considerable benefit to the field.

The mid-19th Century American philosopher Charles Peirce coined the term "abduction" (which he also called "retroduction") to fill a gap he perceived in the territory occupied by induction and deduction. As distilled by Professor Burch [1], Peirce used syllogisms to explain this term, substituting Rule, Case, and Result for the more familiar Major Premise, Minor Premise, and Conclusion. But perhaps more interesting to epidemiologists and social network analysts, he related this logical process to sampling. As Professor Burch explains it, a standard valid syllogism would progress as follows.

Rule: All balls in this urn are red.

Case: All balls in this particular random sample are taken from this urn.

Result: Therefore, all balls in this particular random sample are red.

Peirce then asked what would happen if we change the order of reasoning, by interchanging the Result and the Rule.

Result: All balls in this particular random sample are red.

Case: All balls in this particular random sample are taken from this urn.

Rule: Therefore, all balls in this urn are red.

Burch points out that this is not a valid syllogism but was the core of Peirce's concept of induction. Extraordinary, how closely it captures the epidemiologic mindset. But take it one step farther, and interchange the Result with the Case.

Rule: All balls in this urn are red.

Result: All balls in this particular random sample are red.

Case: Therefore, all balls in this particular random sample are taken from this urn.

Again, not a valid construct, but if we substitute "Alternate Hypothesis" for "Rule," we appear to capture the essence of hypothesis testing as it is now practiced [2]. Burch maintains that this is neither induction nor deduction, but a new type of argument that Peirce called abduction. Peirce went on to use the three "-ductions" to describe the scientific method as a *circular synthesis* of the scientific method. The process begins with a conjecture or hypothesis that is based on some observation or thought (abduction). From the hypothesis can be derived consequences, and these can be tested. The resulting test observations can be used to confirm or refute the hypothesis, or more generally, either to draw conclusions about the truth or return to the abductive process of conjuring up a new hypothesis.

Popper did not agree [3]. He relegated the process of hypothesis generation to the realm of psychology and stated overtly that he was not interested in it [3, page 39]. In contrast, Albert Einstein embraced it. As described by Adam [4], Einstein wrote a short newspaper article in 1919 that colocated the process of abduction with the creativity inherent in scientific endeavors. Einstein said: "Intuitive comprehension of the essentials about the large complex facts leads the researcher to construct one or several hypothetical fundamental laws. . .he [the researcher] does not arrive at his system of thought in a methodical, inductive way; rather, he snuggles (sic) to the facts by intuitive choice among the imaginable axiomatic theories."

Thus, Peirce and Einstein provide a direct connection between theory, observations, conclusions, and revisions. This view stresses that theory and observation are interdependent, iterative, and connected by creativity. Unfortunately, this connection (though not necessarily the creativity) seems to have attenuated in the application of social network analysis to disease transmission.

2. The Linkage of Theory and Empiricism

Several factors have hindered a tight linkage between theoretical and empirical approaches. First, the cost and time to elucidate sociometric network structure, particularly for hard-to-reach populations such as those who may be at the highest risk for HIV or other communicable diseases, are often viewed as prohibitive. Second, empirical sociometric network ascertainment is imperfect. Since the boundaries of the populations of interest are never known and always changing and the manner in which we find out about connections is not standardized, some connections between individuals or network nodes within those populations are always missed, often in unknown ways that render imputation and interpretation problematic. Third, there is no gold standard and no true or known network against which to measure empirical adequacy. These concerns are all subsumed under the general issue of sampling in networks. Because empirical ascertainment of networks requires a credible sampling procedure, preferably one that justifies the use of standard statistical theory, observations may be suspected. One result has been a movement toward theory-based network simulation wherein the investigator controls the sampling, knows (actually creates) the gold standard, and can test the effect of imposed conditions. The past decade has witnessed a burgeoning of this work and considerable new insight into the structure, function, and dynamics of many types of networks [5, 6].

A persistent problem, however, is the difficulty of relating theoretical network constructs back to some empirical reality. The theoretical biases inherent in sampling are the case in point. There can be no question that sampling matters if one is to have a credible mathematical basis for statistical network inference [7, 8]. Modeling approaches have demonstrated the biases that arise from missing data [9]. In his text, Newman [10] enumerates some of these biases: snowball sampling finds persons in proportion to their eigenvector centrality (i.e., the centrality of their contacts), but the large number of waves required to reach equilibrium may preclude unbiased estimates. Contact tracing suffers from the same problem, with the additional issue of seeking only infected persons, who are a biased sample of the population. Random walk sampling may offer some advantages, since sampling is proportional to degree, and equilibrium can be reached quickly in small groups, but issues of contact recall, unfindable partners, and nonparticipation persist. These assertions are all readily verifiable using mathematical and simulation approaches. There has been little or no empirical validation, however, of many theoretical conclusions that are taken as true. In fact, the assumption of theoretical validity is often so strong that many may find empirical verification unnecessary.

3. Reconnecting Theory to Data

But if the Peirce/Einstein view is to be recaptured, meaningful efforts at falsification of theoretical constructs are needed. As noted, such efforts are generally not attempted, perhaps because of their difficulty, or perhaps because of the *a priori* assumptions about their inadequacy. (You cannot know if you have the right answer, so why bother.) This is perhaps where Peirce's second syllogism—the balls in my random sample are all red, so those in the urn from which they come must be red—needs to be invoked. Though logically defective—in fact, it epitomizes "the inductive problem" that has concerned philosophers since Hume—it is the basis for the inductive reasoning that, as noted, drives the epidemiological mindset. As argued forcefully by Pearce and Crawford-Brown [11], the notion that falsifiability is the hallmark of science fails to recognize the uncertainties of falsifiability, which can be at least as strong as those of induction. In addition, these authors stress the primacy of replication and validation of findings [12], the need for mature theory examined in multiple ways, and the importance of observations whose ongoing renewal and explanation is actually the work of theory.

Table 1: Network features with chronological accrual of respondents.

Number of respondents	10	20	30	40	50	100	150	All (206)
Number of persons in network	62	131	202	284	367	685	981	1314
Degree (mean of interviewed respondents)	7.4	8.1	8.3	8.6	8.8	8.4	8.0	7.6
Degree (mean of all persons in network)	2.3	2.3	2.3	2.3	2.3	2.3	2.3	2.3
Degree (variance)	10.5	13.4	13.1	12.8	12.5	12.1	11.8	10.9
Concurrency (kappa)	5.9	7.1	7.0	6.9	6.8	6.6	6.4	6.1
Clustering coefficient	0.034	0.034	0.033	0.029	0.028	0.033	0.041	0.036
Power coefficient	2.79	2.19	2.23	1.76	1.71	1.65	1.59	1.59
Age assortativity	0.313	0.299	0.348	0.315	0.285	0.329	0.323	0.319

Thus, to complete the loop of theory validation, we require repeated demonstration that theoretical predictions are borne out in real life. Empirical verification of theoretical constructs affirms their validity, provides ongoing refinement of parameters, and furnishes a real basis for applying interventions. In the current realm of social network analysis, it would seem that empirical studies provide parameters to theoreticians, and not much else.

4. Some Other Examples

On the other hand, it is also the case that those involved in delineating real-time social networks have focused more on findings and transmission implications than on the specific validation of theoretical constructs. For example, 15 empirical network studies that were used in a synthesis of findings [13] produced over 100 publications, but none focused primarily on testing theoretical findings. There are some examples, however, of empirical attempts to examine theoretical constructs. Take, for example, Newman's assertion that, with random walk sampling, equilibrium can be reached quickly in small groups. Two empirical observations speak to this issue. First, in a direct test of sampling methods [14], networks ascertained by a chain link random walk (wherein the next person in the chain was chosen at random from the contacts of the current respondent) or by nomination (the next person in the chain nominated by the respondent from his/her contacts) were indistinguishable. Second, using those same networks, the underlying pattern of network configuration was evident from the first 10 interviews (out of 206) (Table 1), supporting the notion that the pattern becomes clear quickly.

In a comparison of centrality measures [15], it was demonstrated that imperfect sample data produced stable network estimates under a variety of circumstances. In a comparison of eight types of centrality measures, high concordance [16] was found among measures ascertained through a complex, mixed sampling scheme despite expectations that these measures would vary because of their differing relationships to the underlying sampling method.

A number of studies, following the observations by Barabási and colleagues of "scale-free" network structure in the world wide web [17–19], attempted to show that networks of persons at risk for HIV and STIs could be fit by a power law curve with a coefficient between 2 and 3 (the statistical requirement for scale-freeness) [13, 20]. Several rigorous statistical analyses [7, 21] of the empirical data from 10 studies found that none of the nine statistical models tested consistently provided the best fit to the degree distributions from those studies. In addition, the best-fit power law model predicted no epidemic threshold for HIV and STIs in the United States, a theoretical observation in obvious contrast to the true condition. This result [21], by providing empirical evidence against the proposed theory, embodies the aforementioned process of "circular synthesis."

As a final example, the history of concurrency as an important feature of HIV and STD transmission is informative. Though disjointed, and at times acerbic, the discussion has gone back and forth between theory and data and provides a good illustration of how the two interact. The role of concurrency in Africa was first suggested nearly 20 years ago, based both on observation [22, 23] and on theoretical considerations and simulation [24]. In a comprehensive followup [25–27], mathematical development of a simple formula for calculating network concurrency and a simple simulation established the importance of concurrency in transmission. Ten years on, extensive claims have been made for the overriding importance of concurrency in sexual transmission of HIV in Africa [28, 29], with the assertion that multiple sites, assessed in multiple ways, have evidence of substantial concurrency. Though the empirical evidence for these claims has been challenged [30, 31], and the challenge contested [32], the pattern of high long-term concurrency with a relatively low degree distribution has been demonstrated in detail in at least one comprehensive study, in Likoma Island, Malawi [33]. This nonlinear chain of events does nonetheless illustrate the importance of the interplay between conjecture, empirical data, and theoretical development. The next step, not yet completed, would be a theoretical demonstration of rapid epidemic spread in an African setting that would incorporate a low-degree high concurrency configuration and reasonable parameters for transmission based on emerging empirical information on infectivity in acute HIV infection [34]. (In another aspect of concurrency—its potential role in explaining the ethnic disparity in HIV infection in the United States—this type of theoretical and empirical interplay has been attempted to confirm its importance [35].)

5. Interlocking Roles

Though there are other examples of the circular process of empirical and theoretical interaction, they are still few in number. The majority of empirical studies (e.g., large-scale surveys) from which parameters are drawn are usually theory-free. In turn, theoretical and simulation studies, as noted, use these parameters but are often data- and context-free. (An unfair characterization, perhaps, but it is difficult to deny that ethnographers generally do not speak mathematics and mathematicians do not speak the language of the street.)

But from these considerations, a clearer role for theory, empiricism, and their interrelationship may emerge. In his Nobel acceptance speech in 1974, Frederich von Hayek, often called the father of complexity theory, said: "*...as we penetrate from the realm in which relatively simple laws prevail [the physical sciences] into the range of phenomena where organized complexity rules...often all that we shall be able to predict will be some abstract characteristic of the pattern that will appear...yet...we will still achieve predictions which can be falsified and which therefore are of empirical significance*" [36]. Despite all their difficulties, empirical descriptions of networks, both qualitative and quantitative, have the potential to find those abstract characteristics of a pattern, a task for which theoretical and simulation studies alone are not well suited. Theoretical studies are well suited to exploring patterns, and they often do it best in ways that make little pretense of reality [37] but are geared rather to demonstrating mechanisms and testing the observations. A greater synergy between theory and data could provide the field with a more systematic approach to experimentation and inference.

Fortunately the process of abduction is a method equally approachable by all scientists. Theoreticians can be just as good abductors as empiricists. Anyone is at liberty to think up ideas, but those who "snuggle to the facts" may have the best chance of success.

Acknowledgment

This work is supported in part by Grant R21 DA024611-01 from the National Institute on Drug Abuse, National Institutes of Health.

References

[1] R. Burch, Charles Sanders Peirce. Stanford Encyclopedia of Philosophy, 2009, http://plato.stanford.edu/entries/peirce/.

[2] S. N. Goodman and D. R. Bellhouse, "Hypothesis tests, and likelihood: implications for epidemiology of a neglected historical debate," *American Journal of Epidemiology*, vol. 137, no. 5, pp. 485–501, 1993.

[3] K. Popper, *The Logic of Scientific Discovery*, Routledge, London, UK, 1959.

[4] A. M. Adam, "Farewell to certitude: einstein's novelty on induction and deduction, fallibilism," *Journal for General Philosophy of Science*, vol. 31, no. 1, pp. 19–37, 2000.

[5] R. M. Anderson and G. P. Garnett, "Mathematical models of the transmission and control of sexually transmitted diseases," *Sexually Transmitted Diseases*, vol. 27, no. 10, pp. 636–643, 2000.

[6] M. E. J. Newman, "The structure and function of complex networks," *SIAM Review*, vol. 45, no. 2, pp. 167–256, 2003.

[7] M. S. Handcock and J. H. Jones, "Likelihood-based inference for stochastic models of sexual network formation," *Theoretical Population Biology*, vol. 65, no. 4, pp. 413–422, 2004.

[8] M. S. Handcock, "Modeling social networks with sampled or missing data," Working Paper 75, CSSS, University of Washington, Seattle, Wash, USA, 2007.

[9] A. C. Ghani, C. A. Donnelly, and G. P. Garnett, "Sampling biases and missing data in explorations of sexual partner networks for the spread of sexually transmitted diseases," *Statistics in Medicine*, vol. 17, no. 18, pp. 2079–2097, 1998.

[10] M. E. J. Newman, *Networks: An Introduction*, Oxford University Press, Oxford, UK, 2010.

[11] N. Pearce and D. Crawford-Brown, "Critical discussion in epidemiology: problems with the Popperian approach," *Journal of Clinical Epidemiology*, vol. 42, no. 3, pp. 177–184, 1989.

[12] C. Buck, "Popper's philosophy for epidemiologists," *International Journal of Epidemiology*, vol. 4, no. 3, pp. 159–168, 1975.

[13] R. Rothenberg and S. Q. Muth, "Large-network concepts and small-network characteristics: fixed and variable factors," *Sexually Transmitted Diseases*, vol. 34, no. 8, pp. 604–612, 2007.

[14] R. B. Rothenberg, D. M. Long, C. E. Sterk et al., "The Atlanta urban networks study: a blueprint for endemic transmission," *AIDS*, vol. 14, no. 14, pp. 2191–2200, 2000.

[15] E. Costenbader and T. W. Valente, "The stability of centrality measures when networks are sampled," *Social Networks*, vol. 25, no. 4, pp. 283–307, 2003.

[16] R. B. Rothenberg, J. J. Potterat, D. E. Woodhouse, W. W. Darrow, S. Q. Muth, and A. S. Klovdahl, "Choosing a centrality measure: epidemiologic correlates in the Colorado Springs study of social networks," *Social Networks*, vol. 17, no. 3-4, pp. 273–297, 1995.

[17] A.-L. Barabási and R. Albert, "Emergence of scaling in random networks," *Science*, vol. 286, no. 5439, pp. 509–512, 1999.

[18] A. L. Barabási, R. Albert, H. Jeong, and G. Bianconi, "Power law distribution of the World Wide Web," *Science*, vol. 287, p. 2115, 2000.

[19] A.-L. Barabási, R. Albert, and H. Jeong, "Scale-free characteristics of random networks: the topology of the world-wide web," *Physica A*, vol. 281, no. 1, pp. 69–77, 2000.

[20] F. Liljeros, C. R. Edling, L. A. Nunes Amaral, H. E. Stanley, and Y. Åberg, "Social networks: the web of human sexual contacts," *Nature*, vol. 411, no. 6840, pp. 907–908, 2001.

[21] D. T. Hamilton, M. S. Handcock, and M. Morris, "Degree distributions in sexual networks: a framework for evaluating evidence," *Sexually Transmitted Diseases*, vol. 35, no. 1, pp. 30–40, 2008.

[22] C. P. Hudson, "Concurrent partnership could cause AIDS epidemics," *International Journal of STD and AIDS*, vol. 4, no. 5, pp. 249–253, 1993.

[23] C. P. Hudson, A. J. M. Hennis, P. Kataaha et al., "Risk factors for the spread of AIDS in rural Africa: evidence from a comparative seroepidemiological survey of AIDS, hepatitis B and syphilis in Southwestern Uganda," *AIDS*, vol. 2, no. 4, pp. 255–260, 1988.

[24] C. H. Watts and R. M. May, "The influence of concurrent partnerships on the dynamics of HIV/AIDS," *Mathematical Biosciences*, vol. 108, no. 1, pp. 89–104, 1992.

[25] M. Kretzschmar and M. Morris, "Measures of concurrency in networks and the spread of infectious disease," *Mathematical Biosciences*, vol. 133, no. 2, pp. 165–195, 1996.

[26] M. Morris and M. Kretzschmar, "Concurrent partnerships and transmission dynamics in networks," *Social Networks*, vol. 17, no. 3-4, pp. 299–318, 1995.

[27] M. Morris and M. Kretzschmar, "Concurrent partnerships and the spread of HIV," *AIDS*, vol. 11, no. 5, pp. 641–648, 1997.

[28] D. T. Halperin and H. Epstein, "Concurrent sexual partnerships help to explain Africa's high HIV prevalence: implications for prevention," *The Lancet*, vol. 364, no. 9428, pp. 4–6, 2004.

[29] T. L. Mah and D. T. Halperin, "Concurrent sexual partnerships and the HIV epidemics in africa: evidence to move forward," *AIDS and Behavior*, vol. 14, no. 1, pp. 11–16, 2008.

[30] M. N. Lurie and S. Rosenthal, "Concurrent partnerships as a driver of the HIV epidemic in sub-saharan Africa? The evidence is limited," *AIDS and Behavior*, vol. 14, pp. 17–24, 2009.

[31] L. Sawers and E. Stillwaggon, "Concurrent sexual partnerships do not explain the HIV epidemics in Africa: a systematic review of the evidence," *Journal of the International AIDS Society*, vol. 13, article 34, 2010.

[32] H. Epstein, "The mathematics of concurrent partnerships and HIV: a commentary on lurie and rosenthal, 2009," *AIDS and Behavior*, vol. 14, no. 1, pp. 29–30, 2009.

[33] S. Helleringer and H.-P. Kohler, "Sexual network structure and the spread of HIV in Africa: evidence from Likoma Island, Malawi," *AIDS*, vol. 21, no. 17, pp. 2323–2332, 2007.

[34] M. S. Cohen and C. D. Pilcher, "Amplified HIV transmission and new approaches to HIV prevention," *Journal of Infectious Diseases*, vol. 191, no. 9, pp. 1391–1393, 2005.

[35] M. Morris, A. E. Kurth, D. T. Hamilton, J. Moody, and S. Wakefield, "Concurrent partnerships and HIV prevalence disparities by race: linking science and public health practice," *American Journal of Public Health*, vol. 99, no. 6, pp. 1023–1031, 2009.

[36] F. A. von Hayek, The Pretence of Knowledge, 2010, http://nobelprize.org/nobel_prizes/economics/laureates/1974/hayek-lecture.html.

[37] D. J. Watts and S. H. Strogatz, "Collective dynamics of 'small-world9 networks," *Nature*, vol. 393, no. 6684, pp. 440–442, 1998.